Biomimetic Fouling Control

Thesis submitted by

Andrew John Scardino BSc (Hons) ***UNSW***

in September, 2006

for the degree of Doctor of Philosophy in the School of Marine Biology & Aquaculture, James Cook University

STATEMENT OF ACCESS

I, the undersigned, author of this work, understand that James Cook University will make this thesis available for use within the University Library and, via the Australian Digital Theses network, for use elsewhere.

I understand that, as an unpublished work, a thesis has significant protection under the Copyright Act and; I do not wish to place any further restriction on access to this work.

ANDREW J SCARDINO	07/03/07
Signature	Date

STATEMENT OF SOURCES

DECLARATION

I declare that this thesis is my own work and has not been submitted in any form for another degree or diploma at any university or other institution of tertiary education. Information derived from the published or unpublished work of others has been acknowledged in the text and a list of references is given.

ANDREW J SCARDINO	07/03/07
Signature	Date

ELECTRONIC COPY

I, the undersigned, the author of this work, declare that the electronic copy of this thesis provided to the James Cook University Library is an accurate copy of the print thesis submitted, within the limits of the technology available.

ANDREW J SCARDINO 07/03/07

Signature Date

Acknowledgements

I would like to sincerely thank my supervisor Rocky de Nys. Rocky has taught me to enjoy science and research, though most importantly to believe in myself. His patience, encouragement and friendly manner has made my candidature extremely enjoyable.

The members of the de Nys lab at JCU have been fantastic. I have found them to be valuable friends as well as supporting colleagues. So, thank you Jana Guenther, Ray Bannister, Piers Ettinger-Epstein, Matt Fraser, Leo Nanvervis, Stevie Whalan, Dan Louden, Mikey Horne and Odette Ison for three memorable years in NQ. Other members of the Aquaculture department have also been very helpful and friendly including Brad Evans, Dean Jerry, Paul Southgate, Hector Acosta-Salmon and Erika Martinez. Wade Sherbrooke, a visiting academic, was a good friend and colleague in 2004.

John Lewis from Defence Science & Technology Organisation enabled this project to be undertaken. He has been extremely supportive for the duration of my candidature and has shown considerable patience during the final write up stage.

Kevin Blake was immensely helpful with analytical techniques, particular SEM.

Zhongxiao Peng and Des Hudleston proved to be excellent collaborators. They provided valuable insight into surface characterisation techniques which were crucial for chapters 2 & 3.

Hua Zhang and Rob Lamb also turned out to be wonderful collaborators. They introduced me to superhydrophobic surfaces and chapter 7 has been the result of this fruitful partnership.

Thanks also to Andrew Stone, Rick Barber and Erol Harvey from MiniFAB for the microtextured surfaces which were used in chapters 4 and 5.

Peter Steinberg kindly allowed me to use bench space and resources at the Centre for Marine Biofouling & Bioinnovation, UNSW.

Nick Paul was extremely helpful with statistical advice.

Kevin Ness provided time and assistance with surface pressure quantification.

The School of Marine Biology & Aquaculture and the Graduate Research School at JCU have been particularly encouraging of my work. For the many opportunities you have afforded me I sincerely thank you.

CRC Reef and the Institute of Marine Engineering, Science & Technology have also been supporters of my research.

Lastly, I would like to thank my family. To my wife, Lauren, parents Roy & Frances, and siblings, David & Pauline – thanks for all your love and support, you have made my life very enjoyable and my candidature has seemed infinitely easier because of this.

ABSTRACT

Any man-made structure immersed in the marine environment rapidly becomes fouled, with significant economic consequences. Solutions to fouling have generally used toxic paints or coatings which have damaging effects on marine life. The subsequent phasing out of these antifoulants has sparked a search for non-toxic antifouling alternatives, including the development of technologies based on natural biofouling defence models (biomimicry). The biomimetic approach to antifouling is the focus of this thesis, with an emphasis on physical fouling defence mechanisms in molluscs. Surface microtextures have been identified as potential fouling deterrent mechanisms in molluscs and have been recorded on the blue mussels *Mytilus galloprovincialis* and *M. edulis*. The aim of this thesis is to develop biomimetic fouling control using marine molluscs as a natural model.

To determine physical defences the surface texture of a range of marine bivalves and gastropods from the Great Barrier Reef was characterised and many unique micro-topographical patterns discovered. Laser scanning confocal microscopy was used to quantify the surface roughness parameters for 36 selected species. This is the first example of the characterisation of natural marine surfaces in terms of mean roughness and waviness profiles, skewness, anisotropy and fractal dimension. The wettability of the selected species was also determined. Subsequently, the 36 species were assessed for fouling resistance over three months and fouling resistance and removal was correlated with the surface roughness parameters generated. Key roughness parameters, in particular skewness, fractal dimension and hydrophobicity, were identified for species specific fouling resistance and also fouling removal. Total fouling cover was positively correlated to fractal dimension and negatively correlated to skewness. Algal cover was negatively correlated to hydrophobicity, Spirorbid tubeworm cover was positively correlated to fractal dimension, and percent fouling removal was positively correlated with mean waviness.

To establish the role of surface microtexture in fouling deterrence, biomimics were created for three bivalves, *Mytilus galloprovincialis* and *Tellina plicata,* which have differing microtopographical patterns, and *Amusium balloti,* which has a smooth

surface. Smooth biomimics were significantly more fouled than microtextured biomimics. The fouling resistance of microtextured biomimics diminished after 6-8 weeks, in contrast to natural shells which maintained their fouling resistant properties for 3 months. The extended fouling resistance of natural shells supports a multiple defence strategy of the surface-bound periostracum, with the proteinaceous nature of the coating providing a defence against microfouling. A theory is proposed that microtextured biomimics only deters macrofouling larvae and that microfoulers that are smaller than the size of the microtexture fill the textures and negate its effects.

This theory is termed ‘attachment point theory’, whereby larval attachment is influenced by the number of attachment points with settling larvae preferring the maximum number of attachment points to enhance successful adhesion and recruitment. To test attachment point theory, microtextured films of varying texture widths (2-512 μm) were developed and attachment to the microtextures by a range of micro- and macro-fouling organisms was determined. Diatoms attached in significantly higher numbers on textures smaller than the width of the diatom cell. In contrast attachment was reduced on textures slightly smaller than the cell width, clearly supporting attachment point theory. Attachment by macrofouling larvae and algal spores to microtextures also supported the theory. Larvae and spores generally settled in higher number on the texture larger than the spore/larval size. Attachment points for settling larvae are identified as important mechanisms in fouling deterrence, or attachment, with the critical factor being the ratio of the width of settling organism to that of the microtexture.

The findings of fouling resistance on micro-rough surfaces were explored further to incorporate nano-scale surface roughness. This novel antifouling mechanism combines micro- and nano-scale roughness to a hydrophobic surface to create superhydrophobicity. A range of surfaces incorporating micro- with nano-scale roughness, and nano-scale roughness alone, were tested against a range of micro- and macro- fouling organisms. Nano-rough surfaces alone significantly deterred all tested organisms. In contrast micro-scale with nano-scale roughness either attracted or repelled larvae. From the mixed preferences recorded on the choice bioassays, factors other than hydrophobicity play a significant role in the selection of a surface on. All coatings were superhydrophobic (> 155º) but differed in roughness and produced very

different settlement responses. The consistently high level of deterrence by the nano-scale surface supports a theory of nano-bubbles at the surface of these coatings as an antifouling mechanism. The confirmation of this theory requires further collaborative investigation between physicists, chemists and biologists, but is a significant outcome.

Overall, the research presented has elucidated a number of novel approaches to biomimetic fouling control and developed novel theories for the mechanisms of action of natural surface-mediated fouling defences. These results also contribute to the development of promising alternatives to toxic antifouling technologies and provide unique approaches to significant new developments in micro- and nano-surface technologies in the field.

CONTENTS

List of Tables

Chapter 2

List of Figures

CHAPTER ONE

Biomimetic antifouling surfaces

1.1 *Biofouling defined and the biofouling sequence*

Biofouling is the colonisation processes of a surface in the aqueous environment and occurs most commonly in the marine environment. Within minutes of immersion a surface will be conditioned by a film of macromolecules such as glycoproteins and polysaccharides (Bakker et al. 2003). After several hours the surface becomes colonised by bacteria and after a few days by diatoms, protozoa and other unicellular eukaryotes. The attachment by diatoms through extracellular polymers creates a biofilm matrix on the surface, known as microfouling or slime (Callow & Callow, 2006). A more complex community develops from the microbial biofilm to include multicellular primary producers. The final stage of biofouling involves the settlement of large marine invertebrates and macro-algae. This macro-fouling stage can take from weeks to years and is often dynamic and complex with many species settling to form a complex three dimensional community. The most common macro-fouling organisms are barnacles, bryozoans, algae, tubeworms and molluscs. The biofouling sequence is described in detail by Wahl (1989) and the stages of fouling outlined by Abarzua & Jakubowsky, (1995) and more recently reviewed by Yebra et al. (2004) and Krug (2006).

The larvae and propagules of macrofouling organisms have finite resources and need to find a suitable place to settle within a limited timeframe. The selection of a suitable substrate is part of a complex recruitment process. Several factors influence larval settlement including hydrodynamics (Butman, 1987), light, salinity and temperature (Rodriguez et al. 1993), larval age and size (Marshall & Keough, 2003a; b; Marshall & Keough, 2004, Gribben et al. 2006), conspecifics (Burke, 1986; Pawlik, 1992; Head et al. 2003; 2004) and chemical cues (Fusetani, 2004). Many larvae settle preferentially to conspecifics or settle on other species which has consequences for both the settler (epibiont) and the host (basibiont) (Wahl, 1989). Unfortunately, they also settle onto available open space and this is often provided by artificial surfaces we place in the marine environment, in particular the hulls of vessels, pylons, oil rigs, aquaculture equipment, and any surface that provides space to settle. The consequence of this is the

settlement and growth of complex fouling communities with very significant biological and economic impacts.

1.2 *Past solutions to biofouling*

Biofouling poses a major problem to all marine industries. The economic cost of fouling is substantial and includes expenses such as dry-docking, hull maintenance, increased fuel consumption (up to 40%, Champ, 2000), delayed transport times and increased cleaning (Yebra et al. 2004). The economic consequences of fouling have lead to numerous solutions for biofouling control, which began many centuries ago. Solutions, which have been trialled from as early as the 5th century B.C, include pitch, tar, wax, copper and lead sheathing as well as arsenic and sulphur combined with oil to deter shipworms (Callow, 1990). Despite the numerous methods used lead sheathing was the most common on ships until the 18th century while copper was patented as an antifoulant in 1625 and was used widely by the British fleet in the 1780's. The introduction of iron ships put a halt to copper sheathing due to corrosion and reignited many other failed solutions to prevent fouling (reviewed in detail by Anderson et al. 2003; Yebra et al. 2004).

More sophisticated antifouling paints were developed in the 19th century generally containing a mixture of copper and rosin and in the 1950's the incorporation of organotins greatly improved the antifouling performance of ships (particularly the tri-butyl-tin (TBT) moiety). TBT was first available in an insoluble polymer matrix which does not erode in seawater restricting the lifespan of its activity to only 18 months. This subsequently led to the development of a soluble paint matrix (Yebra et al. 2004). These paints contain high rosin content with co-binders and plasticisers which improved the overall paint characteristics (Rascio et al. 1988). However, these coatings were ineffective when boats were stationary (del Amo et al. 1984) and the paint eroded too quickly at high operational speeds (Yebra et al. 2004).

In 1974 TBT self-polishing copolymers (TBT-SPC) were patented (Milne & Hails, 1974). These antifouling paints have an acrylic polymer with an ester linkage used to bond TBT groups to the polymer backbone (Swain, 1999). In seawater pigment particles (usually cuprous oxide) are eroded and expose a new layer of paint, which continually provides a self-polishing effect (Kiil et al. 2001). This breakthrough was

seen as the definitive antifouling solution as the polishing rate could be controlled for various vessel operating speeds (Anderson, 1995), and the polishing produced low hull roughness which reduced fuel consumption and emission (Swain, 1998). Furthermore, the paints are not corrosive to aluminium and steel (Pal & Misra, 1993), have short drying times, are durable (Hunter & Cain, 1996) and dry docking periods are extended to 5 years (Anderson, 1998).

Unfortunately TBT-SPC antifouling systems have proved to be far from perfect. These paints have very serious effects on non-target organisms in the marine environment including reduced growth, imposex and malformations in molluscs (Alzieu, 1986; Gibbs & Bryan, 1986; Evans et al. 1995) and accumulation in mammals and fishes (Kannan et al. 1997). These adverse effects have forced the International Maritime Organisation to ban the use of TBT-SPC (Champ, 2000). At present the application of TBT based antifouling paints is banned and its presence on all vessels is to be removed, or sealed in, by 2008 (Champ, 2001). These actions have lead to urgency in the search for a non-toxic environmentally friendly antifouling alternative.

Replacement technologies to TBT include the use of copper and complementing booster biocides. Most replacement paint systems use Cu_2O pigment which is soluble in seawater. When Cu_2O is dissolved in seawater the copper oxidises to form Cu^{2+} which is biocidal to most aquatic biota (Yebra et al. 2004). However copper sensitivity varies between organisms and some macro- and micro-algal species are tolerant to copper (Voulvoulis et al. 1999). The low solubility of copper causes rapid precipitation and reduces its toxicity, and it has limited bioaccumulation in the marine environment (Voulvoulis et al. 1999). However, when the concentration of copper exceeds minimum environmental standards it may cause sub-lethal effects to invertebrates and lethal effects to juveniles of marine organisms (Voulvoulis et al. 1999). Various booster biocides are used in antifouling paint systems to control species that are tolerant to copper. The most common are herbicides such as Irgarol 1051, Diuron, Sea-Nine 211, Kathon 5287 and Thiram (reviewed by Yebra et al. 2004). The most common metal-based biocides are zinc and copper pyrithione which are effective against soft fouling though have little effect on hard fouling (Yebra et al. 2004). The major concerns with the use of booster biocides are the lack of toxicity testing and little knowledge of

potential sub-lethal effects and accumulation (Evans et al. 2000, Kobayshi et al. 2002, Yebra et al. 2004).

1.3 *Non-toxic solutions to biofouling*

Given the recurring problems of non-target effects and bioaccumulation of chemically based antifouling technologies a plethora of new research directions have emerged for the non-toxic control of biofouling, in particular the application of fouling-release coatings and a push towards physically based biomimetic technologies. A variety of non-biocidal antifouling methods have been developed including electric currents (Swain, 1998), acoustics vibrations (Branscomb & Rittschof, 1984), piezoelectric coatings (Rahmoune et al. 1995), bubble curtains (Swain, 1998), ultraviolet radiation (Swain, 1998), magnetic fields (Swain, 1998), radioactive coatings (Gitlitz, 1981), heating and cryogenic treatments (Swain, 1998). All of these are either only effective in the short-term, are species specific, suitable only for specialised structures, or are impractical to handle and apply.

Fouling release coatings

An alternative approach to control biofouling is to allow fouling organisms to settle on a surface though ensuring that the adhesion to the surface is weak enough to release the fouling when vessels reach operating speeds. These fouling release coatings (FRCs) have the advantage of being non-biocidal and they reduce hull roughness which can increase speed and save fuel (reviewed by, Clarkson, 1999; Swain, 1999; Brady, 2005). They also have high durability lasting up to 5 years (Anderson, 1998). It is believed that FRCs can be as economically viable as TBC-SPC and significantly reduce the pollution to the world's oceans (Anderson et al. 2003). FRCs are generally composed of either fluoropolymers or silicones (Brady, 2001). The non-stick characteristics of fluoropolymers are counteracted by the high bulk modulus which results in difficulties in removing fouling which does adhere to the surface (Swain, 1998) and as such silicone elastomers are the most widely used. Silicone elastomers are silicone polymers with repeating -Si - O- backbones and saturated organic moieties attached. Polydimethylsiloxane (PDMS) coatings are the most successful of these (Anderson et al. 2003). These coatings will usually have low surface energy to facilitate the removal of marine adhesives as the mechanical locking of glues is reduced by fluid additives which create slippage and fouling-release (Newby et al. 1995). However, FRCs have

drawbacks as they generally only work on vessels operating above 22 knots (Brady, 2001). Furthermore diatom biofilms may not be removed even at maximum operating speeds (Finlay et al. 2002b). Similarly, not all fouling organisms are deterred by low surface free energy materials and for the bryozoans *Bugula neritina* (Mihm et al. 1981), *Bowerbankia* sp. (Eiben, 1976) and *Watersipora* sp. (Loeb, 1977) attachment is stronger on these surfaces whilst for diatoms adhesion strength is increased on silicone elastomers (Finlay, 2002a). FRCs are therefore not suitable for slow moving vessels and other stationary equipment such as nets, rope, pilings, oil pipelines and aquaculture infrastructure.

1.4 *Biomimetic antifouling approaches*

An alternative to foul release coatings is to develop new approaches to the control and prevention of biofouling. Many organisms in the marine environment have evolved their own antifouling defence strategies because of the many negative impacts fouling has on natural hosts (Wahl 1998; de Nys & Steinberg 1999). The study and copying of natural mechanisms is termed 'biomimicry'. Increasingly researchers are investigating and adopting the biomimetic approach for biofouling control largely due to the deficiencies of FRCs and the banning of TBT-SPCs.

Fouling and being fouled

There are many associations, both negative and positive, between epibionts (settler) and basibionts (host) (reviewed in Wahl, 1989; de Nys & Steinberg, 1999). For the epibiont the advantages are more numerous and include, somewhere to live and grow when space can be limiting, hydrodynamic advantages such as nutrient supply and waste removal (Butman, 1987). Furthermore, light and photosynthesis can be increased (Bronus & Heijs, 1986), free transport and larval dispersal can be facilitated (Wahl, 1989) and protection can be provided by associational defence (Hay, 1986). Advantages for the basibiont include improved vitamin and nutrient supply (Lynch et al. 1979), physical and chemical protection from grazers (Bakus et al. 1986; Wahl & Hay, 1995) and camouflage (Witman & Suchanek, 1984). There are however numerous disadvantages to the basibiont as a result of being settled upon. The primary colonisers, bacteria, can cause tissue damage and mortality (Littler & Littler, 1995; Correa & Sanchez, 1996), boring micro-organisms can cause shell damage and brittleness, while boring sponges can result in death to the host (Alagarswarmi & Chellam, 1976;

Thomas, 1981; Che et al. 1996). Other detrimental effects to the host include reduced reproductive output (D'Antonio, 1985), reduced light and changes in pH (Sandjensen, 1977), reduced water flow and increased competition for food (Novak, 1984).

Biomimetic models

The biomimetic approach has gained increasing momentum over the last decade with breakthroughs in materials science which have allowed the copying of intricate surface details found on naturally fouling resistant marine organisms. Several natural models have been studied for biofouling control including gorgonian corals (Vrolijk et al. 1990), porpoise and killer whale skin (Gucinski & Baier, 1983), pilot whale skin (Baum et al. 2001; 2002), shark skin (Ball, 1999), echinoderms (McKenzie & Grigolava, 1996; Bavington et al. 2004), red algae (de Nys et al. 1998; Dworjanyn et al. 1999; Nylund et al. 2005) and crustose coralline algae (Figueiredo et al. 1997), the dogfish eggcase (Thomason et al. 1994; 1996), and the bivalves *Mytilus edulis* (Wahl et al. 1998; Bers & Wahl, 2004), and *Mytilus galloprovincialis* (Scardino et al. 2003; Scardino & de Nys, 2004). Biomimicry of these surfaces involves the microfabrication of surface topographies through casting (Marrs et al. 1995), photolithography (Petronis et al. 2000) and laser ablation of polymers (Scardino et al. 2006).

Gorgonian corals

In response to the need for non-toxic antifouling surfaces several studies have examined the physical surface properties of fouling free marine organisms with a view to mimicking these surface structures for biofouling control. One of the earliest reports of the physical properties of a fouling resistant marine organism was for the gorgonian corals (sea fans) *Pseudopterogorgia americana* (Gmelin) and *Pseudopterogorgia acerose* (Pallas) (Vrolijk et al. 1990). The surface of the gorgonians had a surface free energy in the range for minimal bioadhesiveness (20-30 dynes/cm; Baier et al. 1968). This optimal surface free energy could be combined with mechanical sloughing, the production of secondary metabolites and sulphated polysaccharide mucus, similar to that documented for echinoderms (Bavington et al. 2004), to produce a surface free of fouling. The two gorgonian species had surfaces with an arithmetic average roughness (vertical distance between peaks and troughs) values of between 2-4 µm as measured by profilometry (Vrolijk et al. 1990), which is of a similar scale to the microroughness found on fouling resistant marine bivalves (Scardino et al. 2003; Scardino & de Nys,

2004). When visualised by Scanning Electron Microscopy the surface of *P. americana* was smooth though potential surface microtopographical features may have been masked by a mucus layer covering the entire surface. In contrast *P. acerose* has spicules (Vrolijk et al. 1990) which may provide reduced numbers of attachment points to potential settling larvae/propagules (Scardino et al. 2006). Whilst marine bacteria were present on both gorgonian surfaces there was no occurrence of microalgae or diatoms on the surface (Vrolijk et al. 1990). Interestingly dead gorgonians foul rapidly (Vrolijk et al. 1990) indicating that surface mechanisms alone are not enough to maintain fouling resistance.

Marine mammal skin

Other early reports of biomimicry include the skin of porpoises and killer whales (Gucinski & Baier, 1983) which have critical surface tensions in the range for minimal bioadhesiveness (20-30 dynes/cm; Baier et al. 1968). These surfaces provide low drag and have microtopographical features that may contribute to a fouling free surface (Gucinski & Baier, 1983; Anon, 2002). Surface texture replicas were made, and attempts to mimic the superficial layer of porpoise skin using tethered polymer chains were undertaken, but the antifouling potential of these replicas has not been documented (Gucinski & Baier, 1983). Another study (not yet peer reviewed) of the surface of a fouling resistant marine mammal is on dolphin skin which has a rippled topography in the nanometer range (Anon, 2002) which is also similar to the micro-rippled surface of the mussel *Mytilus galloprovincialis*. The surface topography of the dolphin skin was mimicked using polymer crosslinking to produce nano-sized ‘treacherous terrain’ which can be varied in scale of texture and degree of hydrophobicity (not yet peer reviewed: Anon, 2002; Wooley et al. 2003; Brown et al. 2004). The nano-scale roughness is thought to interfere with protein binding of marine adhesives (Anon, 202) and combined with the high speed of dolphin movement may produce fouling-release performance. The antifouling performance of the biomimicked dolphin skin has yet to be documented. While highlighting the potential importance of biomimetic approaches confirmation of the effects of dolphin skin and treacherous terrain on biofouling are not yet described in the peer reviewed literature.

It seems many species of cetaceans have a remarkably clean surface free of all epibionts (Baum et al. 2001; 2002; 2003) and in the case of the pilot whale,

Globicephala melas, this is attributed to the nano-ridge pores on the surface of the skin (Baum et al. 2002). The nano-ridge pores (0.1-1.2 μm^2) are smaller than most fouling organisms and provide few microniches or contact points to adhere to. The skin surface properties combined with the speed of movement, surfacing and jumping may contribute to removing weakly adhered epibionts. The skin of the pilot whale also contains a zymogel which hydrolyses the adhesives of settling organisms (Baum et al. 2001), whilst attachment into the nano-ridged pores is prevented by heavy enzymatic digestion (Baum et al. 2002). The surface of the pilot whale skin and intercellular gel contain both polar and non-polar groups and this chemical heterogeneity is thought to produce opposite wettability on the same surface which could contribute to short and long-term fouling reduction (Baum et al. 2003). Biomimetic antifouling technologies based on the multiple defence principles of the pilot whale skin were reported as under investigation (Baum et al. 2003) however there are no reports of any potential technologies developed directly from this work.

Shark skin

Shark skin has also been studied for biomimetic technologies, initially due to their drag reduction properties for aircraft (Ball, 1999; Bechert et al. 2000) and more recently due to their antifouling properties (Carman et al. 2006). A variety of shark skins have been analysed and have microtopographical ridges with the number of ribs per scale and the length and spacing of the microtexture varying slightly between species (Bechert et al. 2000). However, the patterns are essentially the same across species (Berchert et al. 2000 and references therein). The surface micropatterns on shark skin have inspired the design of several antifouling films where surface patterns are etched into silicone wafers using photolithography (Hoipkemeier-Wilson et al. 2005; Carman et al. 2006). The design is inspired from the shark skin, which has the same placoid pattern though with different dimensions and the tips of the ribs are flattened. Hoipkemeier-Wilson et al. (2005) used a design termed ‘sharklet’ which is inspired from the placoids of fast moving sharks and has microtextured ribs 4 µm high and 2 µm wide, and are spaced 2 µm apart. The rib lengths vary with the middle of seven ribs being the longest at 16 µm and the first and seventh ribs the shortest (4 µm). The sharklet pattern is scaled down from the real shark skin topography size of between 100-200 µm (Berchert et al. 2000) to be less than the spore size of the ubiquitous fouling alga *Ulva*. The sharklet pattern reduced *Ulva* spore settlement compared to smooth films regardless of the surface

chemistry, however spores that did adhere to the sharklet surface were less easily removed by flow than smooth surfaces (Hoipkemeier-Wilson et al. 2005). The sharklet design has also been produced onto polydimethylsiloxane elastomers (PDMSe) and tested against *Ulva* zoospores (Carman et al. 2006). The sharklet pattern was also compared against a range of microtopographical patterns including pillars, pits, channels and ridges which were 5 µm wide and spaced by intervals of 5, 10 and 20 µm with feature heights of 1.5 and 5 µm (Carman et al. 2006). The sharklet design increased the wettability of PDMSe by 20% (108º) and had the highest water contact angle (135º) of all the microtopographical patterns. The sharklet topography reduced *Ulva* spore settlement by 86% compared to smooth PDMSe. In contrast ridges spaced 5 µm apart and 5 µm high increased *Ulva* settlement by 150% compared to the smooth surface. Spores which did settle on the sharklet design were mostly confined to 'defects' in the pattern which create wider spaces for the spores to settle (Carman et al. 2006).

Bioinspired shark patterns are also successful in reducing barnacle settlement. Liedert & Kesel (2005) examined a range of microtextures etched onto silicone of differing complexions in the field over 3 months. The most successful surface, which had texture spacing of 76 µm and was composed of soft silicone material with a low surface energy, reduced barnacle settlement by 95% compared to smooth surfaces made of hard silicones (Liedert & Kesel, 2005). This study has not yet appeared in the peer-reviewed literature.

The studies on bioinspired shark skin microtopographies demonstrate that fouling rates can be controlled to either promote or reduce settlement based on texture spacing for *Ulva* zoospores. The antifouling performance of the sharklet design against a broader suite of fouling organisms and its longevity in field exposures remains to be determined. Several other studies have examined microtopographies which although not bioinspired have similar patterns to shark skin. Microriblets and pyramids reduced barnacle cyprid settlement by up to 92% compared to smooth surfaces (Berntsson et al. 2000a; Petronis et al. 2000; Berntsson et al 2004). The most successful surfaces are smaller than the cyprid body size and therefore reduce the number of attachment points which may be a potential mechanism of action although as yet is unproven. Barnacle

cyprids demonstrated a behavioural aversion to microtextures spending less time exploring the surface than on smooth surfaces (Berntsson et al. 2000).

Echinoderms

Most marine echinoderms appear to be remarkably free of fouling on their surface, even at the bacterial level (McKenzie & Kelly, 1994; Kelly & McKenzie, 1995). However, this has in most cases not been quantified, and there remains limited data on the presence and composition of fouling community on most marine organisms. Echinoderms such as sea urchins, star fish and brittle stars are believed to use a combination of defence strategies to combat fouling (McKenzie & Grigolava, 1996). The pedicellariae of echinoids and asteroids are thought to contribute to cleaning and possibly removal of macrofouling organisms but is unlikely to be effective against settling larvae or microfouling (McKenzie & Grigolava, 1996). Echinoderms also slough cuticle which removes fouling along with the old cuticle, however this is a slow process (>25 days) and cannot explain the lack of bacterial and diatom fouling which only requires hours to days to settle (Grigolava & McKenzie, 1995). The cuticle of echinoderms also contains proteolytic enzymes and chondroitin sulphate which are thought to alter the adhesion of bacteria by preventing the formation of hydrophobic bonds between the bacteria and the surface (McKenzie & Grigolava, 1996). Mucus secretions are also believed to remove adhered bacteria however shear forces of mucus on bacteria have not been quantified (McKenzie & Grigolava, 1996). Bavington et al. (2004) examined glycoproteins from mucus secretions of the starfish *Marthasterias glacialis* and *Porania pulvillus* and the brittle star *Ophiocomina nigra* on bacterial adhesion. Glycoproteins from *M. glacialis* and *O. nigra* blocked bacterial adhesion whilst adhesion was promoted for *P. pulvillus* (Bavington et al. 2004). Under flow mucus glycoproteins from *M. glacialis* caused bacterial clumpings which were subsequently washed away. It is proposed that the non-stick properties of the echinoderm cuticle coupled with a mucus film is able to keep the surface completely free of fouling (Bavington et al. 2004). More broadly, a range of chemical extracts have been extracted from the body wall of echinoderms with demonstrated effects on settling organisms in laboratory bioassays (Greer et al. 2003; Iken et al. 2003). However, the ecological significance of these extracts is often not understood or the natural surface concentrations only estimated. Therefore while supporting a potential chemical defence for echinoderms the role of natural products as a defence mechanism is unproven.

Algal defences

In contrast chemical defences against fouling are deployed by algae. The most widely studied are surface bound secondary metabolites (reviews Steinberg et al. 2001; Steinberg & de Nys, 2002). A host of naturally produced chemicals have been extracted and have antifouling effects in bioassays. However, to be relevant as a natural defence they need to be produced in ecologically relevant concentrations at a relevant site to interact with fouling organisms. The best example of this defensive strategy is the red alga *Delisea pulchra* which has halogenated furanones produced at the surface of the thallus (de Nys et al. 1998; Dworjanyn et al. 1999; reviewed by de Nys et al. 2006) and concentrations of individual compounds strongly inhibit settlement of various fouling propagules in the field and laboratory (de Nys et al. 1995; Maximilien et al. 1998; Dworjanyn, 2002; Dworjanyn et al. 2006). For the brown alga *Dictyota menstralis* surface extracts deterred settlement by the cosmopolitan bryozoan *Bugula neritina* (Schmitt et al. 1995).

In more recent studies crude extracts for various red algae have been incorporated onto stable gels and have inhibiting effects on several strains of bacteria at ecologically relevant concentrations (Nylund et al. 2005). The algal extracts did not have broad-spectrum antibacterial effects against attachment but rather strain-specific effects (Nylund et al. 2005). However, *Bonnemaisonia hamifera* did have broad-spectrum growth-inhibiting effects. Crude extracts from red algae also have antisettlement effects on the barnacle cyprids *Balanus improvisus* (Nylund & Pavia, 2003). *B. improvisus* cyprids are also inhibited by brown algal phlorotannins (Wikstrom & Pavia, 2004).

For the red alga *Dilsea carnosa* antisettlement properties are not attributed to chemical defences such as the production of metabolites, but rather a mechanical defence through surface renewal. *D. carnosa* is able to shed the outermost cell layers and along with it the associated epibiota (Nylund & Pavia, 2005). Crustose coralline algae have multiple defences against fouling including mechanical and chemical defences. Two species, *Phymatolithon lenormandii* (Aresch) Adey and *P. purpureum* (P. & H. Crouan) Woelkerling and Irvine, were tested for algal settlement in the field and laboratory. Replicate and dead crusts were used for comparison (Figueiredo et al. 1997). *P. lenormandii* has a rough surface with 100 µm protuberances whilst *P.*

purpureum has a smooth surface (Figueiredo et al. 1997). In the field fouling by *Ulva* spp. was higher on the rough *P. lenormandii* replicates than the smooth *P. purpureum* replicates whilst in laboratory experiments the same trend was apparent for settlement by *Fucus* zygotes (Figueiredo et al. 1997). The surface roughness of *P. lenormandii* (100 µm) is larger than both *Ulva* (8-15 µm) zoospores and *Fucus* zygotes (35-50 µm) thereby providing microrefuges (Figueiredo et al. 1997). Overall dead crusts and replica crusts were more heavily fouled than live crusts indicating other factors contribute to antifouling defence on live crusts (Figueiredo et al. 1997). Other potential antifouling mechanisms include thallus shedding and thallus sloughing as well as chemical substances released by the crusts such as bromophenols (Figueiredo et al. 1997). Shading also plays a significant role in antifouling defences of coralline crusts as *Fucus* settlement was greatly increased on live crusts under high light regimes (Figueiredo et al. 1997). Biomimetic studies on algae demonstrate that there are a variety of chemical, physical and mechanical defences to combat fouling. Biomimetic technologies will need to embrace all three strategies to successfully deter a broad range of fouling organisms. Biomimicry based solely on chemical defences will always suffer the criticism of release into the environment and effects on non-target species, unless bound to the surface to prevent release.

The dogfish eggcase

The eggcase of the dogfish *Scyliorhinus canicula* (L.) has been studied due to its fouling free surface despite strong fouling pressure. The eggcases, which are nonliving, are able to resist macrofouling for up to 6 months (42% fouling cover after 300 days in the field and < 15% cover after 200 days under controlled conditions) however microfouling is not prevented as there is a heterogeneous bacterial population present on the surface of the cases from an early stage (Thomason et al. 1994). There is a lack of EPS-producing bacteria which may slow the colonisation of macrofoulers (Thomason et al. 1994). The eggcases were fouled rapidly by macroalgae (*Enteromorpha prolifera* and *Ectocarpus* sp.) under high light conditions and this is avoided in nature by female dogfish laying eggs in dim lit environments (Davenport et al. 1999). Unlike other fouling free natural surfaces the surface free energy is not in the optimal range for minimal bioadhesiveness and is similar to glass and slate which are readily fouled. The metal properties of the surface, such as iron and manganese, form free radicals through the Fenton reaction and are attributed to reduce fouling

(Thomason et al. 1996; Davenport, 1999). Extracted eggcase material produced several 'miscellaneous compounds' which have deterrent effects against micro and macro-foulers though toxicity and the structure of the compounds is unknown (Davenport, 1999). The arithmetic mean roughness of the eggcases was 3.7 µm (Davenport, 1999) which is similar to the scale of roughness found on other fouling resistant marine surfaces (Scardino et al. 2003; Scardino & de Nys, 2004). When the eggcases were roughened they became more attractive to the barnacle *Semibalanus balanoides* cyprids (Thomason et al. 1996; Davenport, 1999). Both abraded and natural eggcases were unattractive to *Enteromorpha intestinalis* zoospores (Thomason et al. 1996; Davenport, 1999), the zoospores (6-10 µm) are far smaller than barnacle cyprids (~ 300 µm) and while the roughened surfaces were not quantified for surface roughness they may have provided differing numbers of attachment points or potential settling sites for the zoospores.

The dogfish eggcase was replicated to assess marine biofilms non-destructively (Marrs et al. 1995). The replication process involves using a dental impression material (polyvinylsiloxane; Kerr's extrude wash type 3 – Kerr UK Ltd) which is extruded onto the surface and peels off forming a negative impression, the negative is filled with epoxy resin (Devcon 2-ton – Devcon, UK) which after curing creates a positive mimic of the surface features at the sub-micron level (Marrs et al. 1995). Diatoms and cocci-type bacteria were successfully copied from the surface of the dogfish eggcase without damage to the original surface. The replication of the eggcase is one of the first reports at biomimicking a natural antifouling surface and led to the production of future biomimics on fouling resistant bivalves (Bers & Wahl, 2004; Scardino & de Nys, 2004) which used the same production methodologies.

Molluscs, crustaceans and multiple defensive strategies

A consistent theme occurs for organisms to have multiple defensive strategies and this approach of multiple non-toxic antifouling defences was examined by Wahl et al. (1998) on the blue mussel *Mytilus edulis*, the gastropod *Littorina littorea*, the colonial ascidian *Cystodytes lobatus* and the crustacean *Carcinus maenas*. A variety of defence strategies were observed including grazing, burrowing, moulting, mucus secretion, cumulative filtration and unidentified surface properties (Wahl et al. 1998). Potential physical defences including surface microtopography were examined by Bers and Wahl

(2004) for *M. edulis*, the crab *Cancer pagurus*, the brittle star *Ophiura texturata* and the dogfish eggcase of *S. canicula*. These natural surfaces were mimicked using resin casts and compared against smooth casts without microtopography. The surface features ranged from 1-1.5 µm ripples on *M. edulis* to 200 µm circular elevations on *C. pagurus* which are interspersed by 2-2.5 µm spicules. The dogfish eggcase has longitudinal and lateral ridges spaced between 30-50 µm whilst the brittle star has 10 µm knobs on its surface (Bers & Wahl, 2004). All four mimicked surface microtopographies had some antifouling effects compared to the smooth control replicas; barnacle cyprids were repelled by *C. paguras* mimics and were temporarily reduced by *M. edulis* and *S. canicula* replicas whilst *O. texturata* deterred the microfoulers *Zoothamnium commune* and *Vorticella* sp. (Bers & Wahl, 2004). The antifouling properties of the mimicked microtopographies were species specific and diminish with time (< 4 weeks) which suggest other defences act in concert with topography on natural surfaces to provide long-term protection from fouling (see Wahl et al. 1998).

For bivalves and gastropods the natural microtexture of their shells is related to the outermost proteinaceous layer on the shell surface, the periostracum. Several studies have reported the significance of this layer in fouling deterrence (Wahl et al. 1998; Scardino et al. 2003) and the prevention of boring initiation (Harper & Skelton, 1993; Che et al. 1996). For the pearl oyster *Pinctada margaritifera* the presence of an intact periostracum in juvenile oysters correlated with no borings of the shell, however 1 year old oysters with reduced periostracum cover have a significant increase in borings, particularly at the apex which is the oldest portion of the shell (Che et al. 1996). The periostracum of the blue mussel *Mytilus edulis* also has antifouling properties. When the periostracum was physically removed from one valve of juvenile *M. edulis* shells borings increased on the abraded valves (Harper & Skelton, 1993) as did algae and barnacle settlement (Wahl et al. 1998). The thick and hairy periostracum of the gastropod *Fusitriton oregonensis* has also been reported to reduce fouling by borers and epizoans (Bottjer, 1981). Scardino et al. (2003) demonstrated that *Mytilus galloprovincialis* shells which had an intact periostracum were significantly less fouled in the field than the oyster *Pinctada imbricata* which had little periostracum cover. When the periostracum was removed from *M. galloprovincialis* there was a strong preference by *Balanus amphitrite* cyprids to settle in naturally abraded portions of the shell (Scardino et al. 2003). Intact portions of the shell had a homogeneous

microtextured ripple of 1-2 µm which was associated with periostracum presence (Scardino et al. 2003). However, other unidentified properties of the periostracum may contribute to fouling deterrence in molluscs as resin replicates of *M. galloprovincialis* did not resist fouling to the same degree as the intact Mytilid shell (Scardino & de Nys, 2004).

In a recent study examining the microtextures of two Mytilid bivalve species, *M. edulis* and *Perna perna*, resin replicas were less fouled by the barnacle *Semibalanus balanoides* than roughened mimics (Bers et al. 2006). *M. edulis* species from varying geographical localities had similar settlement deterrent effects. Interestingly, the arithmetic mean roughness of both the mimicked shells and the roughened mimics were similar, indicating the isotropy of the texture is important to *S. balanoides* settlement (Bers et al. 2006). Smooth control mimics were less fouled than roughened mimics, though not significantly different to natural mimics (Bers et al. 2006). The antifouling performance of the Mytilid mimics were assessed over 2 weeks only, to coincide with peak cyprid settlement, hence the long-term potential of the mimics or broad spectrum antifouling effects are unknown.

Biomimetic antifouling surfaces have produced promising results and researchers have only scratched the surface of the suite of potential surfaces to be mimicked. Microtopography is just one defensive mechanism and future research will incorporate multiple biomimicked/bioinspired antifouling strategies to lay the platform for the development of non-toxic commercial antifouling technologies.

1.5 *Chapter summaries*

The overall goal of this thesis is to investigate marine molluscs as a model for the development of new antifouling technologies. Marine molluscs provide an excellent model to study non-toxic antifouling mechanisms. They have hard surfaces without any apparent chemical defences and some species remain relatively free of fouling in contrast to other heavily fouled species. Bivalves and gastropods will be used as model templates in this thesis to study biomimetic approaches to fouling control.

Chapter Two identifies and characterises the surface of 111 species of molluscs from the Great Barrier Reef. In this chapter a range of microtopographies were identified

from bivalves and gastropods that were free of fouling *in situ*. A subset of 36 species were quantified for surface roughness parameters using confocal laser scanning microscopy. The roughness parameters generated were mean roughness and waviness, Rsk roughness and waviness, anisotropy and fractal dimension, and the wettability of the shells were also recorded. Several roughness parameters differed significantly at the class, family and species taxonomic levels. This study is the first to quantify a range of surface characteristics for a broad range of natural surfaces.

Chapter Three examines the fouling resistance of the 36 species characterised from chapter 2. The total fouling cover, species specific fouling cover and fouling removal rates were assessed over 3 months in the field. Fouling resistances and removal were correlated to surface roughness parameters generated in chapter 2. Key roughness parameters were identified to minimise fouling and will be used for future recommendations in novel surface biomimics. For the first time roughness parameters from natural surfaces were correlated to fouling resistance and removal.

Chapter Four assesses the fouling resistance of shell surfaces and their biomimics to establish the role of surface microtexture in fouling deterrence. Biomimics were created for three bivalves, *Mytilus galloprovincialis* and *Tellina plicata* having differing microtopographical patterns, and *Amusium balotti* which has a smooth surface. Smooth biomimics were significantly more fouled than microtextured biomimics. The fouling resistance of microtextured biomimics diminishes after 6-8 weeks in contrast to natural shells which maintained fouling resistance for 3 months. The loss of resistance over time and multiple defence mechanisms of natural shells are discussed.

Chapter Five moves to a mechanistic understanding of fouling resistance. This chapter assesses diatom attachment to biomimicked microtexture. The surface microtextures characterised on *M. galloprovincialis* and *T. plicata* were microfabricated onto polyimide films and tested against four fouling diatoms of differing cell sizes. The attachment of diatom cells to microtexture was dependent on the number of available attachment points to the surface. Diatoms smaller than the width of microtexture attach in higher numbers than cells which are larger than the width of microtexture. The implications of attachments points for future biomimetic surfaces are discussed.

Chapter Six broadens the findings from chapter 5 to incorporate macrofouling larvae. Microtexture matrices were produced with nine texture widths ranging from 4-512 µm. Attachment rates to the microtextured matrices were examined for a range of common fouling organisms and other larvae which vary in size. They are *Ulva rigida* gametes, *Amphora* sp. cells, *Polysiphonia sphaerocarpa* and *Centroceras clavulatum* cystocarps and *Bugula neritina* larvae. The results provide further support to attachment point theory which was tested in chapter 5. The potential importance of attachments points to novel foul release surfaces is discussed.

Chapter Seven extends the findings of the previous chapters on fouling resistance of microroughness to incorporate surface nanoroughness. For the first time nano-rough surfaces with superhydrophobicity (water contact angles > 150º) were tested for fouling resistance. The four coatings tested had similar superhydrophobicities however differed in the scale and architecture of surface roughness. Three coatings had nano-roughness overlain on microroughness whilst the fourth coating had nano-scale roughness only. The coating containing nanoscale roughness deterred all five tested fouling organisms in static bioassays. Possible mechanisms for the fouling resistance of nanorough surfaces, including the formation of nano-bubbles, are discussed.

Chapter Eight provides a summary and discussion of the results and examines future research directions for biomimetic antifouling surfaces.

CHAPTER TWO

Surface characterisation of bivalves and gastropods from the Great Barrier Reef

2.1 Introduction

Biofouling is a significant issue for marine transport which causes increases in fuel consumption (up to 44%) and increases in overall voyage costs (up to 77%)(reviewed by Yebra et al. 2004). Increasingly non-toxic solutions to biofouling are being sought and in many cases nature can provide models for new antifouling technologies (de Nys & Steinberg, 2002). New surface based technologies in particular are being inspired from natural models as physical surface effects or surface bound chemical signals have the advantage of preventing any non-target environmental effects. Novel antifouling surfaces from natural models not only offer new approaches, but by understanding their mechanisms of action allow the development of new surface based approaches to controlling biofouling. Natural surfaces that have been investigated for their antifouling properties include the skin of sharks (Ball, 1999) and whales (Baum et al. 2002; 2003), Lotus leaves (Barthlott & Neinhuis, 1997), mussel shells (Scardino et al. 2003; Scardino and de Nys, 2004; Bers and Wahl, 2004), the dogfish eggcase (Thomason et al. 1994; Thomason et al. 1996; Davenport, 1999) and other marine invertebrates such as crab carapaces and brittle stars (Wahl et al. 1998; Bers & Wahl, 2004). These natural surfaces exhibit little or no fouling and have no apparent chemical defences, highlighting potential physical surface characteristics, which resist fouling. Physical properties that affect fouling include surface roughness, wettability and microtexture, or any of these properties in combination.

In nature, smaller scale surface microtexture associated with a defence against fouling has been found on the blue mussel *Mytilus galloprovincialis* (Scardino et al. 2003; Scardino & de Nys, 2004) and *Mytilus edulis* (Wahl et al. 1998; Bers & Wahl, 2004). These mussel shells have homogeneous micro-ripples 1-2 µm wide and are rarely fouled. Furthermore they resist fouling compared to non-textured surfaces for up to 12 weeks in the field (Scardino et al. 2003; Bers & Wahl, 2004; Scardino & de Nys, 2004). Similarly, types of shark skin display microtextured diamond patterns which are also thought to help resist fouling (Ball, 1999). Biomimics inspired from the placoid

scales on shark skin are of a similar scale to mussel microtexture and have been reported to reduce *Ulva linza* zoospore settlement by 85% (Carman et al. 2006). In contrast the pilot whale, *Globicephala melas*, has nano-sized pores (Baum et al. 2002) which combined with the production of a zymogel (Baum et al. 2001) that produces chemically heterogeneous patches on the `skin (Baum et al. 2003) are believed to contribute to fouling resistance.

In addition several artificial surfaces with varying degrees and shapes of microtexture without a relation to natural models have been studied and reduce fouling by barnacle cyprids (Berntsson et al. 2000a; b; Petronis et al. 2000) and zoospores of *Ulva linza* (Callow et al. 2002; Hoipkemeier-Wilson et al. 2004).

For shellfish that are naturally free of fouling in the marine environment, resistance is correlated to the presence of an intact periostracum (Che et al. 1996; Harper, 1997; Scardino et al. 2003). The periostracum is a thin proteinaceous uppermost layer of the shell surface. On the mussel shell, *Mytilus galloprovincialis*, areas of the shell devoid of periostracum are preferred by *Balanus amphitrite* cyprids, while the oldest areas of the shell surface which have the least cover of periostracum are most heavily fouled (Scardino et al. 2003). The presence and nature of the periostracum on all shellfish and the development of *Mytilus galloprovincialis* as a model for antifouling surfaces makes shellfish excellent natural models to assess potential fouling resistant surfaces.

The aim of this chapter is to identify natural surface microtextures from marine molluscs that generally had low levels of fouling *in-situ*, and to characterise these surfaces by generating surface roughness parameters. The second aim is to determine relationships between the generated surface roughness parameters and between classes, families and species of molluscs. 111 bivalves and gastropods which were collected and analysed for surface microtexture, a subset (36 of 111 species) was then analysed for six selected roughness parameters using Laser Scanning Confocal Microscopy (LSCM) 1. average roughness (Ra), 2. average waviness (Wa), 3. skewness of the surface roughness profile (Rsk), 4. skewness of the surface waviness profile (Wsk), 5. texture aspect ratio (Str), and 6. fractal dimension (Fd) and surface hydrophobicity. These surfaces are correlated with their resistance to fouling in Chapter 3 to elucidate potential key physical parameters associated with fouling resistance in molluscs, and to

develop model artificial surfaces and hypotheses to directly test the efficacy of natural models and their mechanisms of action in Chapters 4-7.

2.2 Methods

2.2.1 Study sites

Field surveys were conducted on the fringing reefs of Lizard (14º.40'S, 145º.27'E), Orpheus (18º.37'S, 146º.30'E), Magnetic (19º.10'S, 146º.50'E) and Palm Islands (146º.35'S, 18º.44'E) as well as the intertidal mud flats off Townsville (19º.16'S, 146º.49'E). Bivalves and gastropods were collected and brought back to the laboratory for identification and surface characterisation. The majority of shells were dead and the few molluscs which were alive were shucked prior to surface characterisation.

2.2.2 Collections of bivalves and gastropods

In total 111 species of molluscs from the Great Barrier Reef (GBR) were identified using keys and reference texts (Abbott & Dance, 1986; Lamprell & Whitehead, 1992; 1998; Wilson, 1993; 2002; Gosling, 2003). The collected species came from two classes, Bivalvia and Gastropoda. Sixty one species were bivalves from 18 families, while 48 species were gastropods from 20 families. In addition, two echinoderm species, both from different families, were included due to their clean surfaces observed during collection. All species with taxonomical detail are listed in Table 2.1 along with the collection site. All specimens were collected under Permit # G03/8695.1 with the exception of Lizard island specimens which were collected under the Marine Parks permit issued to the Australian museum (G02/044).

Figure 2.1 Map of North Queensland collection sites. Molluscs were collected at various intertidal shores, fringing and mid-reef locations between Cooktown and Townsville

2.2.3 Surface characterisation

The surfaces of all collected species were examined at 10x, 100x, 1,000x and 10,000x magnification for microtextures. Light microscopy (Leica Microsystems, camera DC300) and the IM50 measurement software (Leica Microsystems) were used for image analysis at 10x and 100x. Higher resolution examination used a JEOL JSM-5410LV scanning electron microscope (SEM). Surfaces were prepared for SEM by cutting into approximately 1 cm^2 pieces, mounting on stubs using carbon paint and sputter coated with gold. The range of discovered microtextures is displayed in Table 2.1. Two number ranges indicate macro (> 500 µm) and micro-texture (< 100 µm) scales present.

Table 2.1 Molluscs and echinoderms collected from the Great Barrier Reef. Species in bold were used for further surface analysis. Two number ranges indicate multiple scales of texture were present. # Echinoderm, ~Gastropod, ^ Temperate species.

Species	**Family**	**Location**	**Surface Texture (µm)**
Architectonica perspectiva	Architectonicidae~	Hinchinbrook Island	150-200
Anadara crebriotata	Arcidae	Orpheus Island	700
Atlanta peroni	Atlantidae	Pelorus Is./ Mission beach	70
Monia deliciosa	Bimyidae~	Hinchinbrook Island	Smooth, fouled
Nassarius albescens	Buccinidae~	Cockle Bay	150-300, 50-90
Nassarius coronatus	Buccinidae~	White Lady Bay	50
Nassarius luridus	Buccinidae~	White Lady Bay	25-30
Acrosterigma reeveanum	Cardiidae	Cockle Bay	300
Fragum retusum	Cardiidae	Cockle Bay	200, 1mm
Fragum scrposium	Cardiidae	Cockle Bay	200-250, 10
Fragum unedo	Cardiidae	Lizard Island	200
Fragum sp.	Cardiidae	Orpheus Island	300
Semicassis bisculata	Cassidae~	Hinchinbrook Island	400-500
Cerithium zonatum	Cerithiidae~	Cockle Bay	1mm, 60
Rhinoclavis articulata	Cerithiidae~	Lizard Island	smooth

Species	Family	Location	Surface Texture (µm)
Conus textile	Conidae~	Orpheus Island	200-300
Cyprae annulus	Cypraceae~	Orpheus Island	300
Cyprae erosa	Cypraceae~	Orpheus Island	smooth
Cyprae walkeri	Cypraceae~	Orpheus Island	smooth
Cyprae sp.	Cypraceae~	Orpheus Island	smooth
Diadema savignyi#	Diadematidae	Pelorus Island	100, 5-10
Donax cuneatus	Donacidae	Hinchinbrook Island	smooth
Donax faba	Donacidae	Hinchinbrook Island	80, 150
Haliotes asinine	Haliotidae~	Outer reef Mission beach	70
Haliotes ovina	Haliotidae~	Lizard Island	smooth
Haliotes varia	Haliotidae~	Lizard Island	smooth
Hemidonax sp.	Hemidonacidae	White Lady Bay	350, 60
Laganum laganum#	Laganidae	Cockle Bay	80
Limaria fragilis	Limidae	Orpheus Island	500, 10-20
Littoraria philippiana	Littorinidae~	White Lady Bay	smooth
Anodontia bullula	Lucinidae	White Lady Bay	400, 5-20
Codakia interrupta	Lucinidae	Lizard Island	smooth
Divaricella ornata	Lucinidae	White Lady Bay	200, 5
Mactra antiquata	Mactridae	White Lady Bay	100
Mactra mera	Mactridae	Kissing Point	450
Mactra olorina	Mactridae	Orpheus Island	150
Mactra dissimilis	Mactridae	Orpheus Island	250
Meropesta nicobarica	Mactridae	Kissing Point	200, 25
Mactridae sp	Mactridae	Lizard Island	smooth
Davila plana	Mesodesmatidae	Lizard Island	1-2
Paphies elongata	Mesodesmatidae	Hinchinbrook Island	10
Paphies striata	Mesodesmatidae	Hinchinbrook Island	10-20
Costellaridae sp.	Mitridae~	Lizard Island	smooth
Morula marginalba	Muricidae~	Cockle Bay	800(pr), 160, 60
Mucuridae sp.	Mucuridae~	Lizard Island	smooth
Amygdalum glaberrima	Mytilidae	Cardwell	1mm
Modiolus micropterus	Mytilidae	Lizard Island	150, 40
Modiolus trailii	Mytilidae	Cockle Bay	20-100
*Mytilus galloprovincialis^*	Mytilidae	Eden, NSW	1-2
Septifer bilocularis	Mytilidae	Cockle Bay	280, 40
Septifer sp.	Mytilidae	Orpheus Island	130
Naticarius oncus	Naticidae~	White Lady Bay	60
Natica robillardi	Naticidae~	Cockle Bay	50
Natica zonalis	Naticidae~	Cockle Bay	smooth
Polinices conicus	Naticidae~	White Lady Bay	50
Polinices didyma	Naticidae~	Cockle Bay	150, 20
Polinices sordidus	Naticidae~	Pelorus Island	20-30
Polinices tumidus	Naticidae~	Cockle Bay	2-5
Polinices mammilia	Naticidae~	Pelorus Island	30
Nerita albicillia	Neritidae~	Lizard Island	500, 5
Nerita chamaeleon	Neritidae~	Lizard Island	100
Nerita planosipira	Neritidae~	Lizard Island	400, 50
Nerita plicata	Neritidae~	Lizard Island	200, 30
Nerita polita	Neritidae~	White Lady Bay	20-30
Nerita undata	Neritidae~	Pelorus Island	10
Ovidae sp.	Ovulidae~	Lizard Island	smooth
Cellana radiata	Patellidae~	Lizard Island	200, 10
Phenacolepas crenulata	Phenacolepadidae~	Lizard Island	smooth
Pinna bicolor	Pinnidae	Orpheus Island	1000
Telescopium telescopium	Potamididae~	Cockle Bay	650, 80
Amusium balloti	Propeamussiidae	Trawler	smooth
Asaphis violascens	Psammobiidae	Lizard Island	3-4
Psammobiidae sp.	Psammobiidae	Cockle Bay	280, 80
Soletellina atrata	Psammobiidae	Cockle Bay	150
Pteria peasei	Pteridae	Orpheus Island	400, 1
Pteria chinensis	Pteridae	Orpheus Island	100, 1
Pteria sp.	Pteridae	Cardwell	50
Semele crenulata	Semelidae	Orpheus Island	150-250
Strombus campbelli	Strombidae~	Cockle Bay	140/780, 20-50
Exotica clathrata	Tellinidae	Lizard Island	20-30
Exotica virgulata	Tellinidae	Orpheus Island	70-80

Species	Family	Location	Surface Texture (µm)
Tellina capsoides	Tellinidae	Orpheus Island	100
Tellina inflata	Tellinidae	Orpheus Island	50, 30, 5
Tellina linguafelis	Tellinidae	White Lady Bay	1-10
Tellina piratica	Tellinidae	Kissing Point	1-10
Tellina plicata	Tellinidae	Orpheus Island	500, 2
Tellina serricostata	Tellinidae	Kissing Point	150, 30
Tellina virgata	Tellinidae	White Lady Bay	250, 40
Tellinidae sp	Tellinidae	Lizard Island	smooth
Neotrigonia sp.	Trigoniidae	Orpheus Island	450
Neotrigonia lamarckii	Trigoniidae	Cockle Bay	220-350, 50
Chrysostoma paradoxum	Trochidae~	Lizard Island	smooth
Clanculus clanguloides	Trochidae~	White Lady Bay	70
Monilea belcheri	Trochidae~	Hinchinbrook Island	200-300
Monodenta labio	Trochidae~	Lizard Island	smooth
Pseudostomatella deolorata	Trochidae~	White Lady Bay	70-200, 20-30
Trochus sp.	Trochidae~	Lizard Island	smooth
Turbo petholatus	Turbinidae~	Lizard Island	smooth
Haustator cingulifera	Turritellidae~	Hinchinbrook Island	100, 30
Circe scripta	Veneridae	White Lady Bay	30
Dosinia juvenilis	Veneridae	White Lady Bay	500
Gafrarium equivocum	Veneridae	White Lady Bay	40
Gafrarium tumidum	Veneridae	White Lady Bay	300, 100, 1
Globivenus toreuma	Veneridae	Lizard Island	300, 100
Lioconcha fastigiata	Veneridae	Orpheus Island	250, 1
Lioconcha annettae	Veneridae	Orpheus Island	250
Pitar affinis	Veneridae	Lizard Island	smooth
Tapes sericeus	Veneridae	Cockle Bay	180
Tapes sulcarius	Veneridae	Cockle Bay	150, 20
Tapes variegatus	Veneridae	Kissing Point	500, 10-25
Nannamoria gotoi	Volutidae~	Lizard Island	smooth

2.2.4 Roughness parameters

To further examine the surface properties associated with the periostracum 36 species were selected which were representative of the range of microtextures discovered and cover the major families collected from both Bivalvia and Gastropoda classes. Polyvinylchloride (PVC), a commonly fouled material, was also included as a comparison surface. SEM photos for each of the 36 species examined in detail and PVC are presented in Figure 2.3. Scale bars range from 1-500 µm depending on the scale of microtexture for each species. Note species # 8, *Mytilus galloprovincialis*, is a temperate species and was not collected from the GBR.

The 36 species were analysed for surface roughness parameters using laser scanning confocal microscopy (LSCM). LSCM has several advantages over the other types of microscopic systems, including minimal sample preparation time and cost, images of the specimens can be produced in a shorter time frame, and images can be generated in an open environment (Peng, 2002). Researchers have previously quantified surface topography characteristics using stylus profilometry (Hills et al. 1999; Berntsson et al. 2000a), atomic force microscopy (Scardino et al. 2003) and scanning electron

microscopy (Berntsson et al. 2000b; Petronis et al. 2000). However, these techniques provide limited information about the scale of the surface topography as the profilometry is limited by the stylus size and scanning electron microscopy only produces two-dimensional images losing all information in the third dimension. Additionally, these image scanning techniques require time consuming and expensive surface preparation and these techniques are destructive to the surface.

A BIO-RAD Laser Scanning Radiance 2000 LSCM was used for imaging. Lasersharp 2000 software was used for all image acquisitions. Each test specimen was imaged three times at three random locations on the shell surface. The LSCM settings used are in Table 2.2 and were kept constant for all shells. Laser intensity was the only setting which was optimised between specimens, as lower laser intensity darkens images making it difficult to discern the surface in the focal plane. Alternatively, higher laser intensity whitens images as regions of the focal plane become saturated (Pawley, 1995; Sheppard & Shotton, 1997).

Table 2.2 LSCM settings configuration

Confocal Parameter	**Value**
Objective lens	50x NCG Nikon NA 0.8
Laser intensity	Variable
Iris	2.2326 mm
Gain	0.4
Zoom	3.21
Frame size	512 x 512 x 256
Step size	0.05 µm
Scan rate	500 lines per second (lps)
Kalman averaging	3
Dichroic mirrors	100 % Detection
Emission filter	Open
XY pixel	0.15 µm

The scan area on each shell was 79 x 79 µm. This area provides a representation of the microtextured scales on the mollusc surfaces and detects roughness features to 50 nm

while not compromising image quality. The specimen's surface was aligned parallel to the objective lens in order to reduce excessive image sections caused by the concave nature of mollusc shells. For all imaging 500 lps was used in order to reduce excessive imaging time and any introduced noise was mitigated by filtering (Kalman averaging).

The LSCM uses a step-motor to scan sections of the shell surface, each section (step at 0.05 μm) is then merged together to form a maximum brightness image (MBI). The maximum brightness projection is composed of points of maximum brightness for each pixel location for each individual image in the stack of optical sections (Anamalay et al. 1995) resulting in a reflectance image of the specimen's surface. The MBI was then used to create a height encoded image (HEI) based on pixel intensity. Each pixel is assigned a value on a 0-255 greyscale with 0 representing a pure white pixel and 255 a completely black pixel. The HEI is similar to a contour map providing surface parameters. The information obtained from the HEI is used to generate surface roughness parameters using the MatLab and Optimus 6.1 software (Yuan et al. 2004).

The surface roughness parameters selected for use in this study are 1. average roughness (Ra), 2. average waviness (Wa), 3. skewness of the surface roughness profile (Rsk), 4. skewness of the surface waviness profile (Wsk), 5. texture aspect ratio (Str), and 6. fractal dimension (Fd). The software package Matlab 6.0 was used to calculate Ra, Wa, Rsk and Wsk, while the software package Optimas 6.1 along with code developed by Dr Zhongxiao Peng (Yuan et al. 2004) was used to quantify Str and Fd of the imaged surfaces. The Ra and Rsk for roughness and waviness are amplitude parameters that describe the amplitude and height distribution of the surface which was calculated after separating the original surface profile into three profiles being form, waviness and roughness as illustrated in Figure 2.2. The fractal dimension measures the irregularity or complexity of the surface texture while texture aspect ratio characterises the periodic features or the uniformity of the surface texture patterns. These six parameters allow for analysis of quantified relationships between surface topography characteristics. The equations used to generate these parameters and the implications of high and low values for a surface are listed below.

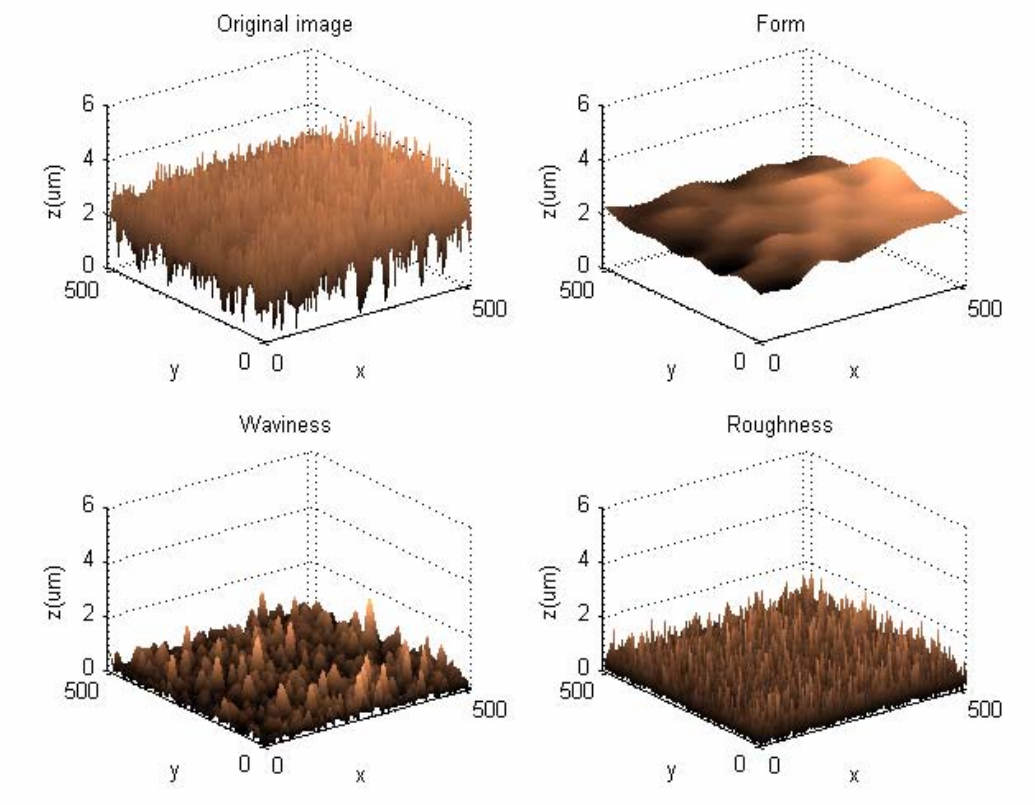

Figure 2.2 Original surface profiles of *Mytilus galloprovincialis* separated into its three profiles being form, waviness and roughness. The 3-D scale is measure in microns. The x and y axis are 0-500 µm and the z axis (height) is 0-6 µm.

Ra

The average roughness (Ra) is defined as the arithmetic mean of the departure of the surface profile from the mean line, and is calculated by $R_a = \frac{1}{L}\int_0^L |z| dx$ over 2 – 20 consecutive sampling lengths, where L is the number of sampling points and z is the residual surface. The average roughness (Ra) values for the test specimens represent the average departure of the roughness profile from the mean line of the surface. Therefore, the larger the value of Ra the greater the roughness profile of the surface roughness.

Wa

As with the roughness results the Wa values obtained represent the average departure of the waviness profile from the mean line of the surface. Therefore, the larger the value of Wa the greater the waviness profile of the surface waviness.

Rsk & Wsk

The average skewness (Rsk) is defined as the symmetry of the amplitude distribution curve about the mean line, and calculated by $R_{sk} = \frac{1}{(n \times j)R_q^3}\left[\sum_{i=1}^{i=n\times j} y(i)^3\right]$

Rsk indicates the symmetry of the amplitude distribution curve about a mean line for the surface roughness profile (and surface waviness profile – Wsk). Skewness indicates whether the surface consists of mainly peaks, valleys, or an equal combination of both. A positive value of Rsk indicates a greater distribution of peaks about the mean line as the amplitude distribution curve is skewed below the mean line and a negative Rsk value indicates a greater distribution of valleys about the mean line as the amplitude distribution curve is skewed above the mean line.

Str

The texture aspect ratio of the surface Str is used to identify texture pattern, isotropy or anisotropy, by examining its value within a range (0 to 1) (Scott, 1994; Peng, 1999). The texture aspect ratio is defined by the areal autocorrelation function (AACF) and is given by (Scott, 1994):

$$0 < S_{tr} = \frac{\text{The fastest decay distance to 0.2 on the normalised AACF}}{\text{The slowest decay distance to 0.2 on the normalised AACF}} \leq 1$$

Str indicates the randomness or directionality of surface texture. Larger values of texture aspect ratio (S_{tr}>0.5) indicate stronger isotropy of the surface texture, whereas smaller values of the texture aspect ratio (S_{tr}<0.3) indicates stronger anisotropy of the surface texture (Scott, 1994; Peng, 1999).

Fractal dimension

Fractal dimension (Fd) quantifies whether irregular shapes have a common characteristic feature in that they are self-similar, meaning that on magnification sub-structures are nearly exact copies of the original specimen. Fd is measured on a scale of 2-3, a perfectly flat surface will have an Fd value of 2 against an Fd of 3 for a very complex self replicating surface.

2.2.5 Surface wettability

Water contact angles were used to quantify the hydrophobicity of each surface. The sessile drop method was used and the mean of the left and right angles used (Uyama et al. 1991). For each shell, three measurements on each surface were taken using a goniometer (Ramé-hart: model # 100-00) and compatible imaging software (RHI 2001 Imaging System). Shells were tilted horizontal to the camera to enable image to be taken before droplet rolled off the surface. For shells with fine microtextures the size of the droplet was reduced. Occasionally new areas on the shell had to be chosen to overcome droplet distortion.

2.2.6 Correlations of surface parameters

As some of the surface parameters could be good predictors of others, it is useful to determine if any relationships exist between each of the seven surface parameters. Pair-wise correlations were made using mean values (n = 3) from the 36 species and PVC. Pearson's correlation coefficients are reported with the critical value at $\alpha = 0.05$.

2.2.7 Univariate analyses

As well as determining if correlations exist amongst the surface properties (i.e. the main aim of this chapter), there are also some univariate comparisons between taxonomic groups that will be of interest. The 36 species examined in this chapter can be classified into two classes (bivalve and gastropod) and 14 families (see Table 2.3). Differences between taxonomic groups at any one level (i.e. differences between species, families or classes) were analysed separately for each surface characteristic. Separate analyses had to be performed as nested ANOVAs could not be used due to the disproportionate number of families within classes and species within families (Table 2.3). This meant that differences in surface characteristics between the two classes were analysed by t-tests (using the mean value for each species as a replicate: bivalve n = 26 species, gastropod n = 10 species). Differences between families were examined by 1-way ANOVA (again with species means as replicates), but in this case only those families that contained two or more replicate species were included in the formal analysis (n = 8). Differences between the individual species (n = 36) were analysed by 1-way ANOVA. As well as the 36 species, the artificial substratum PVC was included in this analysis.

Student-Newman-Keuls (SNK) multiple comparisons were used for post-hoc analysis of the ANOVAs with families and species. In many cases the SNK groupings for species showed much overlap, and for this reason the groups are not indicated on the figures but are listed in full in Appendix 1.

The assumptions of ANOVA were assessed using histograms of standardized residuals, for normality, and scattergrams of standardized residuals versus predicted means, for homogeneity of variance (Quinn & Keough, 2002). If the assumptions were not met, then data were transformed to satisfy the assumptions of the ANOVA, as indicated in the results. All analyses were performed on SPSS v 12.

2.3 Results

The 109 mollusc and 2 echinoderm species identified were characterised for surface microtextures under SEM and light microscopy and ranged in shape, structure and scale of microtextures from 1 µm to 1 mm (Figure 2.3). Most species had micro-ripples or valleys, some displayed pits (species # 11, 17, 18, 19, 33, Figure 2.3) and others micro-projections/pyramids (species # 1, 10, 15, 28, Figure 2.3). Some species displayed multiple scales of microtexture such as *Modiolus micropterus* (#7) (400 µm growth lines and 40 µm underlying texture) and *Gafrarium tumidum* (#15) (300 µm growth lines, 100 µm texture and 1 µm projections; Figure 2.3). All species with microtextures are listed in Table 2.1. *Mytilus galloprovincialis* had the shortest wavelength of microtexture (1-2 µm) and *Fragum retsum* had the longest (1 mm). Some species such as *Amusium balloti* (# 34) and *Donax cuneatus* (# 30) had smooth surface profiles free of microtexture, as did PVC (# 6) (Figure 2.3).

1.Tellina inflata

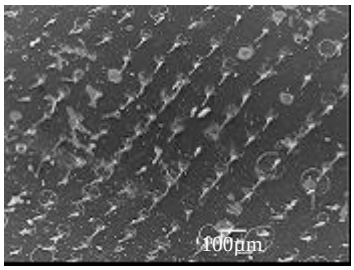

2.Tellina linguafelis

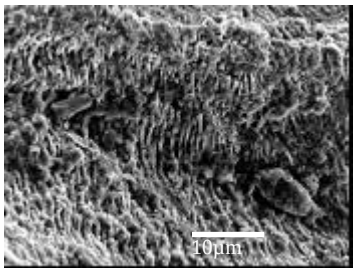

3.Tellina capsoides

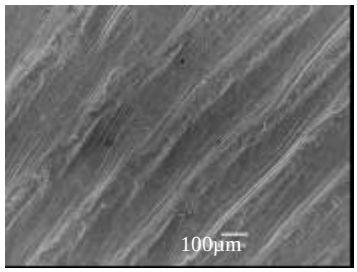

4.Tellina serricostata

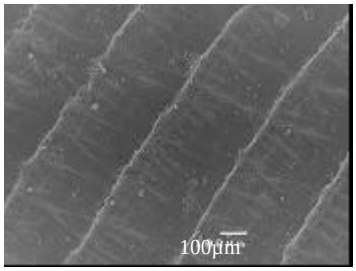

5.Tellina virgata

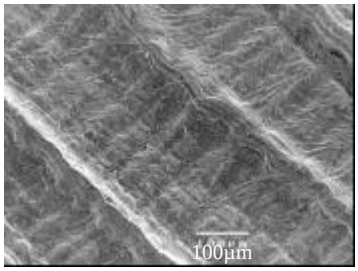

6.PVC

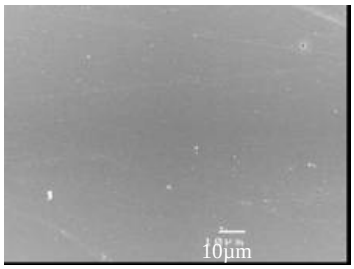

7.Modiolus micropterus

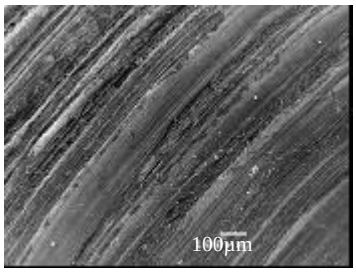

8.Mytilus galloprovincialis

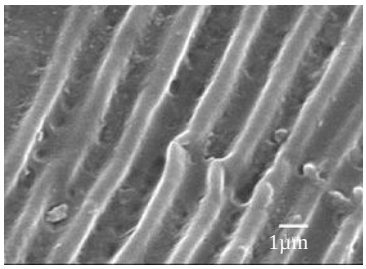

9.Septifer bilocularis

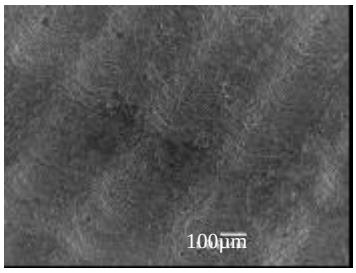

10.Tapes sulcarius

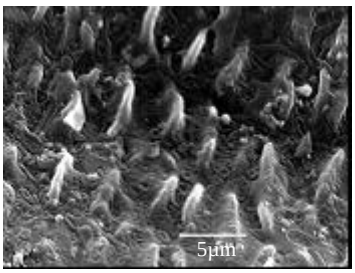

11. Lioconcha fastigata

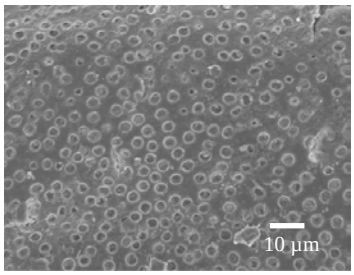

12.Tapes varieagatus

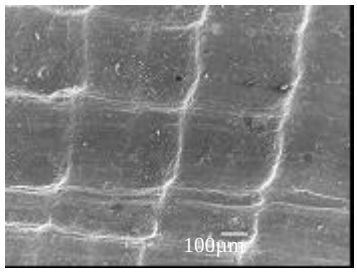

13.Dosinia juvenilis

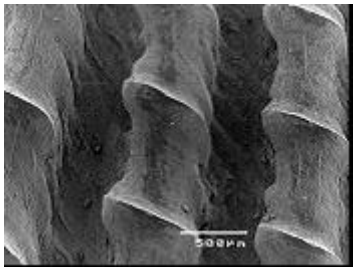

14.Globivenus toreuma

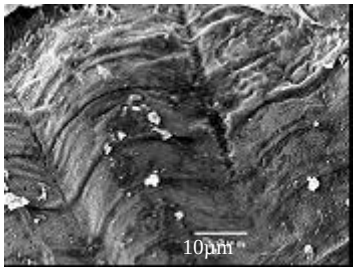

15.Gafrarium tumidum

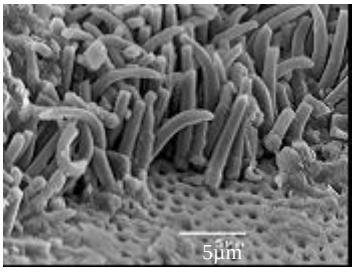

16.Nerita plicata

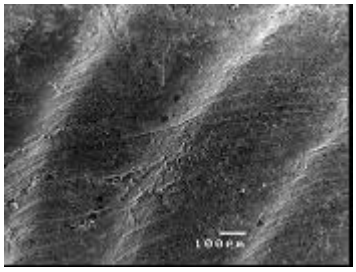

17.Nerita albicillia

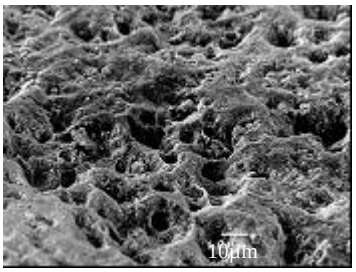

18.Nerita planosipora

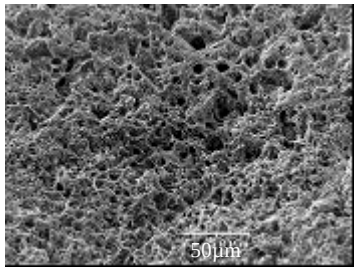

19.Nerita polita

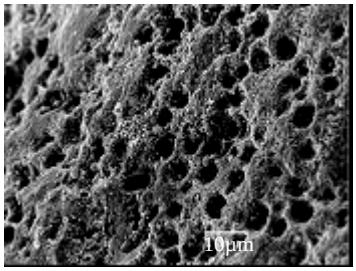

20.Nerita undata

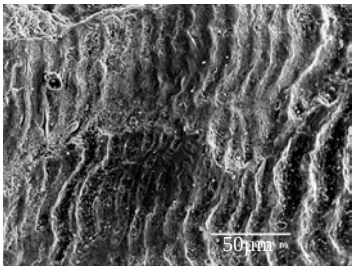

21.Nerita chamaeleon

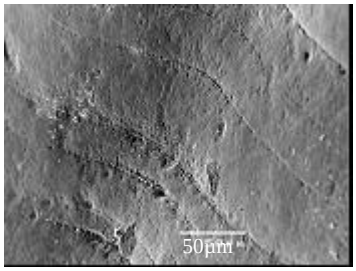

22.Polinices conicus

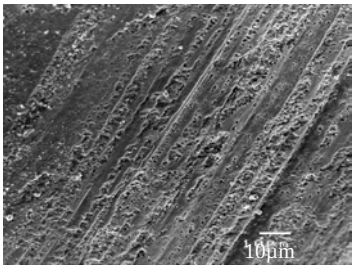

23.Natica zonalis

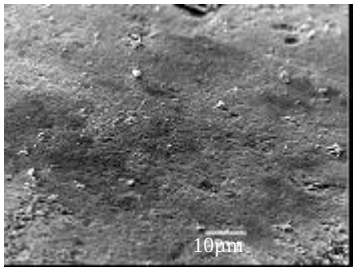

24.Polinices mammailia

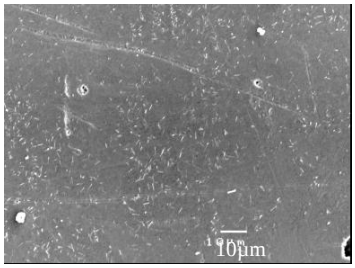

25.Natica robillardi

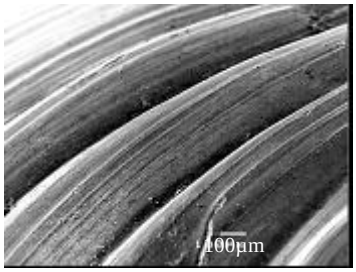

26.Mactra disimilis

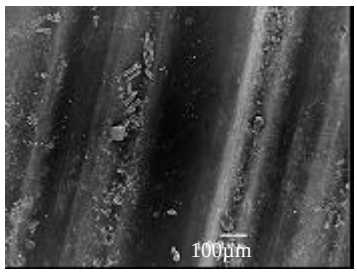

27.Mactra olorina

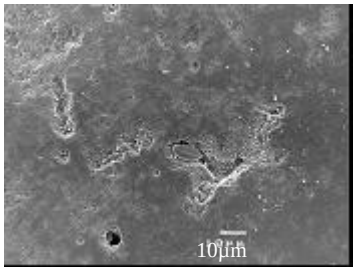

28.Asaphis violascens

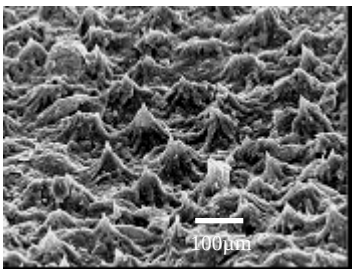

29.Soletellina atrata

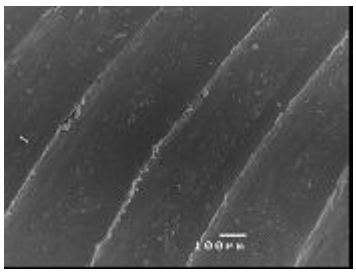

30.Donax cuneatus

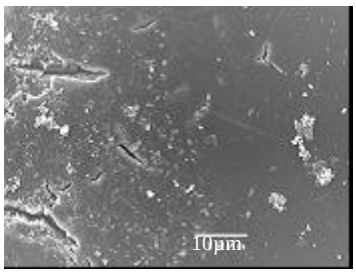

31.Donax faba ***32.Davila plana*** ***33.Divaricella ornate***

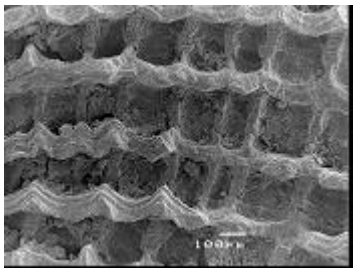

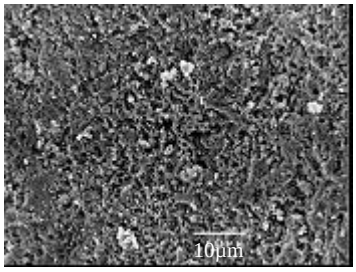

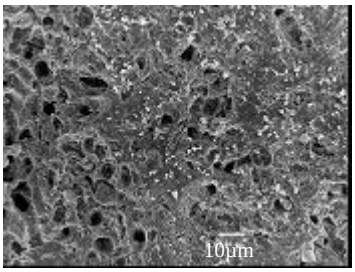

34.Amusium balloti ***35.Hemidonax* sp.** ***36.Semele crenulata***

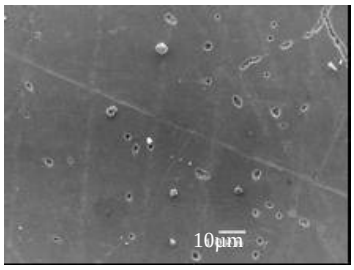

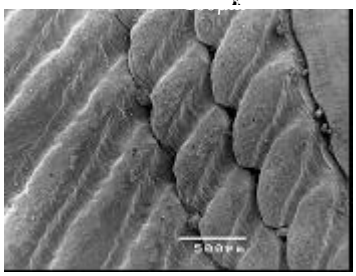

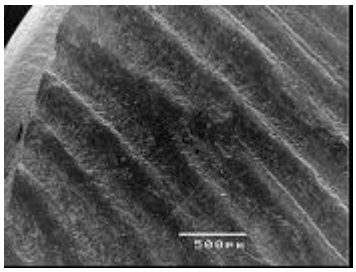

37.Acrosterigma reeveanum

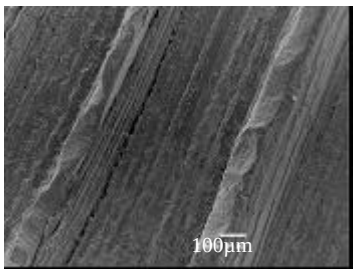

Figure 2.3 Scanning electron microscopy photos of 36 species of bivalves and gastropods and PVC examined. Scale bars range from 1-500 µm depending on the scale of microtexture for each species.

2.3.1 Surface roughness parameters on shell surfaces

The 36 selected species and PVC were characterized for the six surface roughness parameters and hydrophobicity, which are summarized in Table 2.3. Each parameter was also analysed separately for taxonomic differences at the class, family and species levels.

Table 2.3 The six surface roughness parameters and hydrophobicity for the 36 species and PVC. The species are listed by families. Mean roughness (Ra) and Mean waviness (Wa) are measured in microns (µm). Values closer to zero indicate a smooth surface. Rsk roughness (Rsk) and waviness (Wsk) are also measured in microns (µm). Positive values indicate more peaks about the mean line and negative values indicate valleys below the mean line. Str is a measure between 0 and 1 with values approaching 1 indicating randomness and reduced directionality. Fractal dimension (Fd) is a measure between 2 and 3 with values approaching 3 indicating the surface is more fractal or complex. Hydrophobicity is expressed as the contact angle formed by a drop of water on the surface (0- 180 °).

Species #	**Family**	**Ra (µm)**	**Wa (µm)**	**Str (0-1)**	**Fd (2-3)**	**Rsk (µm)**	**Wsk (µm)**	**Hydro-phobicity (°)**
1.Tellina inflata	Tellinidae	0.061	0.098	0.804	2.339	2.53	1.36	50
2.Tellina linguafelis	Tellinidae	0.179	0.11	0.802	2.894	0.18	0.45	18
3.Tellina capsoides	Tellinidae	0.138	0.127	0.791	2.934	-0.015	0.045	46
4.Tellina serricostata	Tellinidae	0.103	0.38	0.808	2.52	1.845	1.365	52
5.Tellina virgata	Tellinidae	0.172	0.111	0.778	2.856	2.388	0.981	36
6. **PVC**		0.093	0.148	0.823	2.5	3.573	1.783	70
7.Modiolus micropterus	Mytilidae	0.362	0.19	0.751	2.855	0.002	-0.015	50
8.Mytilus galloprovincialis	Mytilidae	0.274	0.183	0.801	2.826	-0.018	-0.05	58
9.Septifer bilocularis	Mytilidae	0.201	0.237	0.796	2.874	0.018	-0.297	37
10.Tapes sulcarius	Veneridae	0.114	0.074	0.81	2.81	-0.004	0.057	50
11.Lioconcha fastigata	Veneridae	0.072	0.076	0.791	2.839	-0.005	0.016	75
12.Tapes varieagatus	Veneridae	0.175	0.362	0.808	2.51	3.09	1.86	45
13.Dosinia juvenilis	Veneridae	0.182	0.482	0.757	2.531	2.63	1.3	56
14.Globivenus toreuma	Veneridae	0.105	0.412	0.81	2.45	3.35	1.45	60
15.Gafrarium tumidum	Veneridae	0.13	0.195	0.806	2.513	1.83	1.32	30
16.Nerita plicata	Neritidae	0.173	0.174	0.77	2.938	0.092	0.475	43
17.Nerita albicillia	Neritidae	0.228	0.309	0.778	2.949	-0.053	0.128	35
18.Nerita planosipora	Neritidae	0.179	0.098	0.806	2.905	-0.002	0.092	42
19.Nerita polita	Neritidae	0.19	0.158	0.792	2.9	0.002	-0.116	70
20.Nerita undata	Neritidae	0.177	0.102	0.801	2.867	0.029	0.33	46
21.Nerita chamaeleon	Neritidae	0.075	0.183	0.815	2.446	3.02	2.3	66
22.Polinices conicus	Naticidae	0.156	0.08	0.801	2.864	0.008	0.119	65
23.Natica zonalis	Naticidae	0.072	0.166	0.818	2.429	1.86	1.48	61
24.Polinices mammailia	Naticidae	0.132	0.061	0.788	2.787	-0.002	0.168	75
25.Natica robillardi	Naticidae	0.122	0.058	0.804	2.784	0.003	0.007	70
26.Mactra disimilis	Mactridae	0.057	0.128	0.814	2.335	2.8	1.38	64
27.Mactra olorina	Mactridae	0.054	0.125	0.816	2.39	2.21	1.49	81
28.Asaphis violascens	Psammobiidae	0.161	0.392	0.812	2.435	3.86	1.77	23
29.Soletellina atrata	Psammobiidae	0.052	0.183	0.814	2.39	2.51	1.36	61
30.Donax cuneatus	Donacidae	0.164	0.385	0.813	2.507	2.92	1.907	62
31.Donax faba	Donacidae	0.067	0.149	0.807	2.44	2.73	1.29	70

Species #	Family	Ra (µm)	Wa (µm)	Str (0-1)	Fd (2-3)	Rsk (µm)	Wsk (µm)	Hydro-phobicity (°)
32.Davila plana	Mesodesmatidae	0.084	0.166	0.815	2.39	3.5	1.94	65
33.Divaricella ornate	Lucinidae	0.114	0.354	0.81	2.508	2.99	1.46	46
34.Amusium balloti	Propeamussiidae	0.12	0.073	0.785	2.76	1.12	1.26	51
35.Hemidonax sp.	Hemidonacidae	0.054	0.148	0.818	2.351	5.49	2.42	75
36.Semele crenulata	Semelidae	0.146	0.295	0.813	2.56	2.735	1.43	66
37.Acrosterigma reeveanum	Cardiidae	0.167	0.355	0.814	2.502	2.66	1.36	77

Mean Roughness (Ra)

There was no significant difference (P = 0.539, Figure 2.4a) in the mean roughness of surfaces between bivalves and gastropods. However, there were significant differences between families (P = 0.003, Figure 2.4b) with species from the Mytilidae family having the highest Ra values (0.279 ± 0.05 µm), significantly higher than all other families (SNK post-hoc comparison, Figure 2.4b – note only families comprising two or more species were formally analysed). The two families with the lowest Ra were Hemidonacidae (0.052 ± 0.01 µm) and Mactridae (0.055 ± 0.002 µm). There were also several significant differences at the species level (P < 0.001, Figure 2.4c, post-hoc comparisons in Appendix 1). For individual species, the roughest surfaces occurred on two Mytilid species *Modiolus micropterus* (#7) (0.36 ± .03 µm) and *Mytilus galloprovincialis* (#8) (0.27 ± .03 µm) which were five times as rough as *Soletellina atrata* (#29) (0.052 ± .03 µm), *Mactra olorina* (#27) (0.054 ± 0.003 µm) and *Hemidonax* sp. (#35) (0.054 ± 0.01 µm) (Figure 2.4c). For the gastropods the roughest surface was *Nerita albicillia* (#17) (0.23 ± 0.02 µm) which was three times as rough as *Natica zonalis* (0.072 ± 0.01 µm) (Figure 2.4c).

a)

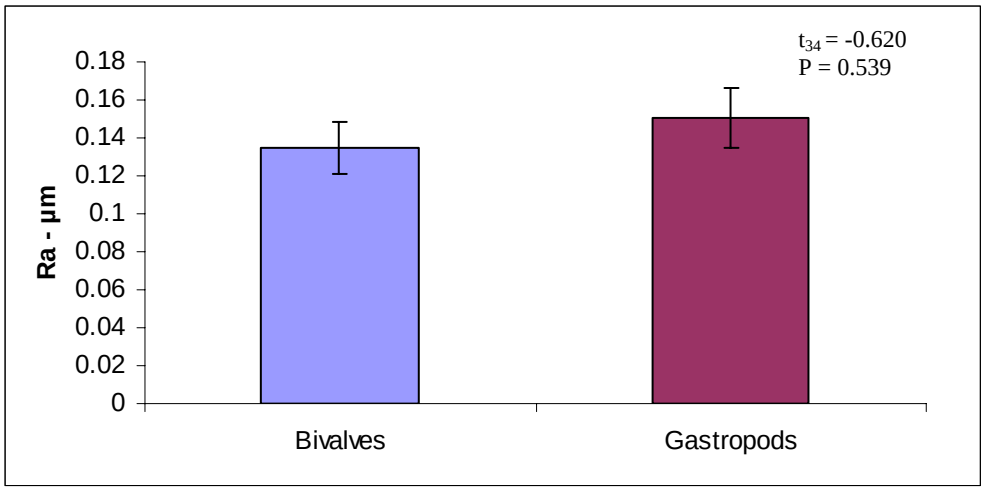

b)

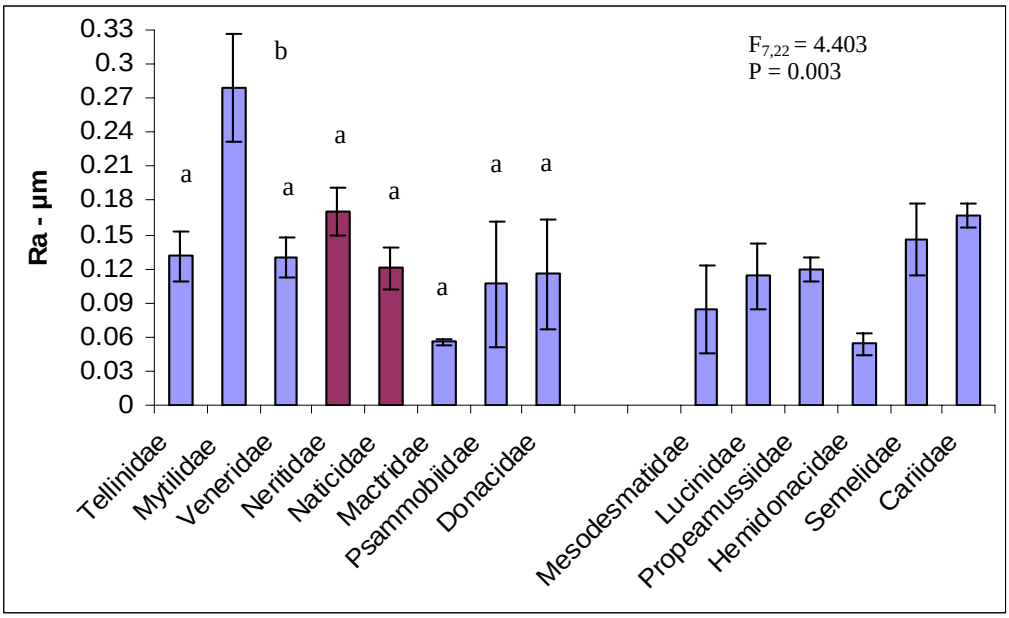

c)

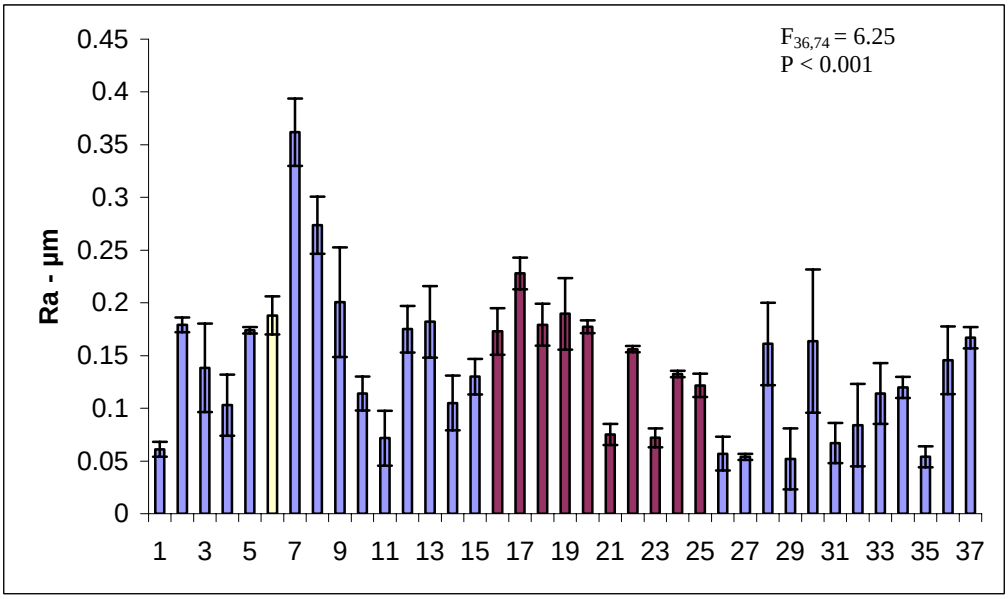

Figure 2.4 Mean roughness between a) Classes b) Families and c) the 36 species and PVC. Data are means ± one SE. Bars sharing the same letter are not significantly different at α = 0.05, Student-Newman-Keuls post-hoc comparison. Columns in blue represent bivalves and those in red are gastropods while the yellow column is PVC. Due to many overlapping groups in multiple comparisons individual pair-wise comparisons are not displayed on Figure c) but are displayed in Appendix 1. In Figure b) only families on the left hand side of the x-axis are formally analysed as they contain 2 or more species.

Mean waviness (Wa)

Mean waviness data for bivalves and gastropods was not heteroscedastic. Natural log transformation did improve the homogeneity of the variances, as such this data was analysed. Untransformed data is presented in Figure 2.5. In general gastropods had surfaces with lower waviness than bivalves which was significant (P = 0.048, Figure 2.5a). There were no significant differences at the family level (P = 0.234, Figure 2.5b). The species from the Cardiidae (0.355 ± 0.02 µm) and Lucinidae (0.354 ± 0.04 µm) family had the largest waviness profiles (Figure 2.5b) which were four times as large as the Naticidae (0.09 ± 0.025 µm) (gastropods) family. There were several significant differences for Wa values at the species level (P < 0.001, Figure 2.5c, post-hoc comparisons in Appendix 1). The species with the highest waviness were *Dosinia juvenilis* (#13) (0.48 ± 0.09 µm) and *Globivenus toreuma* (#14) (0.41 ± 0.07 µm) which have waviness profiles eight times that of *Natica robillardi* (#25) (0.058 ± 0.004 µm) and *Polinices mammailia* (#24) (0.061 ± 0.003 µm) (Figure 2.8).

a)

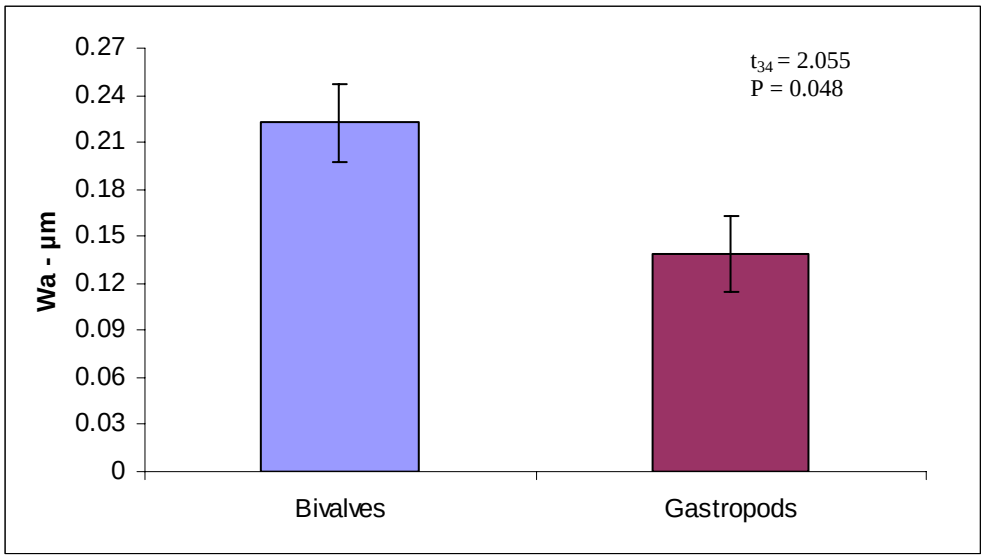

b)

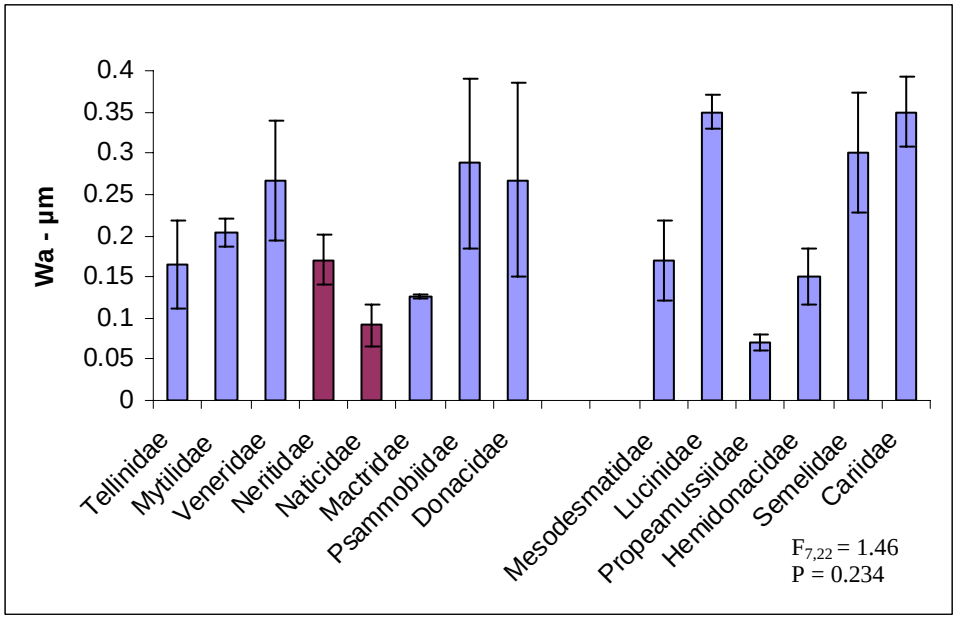

c)

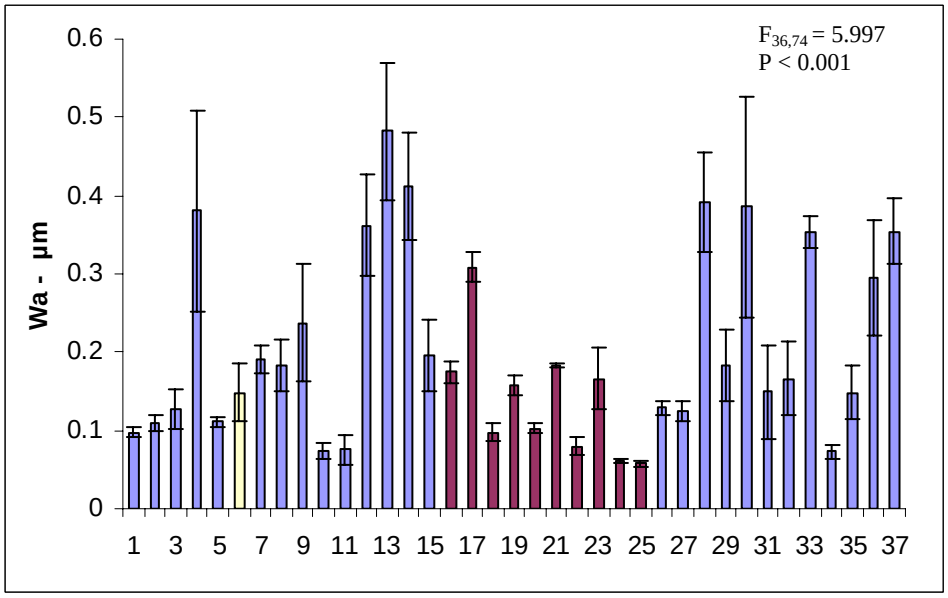

Figure 2.5 Mean waviness values between a) Classes b) Families and c) the 36 species. Data are means ± one SE. Columns in blue represent bivalves and those in red are gastropods while the yellow column is PVC. Due to many overlapping groups in multiple comparisons individual pair-wise comparisons are not displayed on Figure c) but are displayed in Appendix 1. In Figure b) only families on the left hand side of the x-axis are formally analysed as they contain 2 or more species.

Skewness of the surface roughness profile (Rsk)

Bivalves had roughness profiles 4 times more skewed than gastropods (P = 0.005, Figure 2.6a). There were also significant differences at the family level (P = 0.020, Figure 2.6b). The two gastropod families and the Mytilidae family had very low Rsk roughness values, whilst the family with the most skewed surfaces was Psammobiidae which was significantly more skewed than the Mytilidae family (SNK post-hoc comparison, Figure 2.6b). There were also several significant differences at the species level (P < 0.001, Figure 2.6c, post-hoc comparisons in Appendix 1). The species with the highest Rsk values and therefore the greatest distribution of peaks about the mean line were *Hemidonax* sp. (#35) (5.49 ± 1.52 µm), *Asaphis violascens* (#28) (3.86 ± 0.88 µm) and PVC (3.57 ± 0.52 µm) (Figure 2.6c). No surfaces had large negative values indicating there were few surfaces with a high distribution of valleys. Several surfaces had Rsk values of close to zero indicating periodic texture features with neither a high distribution of peaks or valleys.

a)

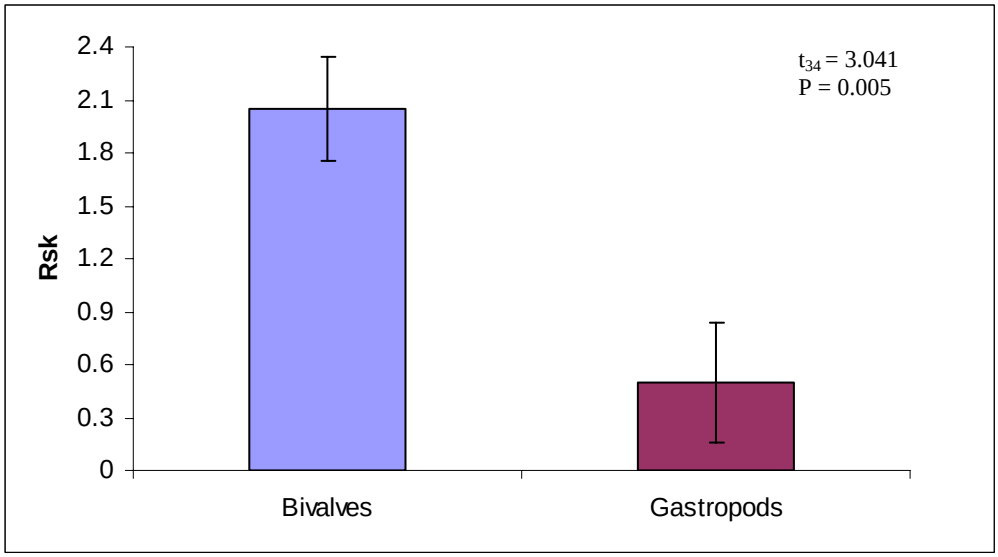

b)

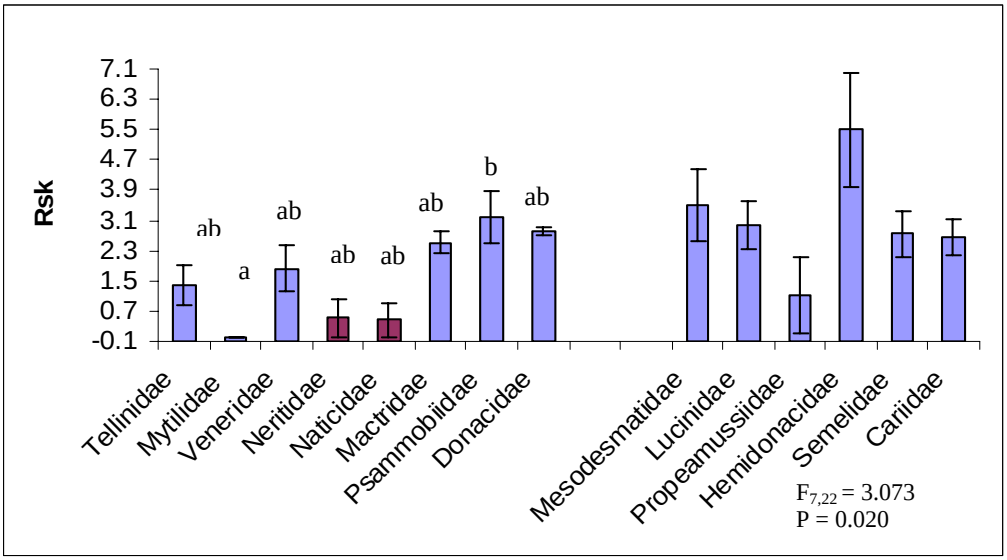

c)

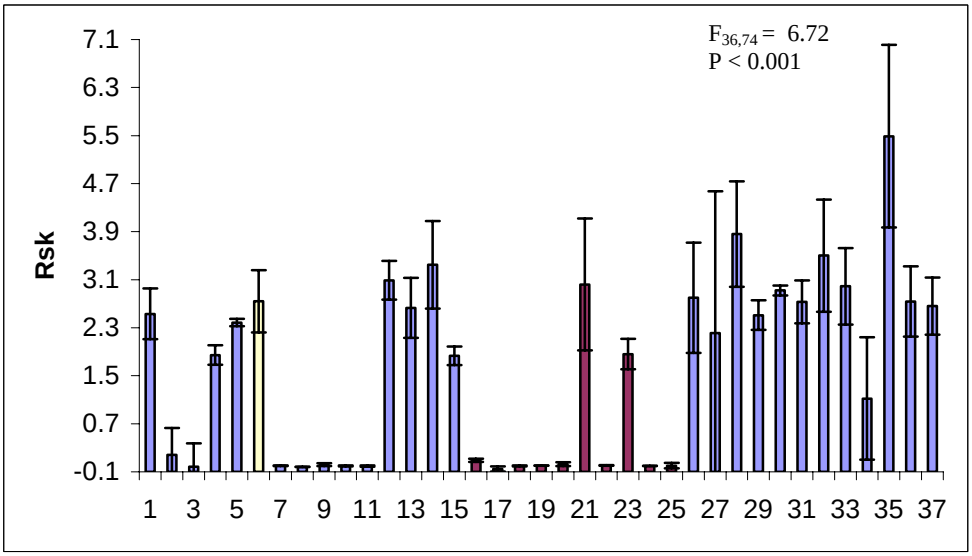

Figure 2.6 Rsk roughness between a) Classes b) Families and c) the 36 species and PVC. Data are means ± one SE. Bars sharing the same letter are not significantly different at α = 0.05, Student-Newman-Keuls post-hoc comparison. Columns in blue represent bivalves and those in red are gastropods while the yellow column is PVC. Due to many overlapping groups in multiple comparisons individual pair-wise comparisons are not displayed on graph c) but are displayed in Appendix 1. In figure b) only families on the left hand side of the x-axis are formally analysed as they contain 2 or more species.

Skewness of the surface waviness profile (Wsk)

Wsk values followed the same pattern as for Rsk values with bivalve surfaces having significantly higher values and a greater distribution of peaks than gastropods ($P < 0.034$, Figure 2.7a). As for Rsk roughness values the two gastropod families and the Mytilidae family had very low values, whilst the families with the most skewed surfaces were Psammobiidae and Donacidae. However, there were no significant differences at the family level ($P = 0.077$, Figure 2.7b). There were vast differences at the species level ($P < 0.001$, Figure 2.7c, post-hoc comparisons in Appendix 1). Several species had periodic texture features (values close to zero) though only two surfaces, *Septifer bilocularis* (#9) (-0.297 ± 0.17 µm) and *Nerita polita* (#19) (-0.116 ± 0.14 µm), had large negative values indicating a greater distribution of valleys (Figure 2.7c). The species with the highest Wsk values and the greatest distribution of peaks were *Hemidonax* sp. (#35) (0.242 ± 0.26 µm) and *Nerita chamaeleon* (#21) (0.23 ± 1.1 µm) (Figure 2.7c).

a)

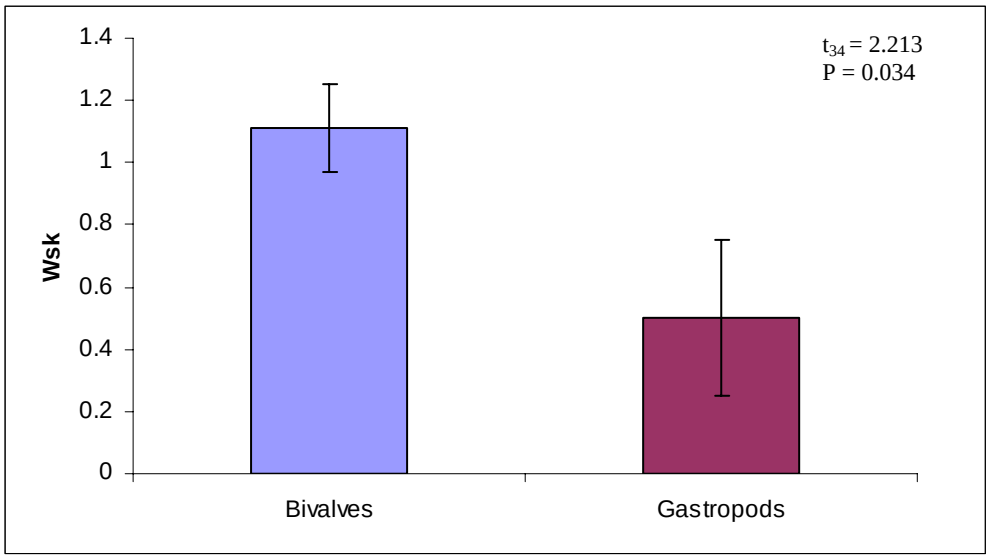

b)

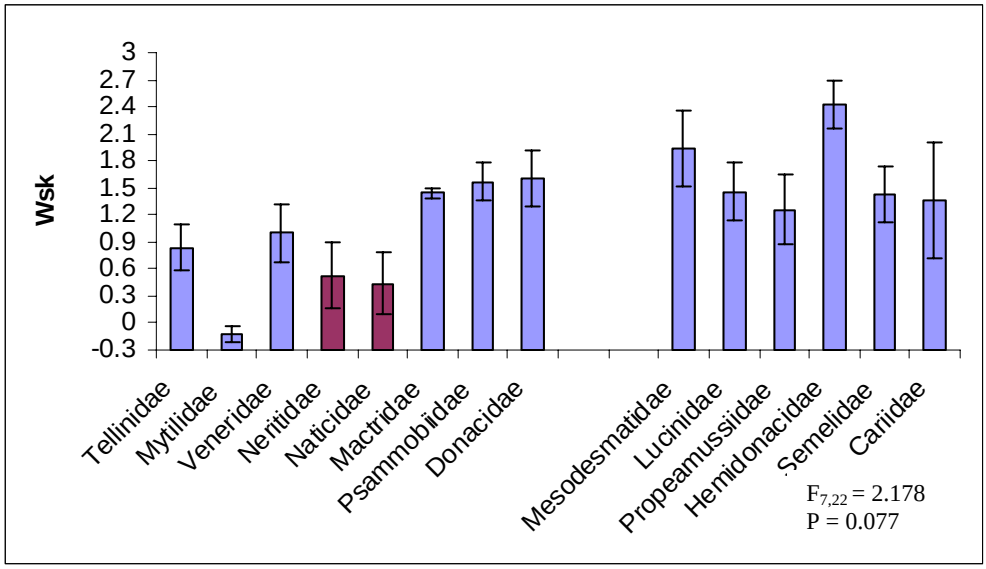

c)

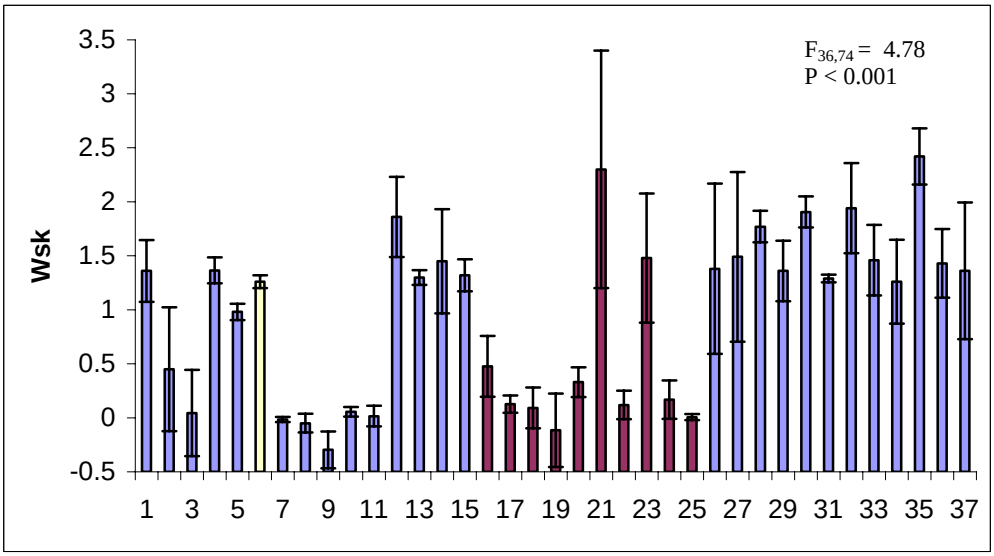

Figure 2.7 Wsk waviness values between a) Classes b) Families and c) the 36 species and PVC. Data are means ± one SE. Columns in blue represent bivalves and those in red are gastropods while the yellow column is PVC. Due to many overlapping groups in multiple comparisons individual pair-wise comparisons are not displayed on Figure c) but are displayed in Appendix 1. In Figure b) only families on the left hand side of the x-axis are formally analysed as they contain 2 or more species.

Texture aspect ratio (Str)

All surfaces displayed a high degree of isotropy (as all values > 0.5), indicating highly random surfaces with low directionality. There were no significant differences for Str at the class level (P = 0.496, Figure 2.8a) though bivalves had slightly more isotropic

surfaces than gastropods. There were also no significant differences between the families with all families having isotropic surfaces (P = 0.387, Figure 2.8b). There was also very little variance within families. The most isotropic family was Mactridae and the least Mytilidae. At the species level there were significant differences (P < 0.001, Figure 2.8c, post-hoc comparisons in Appendix 1). The least random surface was *Modiolus micropterus* (#7) (0.751 ± 0.014) while the most isotropic surface was *Natica zonalis* (#23) (0.818 ± 0.005) (Figure 2.7c). PVC had a high mean isotropy (0.823± 0.004, Figure 2.7c).

a)

b)

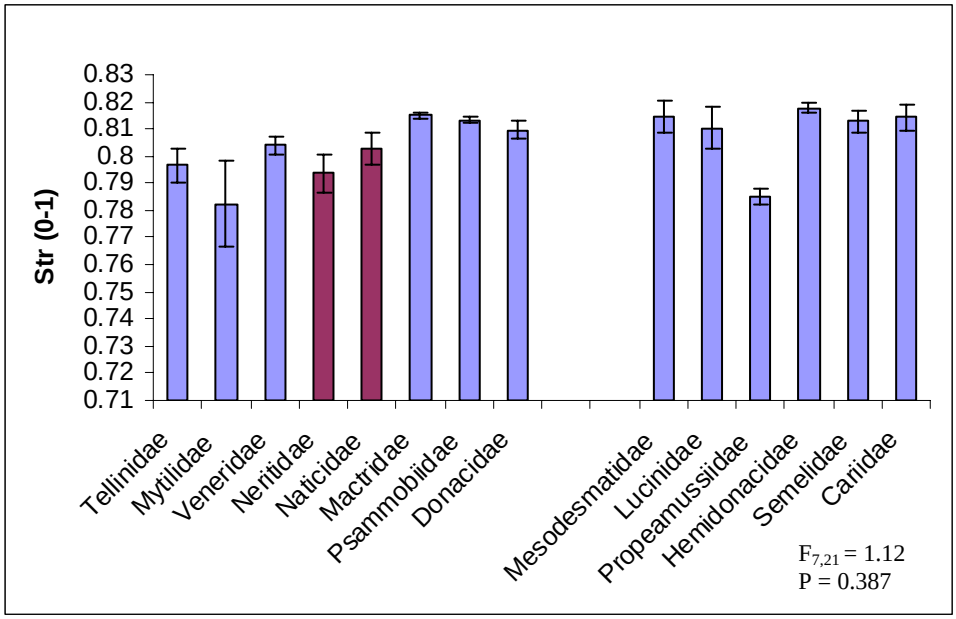

c)

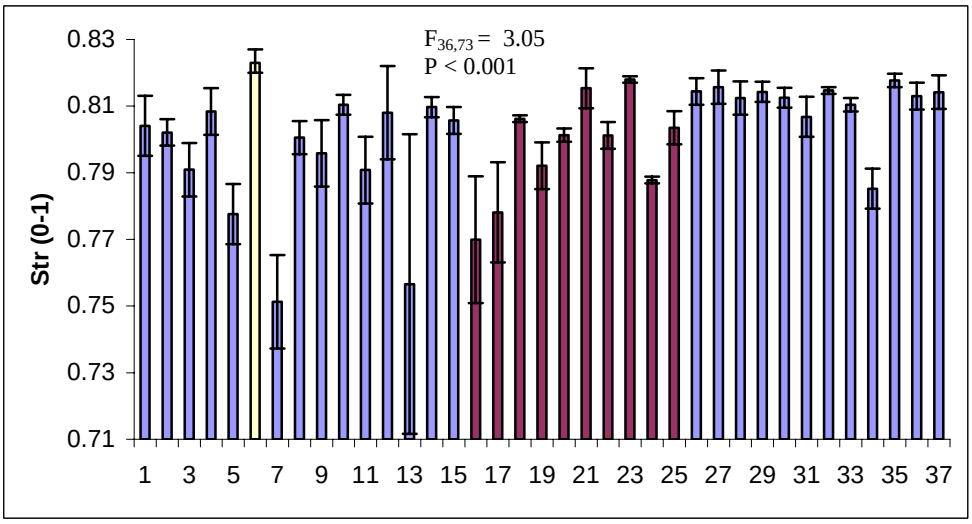

Figure 2.8 Str values between a) Classes b) Families and c) the 36 species and PVC. Data are means ± one SE. Columns in blue represent bivalves and those in red are gastropods while the yellow column is PVC. Due to many overlapping groups in multiple comparisons individual pair-wise comparisons are not displayed on Figure c) but are displayed in Appendix 1. In Figure b) only families on the left hand side of the x-axis are formally analysed as they contain 2 or more species.

Fractal dimension (Fd)

Fractal dimension data for bivalve and gastropod families was not heteroscedastic. Natural log transformation did improve the homogeneity of the variances, as such this data was analysed. Untransformed data is presented in Figure 2.9. The surfaces

examined displayed a range of fractal complexities. Bivalves had a significantly lower degree of self similarity than gastropods (P = 0.012, Figure 2.9a). At the family level there were significant differences (P = 0.022, Figure 2.9b). The most complex surfaces were from the two gastropod families and the Mytilidae family whilst the least complex family was Mactridae which was significantly less fractal than the Mytilidae and Neritidae families (SNK post-hoc comparison, Figure 2.9b). At the species level there were also significant differences (P < 0.001, Figure 2.9c, post-hoc comparisons in Appendix 1). *N. albicillia* (#17), *N. plicata* (#16), *N. planosipora* (#18) and *N. polita* (#19) all had very high fd values, while surfaces with the lowest degrees of self-similarity were *Mactra dissimilis* (2.335 ± .031) and *Tellina inflata* (2.339 ± 0.017) (Figure 2.9c). There were little variance observed within families and species.

a)

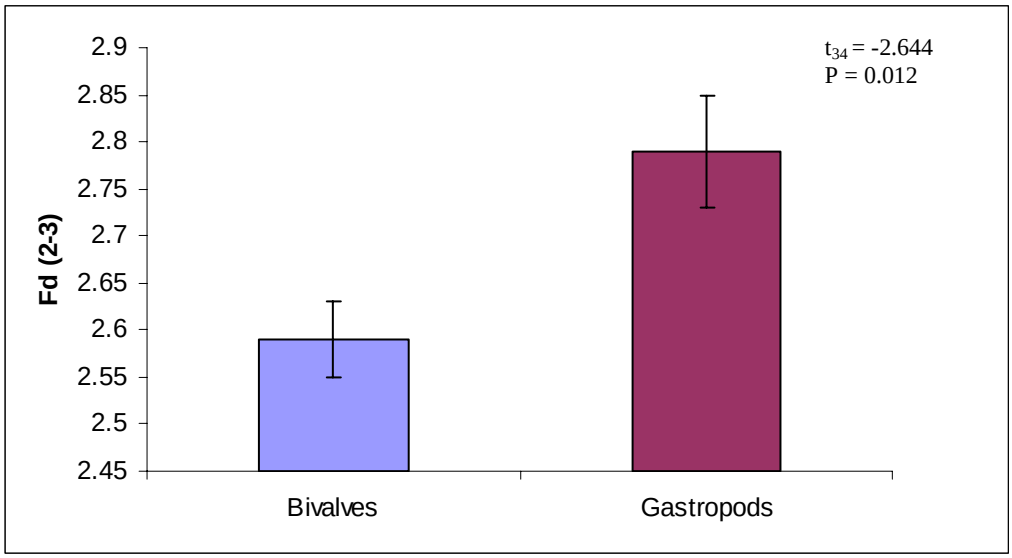

b)

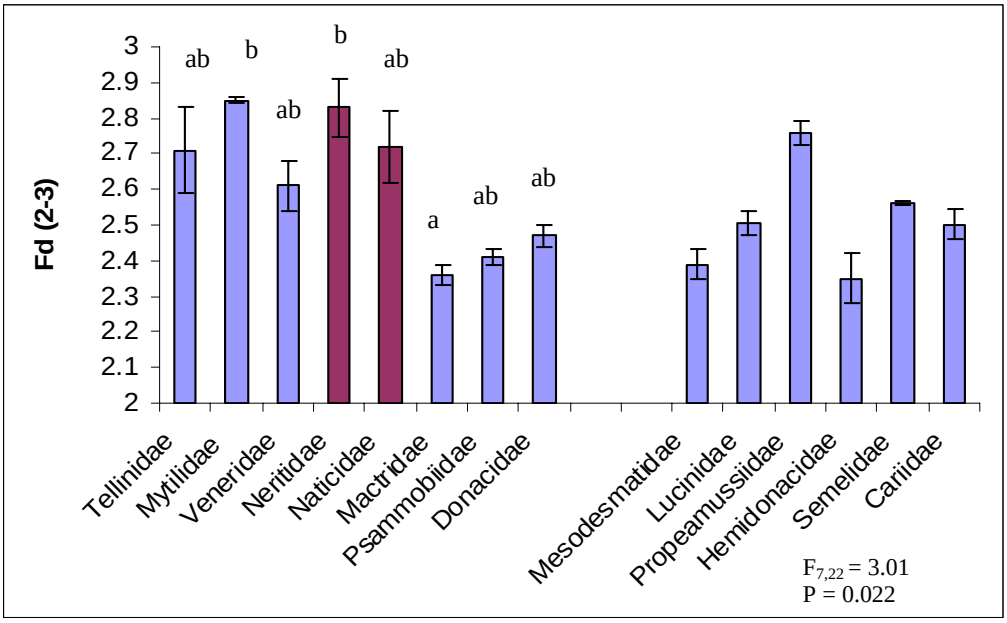

c)

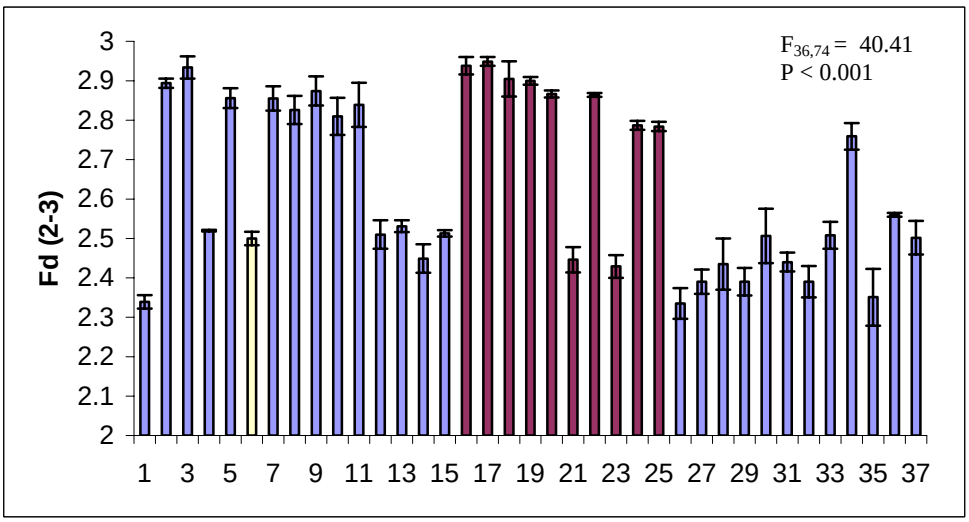

Figure 2.9 Fractal dimensions values (scale 2-3) between a) Classes b) Families and c) the 36 species and PVC. Data are means ± one SE. Bars sharing the same letter are not significantly different at α = 0.05, Student-Newman-Keuls post-hoc comparison. Columns in blue represent bivalves and those in red are gastropods while the yellow column is PVC. Due to many overlapping groups in multiple comparisons individual pair-wise comparisons are not displayed on Figure c) but are displayed in Appendix 1. In Figure b) only families on the left hand side of the x-axis are formally analysed as they contain 2 or more species.

2.3.2 Surface wettability water contact angles

The bivalve and gastropod surfaces displayed moderate degrees of hydrophobicity with most surfaces having water contact angles of 45º – 75º (Figure 2.10). There was no significant differences in surface hydrophobicity at the class level (P = 0.573, Figure 2.10a). There were also no differences at the family level (P = 0.059, Figure 2.10b). The family Tellinidae (40.4º) had the lowest hydrophobicity whilst the Mactridae family had the most hydrophobic surfaces (72.6º). There were no significant differences at the species level (P = 0.442, Figure 2.10c). The most hydrophobic species were the bivalves *Mactra olorina* (#27) (81.3º ± 18.1) and *Acrosterigma reeveanum* (#37) (77.2º ± 3.9) while the most hydrophilic surfaces were *Tellina linguafelis* (#2) (17.7º ± 10.6) and *Asaphis violascens* (#28) (23.5º ± 1.5) (Figure 2.10c).

a)

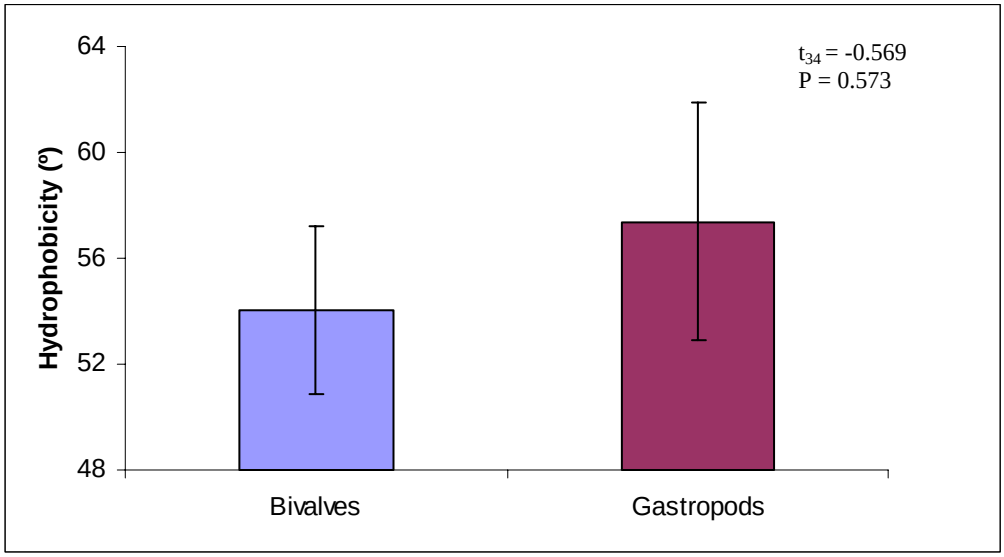

b)

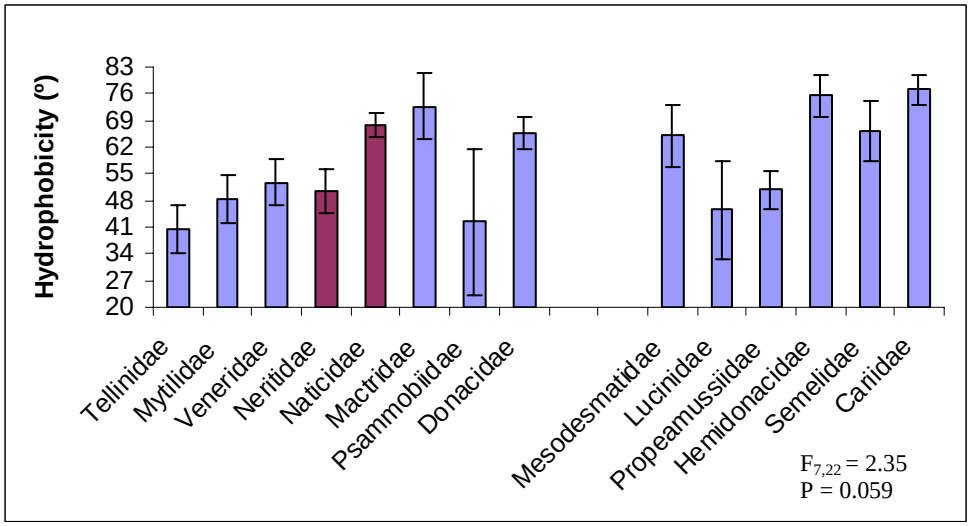

c)

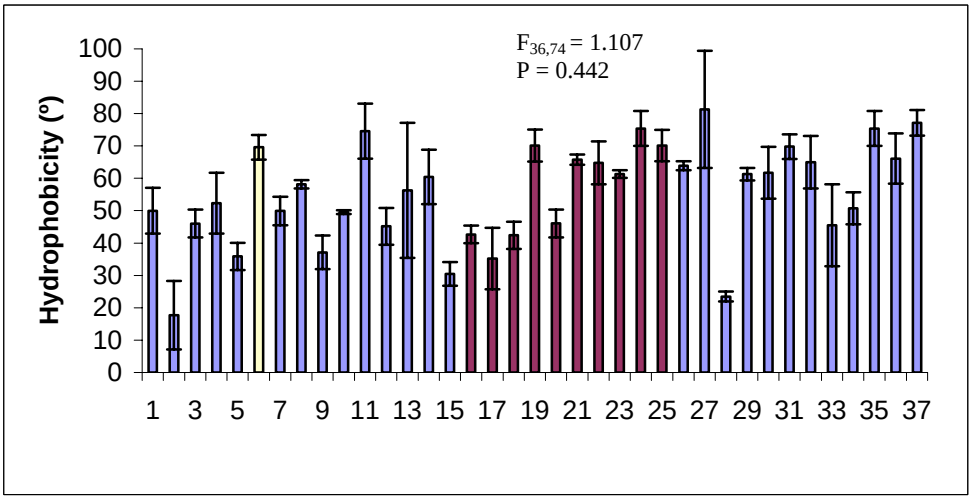

Figure: 2.10 Hydrophobicity values (water contact angles) between a) Classes b) Families and c) the 36 species and PVC. Data are means ± one SE. In Figure b) only families on the left hand side of the x-axis are formally analysed as they contain 2 or more species. Columns in blue represent bivalves and those in red are gastropods while the yellow column is PVC.

2.3.3 Correlations of surface parameters

The tested species demonstrated broad ranges of mean roughness and waviness and the surfaces had either a high distribution of peaks or periodic texture. Surfaces also displayed varying degrees of directionality, randomness and complexity. Surface hydrophobicity ranged from weakly hydrophobic to moderately hydrophobic. Due to the complex nature of the seven surface parameters measured bivariate correlations were undertaken to determine if one variable can be used to predict the other variables.

The seven surface parameters demonstrated several significant correlations (Table 2.4). Mean surface roughness correlated significantly with all parameters except mean waviness. Mean roughness was negatively correlated with Str, Rsk roughness, Rsk waviness and hydrophobicity while it was positively correlated to fractal dimension. Therefore as the shell surfaces increase in roughness they also become more directional, less random, display more periodic texture, have weaker levels of hydrophobicity and become more complex.

Fractal dimension, or the level of self-replication of a surface, was significantly correlated with all surface parameters. Fd had a positive correlation with Ra and a negative correlation with all other parameters (Table 2.4) and would therefore be a good predictor of the other six surface parameters. This means surfaces with high complexity and self-replication are rougher, less wavy, have higher directionality, have more periodic texture features and have weaker hydrophobicity.

In contrast, mean waviness had few significant correlations and would therefore be a poor predictor of the other surface features. Mean waviness was negatively correlated with fractal dimension and positively correlated to Rsk roughness and waviness (Table 2.4). As such, a surface with higher waviness profiles will be less complex and have a greater distribution of peaks about the mean line.

Str, which measures directionality, was significantly correlated with all parameters except mean waviness. Str had a negative correlation with Ra and Fd and a positive correlation with hydrophobicity, Rsk roughness and Rsk waviness (Table 2.4). Therefore a surface with little directionality and increased randomness will be less rough and have little self-replication, it will also be more hydrophobic and have a higher distribution of peaks about the mean line.

Hydrophobicity correlated negatively with Ra and Fd and positively with Str (Table 2.4). As such a surface that repels water and is more strongly hydrophobic will be less rough and have lower complexity and will have little directionality.

Both Rsk roughness and Rsk waviness displayed the same correlations with positive relationships to Ra waviness, Str and each other while having negative correlations to Ra roughness and Fd, there was no correlation with hydrophobicity (Table 2.4). As such a surface with a higher distribution of peaks on the roughness and waviness profiles will have higher waviness, lower roughness and complexity and reduced directionality.

Table 2.4 Surface roughness parameter correlations for the 36 species. Pearson's correlation coefficients are used. * denotes correlation is significant at the 0.05 level (2-tailed) and ** denotes correlation is significant at the 0.01 level (2-tailed).

	Ra roughness	**Ra waviness**	**Str**	**Fractal dimension**	**Rsk roughness**	**Rsk waviness**	**Hydro phobicity**
Ra roughness		.232	-.642(**)	.757(**)	-.442(**)	-.541(**)	-.493(**)
		.166	.000	.000	.006	.001	.002
Ra waviness	.232		.162	-.353(*)	.447(**)	.393(*)	-.210
	.166		.338	.032	.006	.016	.212
Str	-.642(**)	.162		-.760(**)	.664(**)	.754(**)	.388(*)
	.000	.338		.000	.000	.000	.018
Fractal dimension	.757(**)	-.353(*)	-.760(**)		-.768(**)	-.778(**)	-.420(**)
	.000	.032	.000		.000	.000	.010
Rsk roughness	-.442(**)	.447(**)	.664(**)	-.768(**)		.895(**)	.181
	.006	.006	.000	.000		.000	.285
Rsk waviness	-.541(**)	.393(*)	.754(**)	-.778(**)	.895(**)		.197
	.001	.016	.000	.000	.000		.242
Hydro phobicity	-.493(**)	-.210	.388(*)	-.420(**)	.181	.197	
	.002	.212	.018	.010	.285	.242	

2.4 Discussion

This study has discovered a wide variety of surface microtextures on marine molluscs *in-situ*. For the first time natural surfaces have been quantified for roughness parameters and hydrophobicity. These roughness parameters have several significant correlations to each other and one variable, fractal dimension, can be used to predict the six other surface parameters. The quantified surface parameters may now be used to determine critical roughness/surface factors that resist or promote fouling (Chapter 3).

The use of CLSM as used in this study has several advantages over other surface analytical techniques. Algorithms used (Yuan et al. 2004) have enabled quantification

of directionality, randomness and complexity, which is rarely studied in relation to biofouling. Few of the surface parameters characterised for species have been examined in detail across a broad range of values for their effects on biofouling.

The mollusc surfaces examined displayed small scales of roughness and waviness, predominately in the nanometer range. Most surfaces were highly complex with Fd values close to the maximum. Surfaces had either periodic texture or a greater distribution of peaks, but not valleys. All surfaces were highly isotropic and therefore had less directionality and more randomness. The surfaces had a moderate hydrophobicity. The mollusc surfaces characterised differed at the class, family and species level. Bivalves had significantly higher waviness profiles and were more positively skewed in the roughness and waviness profiles whilst gastropods had significantly greater fractal dimensions. The Ra, Wa, Rsk and Fd parameters differed significantly between families, whilst at the species level all parameters differed significantly except hydrophobicity. Several of the surfaces parameters were correlated together.

In one of the few studies which has explored the concept of fractals in relation to fouling Hills et al. (1999) examined the influence of fractals on barnacle cyprid recruitment. Fractals were found to be positively correlated to cyprid recruitment though it was believed cyprids were responding to potential settling sites rather than complexity (Hill et al. 1999). Le Tournequey & Bourget (1988) found higher fractal dimensions on preferred cyprid settlement sites. Fractal dimensions have also been correlated to changes in recruitment on artificial pond weed (Jeffries, 1993) and macroalgae (Gee & Warwick, 1994; Davenport et al. 1996) though causation was not demonstrated.

A few studies have examined mean roughness, width and heights of surfaces in relation to fouling, though not on the waviness profiles of a surface, and they are mostly on artificial surfaces. The microstructure of mollusc shells has been studied including the nacreous layers (Hedegaard & Wenk, 1998) however topography features on the surface of mollusc's shells have never before been quantified. In one of the few examples of natural surface characterisation Holmes et al. (1997) studied Ra and Rz (mean height) values for rock types though were unable to predict cyprid settlement

based on these parameters. Berntsson et al. (2000a; b) studied cyprid recruitment on artificial surfaces with varying Ra, Rsm (width) and Rz. They found settlement was reduced on longitudinal textures rather than separate topographical structures such as pits and peaks. The scales used however (20 -500 µm) were orders of magnitude larger than the present study. Only the smooth surface had an Ra value (0.2 µm) applicable to the present study and Rsm, the mean width of spacing (112 µm), was much higher than the values determined here (Berntsson et al. 2000a; b). Critical roughness values determined were Rz – 30-45 µm, Ra – 5-10 µm and Rsm – 150-200 µm, all of which are several times larger than the roughness values measured on mollusc surfaces in this study. These studies only examine the settlement response of one species, not overall fouling. A non-preferred roughness could easily be preferred by other fouling species. Petronis et al. (2000) examined artificial pyramids and riblets on cyprid recruitment. They measured Ra, Rz, Rsm and Rdsr (projected surface area ratio) and Rdva (developed structure volume per projected area) and hydrophobicity. Surfaces were characterised using SEM based on dimensions of measured microstructures. Barnacle density decreased with increasing Ra and Rdsr values and was positively correlated with hydrophobicity. In addition to attachment surface characteristics affect detachment. Granhag et al. (2004) found that *Enteromorpha* (*Ulva*) spores were removed least from surfaces with an Rz of 25 µm compared to smooth (Rz 1 µm) and the roughest surface (Rz 100 µm) after exposure to a water jet.

The roughness parameters generated from the mollusc surfaces will be correlated to their antifouling resistance (Chapter 3). The critical roughness features of the best and worst performing species will be identified and used for recommendations for future biomimics and as a basis to determine the underlying mechanisms that determine fouling resistance.

CHAPTER THREE

Fouling resistance of selected mollusc shells with quantified roughness properties

3.1 Introduction

Nature provides unique examples of inherently fouling resistant surfaces based on physical properties. For instance, shark skin (Ball, 1999) and whale skin (Baum et al. 2001; 2002) are two examples where natural microtextures contribute to the reduction in fouling settlement. Gorgonian corals (Figuerido et al. 1997), crab carapaces and brittle stars (Bers & Wahl, 2004) as well as dogfish egg cases (Davenport et al. 1999) may also have potential physical fouling resistant properties. By far the most well researched models of natural fouling resistant surfaces are the mussels *Mytilus galloprovincialis* (Scardino et al. 2003; Scardino & de Nys, 2004) and *Mytilus edulis* (Wahl et al. 1998; Bers & Wahl, 2004). These species have micro-ripples on their surface with wavelengths of 1-2 µm that are believed to deter the settlement of macrofouling organisms. Mussel shells and mollusc shells in general have no known chemical defences and are composed of calcium carbonate thereby making them excellent candidates for biomimics. The surface of shell fish also has a thin proteinaceous top-layer, the periostracum, the presence of which correlates to reduced fouling (Harper & Skelton, 1993; Che et al. 1996; Scardino et al. 2003).

The strong fouling resistance of mussel species and the universal nature of the periostracum suggest that this phenomenon may be present across a broader range of mollusc species and that species with fouling resistance may share common surface features. These critical surface features could guide development of future biomimetic surfaces with potential applications in shipping, aquaculture and biomedical devices as well as providing new input for foul-release coatings.

The Great Barrier Reef (GBR) in northern Australia has a broad range of molluscs (Wilson, 1993; 2002; Lamprell, 1993), many of which anecdotally appear free of fouling despite strong fouling pressure of tropical waters. In the previous chapter, the surfaces of 111 mollusc species were characterised for surface microtextures and a

subset of 36 were quantified for surface roughness parameters. However, no study has correlated the fouling resistance of multiple natural surfaces with quantified surface roughness parameters. In the present chapter, the fouling resistance, and the relative attachment strength as measured by fouling removal of the same 36 characterised species, are quantified and correlated with the predetermined roughness parameters (Chapter 2). The aim of this chapter is to determine the key parameters that define surfaces that are resistant to species specific fouling organisms, or have high foul release properties, and further examine the broader theoretical mechanisms responsible for fouling resistance.

3.2 Methods

3.2.1 Selection of species

A subset of the collected molluscs characterised from Chapter 2 were used for the analysis of fouling resistance. Thirty six species were chosen as they represent the broad range of surface textures as characterised in Chapter 2. The 36 species are from 14 different families (Table 2.1 in bold) with their collection location also listed in Table 3.4. Five replicates of each species were used to assess fouling resistance in the field after 3 months and the level of fouling removal at the completion of the field experiment. Polyvinylchloride (PVC) was used as a control as it is known to foul rapidly (Scardino & de Nys, 2004). Five pieces of PVC (30 mm x 30 mm) were used to mimic the size of the mollusc shells.

3.2.2 Experimental design and measurements

The fouling resistance experiments were conducted at Ross Creek (19° 15'S; 146° 50'E), Townsville. This site has strong fouling pressure throughout the year (Floerl, 2002) and is typically dominated by the bryozoan *Bugula neritina*, spirorbid and *Hydroides* spp. tubeworms, encrusting bryozoans including *Schizoporella* and *Watersipora* species and colonial ascidians, particularly *Diplosoma* and *Botrylloides* species (Floerl & Inglas, 2003; Scardino & de Nys, 2004). One valve of each individual was cleaned and dried. A small drop of resin (DEVCON® 2-TON®; DEVCON, Wellingborough NN8 6QX, UK) was then placed inside the valve. After 10 minutes of partial curing a stainless steel thread was placed in the resin and allowed to set for 12

hours. PVC panels were then used as the base to bolt in test shells. Small holes were drilled into the PVC and 1 replicate of each species was randomly assigned a position on each of the five PVC panels. The shells were bolted into the PVC panel and secured with stainless steel nuts. There were five replicate panels, each with one replicate of the 36 species of shell and PVC.

The PVC panels were submerged at Ross Creek at a depth of 1-2m. The panels were removed weekly and each replicate photographed with a digital camera (SONY DSC-W5 Cyber-shot, 5.1 mega pixel, 3.0 x zoom). The digital pictures were analysed with the measurement module of the image analysis program IM50 (Leica Microsystems). The area of each shell was traced along with the area of each fouling organisms. This allowed a comparison of total percent of fouling of the shell and percent fouling cover by each fouling species.

3.2.3 Antifouling paint trial

Edge effects are often an issue in field based fouling experiments. Fouling organisms are known to establish inside the valves of shucked shells or on the adjacent paneling and grow over onto the top of the shell surface (Scardino & de Nys, 2004). To avoid these potential edge effects a new methodology trial was conducted over 6 weeks whereby the panels which were to hold the shells are painted with a commercial antifouling paint. To ensure the antifouling paint had no 'halo effect' which might deter fouling organisms from settling on shells attached to panels painted with antifouling a trial experiment was run. The test involved painting half the panel (PVC) which would hold the shells with antifouling paint and leaving the other half of the panel as unmodified PVC to determine if there were any differences in numbers of recruits and percent fouling cover on shells attached to painted and unpainted PVC. Test shells *Amusium balloti* and *Mytilus galloprovincialis* were used as these species are in high abundance and their fouling resistance is reported (Scardino & de Nys, 2004). Shells were fixed onto PVC panels (as described in 3.2.1) with 1 replicate of each species bolted onto one half of the PVC panel and secured with stainless steel nuts. The other half of the PVC panel was coated with the commercial antifouling paint (active constituent: 543-559 g/L copper present as cuprous oxide, 62 g/L diuron) (Wattyl Protective and Marine Coatings - Sigmaplane Ecol HA120). One replicate of each species was also bolted onto the painted half of the PVC panel. There were three

replicate panels. Percent fouling cover and number of recruits was measured after 6 weeks and compared between shells on the coated and uncoated sections of the panels.

3.2.4 Fouling resistance experiments

The fouling resistance measurements were conducted at Ross Creek (19° 15'S; 146° 50'E), Townsville. Each of the 36 species and PVC control were gently cleaned and then randomly assigned a place on a panel and bolted in with stainless steel threads as outlined in 3.2.3. There were five panels, each with one replicate of the 36 species and PVC. The panels were completely coated with antifouling paint (as described in 3.2.3) to remove edge effects. The fouling cover was measured as described in 3.2.1.

3.2.5 Fouling adhesion and removal

To determine a relative measure of adhesion strength by fouling organisms to different shells, each replicate was subject to a water jet at the completion of the field exposure experiment. After 16 weeks the panels were removed and a water jet (Gerni – Crown compact) was used to remove fouling. The water jet was locked into place on a stage vertically above the test surfaces. A slider allowed the water jet to be moved vertically (75-15cm) along the stage to within 1cm. The pressure from the water jet acting on the shell surface was calculated by $\mathbf{Pa=N/m^2}$, where Pa = the surface pressure in Pascals, N = force in Newtons. The water jet was delivered at a flow rate of 6L/min from a series of heights starting at 75cm. The weight of the water jet was measured from a strain gauge (Scale Components P/L; Model: STC - 250 kg; calibration # - mV/V: 2.9991; serial # - W13397) and was constant (1.23 kg) for varying distances from the surface. The area of the water jet acting on the surface was determined by measuring the diameter of a series of holes left by the water jet. The surface pressures acting on the shell surfaces from varying heights from 75cm to 15cm and are listed in Table 3.1.

The percent removal of fouling from each shell was quantified by analysing images before and after exposure to the water jet from 75cm, 60cm, 45cm, 30cm and 15cm from the surface. Each replicate was photographed with a digital camera before and after exposure to the water at each level. Digital pictures were analysed with the measurement module of the image analysis program IM50. The area of each shell and

fouling organism was traced allowing a comparison of total percent of fouling covering the shell.

Table 3.1 Surface pressure delivered from water jet at varying heights.

Height (cm)	Pressure (kPa)
75	76.28
60	85.13
45	97.07
30	129.9
15	195.51

3.2.6 Statistical Analysis

The antifouling paint trial was analysed by a 3-way mixed model ANOVA. The two fixed factors were “species” and “coating”, and panel was the random factor. As there was only one replicate on each coated side of the panel, the only interaction term reported for this analysis is species by coating.

It was not possible to use the same individuals for both the fouling and surface characterisation experiments. For this reason the mean values of each species were used in the bivariate correlations between each of the seven surface parameters and fouling resistance. Pearson’s correlation were used with a significance level of $\alpha = 0.05$.

Differences between taxonomic groups at any one level (i.e. differences between species, families or classes) were analysed separately for total fouling cover, species specific fouling cover and fouling removal. Separate analyses had to be performed as nested ANOVAs could not be used due to the disproportionate number of families within classes and species within families (Table 3.4). This meant that differences in fouling between the two classes were analysed by t-tests (using the mean value for each species as a replicate: bivalve n = 26 species, gastropod n = 10 species). Differences between families were examined by 1-way ANOVA (again with species means as replicates), but in this case only those families that contained two or more replicate species were included in the formal analysis (n = 8). Differences between the individual species (n = 36) were analysed by 1-way ANOVA. As well as the 36 species, the

artificial substratum PVC was included in this analysis. Student-Newman-Keuls (SNK) multiple comparisons were used for post-hoc analysis of the ANOVAs with families and species. In the case of total fouling cover between families, there was a significant effect detected by ANOVA but SNK post-hoc comparisons could not separate the means of any individual groups. For this analysis a less conservative multiple comparison, Tukey's Least Significant Differences (LSD), was used in order to determine which groups were driving the significant result in the ANOVA (Figure 3.7b).

The assumptions of ANOVA were assessed using histograms of standardized residuals for normality, and scattergrams of standardized residuals versus predicted means for homogeneity of variance (Quinn & Keough, 2002). If the assumptions were not met then data were transformed, as indicated in the results. All analyses were performed on SPSS v 12.

3.3 Results

3.3.1 Antifouling paint trial

The antifouling paint did not reduce the number of recruits or the percent fouling cover on *A. balloti* and *M. galloprovincialis* shells compared to those without paint (Figure 3.2). In some cases fouling on the shells was higher on panels with the antifouling paint (possibly a concentration effect due to less area available to settle), for example, the number of recruits of ($P = 0.037$, Table 3.2) and percent cover ($P = 0.003$, Table 3.3) by spirorbid tubeworms were present in significantly higher numbers on shells attached to painted panels than on PVC. Percent cover by colonial ascidians was also higher on *A. balloti* shells on painted panels than PVC ($P = 0.01$, Table 3.3). *Hydroides* spp. tubeworm recruits and percent cover were significantly higher on *M. galloprovincialis* shells on painted panels than PVC (Figure 3.3; 3.5). *A. balloti* shells were fouled more heavily by all fouling organisms than *M. galloprovincialis* shells regardless of coating or PVC (Table 3.2).

Spirorbid tubeworms recruited on *A. balloti* shells in the highest numbers with an average of 30.33 ± 10.4 tubeworms settling on shells attached to uncoated PVC and 148.33 ± 46.4 settling on shells attached to painted PVC. *Hydroides* spp. tubeworms

recruited on *A. balloti* shells in similar numbers to shells attached to PVC (29 ± 8.1) and shells attached to painted PVC (8.7 ± 2.9 P = 0.178) (Figure 3.2). This trend was consistent for all other fouling organisms settling on *A. balloti* shells. Colonial ascidian colonies between uncoated PVC (12.33 ± 7.3 colonies) and coated PVC was not significantly different (26.33 ± 8.8 colonies, P = 0.313) (Table 3.2; Figure 3.2). Barnacle cyprid settlement was also not significantly different between *A. balloti* shells attached to uncoated PVC (12.7 ± 7.2) and coated PVC (8.3 ± 7.2, P = 0.728) (Table 3.2; Figure 3.2). Encrusting bryozoan recruits on *A. balloti* shells were not significantly different between coated (2.7 ± 1.8) and uncoated (6.7 ± 0.9, P = 0.151) PVC (Table 3.2; Figure 3.2).

Aside from spirorbid tubeworms, the number of fouling recruits settling on *M. galloprovincialis* shells was not significantly different between uncoated PVC and coated PVC. Spirorbids settled in significantly higher numbers on shells attached to coated PVC (23 ± 4) than on shells attached to uncoated PVC (3 ± 1.5, P = 0.037) (Table 3.2; Figure 3.3). There were no other fouling recruits on *M. galloprovincialis* shells attached to uncoated PVC. In contrast, both *Hydroides* spp. tubeworms (1.7 ± 1.2) and barnacle cyprids (0.7 ± 0.6) settled in small numbers on *M. galloprovincialis* shells attached to coated PVC (Figure 3.3).

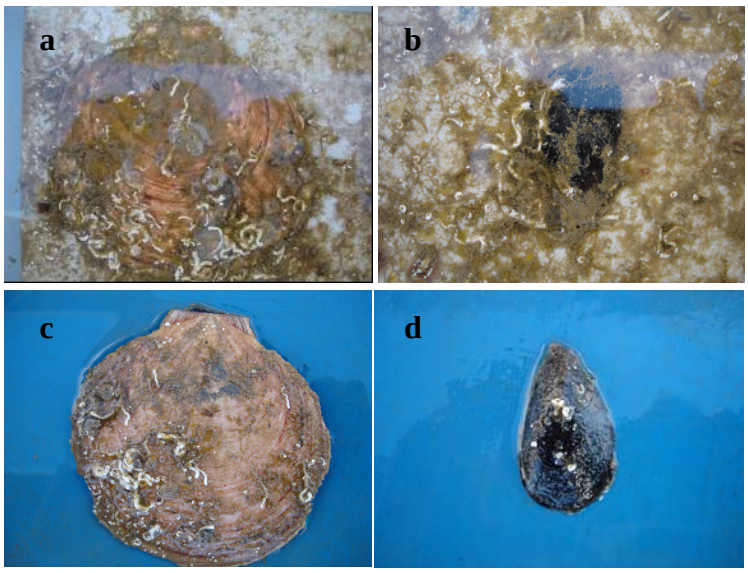

Figure 3.1 *Amusium balloti* and *Mytilus galloprovincialis* shells after 6 weeks exposure to fouling a) *A. balloti* shell on uncoated PVC panel b) *M. galloprovincialis* shell on uncoated PVC panel c) *A. balloti* on PVC panel with antifouling paint d) *M. galloprovincialis* shell on PVC panel with antifouling paint.

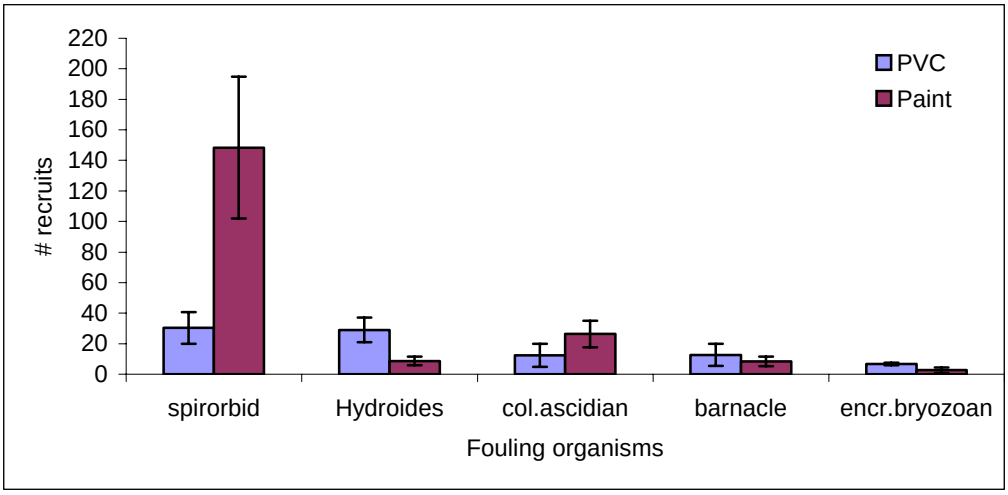

Figure 3.2 Number of recruits on *A. balloti* shells fixed to PVC and painted panels after 6 weeks. Data are means ± one SE.

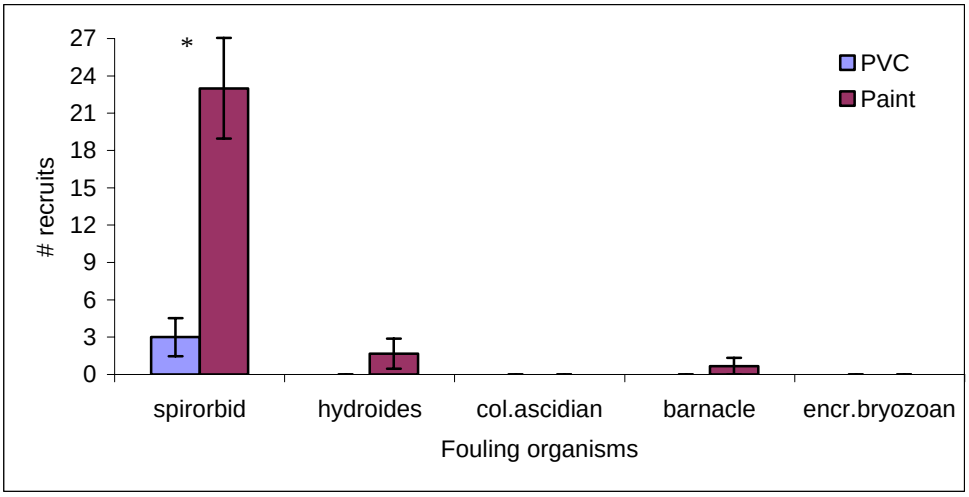

Figure 3.3 Number of recruits on *M. galloprovincialis* shells fixed to PVC and painted panels after 6 weeks. Data are means ± one SE. * = significant difference at α = 0.05.

Table 3.2. Three way mixed model ANOVA for fouling recruits on *A. balloti* and *M. galloprovincialis* shells attached to painted or unpainted PVC. Fixed factors are coating and species, random factor is panel.

Variable	**Factor**	**df**	**F**	**P**
# spirorbid recruits	Coating	1,6	7.18	0.037
	Species	1,6	8.78	0.025
	Coating*Species	1,6	3.62	0.106
	Panel	2,6	0.430	0.669

# *Hydroides* recruits	Coating	1,6	8.93	0.024
	Species	1,6	200.2	<0.001
	Coating*Species	1,6	8.93	0.024
	Panel	2,6	1.35	0.328
# colonial ascidian colonies	Coating	1,6	1.12	0.313
	Species	1,6	20.40	0.004
	Coating*Species	1,6	1.12	0.313
	Panel	2,6	0.582	0.588
# barnacle recruits	Coating	1,6	0.133	0.728
	Species	1,6	39.05	0.001
	Coating*Species	1,6	0.133	0.728
	Panel	2,6	0.055	0.947
# encrusting bryozoan colonies	Coating	1,6	2.71	0.151
	Species	1,6	24.62	0.003
	Coating*Species	1,6	2.71	0.151
	Panel	2,6	0.541	0.608

The percent coverage of fouling organisms on *A. balloti* and *M. galloprovincialis* shells was not reduced by the antifouling paint. In fact for *A. balloti* shells both spirorbid (P = 0.003) and colonial ascidian cover (P = 0.01) were significantly higher on coated PVC than on uncoated PVC (Figure 3.4; Table 3.3). This was consistent for spirorbid cover on *M. galloprovincialis* shells (P = 0.003, Figure 3.5; Table 3.3). In contrast fouling cover by multiple spp. of *Hydroides*, barnacles and encrusting bryozoans was not significantly different on *A. balloti* and *M. galloprovincialis* shells stuck to painted and unpainted PVC panels (Figure 3.4 & 3.5; Table 3.3).

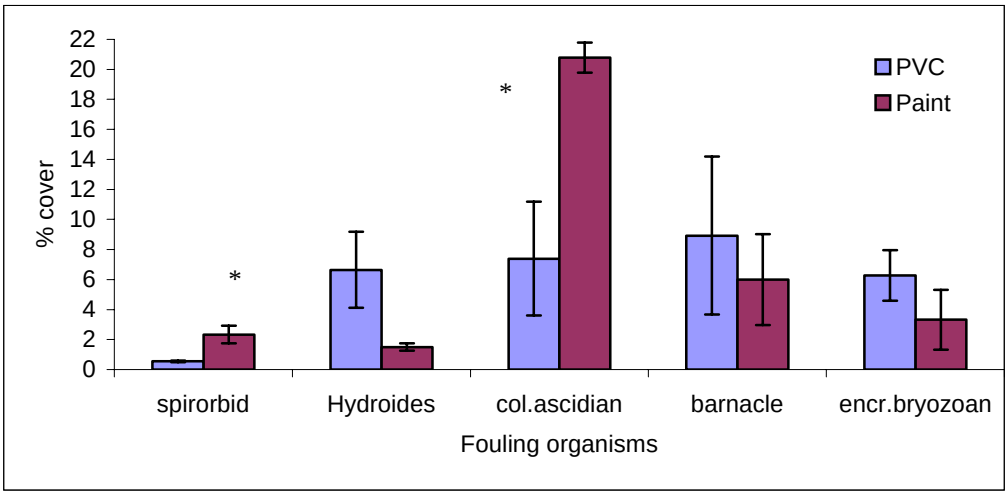

Figure 3.4 Percent cover of fouling organisms on *A. balloti* shells fixed to PVC and painted panels after 6 weeks. Data are means ± one SE. * = significant difference at α = 0.05.

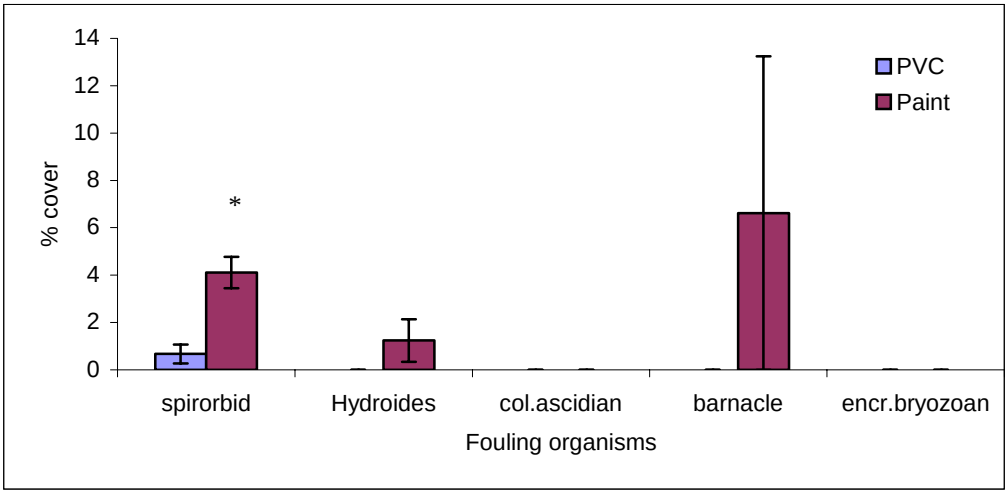

Figure 3.5 Percent cover of fouling organisms on *M. galloprovincialis* shells fixed to PVC and painted panels after 6 weeks. Data are means ± one SE. * = significant difference at α = 0.05

Table 3.3. Three way mixed model ANOVA for percent fouling cover on *A. balloti* and *M. galloprovincialis* shells attached to painted or unpainted PVC. Fixed factors are coating and species, random factor is panel.

Variable	**Factor**	**df**	**F**	**P**
% spirorbid cover	Coating	1,6	22.74	0.003
	Species	1,6	1.12	0.330
	Coating*Species	1,6	1.69	0.241
	Panel	2,6	0.615	0.572

% *Hydroides* cover	Coating	1,6	7.24	0.036
	Species	1,6	55.06	<0.001
	Coating*Species	1,6	7.24	0.036
	Panel	2,6	1.08	0.398
% colonial ascidian cover	Coating	1,6	13.96	0.01
	Species	1,6	61.75	<0.001
	Coating*Species	1,6	13.96	0.01
	Panel	2,6	1.78	0.248
% barnacle cover	Coating	1,6	0.164	0.699
	Species	1,6	14.05	0.01
	Coating*Species	1,6	0.164	0.699
	Panel	2,6	0.029	0.971
% encrusting bryozoan cover	Coating	1,6	1.03	0.350
	Species	1,6	10.86	0.017
	Coating*Species	1,6	1.026	0.350
	Panel	2,6	0.199	0.825

3.3.2 Fouling resistance of the 36 species

The dominant fouling organisms occurring on the 36 species and PVC control were encrusting bryozoans, colonial ascidians, the erect bryozoan *Bugula neritina*, spirorbid tubeworms and algae. Of these major fouling organisms the most dominant were colonial ascidians accounting for approximately 40% of the total fouling cover, then encrusting bryozoans (~25%) and *Bugula neritina* (~15%). There were large differences in total and species specific fouling cover between classes, families and species of molluscs. Bivalves had significantly lower total fouling cover than gastropods ($P < 0.001$, Figure 3.8a) and significantly lower cover by encrusting bryozoans ($P = 0.027$, Figure 3.13a). There were also significant differences between families (Figures 3.8b-3.10b).

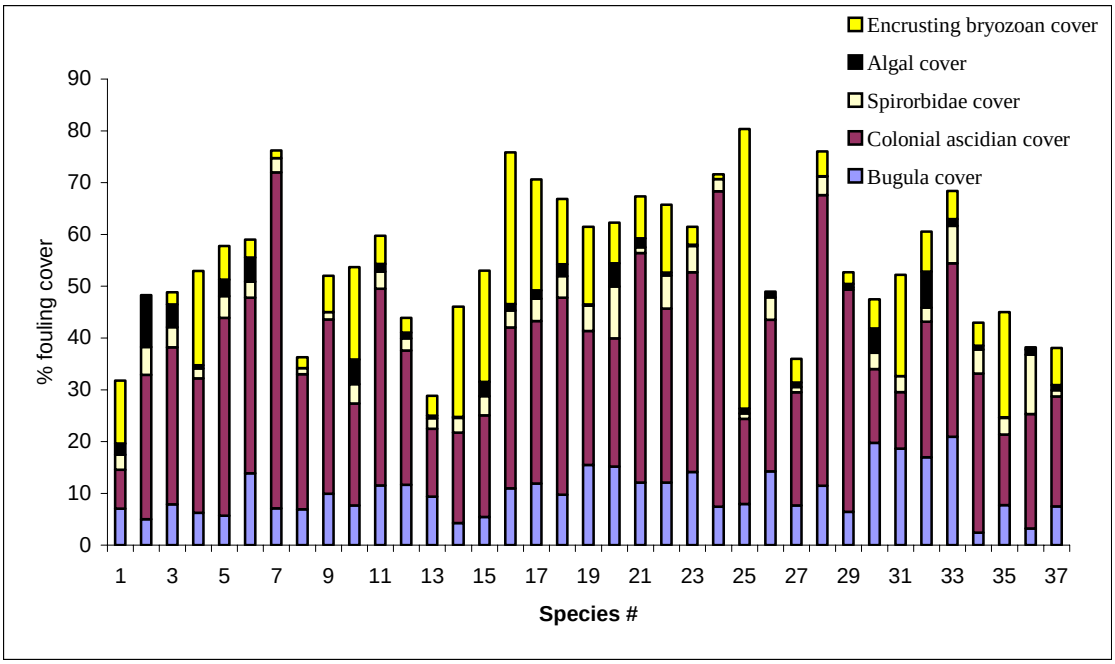

Figure 3.6 Mean species specific fouling cover on the 36 species and PVC after 12 weeks exposure

Table 3.4 The 36 species used for fouling resistance studies. * = Gastropod

Species #	**Family**	**Species #**	**Family**
1.Tellina inflata	Tellinidae	*20.Nerita undata*	Neritidae*
2.Tellina linguafelis	Tellinidae	*21.Nerita chamaeleon*	Neritidae*
3.Tellina capsoides	Tellinidae	*22.Polinices conicus*	Naticidae*
4.Tellina serricostata	Tellinidae	*23.Natica zonalis*	Naticidae*
5.Tellina virgata	Tellinidae	*24.Polinices mammailia*	Naticidae*
6. PVC		*25.Natica robillardi*	Naticidae*
7.Modiolus micropterus	Mytilidae	*26.Mactra disimilis*	Mactridae
8.Mytilus galloprovincialis	Mytilidae	*27.Mactra olorina*	Mactridae
9.Septifer bilocularis	Mytilidae	*28.Asaphis violascens*	Psammobiidae
10.Tapes sulcarius	Veneridae	*29.Soletellina atrata*	Psammobiidae
11.Lioconcha fastigata	Veneridae	*30.Donax cuneatus*	Donacidae
12.Tapes varieagatus	Veneridae	*31.Donax faba*	Donacidae
13.Dosinia juvenilis	Veneridae	*32.Davila plana*	Mesodesmatidae
14.Globivenus toreuma	Veneridae	*33.Divaricella ornate*	Lucinidae
15.Gafrarium tumidum	Veneridae	*34.Amusium balloti*	Propeamussiidae
16.Nerita plicata	Neritidae*	*35.Hemidonax sp.*	Hemidonacidae
17.Nerita albicillia	Neritidae*	*36.Semele crenulata*	Semelidae
18.Nerita planosipora	Neritidae*	*37.Acrosterigma reeveanum*	Cardiidae
19.Nerita polita	Neritidae*		

Total fouling cover

Percentage data was generally not heteroscedastic. To improve the homogeneity of the variances, and to satisfy the assumptions of ANOVA, all percentage data was transformed (arcsine square root) for analyses. Untransformed data is presented in Figures 3.7- 3.14.

Overall, gastropods were fouled more than bivalves ($P < 0.001$, Figure 3.7a). There were also significant differences between families ($P = 0.011$, Figure 3.7b). The two gastropod families had significantly higher fouling cover than the molluscan Tellinidae, Mactridae and Veneridae families, whilst the Psammobiidae family was also significantly more fouled than the Mactridae family (LSD post-hoc comparison, Figure 3.7b). There were however no significant differences at the species level ($P = 0.112$, Figure 3.7c). The most fouling resistant species after 12 weeks were *Dosinis juvenilis* (# 13) (28.9% total cover) followed by *Tellina inflata* (# 1) (31.87%) and *Mactra olorina* (# 27) (36.12%). In contrast the species that exhibited the greatest fouling were *Natica robillardi* (# 25) (81.4%), *Modiolus micropterus* (# 7) (77%) and *Asaphis violascens* (# 28) (76.1%) (Figure 3.7c).

a)

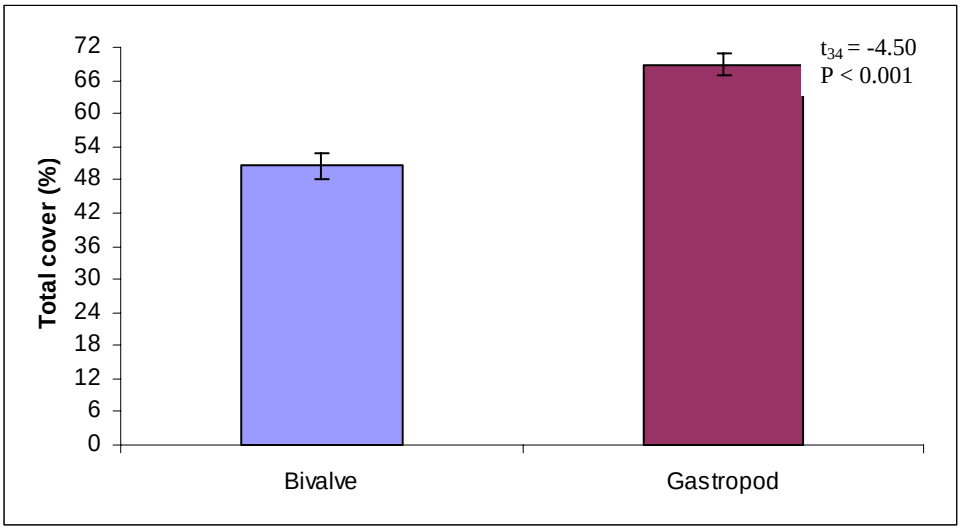

b)

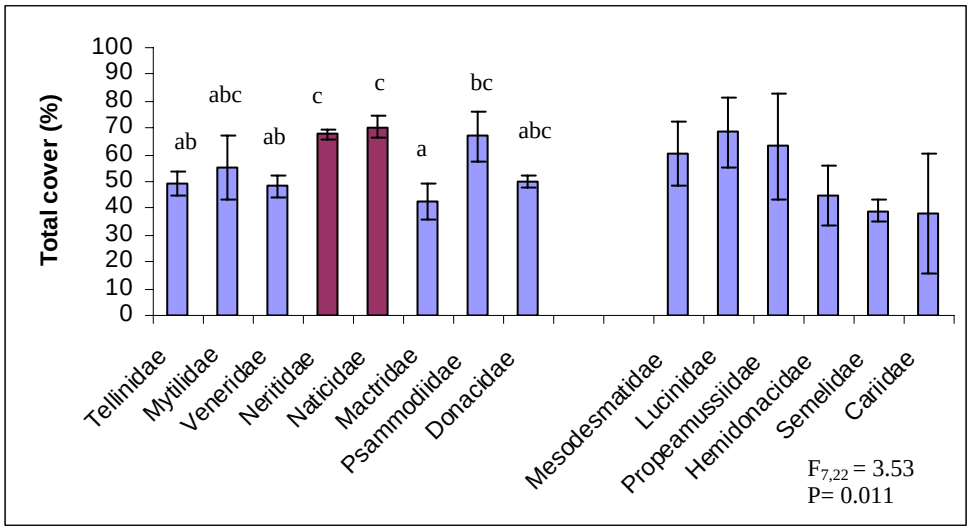

c)

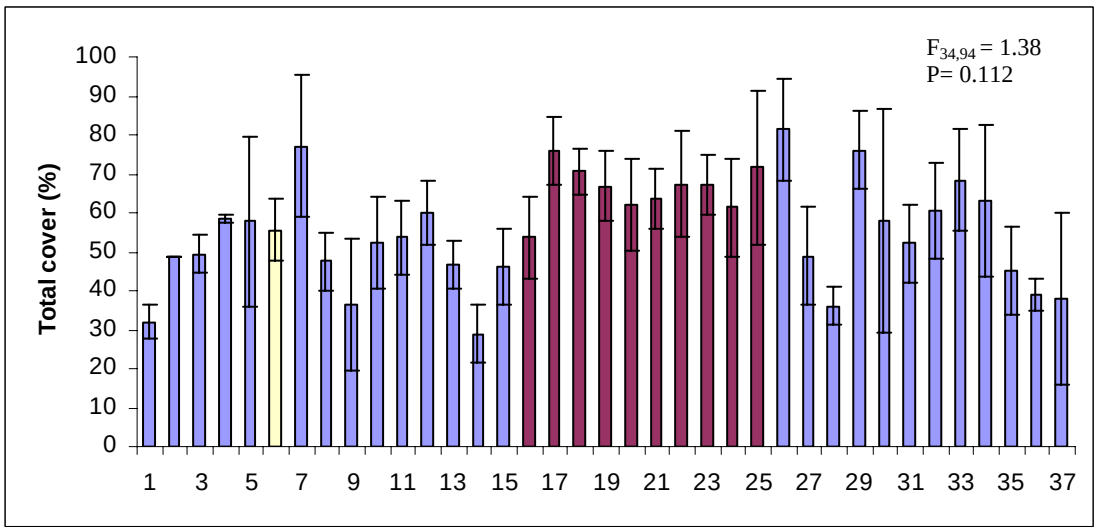

Figure 3.7 Total fouling cover between: a) classes b) families and c) the 36 species and PVC after 12 weeks. Data are means ± one SE. Bars sharing the same letter are not significantly different at α = 0.05, Tukey's Least Significant Difference post-hoc comparison. Columns in blue represent bivalves and those in red are gastropods while the yellow column is PVC. In Figure b) only families on the left hand side of the x-axis are formally analysed as they contain 2 or more species.

Bugula neritina *cover*

The bryozoan *Bugula neritina* was one of the dominant fouling species, occurring on all 36 species. There was no significant difference in *B. neritina* cover at the class level (P = 0.170, Figure 3.8a). At the family level there were significant differences in *B. neritina* cover (P = 0.001, Figure 3.8b). The molluscan family, Donacidae, had a

significantly greater covering of *B. neritina* than all other families with two or more species (SNK post-hoc comparison, Figure 3.8b). There were no significant differences at the species level (P = 0.423, Figure 3.8c). The species with the least fouling cover by *B. neritina* were *A. balloti* (#34) (2.38%), *S. crenulata* (#36) (3.22%) and *G. toreuma* (#14) (4.3%). The species with the highest cover of *B. neritina* were *D. ornate* (#33) (20.91%), *D. cuneatus* (#30) (19.78%) and *D. faba* (#31) (18.64%) (Figure 3.8c).

a)

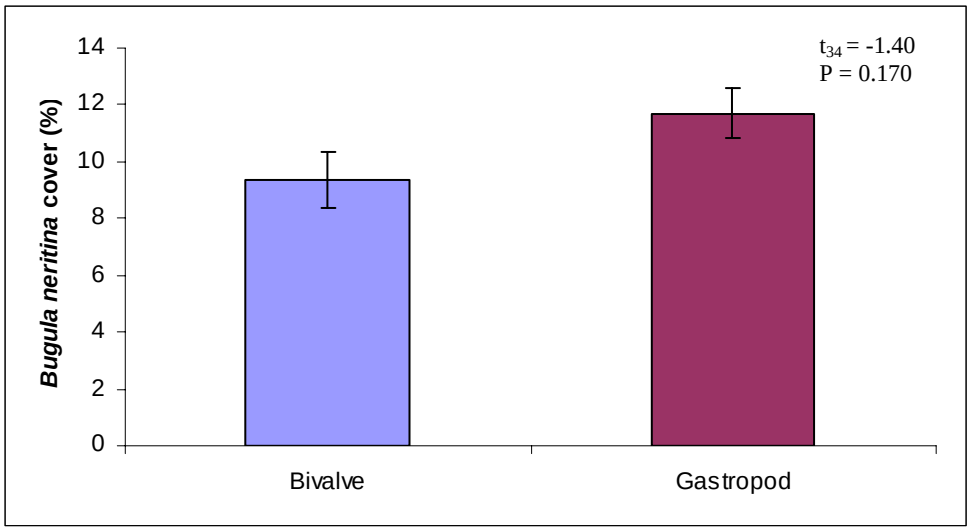

b)

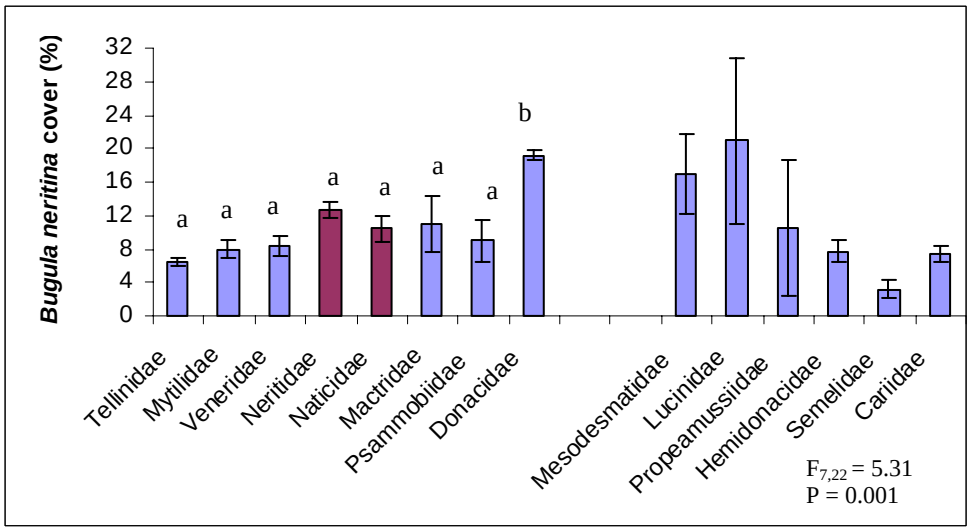

c)

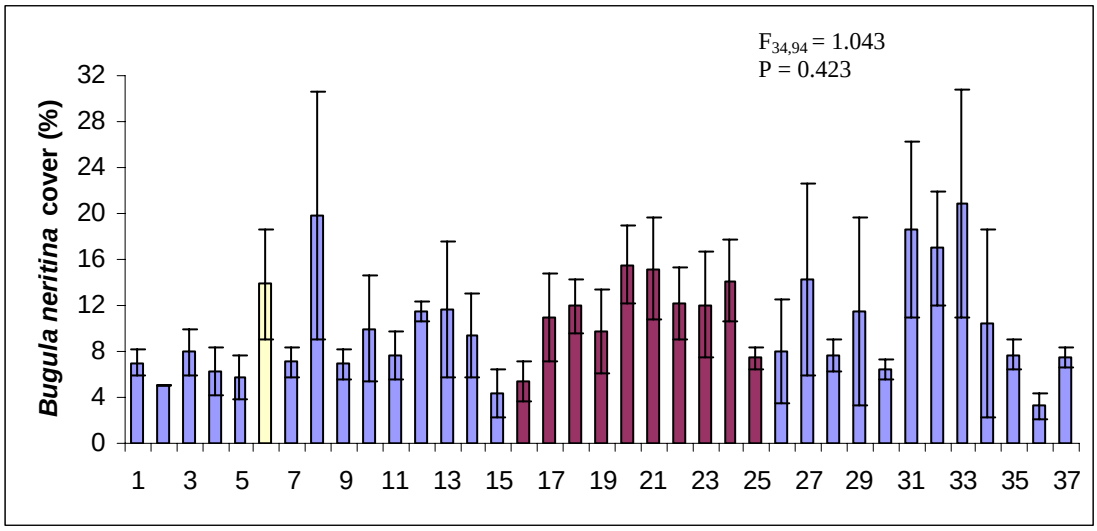

Figure 3.8 *Bugula neritina* fouling cover between: a) classes b) families and c) the 36 species and PVC after 12 weeks. Data are means ± one SE. Bars sharing the same letter are not significantly different at α = 0.05, Student-Newman-Keuls post-hoc comparison. Columns in blue represent bivalves and those in red are gastropods while the yellow column is PVC. In Figure b) only families on the left hand side of the x-axis are formally analysed as they contain 2 or more species.

Colonial ascidian cover

All species were fouled to some extent by colonial ascidians over the 12 weeks of submergence. There were no significant differences between the Bivalves and Gastropods (P = 0.147, Figure 3.9a). At the family level there were significant differences (P = 0.043, Figure 3.9b). The Psammobiidae family had the highest colonial ascidian cover, which was significantly greater than cover on the Donacidae family (SNK post-hoc comparison, Figure 3.9b). However there were no significant differences at the species level (P = 0.436, Figure 3.9c). The species with the most resistance to fouling by colonial ascidians were *T. inflata* (#1) (7.53%), *D. faba* (#31) (10.91%) and *D. juvenilis* (#13) (13.1%). The species with the highest fouling cover by colonial ascidians were *M. micropterus* (#7) (64.92%), *P. mammailia* (#24) (60.95%) and *A. violascenes* (#28) (56.08%) (Figure 3.9c).

a)

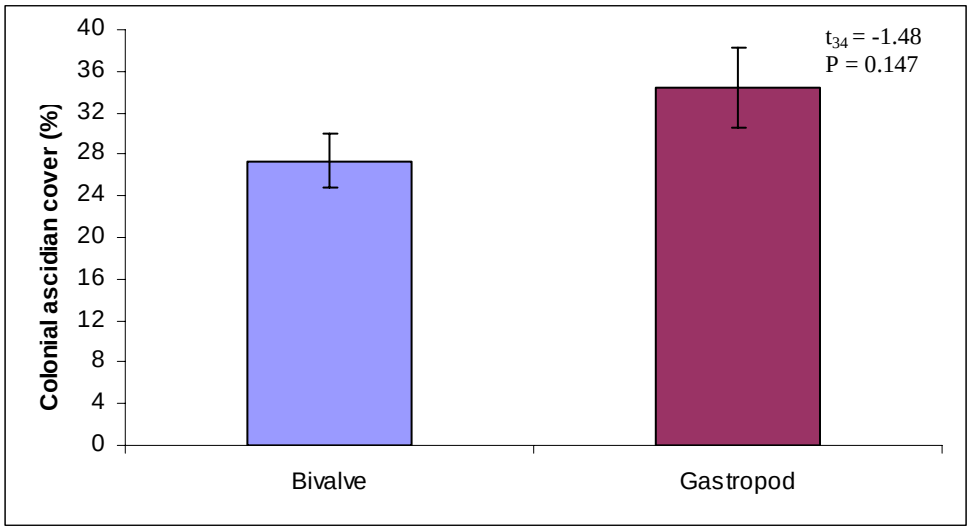
Colonial ascidian cover (%)
40
36
32
28
24
20
16
12
8
4
0
t_{34} = -1.48
P = 0.147
Bivalve
Gastropod

b)

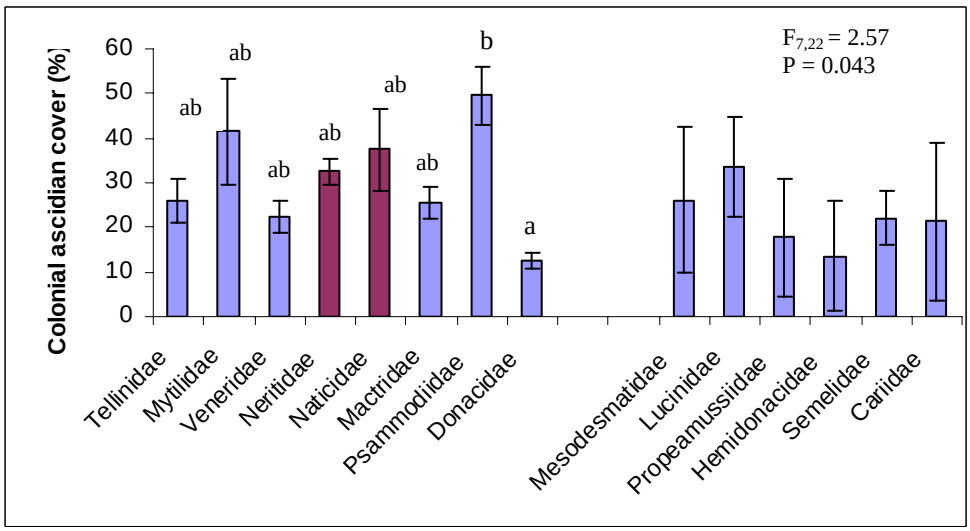
Colonial ascidian cover (%)
60
50
40
30
20
10
0
$F_{7,22}$ = 2.57
P = 0.043
ab
ab
ab
ab
ab
ab
b
a
Tellinidae
Mytilidae
Veneridae
Neritidae
Naticidae
Mactridae
Psammodiidae
Donacidae
Mesodesmatidae
Lucinidae
Propeamussiidae
Hemidonacidae
Semelidae
Cariidae

c)

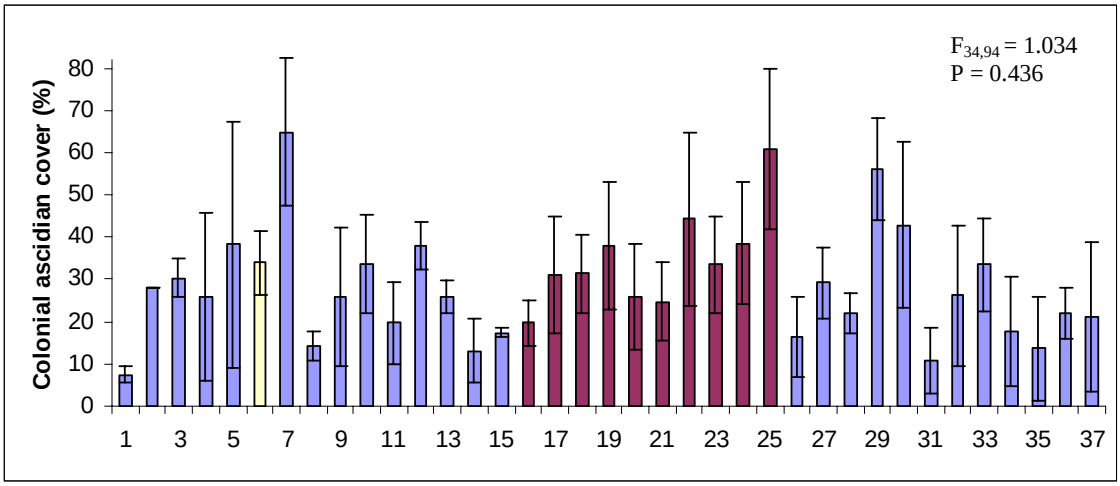

Figure 3.9 Colonial ascidian fouling cover between: a) classes b) families and c) the 36 species and PVC after 12 weeks. Data are means ± one SE. Bars sharing the same letter are not significantly different at α = 0.05, Student-Newman-Keuls post-hoc comparison. Columns in blue represent bivalves and those in red are gastropods while the yellow column is PVC. In Figure b) only families on the left hand side of the x-axis are formally analysed as they contain 2 or more species.

Spirorbid cover

There were no significant differences in covering of spirorbid tubeworms between bivalves and gastropods (P = 0.315, Figure 3.10a). There was also no significant difference in spirorbid covering between families (P = 0.532, Figure 3.10b) with most having between 2-6% cover. The spirorbid tubeworms occupied the surface of all 36 species and there was no significant differences at this level (P = 0.092, Figure 3.10c). Most species had less than 5% fouling cover by spirorbid tubeworms, the least cover occurred on *S. atrata* (#29)(0.44%), *N. robillardi* (#25)(1.04%) and *M. olorina* (#27)(1.06%). In contrast *S. crenulata* (#36) (11.44%), *N. undata* (#20) (9.98%) and *D. ornate* (#33) (7.26%) had a higher covering by spirorbid tubeworms (Figure 3.10c).

a)

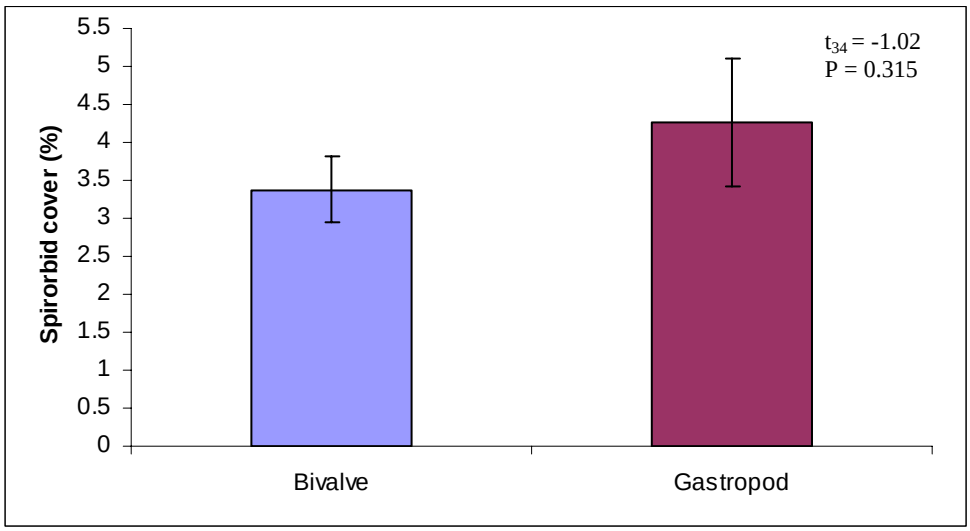

b)

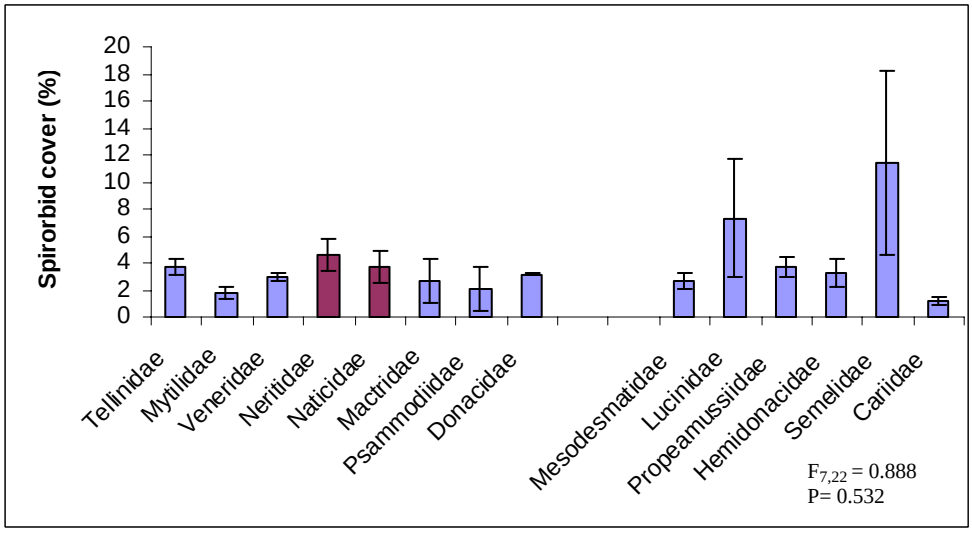

c)

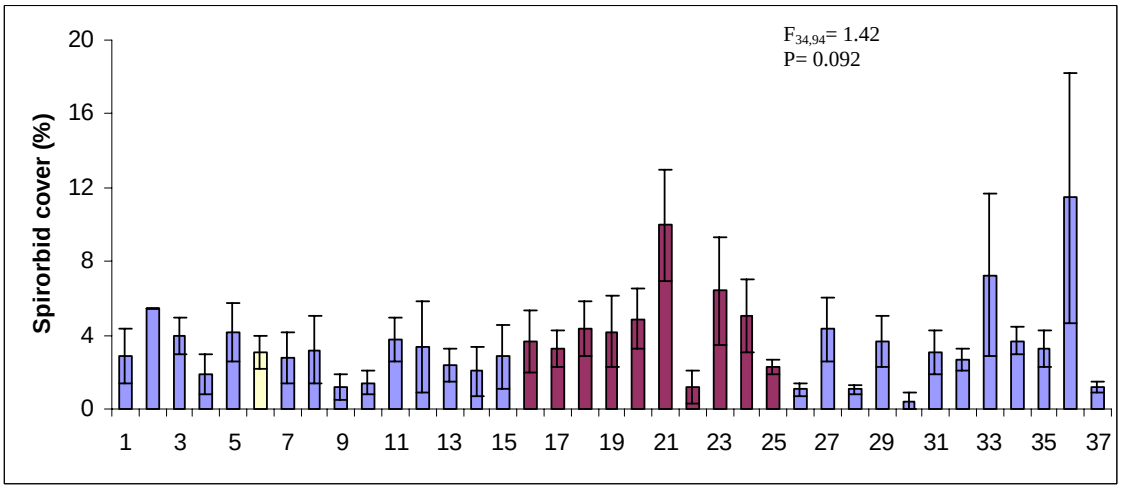

Figure 3.10 Spirorbidae fouling cover between: a) classes b) families and c) the 36 species and PVC after 12 weeks. Data are means ± one SE. Columns in blue represent

bivalves and those in red are gastropods while the yellow column is PVC. In Figure b) only families on the left hand side of the x-axis are formally analysed as they contain 2 or more species.

Algal cover

Algal cover did not differ significantly between classes (P = 0.483, Figure 3.11a). There were also no significant differences at the family level (P = 0.149, Figure 3.11b). However, the Mytilidae family had no algal cover. Five of the 36 species resisted algal fouling completely, whilst the remaining species had between 1 and 10% cover. However, there were no significant differences at this level (P = 0.092, Figure 3.11c). The highest covering of algae was on *T. linguafelis* (#2)(9.99%), *D. plana* (#32)(7%) and PVC (#6)(4.74%), while the five species with no algal cover were *M. micropterus* (#7), *M. galloprovincialis* (#8), *S. bilocularis* (#9), *P. mammailia* (#24) and *D. faba* (#31)(Figure 3.11c). All three Mytilidae species had zero algal cover.

a)

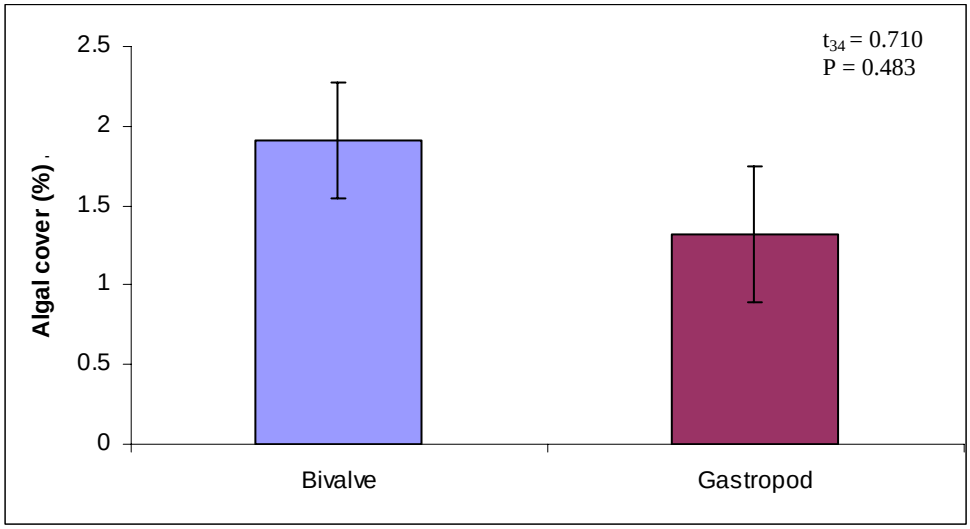

b)

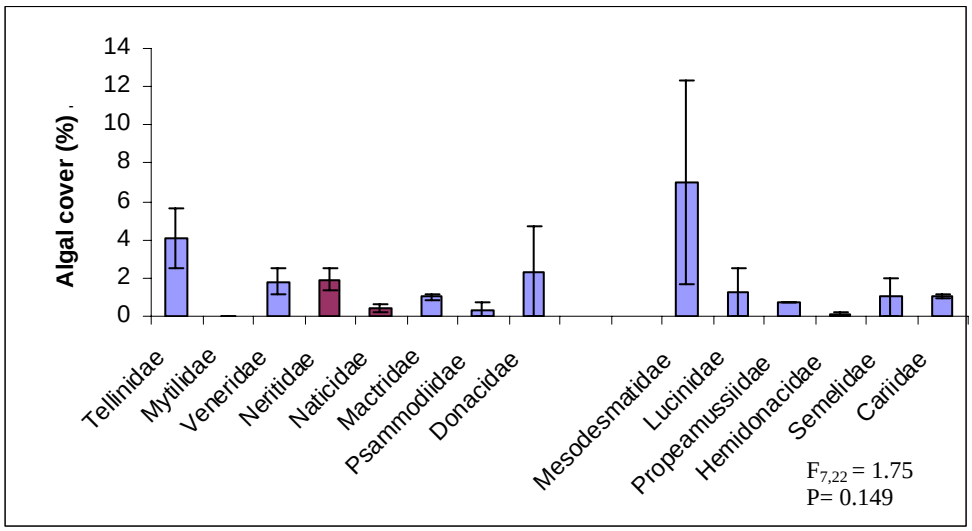

c)

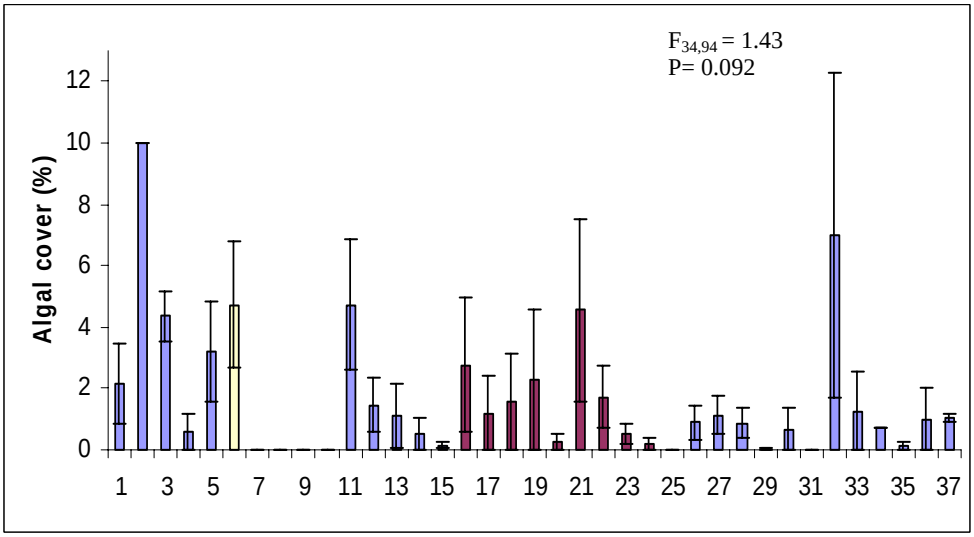

Figure 3.11 Algal fouling cover between: a) classes b) families and c) the 36 species and PVC after 12 weeks. Data are means ± one SE. Columns in blue represent bivalves and those in red are gastropods while the yellow column is PVC. In Figure b) only families on the left hand side of the x-axis are formally analysed as they contain 2 or more species.

Encrusting bryozoan cover

Fouling cover by encrusting bryozoans varied extensively between the 36 species from complete resistance up to 54% cover. Bivalves had significantly lower encrusting bryozoan cover than gastropods (P = 0.027, Figure 3.12a). At the family level there were no significant differences (P = 0.339, Figure 3.12b). The Mactridae family had the highest encrusting bryozoan cover and the Mytilidae family had the least cover (Figure

3.12b). There were also no significant differences at the species level (P = 0.290, Figure 3.12c). Two species, *T. linguafelis* (#2) and *M. dissimilis* (#26), had no encrusting bryozoan cover after 12 weeks, in contrast the species with the least resistance were *N. robillardi* (#25)(54%), *N. plicata* (#16)(29.33%) and *G. tumidum* (#15)(21.5%)(Figure 3.12c).

a)

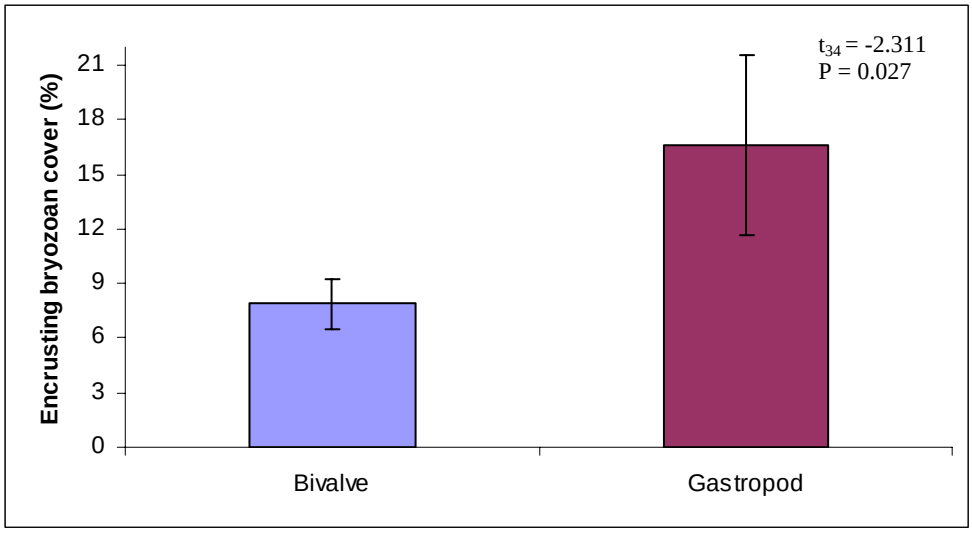

b)

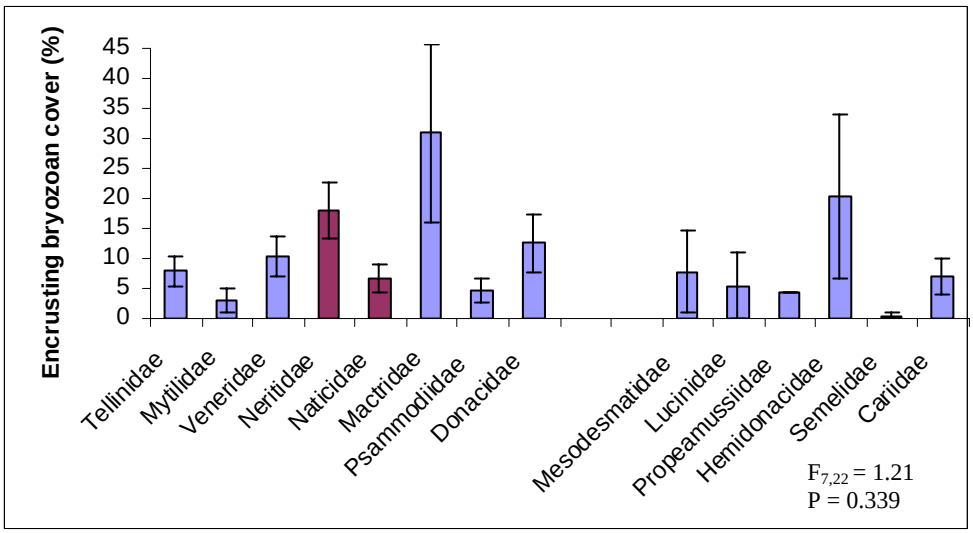

c)

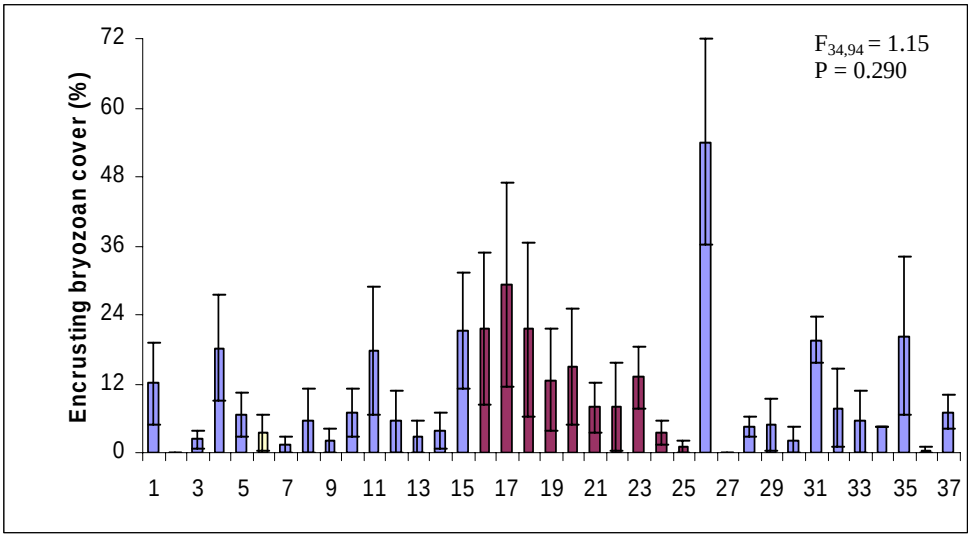

Figure 3.12 Encrusting bryozoan fouling cover between: a) classes b) families and c) the 36 species and PVC after 12 weeks. Data are means ± one SE. Columns in blue represent bivalves and those in red are gastropods while the yellow column is PVC. In Figure b) only families on the left hand side of the x-axis are formally analysed as they contain 2 or more species.

3.3.3 Surface roughness and fouling cover correlations

There were a number of significant correlations between total fouling cover, species specific fouling cover, and the individual roughness parameters generated in Chapter 2 (highlighted in Table 3.5). Total fouling cover was positively correlated to the fractal dimension of a surface (Figure 3.13g, r = 0.376, P = 0.022) and therefore the more fractal or complex a surface is the more likely it is to have a higher overall fouling cover. In contrast, total fouling cover was negatively correlated to Rsk (Figure 3.13i, r = -0.357, P = 0.030) and Wsk (Figure 3.13c, r = -0.371, P = 0.024). This means that surfaces with a greater distribution of peaks about the mean line had lower overall fouling cover. Algal cover was negatively correlated to hydrophobicity (Figure 3.13f, r = -0.395, P = 0.021) and therefore surfaces which were most hydrophobic had lower algal cover. In accordance with total fouling cover, spirorbid tubeworm cover was positively correlated to fractal dimension (Figure 3.13h, r = 0.342, P = 0.039). Encrusting bryozoan cover was negatively correlated to both Rsk (Figure 3.13a, r = -0.329, P = 0.046) and Wsk (Figure 3.13d, r = -0.367, P = 0.025). This means those surfaces with few peaks about the mean line had the highest encrusting bryozoan cover.

In contrast macro-algal cover was positively correlated to both Rsk (Figure 3.13e, r = 0.469, P = 0.003) and Wsk (Figure 3.13b, r = 0.423, P = 0.009).

Table 3.5 Correlations between surface roughness parameters and species specific fouling cover for the 36 species. Pearson's coefficients (r) and p-values (beneath) are listed for each correlation.

	Total cover	*B. neritina* cover	Col. ascidian cover	Spirorbid cover	Algal cover	Encrusting byryozoan
Ra	.194	-.116	.317	.087	-.038	-.099
	.249	.494	.056	.609	.824	.560
Wa	-.213	.117	-.138	-.074	-.224	-.110
	.205	.492	.415	.664	.182	.518
Str	-.174	.204	-.268	.031	.158	-.020
	.303	.226	.109	.858	.349	.906
Fractal dimension	**.376(*)**	-.155	.274	**.342(*)**	.151	.135
	.022	.359	.100	**.039**	.374	.427
Rsk	**-.357(*)**	.152	-.247	-.101	**.469(*)**	**-.329(*)**
	.030	.369	.141	.554	**.003**	**.046**
Wsk	**-.371(*)**	.149	-.225	-.088	**.423(*)**	**-.367(*)**
	.024	.378	.181	.603	**.009**	**.025**
Hydrophobicity	-.145	.149	-.163	-.168	**-.395(*)**	.077
	.413	.399	.357	.343	**.021**	.666
Total fouling cover	1	.293	**.623(**)**	.071	-.061	**.361(*)**
		.078	**.000**	.676	.718	**.028**
Bugula neritina cover	.293	1	-.036	.143	.095	-.036
	.078		.834	.398	.576	.833
Colonial ascidian cover	**.623(**)**	-.036	1	-.039	-.164	**-.385(*)**
	.000	.834		.820	.333	**.019**
Spirorbis cover	.071	.143	-.039	1	.213	-.174
	.676	.398	.820		.205	.303
Algal cover	-.061	.095	-.164	.213	1	-.146
	.718	.576	.333	.205		.390
Encrusting bryozoan cover	**.361(*)**	-.036	**-.385(*)**	-.174	-.146	1
	.028	.833	**.019**	.303	.390	

** Correlation is significant at the 0.01 level (2-tailed).
* Correlation is significant at the 0.05 level (2-tailed).

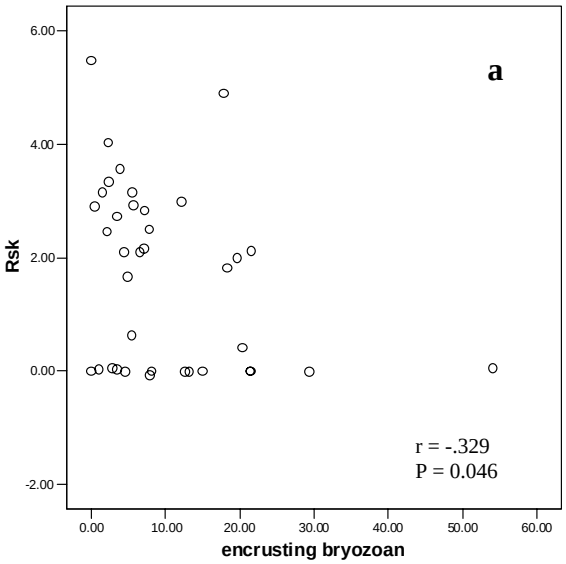
a
Rsk
encrusting bryozoan
r = -.329
P = 0.046

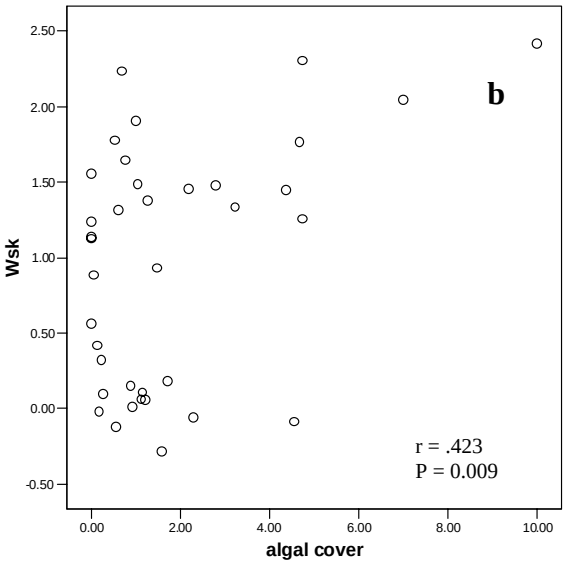
b
Wsk
algal cover
r = .423
P = 0.009

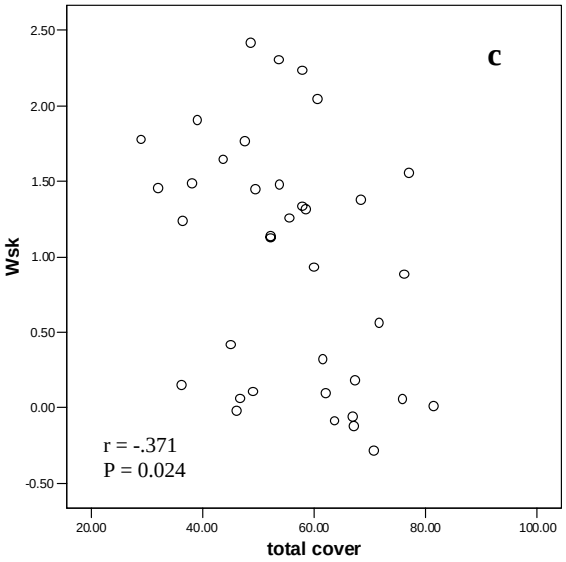
c
Wsk
total cover
r = -.371
P = 0.024

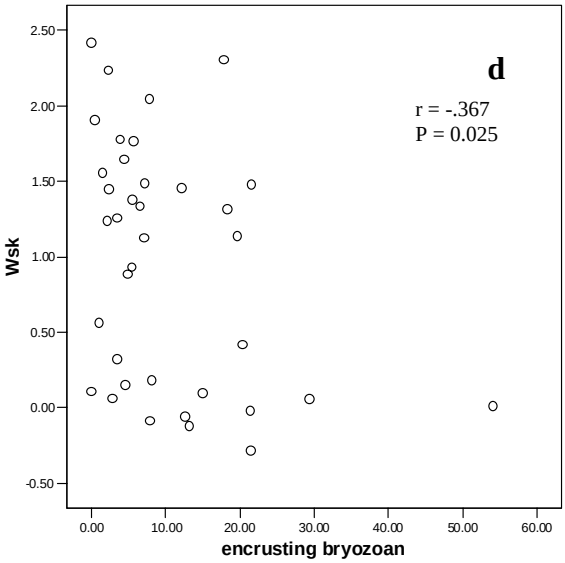
d
Wsk
encrusting bryozoan
r = -.367
P = 0.025

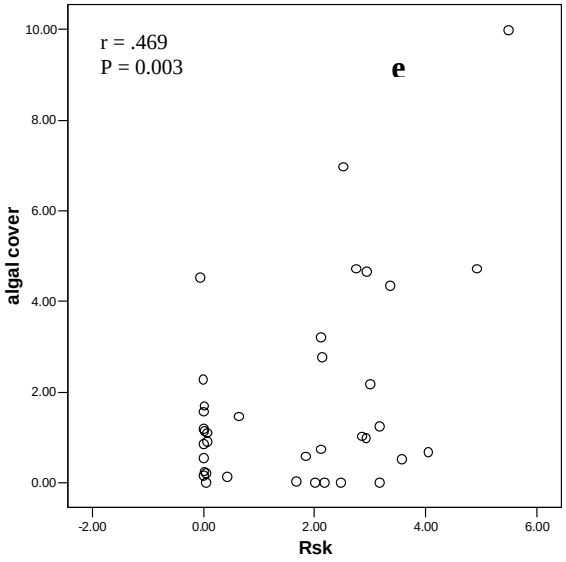
e
algal cover
Rsk
r = .469
P = 0.003

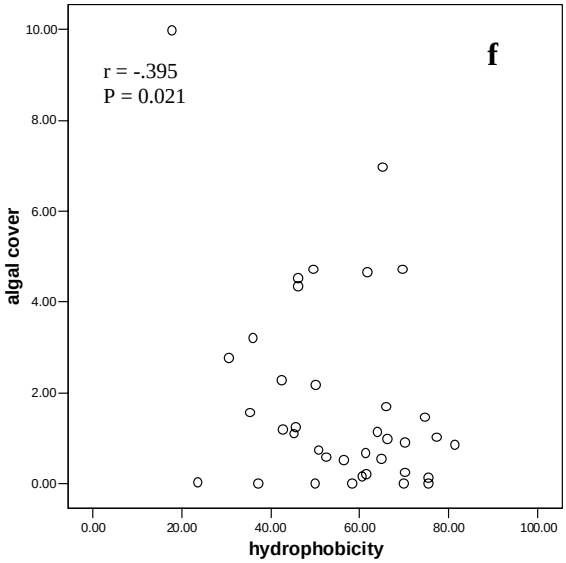
f
algal cover
hydrophobicity
r = -.395
P = 0.021

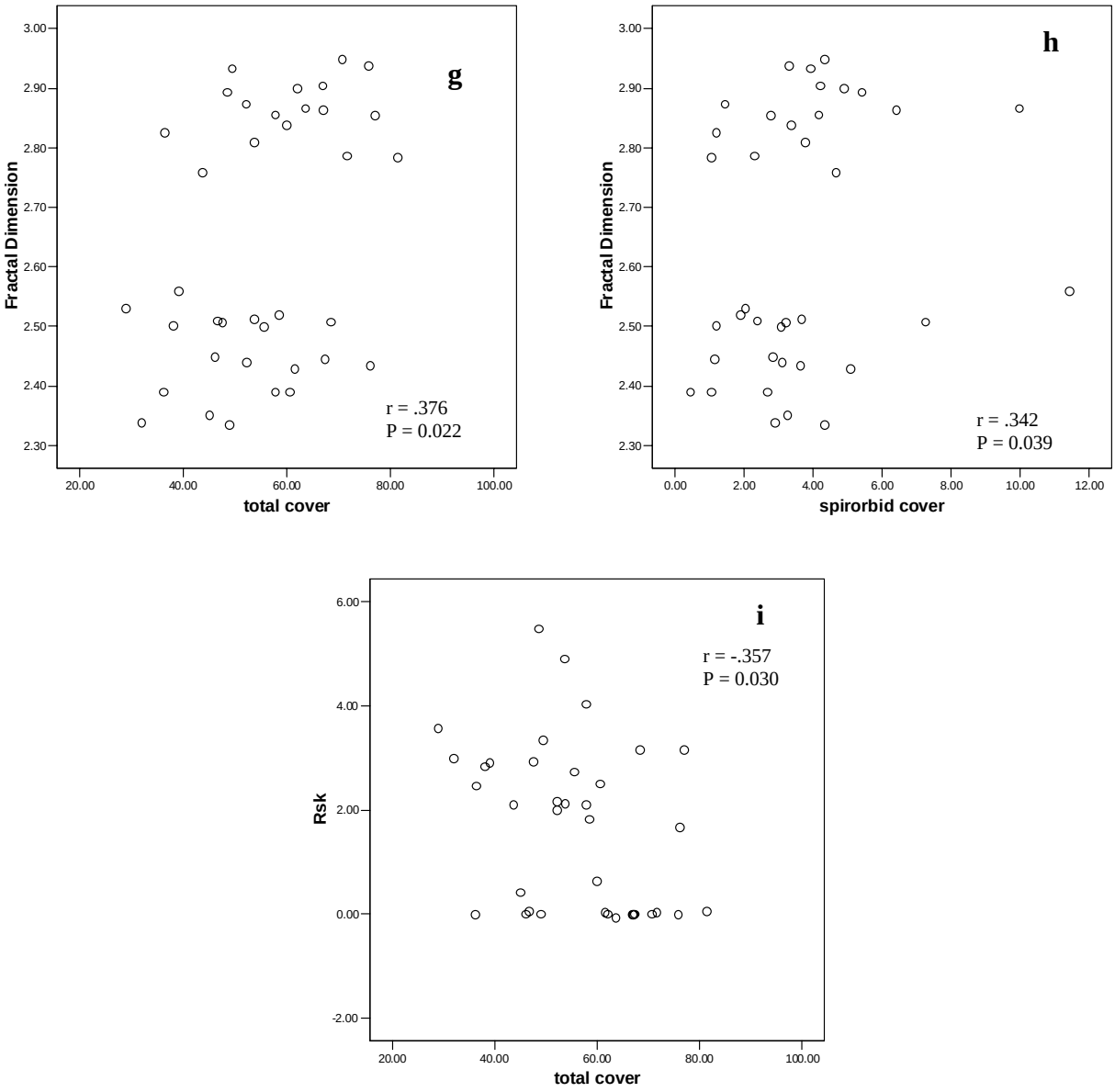

Figure 3.13 Scatter plots of significant correlations between roughness parameters and fouling cover. Data are mean value from the 36 mollusc species and the PVC control. a) Rsk versus encrusting bryozoan cover b) Wsk versus algal cover c) Wsk versus total fouling cover d) Wsk versus encrusting bryozoan cover e) algal cover versus Rsk f) algal cover versus hydrophobicity g) fractal dimension versus total cover h) fractal dimension versus spirorbid cover i) Rsk versus total fouling cover

3.3.4. Fouling adhesion and removal

Percent fouling removal

The lowest surface pressure (76.28 kPa) removed over 70% of the total fouling cover for most mollusc species, including almost all the fouling cover by *Bugula neritina*,

colonial ascidians, encrusting bryozoans and spirorbid tubeworms (Figure 3.14c). However, very little algal cover was removed. Subsequent increases in surface pressures, up to 195.51 kPa, produced no further increases in percent fouling removal from the shell surfaces. Due to the vast majority of fouling organisms being removed at the lowest surface pressure only total fouling cover removal from the first water jet (76.28 kPa) was subsequently analysed (Figure 3.14).

Fouling removal on bivalves (75.5%) was slightly higher than on gastropods (68.4%) at 76 kPa, however this difference was not significant (P = 0.153, Figure 3.14a). There were no significant differences in fouling removal between families (P = 0.141, Figure 3.14b). Fouling removal was highest on the Mytilidae family (88.5%) whilst fouling adhered more strongly to the gastropod Naticidae and bivalve Mactridae families (65% removal) (Figure 3.14b). On most of the 36 species fouling cover was easily removed at the lowest surface pressure (76.28 KPa) used and there were no significant differences at this level (P = 0.413, Figure 3.14c). Fouling adherence was weakest on *Septifer bilocularis* (#9), *M. galloprovincialis* (#8) and *Hemidonax* sp. (#35) with fouling removal of 99.3%, 92.2% and 91.2% respectively (Figure 3.13c). The species on which fouling had the greatest adherence were *Tellina linguafelis* (#2)(37% removal), *Polinices conicus* (#22)(44.7% removal) and *A. balloti* (#34)(58% removal).

a)

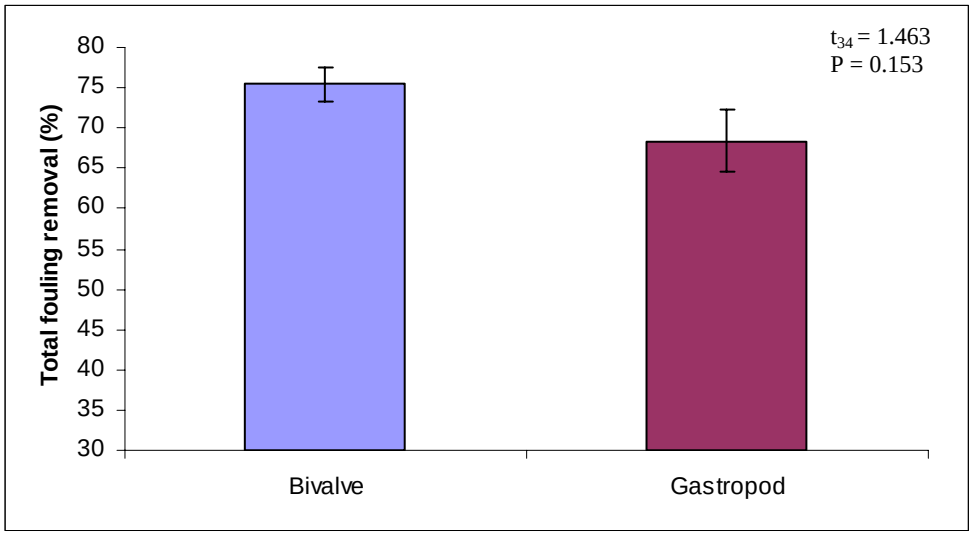

b)

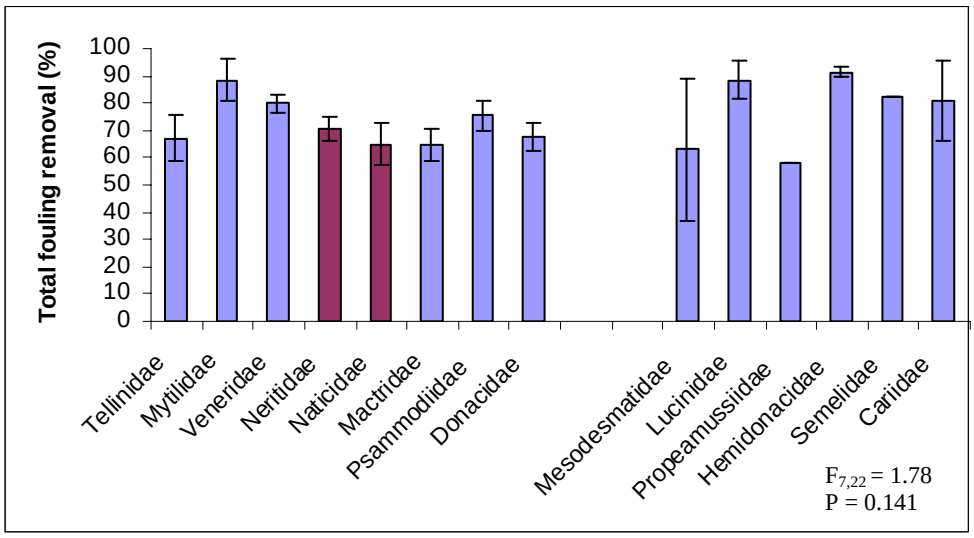

c)

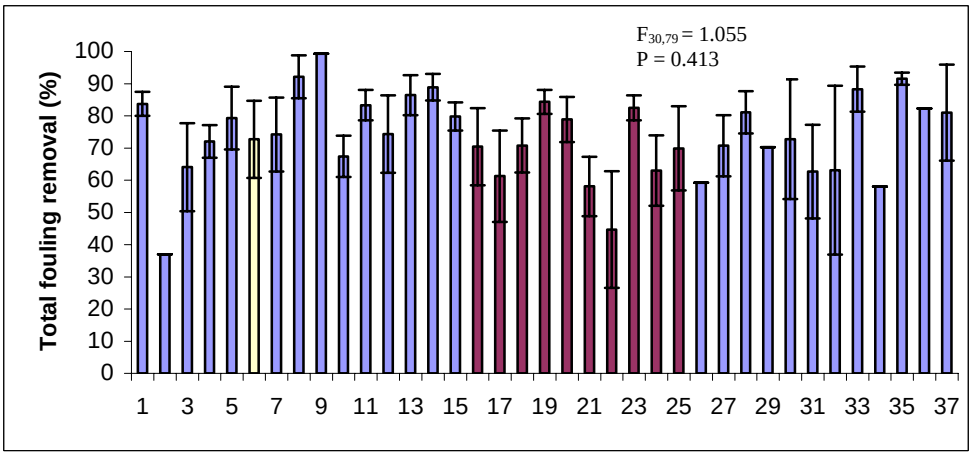

Figure 3.14 Total fouling removal between: a) classes b) families and c) the 36 species and PVC after 12 weeks. Data are means ± one SE. Columns in blue represent bivalves and those in red are gastropods while the yellow column is PVC. In Figure b) only families on the left hand side of the x-axis are formally analysed as they contain 2 or more species.

Algal cover was almost exclusively the only remaining fouling cover after exposure to water jets. The strong adherence of algae is demonstrated by a significant negative correlation with algal percent removal, i.e. species with a higher covering of algae had a lower percent removal of fouling after exposure to a water jet (Table 3.6).

Table 3.6 Correlations between % fouling removal and species specific fouling cover.

	% fouling removal
Total fouling cover	-.237
	.158
Bugula. neritina cover	-.004
	.980
Colonial ascidian cover	-.160
	.345
spirorbid cover	-.066
	.700
Algal cover	**-.451(**)**
	.005
Encrusting bryozoan cover	.018
	.917

** Correlation is significant at the 0.01 level (2-tailed).

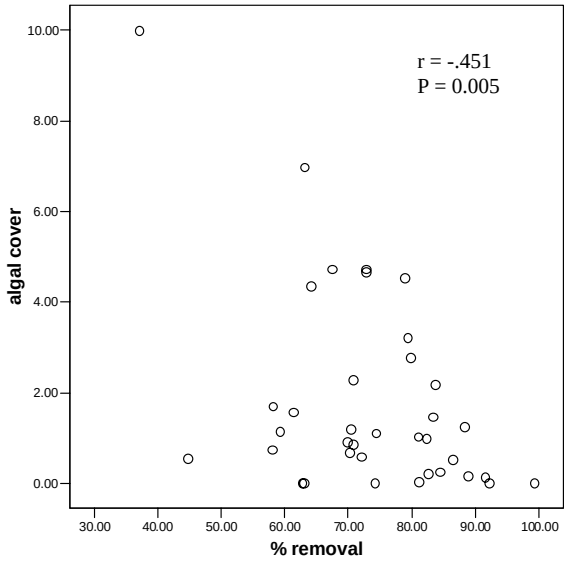

Figure 3.15 Scatter plots of means of algal cover versus percent fouling removal for the 36 species and PVC.

Of the roughness parameters determined for the 36 species and PVC in Chapter 2 only mean waviness was significantly correlated to total percent fouling removal (P = 0.008, Table 3.7). This means that species with higher mean waviness profiles had the highest removal of total fouling after exposure to a water jet.

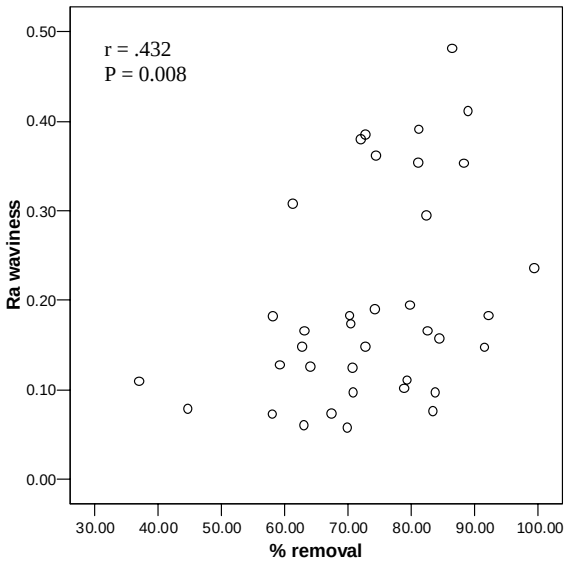

Figure 3.16 Scatter plot of means of waviness profiles (Rw) versus percent fouling removal for the 36 species and PVC.

Table 3.7 Correlations between % fouling removal and roughness parameters of the 36 species and PVC

	Total fouling removal
Total fouling cover	1.000
	.
Ra roughness	.149
	.380
Wa waviness	**.432(**)**
	.008
Str	.019
	.909
Fractal dimension	-.111
	.513
Rsk-rough	.170
	.313
Wsk-waviness	.024
	.888
Hydrophobicity	-.007
	.969

** Correlation is significant at the 0.01 level (2-tailed).

Table 3.8 Summary of significant differences at the Class, Family and Species level between total fouling cover, species specific fouling cover, and total percent fouling removal. Significant correlations between roughness parameters and fouling cover and removal are also listed.

	Total cover	***Bugula neritina***	**Colonial ascidian**	**Spirorbid**	**Algae**	**Encrusting bryozoan**	**% removal**
Class	Y	N	N	N	N	Y	N
Family	Y	Y	Y	N	N	N	N
Species correlation	Rsk , Wsk Fd	-	-	Fd	Rsk , Wsk, Hydrophob	Rsk , Wsk	Wa Algal cov.

Y= significant difference at $\alpha = 0.05$; N= no significant difference at $\alpha = 0.05$

3.4 Discussion

Surface characteristics of molluscs clearly affect the settlement and attachment strength of fouling organisms. The 36 species examined varied widely in the level of fouling cover after 12 weeks exposure. There were also significant differences between classes and families of molluscs in total fouling cover, species-specific fouling cover and fouling removal (i.e. attachment strength of fouling organisms). Correlations determined for fouling resistance and surface roughness parameters further support a role for surface topography as a physical defence against fouling. In addition to deterrence, some correlations between surface characteristics and the strength of attachment of fouling were also evident. This is the first report of natural surfaces affecting attachment strength and its correlation with quantified surface characteristics.

The 36 species tested came from two molluscan classes, Bivalvia and Gastropodia. Overall, gastropods were more fouled than bivalves and, in particular, had higher encrusting bryozoan cover. Significant differences at such a high taxonomic level are unexpected and one possible explanation for these differences is variation in surface properties between these two classes. For example, bivalves have significantly higher Rsk values in both the roughness and waviness profiles whereas gastropods have significantly higher fractal dimensions (Chapter 2). Furthermore, total fouling cover positively correlated with fractal dimension and negatively correlated with Rsk roughness (Table 3.5). This means that total fouling cover is highest on surfaces with a

high fractal dimensions and a low Rsk roughness. Such roughness characteristics are typical of gastropod surfaces.

There were few significant differences in fouling at the family taxonomic level. The two gastropod families, Naticidae and Neritidae, were significantly more fouled than the Tellinidae, Veneridae and Mactridae families. For species specific fouling cover the Donacidae family had significantly more *Bugula neritina* cover than all other families whilst the Psammobiidae family had significantly more colonial ascidian cover than the Donacidae family. The Mytilidae family had no macro-algal cover. All other families did not differ for either the total or any species-specific fouling cover or in fouling removal. Significant differences in fouling cover at this taxonomic level are not unexpected as families differed significantly in all roughness properties measured in Chapter 2. However, there were no significant differences in fouling cover between the 36 species. The comparison of several different means (36 for species) may have contributed to no significant differences being detected at this taxonomic level. Despite the lack of significant differences there were large differences in fouling cover between families and species with some species being fouled more than twice as much as others. For example *Modiolus micropterus* and *Mactra disimilis* had 80% total cover, compared to 30% total cover for *Tellina inflata* and *Globivenus toreuma*. Harper (1997) notes that the periostracum thickness of bivalves and gastropods is highly variable and has most likely evolved based on life habitats such as burrowing, cementing or free swimming. It is plausible that surface roughness characteristics of the shell could also have evolved based on the life habitats of classes and families of molluscs. In the present study all mollusc shells collected were visually examined to ensure the periostracum was intact and free from abrasions.

A complex surface may provide more potential settling sites for fouling organisms. This would explain why total fouling cover was positively correlated to fractal dimension, as surfaces that were more fractal or complex had the highest levels of fouling. A similar concept has been explored for barnacle cyprids (Hills et al 1999) and theoretical attachment points for diatoms (Scardino et al 2006; Chapter 5) and other macrofoulers (Chapter 6). Hills et al. (1999) found that densities of *Semibalanus balanoides* were positively correlated to Potential Settling Sites (PSS) and Minkowski fractal dimensions. It was concluded that PSS which is based on cyprid body size and

behaviour in relation to surface topography was the most important factor driving settlement density. A highly complex surface will have many scales of roughness and hence potentially provide a range of settlement sites for a broad range of larval/cell sizes. This may explain the positive correlation to total fouling cover.

The second most important roughness parameter was Rsk. Surfaces with the highest levels of total fouling cover had lower Rsk values. However, surfaces with high Rsk values, such as those from the Mytilidae family, have a greater distribution of peaks while low Rsk rough surfaces (values close to 0) tend to be smoother as they have neither a high distribution of peaks or valleys about the mean line. Surfaces with homogeneous peaks/ripples have reduced fouling compared to smooth surfaces (Berntsson et al. 2000a; Petronis et al. 2000; Scardino & de Nys, 2004; Chapter 4, Chapter 5). Berntsson et al. (2000a) and Petronis et al (2000) both found significant reductions in *Balanus improvisus* settlement on a range of micro-pyramids and projections compared to smooth surfaces whilst Scardino & de Nys, (2004) found that mussel shells and biomimics of *Mytilus galloprovincialis* which have micro-ripples were significantly less fouled that smooth shells and biomimics of the scallop, *Amusium balloti*. These studies support the present studies findings that smoother surfaces without peaks tend to foul more rapidly.

Algal cover was negatively correlated with surface hydrophobicity. As such, surfaces with the least algal cover had the highest hydrophobicities. Several papers have explored the influence of hydrophobicity on fouling, often demonstrating species specific responses (Finlay et al 2002a). Hydrophobicity is believed to deter certain species of green algae, bryozoans and barnacles though the effects can diminish with time (Zhang et al. 2005). Finlay et al (2002a) found that the green alga *Ulva* (*Enteromorpha*) had the highest adhesion strength on hydrophilic surfaces. Cell detachment was recorded on surfaces of varying hydrophobicities which are similar to the range found on mollusc surfaces in the present study. With a shear stress of 56 Pa, hydrophilic surfaces (< 40º) had < 30% spore removal compared to over 90% removal on hydrophobic surfaces (80-100º) (Finlay et al. 2002a). Interestingly all three Mytilid species used in this study were completely free of algal cover. Mytilids are known to resist fouling longer than other natural surfaces (Scardino et al. 2003; Scardino & de Nys, 2004). The Mytilids species in this study, however, did not have exceptional

hydrophobicities. This points towards other factors which may have prevented algal fouling, including small-scale microtextures or the properties of the periostracum. The presence of an intact periostracum on *Mytilus galloprovincialis* is known to deter *Balanus improvisus* cyprids (Scardino et al. 2003) though this remains untested for algal spores. It should be noted that algae was not a dominant fouling group at this site (< 5%) and more concentrated fouling laboratory bioassays would be warranted to elucidate the aforementioned effects.

The self-cleaning ability of a surface has increased in importance with the advent of foul-release coatings. Surfaces may foul at the same rate, however, the force required to remove fouling can vary markedly. This is of great importance if the force is relevant to boat operating speeds. In this study the removal of fouling from a known surface pressure varied widely across the 36 species. The percent fouling removal correlated positively with mean waviness (Wa) and negatively with algal cover. As such, surfaces with the highest waviness profiles had the weakest fouling adherence. This finding could provide an important consideration for the design of novel surfaces or coatings. Whilst foul-release surfaces are generally characterised for their surface energy and critical surface tensions (Anderson et al. 2003), they have not previously been characterised for waviness profiles. The bulk properties of a surface are also important to fouling-release. The best performing fouling-release surfaces are made from low modulus materials (Anderson et al. 2003). The mollusc shells used in this study were relatively high modulus materials. Future biomimetic design will need to consider adopting optimal roughness parameters coupled with low surface energy and low modulus materials.

The lowest surface pressure used reduced a large quantity of the fouling (70-80%). Ideally lower surface pressures should be used first. The surface pressures chosen in this study were based on approximations to boat operating speeds (Finlay, 2002b). Such high fouling removal rates in the present study was unexpected and could have been due to adhesive or cohesive failure of bioadhesives as the surfaces were briefly exposed to air. Future studies will be designed in flow-chambers which keep the test surface fully immersed and allows for gradual increases in surface pressure.

Surfaces with higher algal cover had the lowest fouling removal as algae adhered to the highest surface pressures tested (195 kPa). This is consistent with Finlay et al. (2002b) which found that spores of *Ulva* (*Enteromorpha*) would not detach after 8 h with surfaces pressures in excess of 250 kPa. Granhag et al. (2004) determined that when roughness was introduced to surfaces a decreased force of 122 kPa was required to remove *Ulva* (*Enteromorpha*) spores.

There have been several studies which have quantified the surface pressure required to remove fouling with a water jet (Swain & Schultz, 1996; Finlay et al. 2002b; Granhag et al. 2004). Finlay et al. (2002b) demonstrated the relevance of surface pressure to the friction caused by operating vessels. Using the Power Law formula they calculated surface pressure and approximated it to equivalent wall shear stress. Therefore surface pressures of between 130-210 kPa equated to wall shear stress values of 194-275 Pa and are equivalent to ship speeds of 25- 35.5 knots (Holland et al. 2004). This study has used a far simpler water jet to detach fouling, however the recorded surface pressures (75-195 kPa) are of comparable magnitude and the technique is similar to that used by boat cleaners universally. Whilst the surfaces pressures should be interpreted with caution they do demonstrate the importance of flow in determining fouling adherence. Future studies will examine biomimetic surfaces in flow chambers to determine more precisely the forces required to remove adhered epibionts.

In summary, this study has shown the importance of surface roughness to fouling resistance and removal. For the first time natural surfaces have been quantitatively characterised and the determined surface parameters correlated to fouling resistance. These findings will aid in understanding the required shape of foul-release coatings to produce a biomimetic surface with effective antifouling properties.

CHAPTER FOUR

Fouling deterrence on natural bivalve surfaces: a physical phenomenon?[1]

4.1 Introduction

This Chapter builds on the findings of the surface characterisation (Chapter 2) and fouling deterrence (Chapter 3) of bivalve surfaces. The broad ranges of fouling resistances observed from the surfaces of the 36 molluscs tested in Chapter 3 leads to questions as to whether resistance to fouling is due to physical and/or chemical forces associated with the shell surface. To address this three bivalves with different surface structures and fouling resistant properties are chosen for biomimicry to test whether the copied surfaces (thereby eliminating potential surface chemistry) will perform as well as the natural surfaces in field exposures.

Surface microtopography influences the settlement and growth of fouling organisms and has primarily been demonstrated using artificially textured surfaces (Hills & Thomason 1998a, b, Andersson et al. 1999, Kohler et al. 1999, Berntsson et al. 2000a, Berntsson et al. 2000b, Petronis et al. 2000, Callow et al. 2002, Thomason et al. 2002). In these studies, the response to surface microtopography is often species specific and dependent on the surface profile (roughness). This settlement response may be related to the number of adhesion points a settling organism can make on a surface (Callow et al. 2002). For example, artificial structures in the order of 5μm to 1mm applied to polydimethyl siloxane (PDMS) elastomers affect the settlement of *Ulva linza* (= *Enteromorpha linza*) spores with preferential settlement in micro-ridges of the same size (5-10μm) as the spores, or against the pillar wall and floor when the ridges are wider (Callow et al. 2002). Microtexture can also deter settlement with a range of feature widths including micro-ridges of 30-45μm (Berntsson et al. 2000a; b) and 50-100 μm (Andersson et al. 1999), and micro-pyramids 33-97μm (Petronis *et al.* 2000) deterring the settlement of cyprids of the barnacle *Balanus improvisus*. In contrast, larger scale roughness (0.5-1mm) is preferred by diatoms, ciliates, bryozoans, the

[1] Chapter 4 is adapted from Scardino, A.J. & de Nys, R. (2004) Fouling deterrence on the bivalve shell *Mytilus galloprovincialis*: A physical phenomenon? *Biofouling* 20(4-5): 249-257.

mussel *Mytilus edulis,* and the barnacle *Balanus improvisus* (Kohler et al. 1999), while settlement tiles with a roughness of 2-4mm reduced settlement by the barnacle *Semibalanus balanoides* (Hills & Thomason, 1998b). No single artificially textured surface prevents the settlement of a range of fouling organisms.

The objective of this study was to mimic the surfaces of selected bivalves collected in Chapter 2 and compare the fouling resistance of the mimics to the shells. Biomimicry, or the copying of natural surface microtopographies, provides a mechanism to identify the role of physical surfaces by removing any chemical or mechanical deterrents associated with surfaces (Figueiredo et al. 1997; Bers & Wahl, 2004). Mimicked surface microtopographies from marine organisms have deterrent effects on the settlement of fouling organisms. Biomimics of the crustose coralline alga *Phymatolithon purpureum* had a lower density of *Ulva* sp. zoospores and *Fucus serratus* zygotes than *P. lenormandii* (Figueiredo et al. 1997). Biomimics of the carapace of the crab *Cancer pagurus* deterred macrofoulers, the egg case of the dogfish *Scyliorhinus canicula,* and the brittle star *Ophiura texturata* deterred microfoulers, and the mussel *Mytilus edulis* initially reduced barnacle settlement (Bers & Wahl, 2004).

Three bivalve surfaces were chosen for mimicry in this study, *Mytilus galloprovincialis*, *Tellina plicata* and *Amusium balloti*. One of the most intriguing examples of a natural surface that deters fouling is the shell of the blue mussel *M. galloprovincialis*. *M. galloprovincialis* has a homogeneous ripple-like microtextured surface (1-2 μm) and is rarely fouled (Scardino et al. 2003). Furthermore, the cosmopolitan fouling organism, *Balanus amphitrite* settles preferentially on portions of *M. galloprovincialis* shell where the periostracum is naturally abraded (Scardino et al. 2003). While there is a strong correlation between fouling deterrence and surface microtopography in *M. galloprovincialis* there is no unequivocal demonstration that this is a physical phenomenon based on surface microtopography or that the surface contributes to a broader defence strategy. The surface microtexture on *Mytilus* shells is now well documented and can be thought of as an 'industry standard' to compare with other natural surfaces. *Tellina plicata* was chosen as it displayed micro-projections at a similar scale to *M. galloprovincialis* and also has larger scale texture 430 μm. Petronis et al. (2000) has demonstrated that on artificial surfaces micro-projections/pyramids

significantly reduced barnacle cyprid settlement compared to smooth surfaces. *Amusium balloti* was used as it has a smooth surface structure free of microtexture and provides a good contrast to surface roughness parameters generated for *M. galloprovincialis* in Chapter 3. Therefore, the aim of this study was to determine the role of surface microtopography when decoupled from surface chemistry. A second aim was to compare different types of surface topography and smooth surfaces for fouling resistance and species specific preferences.

4.2 Materials & Methods

4.2.1 Organisms and study site

The antifouling properties of three species of bivalves, *M. galloprovincialis*, *Tellina plicata* and *Amusium balloti* were investigated. These species were chosen, as they have very different surface microtopographies. *M. galloprovincialis* displays micro-ripples of 1-2 μm (Scardino et al. 2003), *T. plicata* has larger scale growth lines of 437μm and microprojections of 2.24 μm, whilst *A. balloti* has a smooth surface (free of surface texture). *M. galloprovincialis* shell was collected from temperate waters in Eden, New South Wales, Australia. *T. plicata* valves were collected off Orpheus Island (18º.37'S, 146º.30'E), Queensland, Australia. *A. balloti* shell was trawled from tropical waters off Townsville, Queensland, Australia. Field assays were conducted in Ross Creek (19° 15'S; 146° 50'E), which is outside the natural range of *M. galloprovincialis*. This site is easily accessible and has very strong fouling pressure throughout the year with the major fouling species being *Bugula neritina*, *Hydroides elegans*, *Watersipora subtorquata* and *Botrylloides leachi* (Floerl & Inglis, 2003).

4.2.2 Production of biomimics

To determine the antifouling properties of the surface microtopography of *M. galloprovincialis*, *T. plicata* and *A. balloti*, biomimics of their shell surface were created using methodologies adapted from Marrs *et al.* (1995). Biomimics were produced using a polyvinylsiloxane negative impression (KERR's Extrude Wash® Type 3; KERR, Romulus, MI 48174, USA) of the shell surface using an extrude-gun and mixing tip. The wash was extruded evenly over the shell surface, minimizing the formation of air-bubbles. Following curing (15 minutes at room temperature), the

extrude wash was peeled off the shell surface, leaving a negative (opposite) impression of the shell surface. Epoxy resin (DEVCON® 2-TON®; DEVCON, Wellingborough NN8 6QX, UK) was then poured over the negative impression to create a positive mould. The resin is cured at room temperature for 24 hours, after which the negative impression is peeled off leaving a positive mould of the shell, with a casting resolution of < 1 µm (Marrs et al. 1995).

4.2.3 Treatments

Treatments tested were *M. galloprovincialis* shell and mould, *T. plicata* mould, *A. balloti* shell and mould, biomimics of *M. galloprovincialis* treated with sandpaper, grade 80, (which produced a irregular/random pattern however with a consistent amplitude), a smooth resin mould (completely free of texture and surface irregularities) and Polyvinylchloride (PVC) strips (60mm x 30mm). The PVC strips were included to determine the degree of fouling pressure and any effects the resin material may have on fouling. *T. plicata* shell was not used due to limited valve replication.

4.2.4 Surface characterisation of biomimics and controls

Treatments and controls were cut into approximately 1cm^2 pieces, rinsed with Milli Q water, air dried, then mounted onto stubs with carbon paint and sputter coated with gold. The width of surface microtopographies (distance from peak to adjacent peak) of all eight treatments were measured under Scanning Electron Microscopy (JEOL JSM-5410LV) on three replicas of each treatment at four random points on each replica up to 5000x magnification (Figure 4.1, Table 4.1).

a) **b)** **c)**

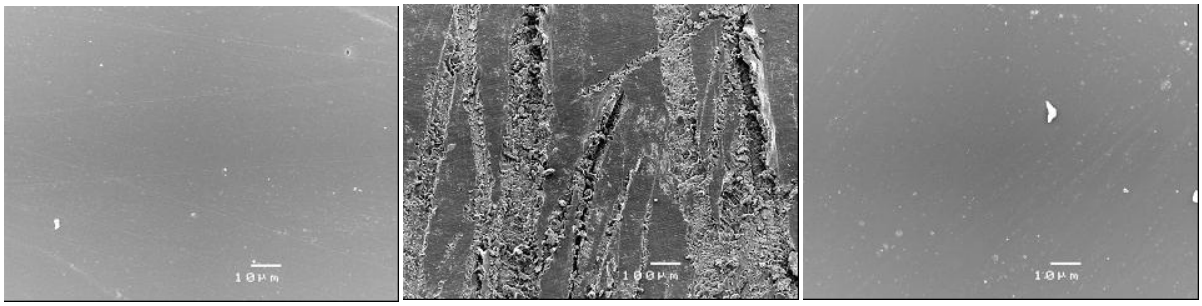

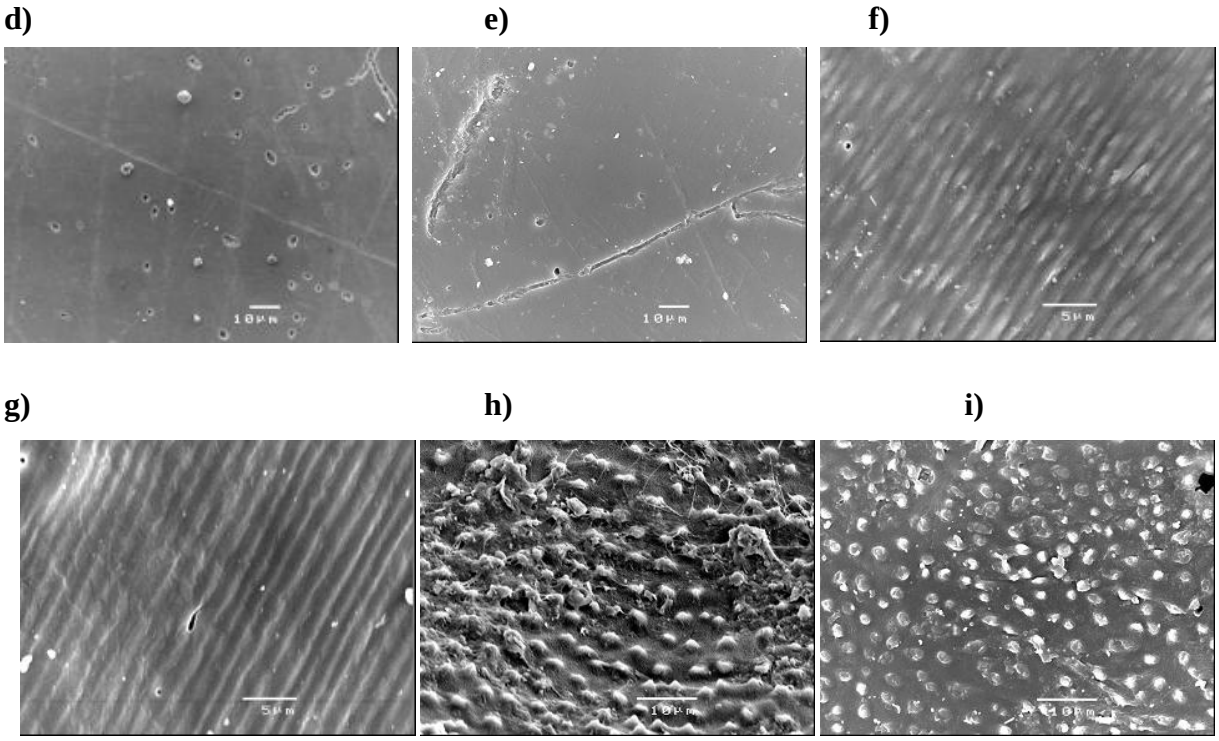

Figure 4.1: Scanning Electron Microscopy of surface microtopography for a) PVC b) sanded mould c) smooth mould d) *A. balloti* shell e) *A. balloti* mould f) *M. galloprovincialis* shell g) *M. galloprovincialis* mould h) *T. plicata* shell i) *T. plicata* mould.

Table 4.1. Surface microtextures measured on the eight treatments. Data show mean ± one S.E.

Treatment	Microtexture (μm)
PVC	0 (smooth)
Sanded	55.4±2.7
Smooth resin	0 (smooth)
A. balloti	0 (smooth)
A. balloti *mould*	0 (smooth)
M. galloprovincialis	1.94±0.03
M. galloprovincialis mould	2.01±0.06
T. plicata *mould*	437±16.4 (growth lines) & 2.24±0.15 (projections)

4.2.5 Field exposure trials

Five replicas of each treatment were used to test fouling resistance *in-situ*. For the bivalve shell treatments, *M. galloprovincialis* and *A. balloti*, one valve (chosen randomly) was used as the shells were opened and cleaned. A small hole was drilled into the top of each of the eight treatments and then placed randomly along fishing line. The line was suspended at a depth of 1-2m at Ross Creek. The treatments were examined fortnightly for 12 weeks for macrofouling from June 2003. The percent cover and number of settled macrofoulers were counted visually using the point-intercept method. Counts were made 5mm from each side to avoid edge effects. For *M. galloprovincialis* shell, two replicas were excluded from the analysis due to strong edge effects caused by the colonial ascidian *Diplosoma* sp. that initially established inside the mussel shell. Transparent grids ($1mm^2$) were placed over each treatment and percent fouling cover calculated by dividing the total number of grids occupied by fouling organisms by the total number of grids covering the treatment. Fouling organisms were identified to species level where possible, using taxonomic keys (OECD, 1967; Millar, 1967; Hutchings, 1984; Monniot *et al.* 1991; Kott, 1992). After 12 weeks the majority of treatments were completely fouled and all individuals were photographed (Kodak DC240, digital) and the experiment concluded.

4.2.6 Statistical analysis

Statistical analysis was performed using SPSS (Version 10.0, SPSS Inc., Chicago). Percent cover of major groups of macrofoulers was recorded and analysed for each treatment by Repeated Measure Analysis of Variance (RMA). The mean width of microtopography was compared between *M. galloprovincialis* shell and mould by one-way ANOVA. The assumptions of ANOVA were met by testing the normality of the data using Q-Q plots of standardized residuals and homogeneity of variance tested using scattergrams of standardized residuals versus predicted means (Underwood 1981). Where assumptions were not met, data were transformed (arcsine square-root). When post-hoc analysis was required, Tukey's HSD test was performed. Standard error bars are not shown on Figures 4.3-4.6 for clarity of presentation.

4.3 Results

4.3.1 Surface characterisation of biomimics and controls

Of the eight treatments, PVC, *A. balloti* shell, *A. balloti* mould, and smooth resin mould, displayed no surface topography. The remaining four treatments had some scale of surface microtopography, the lowest being *M. galloprovincialis* shell with ripples (1.94 μm ± 0.03), which is consistent with Scardino et al. (2003). The microtopography on the *M. galloprovincialis* mould (2.01 μm ± 0.06) was not significantly different from *M. galloprovincialis* shell (one-way ANOVA $F_{1,18} = 1.37$, $P = 0.257$). On *T. plicata* moulds the distance between the microprojections was 2.24 ± 0.15 μm. The random surface microtopography on the sanded mould was 55μm ± 2.7 (mean width of abrasions) (Figure 4.1, Table 4.1).

Field exposure trials

4.3.2 Species diversity on treatments

The mean number of species occurring on the eight treatments and controls was recorded over a 12-week period. In total 11 species were recorded with the major groups of fouling organisms being serpulid tubeworms, encrusting bryozoans, the erect bryozoan *Bugula neritina,* colonial ascidians, and bivalves. Initially, there was little diversity with only the tubeworms, *Hydroides* spp., Spirorbid tubeworms and *B. neritina* settling. After 12 weeks, *A. balloti* shell (5.8 ± 0.5) and mould (3.75 ± 0.48), and PVC (4.0 ± 0.43) had the highest mean number of species settling on their surface with significantly more species settling on these treatments over time than the other treatments (RMA, $P < 0.001$, Figure 4.2). The three dominant fouling organisms occurring on all treatments were a Spirorbid tubeworm, the colonial ascidian *Diplosoma* sp., and the bryozoan *B. neritina.* These contributed to more than 90% of total cover. The response of the three fouling organisms to treatments is analysed in greater detail below.

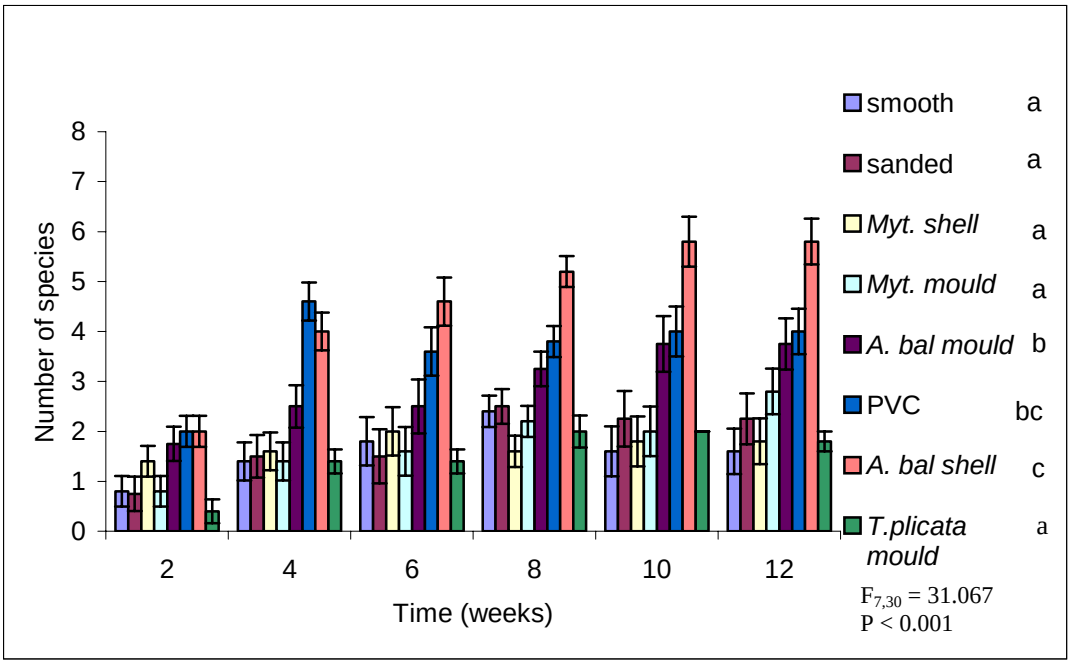

Figure 4.2: The mean number (± one S.E.) of species occurring on the eight treatments over time. Analysis by Repeated Measures Analysis of Variance followed by Tukey's HSD *post hoc* test. Treatments sharing the same letter are not different at $\alpha = 0.05$.

4.3.3 Total fouling cover

To determine if there was a treatment effect on fouling over time, Repeated Measures Analysis of Variance was performed on the percent fouling cover on the seven treatments over a 12-week period. A significant difference in percent fouling cover was found between the treatments over time (RMA, $P < 0.001$, Figure 4.3). *M. galloprovincialis* shell was the least fouled (16.7 ± 7.7% cover) and had a significantly lower fouling cover than all other treatments over time with the exception of *T. plicata* mould (Figure 4.3, Tukey's HSD). *M. galloprovincialis* mould, *T. plicata* mould and the sanded moulds had significantly lower levels of fouling over time than PVC, *A. balloti* shell and *A. balloti* mould (Figure 4.3, Tukey's HSD). After six weeks exposure to fouling the textured surfaces *M. galloprovincialis* shell, *M. galloprovincialis* mould, *T. plicata* mould and sanded mould had low cover (6 ± 2.1%, 17 ± 3.6%, 12 ± 2.8% and 15.5 ± 4.8% cover respectively). In contrast, *A. balloti* shell, *A. balloti* mould, and PVC were heavily fouled, almost to the point of total cover (92.4 ± 3.2%, 75.5 ± 8.3%, 89.4 ± 3.5% respectively). The smooth mould had an intermediate level of total cover (40 ± 13.5%) (Figure 4.3). However, after eight weeks the sanded mould, smooth mould, *T. plicata* mould and *M. galloprovincialis* mould all increased in fouling cover

while fouling cover on *M. galloprovincialis* shell remained low. This trend continued for the remaining four weeks of the experiment where after 12 weeks *M. galloprovincialis* shell maintained a low fouling cover (16.7 ± 7.7%), while all other treatments had total fouling cover greater than 80% with the exception of *T. plicata* mould (59%) (Figure 4.3).

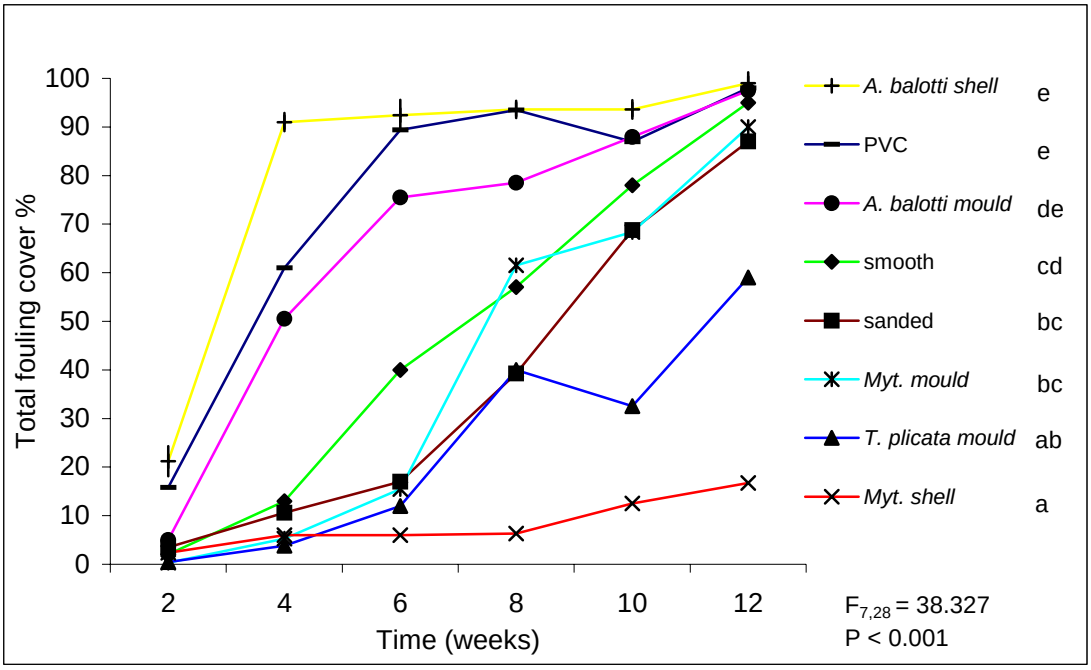

Figure 4.3: Mean percent total fouling cover on the eight treatments over time. Analysis by Repeated Measures Analysis of Variance followed by Tukey's HSD *post hoc* test. Treatments sharing the same letter are not different at $\alpha = 0.05$.

The majority of fouling on the eight treatments was due to three fouling organisms, the bryozoan *B. neritina*, the Spirorbid tubeworm and the colonial ascidian *Diplosoma* sp. However, the response of each organism to the treatments differed markedly. To interpret the response of the major fouling organisms to the treatments, the level of fouling (%) by each of the three organisms was analysed over 12 weeks by Repeated Measures Analysis of Variance.

4.3.4 Spirorbid tubeworm

The calcareous Spirorbid tubeworm occurred on all treatments during the experiment. However, there was significantly less fouling by Spirorbid tubeworms on *M. galloprovincialis* shell than on the *A. balloti* shell and less Spirorbid fouling on the *T.*

plicata mould and sanded mould than on the *A. balloti* mould (RMA, P = 0.004, Figure 4.4). After four weeks exposure, *A. balloti* shell, *A. balloti* mould, and PVC were heavily fouled by Spirorbid tubeworms (47 ± 4.1%, 30.5 ± 5.5%, 21 ± 4.9% cover respectively), while the other treatments had less than 10% cover (Figure 4.4). After six weeks, Spirorbid tubeworm cover on *A. balloti* shell dropped to 17 ± 4.8% due to an increase in cover by *Diplosoma* sp. over Spirorbid tubeworms. From eight to 12 weeks *M. galloprovincialis* shell and the sanded mould maintained a low level of fouling (10%), while fouling by Spirorbid tubeworms increased on the *M. galloprovincialis* and *T. plicata* mould and remained at high levels (25-35%) on *A. balloti* shell and mould, and smooth mould (Figure 4.4).

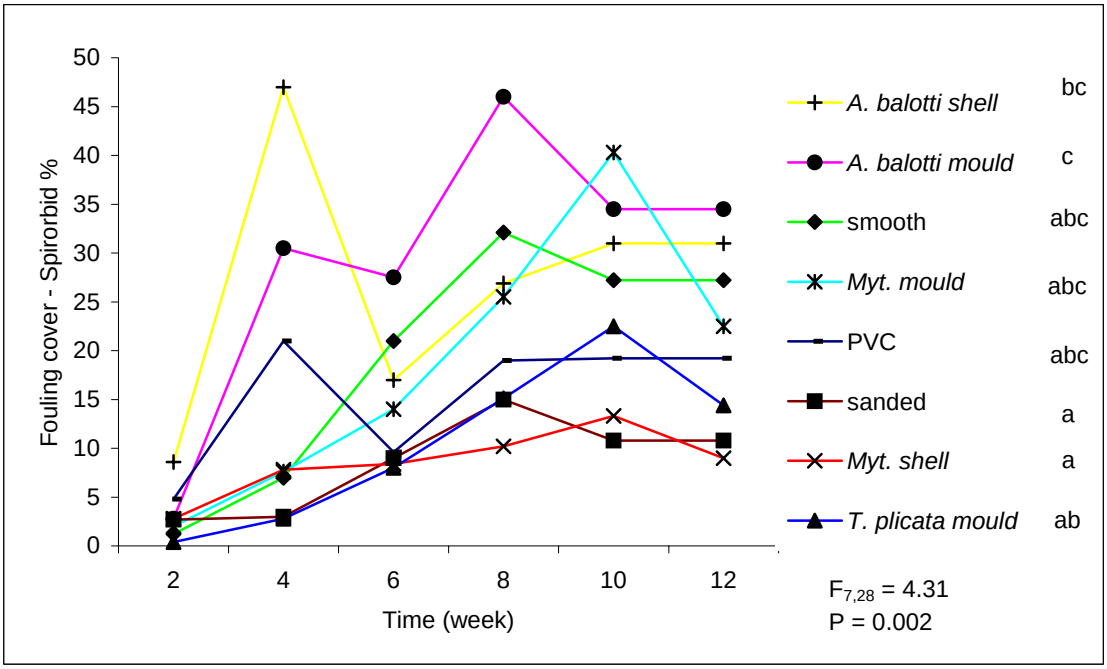

Figure 4.4: Mean percent fouling by a Spirorbid tubeworm on treatments over time. Analysis by Repeated Measures Analysis of Variance followed by Tukey's HSD *post hoc* test. Treatments sharing the same letter are not different at $\alpha = 0.05$.

4.3.5 Diplosoma sp.

The colonial ascidian *Diplosoma* sp. was slow to establish, with only two treatments (*A. balloti* shell and PVC) being heavily fouled by six weeks. Fouling increased on all treatments between six to ten weeks with the exception of *M. galloprovincialis* shell (Figure 4.5). While patterns of fouling changed rapidly after six to eight weeks there was a significant difference in fouling between the least fouled treatments *M. galloprovincialis* shell and mould, *T. plicata* mould, *A. balloti* mould, and PVC (RMA,

P < 0.001, Figure 4.5). After 12 weeks all treatments except *M. galloprovincialis* shell were fouled to some extent by *Diplosoma* sp., *A. balloti* mould (13.9 ± 11.1%) was the least fouled while the sanded mould (50 ± 22%), PVC (51.2 ± 4.2%), and *M. galloprovincialis* mould (47.5 ± 16.9%) had the highest levels. Fouling had increased rapidly on the *M. galloprovincialis* and *T. plicata* moulds after week ten (Figure 4.5).

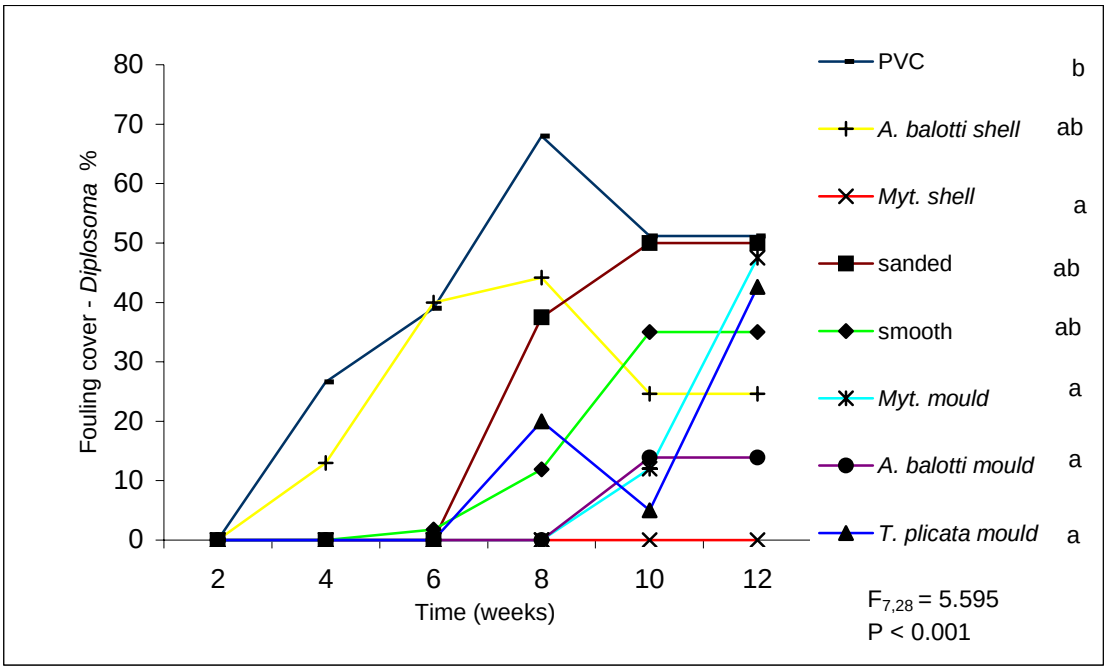

Figure 4.5: Mean percent fouling by *Diplosoma* sp. on treatments over time. Analysis by Repeated Measures Analysis of Variance followed by Tukey's HSD *post hoc* test. Treatments sharing the same letter are not different at $\alpha = 0.05$.

4.3.6 *Bugula neritina*

There were significant differences in fouling by the erect bryozoan *B. neritina* between the eight treatments over time (RMA, P = 0.028, Figure 4.6). *M. galloprovincialis* shell and *T. plicata* mould were significantly less fouled by *B. neritina* than *A. balloti* shell and mould and PVC over ther 12 weeks (Figure 4.6). Again, *M. galloprovincialis* shell remained unfouled throughout the trial and the sanded mould, *T. plicata* and *M. galloprovincialis* mould were virtually unfouled by *B. neritina* for the first 6 weeks. After six weeks, fouling was high on the smooth surfaces, PVC (30 ± 11.5%), *A. balloti* shell (27 ± 7%) and *A. balloti* mould (18.7 ± 14.2%). After 8 weeks, fouling by *B. neritina* increased on the sanded mould (17 ± 2.4%) and *M. galloprovincialis* mould (11.3 ± 8.3%), but dropped substantially on *A. balloti* shell (32 ± 15.5% to 3.8 ±2.3%). After 12 weeks, fouling cover by *B. neritina* had increased on *M. galloprovincialis*

mould (22 ± 6.3%) and the smooth mould (24.2 ± 9.1%) though not on *T. plicata* mould (2.1%), and was constant on all other treatments (Figure 4.6).

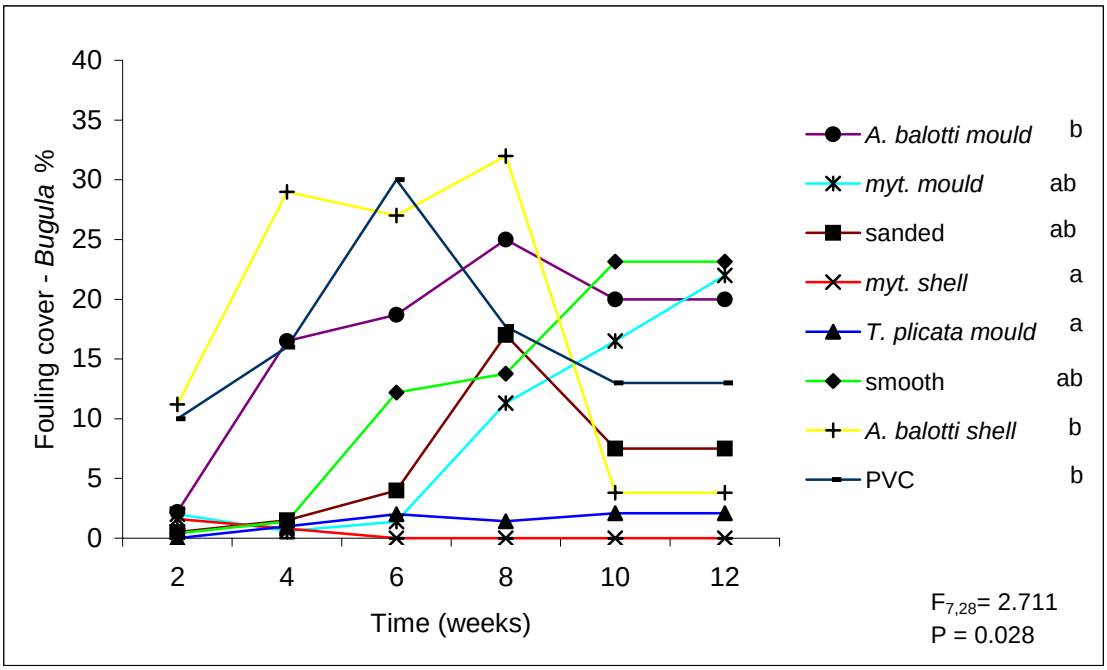

Figure 4.6: Mean percent fouling by *Bugula neritina* on treatments over time. Analysis by Repeated Measures Analysis of Variance.

4.4 Discussion

This study demonstrates the role of surface microtopography as a fouling deterrent mechanism. The shell of *M. galloprovincialis* and mould of *M. galloprovincialis* and *T. plicata* were fouled by significantly fewer species and had significantly less total fouling cover than the shell and mould of *A. balloti* over a 12-week period. Furthermore, the four treatments that had surface microtopography, be it structured as in the case of *M. galloprovincialis* shell and mould (1-2 µm) and the *T. plicata* mould (2 µm), or random as in the case of the sanded mould (55 µm), had lower total cover of fouling organisms than treatments without microtopography after six weeks. There was also no significant difference between the effect of the *M. galloprovincialis* mould (1-2µm), *T. plicata* mould and the sanded mould (55µm). However, the strong fouling deterrent effects of these surfaces diminish rapidly after six to eight weeks (Figure 4.3), while *M. galloprovincialis* shell remained essentially unfouled throughout the experiment.

The finding that surface microtopography reduces the level of fouling compared to smooth surfaces is consistent with studies comparing artificial surface microtexture to smooth controls. For example, barnacle cyprids (*Balanus improvisus*) are deterred by microtopographies ranging from 30-350 μm with the most significant reductions between 30-73 μm, the same micro-scale as the cyprids searching antennules (Andersson et al. 1999, Berntsson et al. 2000a, Berntsson et al. 2000b, Petronis et al. 2000). However, the response to surface microtopography is often species specific with some studies demonstrating that roughness promotes fouling (Chabot & Bourget 1988, Lemire & Bourget 1996, Lapointe & Bourget 1999). In this study there were species-specific responses to the differing treatments, particularly in the first eight weeks of the trial. The most common fouling organism was a calcareous Spirorbid tubeworm that showed a preference for smooth surfaces over those with texture, consistent with previous studies where *Spirorbis borealis* avoided rougher surfaces (Crisp & Ryland 1960). In contrast, *Diplosoma* sp. had no preference for specific settlement surfaces. Settlement was high (40%) on some but not all smooth surfaces after six weeks, and there was no clear preference for surface texture after this time. *B. neritina* was an early coloniser, possibly due to its preference for clean over filmed surfaces (Crisp & Ryland 1960, Maki et al. 1989) and had a strong preference for smooth surfaces. There was high settlement on all smooth surfaces and no settlement on textured surfaces after six weeks. This is in contrast to a reported indifference to surface texture (Crisp & Ryland, 1960). Consistent with the other species, any deterrent effect of surface microtopography or roughness on moulded treatments was reduced after six weeks.

The loss of activity over time of artificial surfaces has been reported for both resin mimics (Bers & Wahl, 2004) and artificially textured (PDMS) surfaces (Andersson et al. 1999). Biomimics of the carapace of *Cancer pagurus* deterred the barnacle *Balanus improvisus*, the egg case of the dogfish *Scyliorhinus canicula* and the brittle star *Ophiura texturata* deterred the ciliates *Zoothamnium commune* and *Vorticella* sp., and the mussel *Mytilus edulis* reduced barnacle settlement for one week (Bers & Wahl, 2004). Any deterrent effects were lost after four weeks resulting in the conclusion that the underlying antifouling mechanisms remain unresolved and physical deterrents are one component of a multiple antifouling defence strategy (Bers & Wahl, 2004). In a similar study the moulded surface features of crustose coralline algae were examined

(Figueiredo et al. 1997). The settlement of algae was lower on replicas of smooth algal surfaces (*Phymatolithon purpureum*), however the lowest settlement was on live alga. In this case the surface properties acted as a defence against fouling in conjunction with thallus shedding by the alga (Figueiredo et al. 1997).

Factors that may explain the loss of fouling deterrence between *M. galloprovincialis* shell, its biomimic, the *T. plicata* biomimic and the roughened surface after six weeks include reduced integrity of the mould after exposure to the marine environment, or differential microfouling development affecting the textured moulded surfaces due to potential differences in the chemical nature of the shell and resin. Reduced integrity is unlikely due to the short exposure time before loss of activity and the durability of material in other studies (Thomason et al. 2002). However, the differential development of microfouling communities may play a role in the differences in fouling cover between the resin moulds and shell after six to eight weeks exposure. The settlement and growth of bacteria and diatom biofilms are influenced by surface chemistry (Maki, 1999; Steinberg *et al.* 2001) and surface free energy (Becker, 1996, Becker et al. 1997, Wigglesworth-Cooksey et al. 1999, Finlay et al. 2002a, Sekar et al. 2004). Bacteria and diatoms can also alter the free energy of a surface (Wigglesworth-Cooksey et al. 1999) and modify the settlement response of some larvae (Maki et al. 1989). The surface of *M. galloprovincialis* may prevent biofilm development due to surface (protein) chemistry and/or surface free energy associated with the periostracum. The potential differential development of a biofilm on the textured moulds may reduce microtexture, resulting in the loss of physical deterrence. Alternatively, the development of a biofilm on textured moulds could provide a cue for subsequent macrofoulers (Wieczorek & Todd, 1997; Patel et al. 2003). This can be addressed by investigating the influence of microtopography on biofilm development and subsequent macrofouling. Furthermore, comparative studies of the effect of the periostracum on microfouling are required to determine a relationship between the periostracum and fouling deterrence.

This study has demonstrated the importance of microtexture to fouling resistance. Microtextured biomimics were able to resist fouling for up to eight weeks in the field. The scale of microtexture will now need to be compared and tested against a range of larval sizes. One scale of texture will provide many different numbers of attachments

points for larvae of differing sizes. The importance of attachments points requires further testing.

CHAPTER FIVE

Testing attachment point theory: Diatom attachment on microtextured polyimide biomimics[2]

5.1 Introduction

In this Chapter the biomimics from Chapter 4 are used as templates for the design of microtextured films for testing against microfouling organisms. The films will determine the importance of attachment points to microfouling by examining varying microtexture widths to the attachment by different diatom cell sizes. Chapter 6 will broaden the range of microtextures to encompass macro fouling larvae.

Physical surfaces are an important cue in the settlement preferences of invertebrate larvae and algal propagules. Whilst many fouling organisms actively search for a suitable surface some organisms, such as diatoms, contact a surface passively through water currents and gravity and can then actively choose where to settle. Diatoms are characterized by silica cell walls known as the frustule, which have two valves. Raphid diatoms, which were used in this study, have an elongated slit (raphe) along the valve which secretes extracellular polymeric substances (EPS). The EPS has a dual function of allowing the cell to adhere to the surface and aiding in motility through gliding along the surface (Edgar and Pickett-Heaps, 1984; Wetherbee et al. 1998). Consequently, understanding the role of physical structures and surfaces in settlement preferences will contribute to the development of surfaces that either prevent settlement and the development of biofouling communities, or allow for selective settlement for target species, for example in aquaculture.

Research into physical deterrents to fouling has focused on artificial surfaces with a range of microtextures and has examined their influence on the settlement of macrofouling organisms (Hills & Thomason 1998a, b, Kohler et al. 1999, Berntsson et al. 2000a, Berntsson et al. 2000b, Petronis et al. 2000, Callow et al. 2002, Thomason et

[2] Chapter 5 is adapted from Scardino, A. J., Harvey, E. & de Nys, R.(2006) Testing attachment point theory: diatom attachment on microtextured polyimide biomimics. *Biofouling* **22**(1): 55-60.

al. 2002, Hoipkemeier-Wilson et al. 2004). Whilst there have been some promising results, the deterrence of fouling organisms is often species specific (Berntsson et al. 2000b, Petronis et al. 2000) and the deterrent effect diminishes with time (Andersson et al. 1999, Bers & Wahl 2004, Scardino & de Nys 2004). The effects of surface microtexture are clearly related to the scale of the test organisms and it is proposed that fouling organisms that are larger than the scale of microtexture will have reduced adhesion strength due to fewer attachment points, whilst fouling organisms that are slightly smaller than the scale of surface topography will have greater adhesion strength due to 'attractive' topographies (Callow et al. 2002) with multiple attachment points - 'attachment point theory' (reviewed by Verran & Boyd, 2001). Fouling organisms that are slightly smaller than the scale of surface topography will also have increased adhesion due to micro-refuges and protection from hydrodynamic forces (Granhag et al. 2004). This concept has been explored for barnacle cyprids (Lemire & Bourget 1996, Kohler et al. 1999, Lapointe & Bourget 1999, Berntsson et al. 2000a, Berntsson et al. 2000b, Petronis et al. 2000) and algal spores (Callow et al. 2002, Hoipkemeier-Wilson et al. 2004) and the results of these studies support the applicability of the theory, at least for barnacle cyprids of various species and the fouling algal species of *Ulva* syn. *Enteromorpha* (Hayden et al. 2003).

In contrast to macrofouling studies, there has been comparatively little research into diatom attachment onto microfabricated surfaces and the effect of structured microtextures on diatom settlement, attachment, and strength of attachment. Considering diatoms are omnipresent fouling organisms that establish on surfaces before macrofouling organisms, and in many cases the diatom film is a prerequisite for macrofouling colonization (Wahl, 1989), it is important to determine the influence of surface microtexture in diatom attachment and the relationship to cell size.

Studies on diatom motility, attachment and adhesion have focused on varying surface effects including wettability (Becker et al. 1997, Wigglesworth-Cooksey et al. 1999, Finlay et al. 2002a), surface roughness (Kohler et al. 1999, Sekar et al. 2004), surface charge (Rasmussen & Ostgaard, 2001) and the presence of surface biofilms (Peterson & Stevenson, 1989). The effects of environmental flow rates and temperature (Cohn et al. 2003), pH of the medium (Sekar et al. 2004), exopolysaccharide (EPS) production (Becker 1996), and adhesive mechanisms (Holland et al. 2004) on diatom motility and

adhesion have also been investigated. Studies of the effects of surface topography and roughness on diatom attachment have focused on anisotropic structures produced through sanding and polishing at scales of 100 to 5000 μm (Kohler et al. 1999), and on uncharacterized surfaces of varying roughness (Sekar et al. 2004). This study is the first to test diatom attachment against homogeneous microtextures at the same scale as the test organisms.

Four species of common benthic fouling diatoms were tested for their ability to attach onto microtextured polyimide modeled on natural fouling resistant surfaces (biomimics) and smooth polyimide controls in static laboratory assays. The four species of diatoms were chosen, as their sizes were above, below, or at the same scale, as the microtextured surfaces. The aim of this study was to determine if the scale and pattern of microtexture reduces diatom attachment in static laboratory bioassays and how this relates to the size of the diatom.

5.2 Methods

5.2.1 Culture of diatom species

The four diatom species used, *Fallacia carpentariae* (CS-346) (Hallegraeff et Burford), *Nitzschia* cf. *paleacea* (CS-429), *Amphora* sp. (CS-255) and *Navicula jeffreyi* (CS-46) (Hallegraeff et Burford), are all Pennales (Class Bacillariophyceae, Order Bacillariales). A 20 ml cultured suspension of each species was obtained from CSIRO microalgal supply service, Tasmania, Australia. Growth conditions for all cells were 12:12 light: dark cycle with a light intensity - 80 μmol photons PAR $m^{-2}S^{-1}$; using Philips daylight or cool white fluorescent tubes. Diatom cultures were supplemented with Guillard's F/2 medium with the exception of *Amphora* sp. that was supplemented with F/E2 medium (Guillard & Ryland, 1962). *F. carpentariae* and *Amphora* sp. were cultured at 25ºC and *N. palacea* and *N. jeffreyi* at 20ºC. The cells were re-suspended with an orbital shaker and their concentration determined using a haemocytometer prior to use in assays.

5.2.2 Production of microtextured surfaces

Test surfaces were produced using methodologies adapted from Duncan et al. (2002). The microtextured surface patterns were laser etched onto Polyimide film (Kapton

HN®, thickness 125 µm, test surface 20 mm x 20 mm) by MiniFAB (Ltd) using a KrF excimer laser beam (248 nm, fluence 1 J/cm^2. impulse, 20 ns per impulse, X10 mask magnification) coupled with an optical device which projects the laser beam through a metal photomask producing 1 µm wide bars with a 2 µm pitch. Three patterns were modeled from the fouling resistant bivalves *Mytilus galloprovincialis* (Figure 5.1a) and *Tellina plicata* (Figure 5.1b). The surfaces were 2 µm ripples modeled from *M. galloprovincialis* (2 µm wavelength, depth 0.4 µm – Figure 5.1c), 4 µm ripples slightly larger than *M. galloprovincialis* microtexture (4 µm wavelength, depth 1.2µm – Figure 5.1d), and 4 µm projections modeled from *T. plicata* (4 µm wavelength, depth 0.5 µm – Figure 5.1e). Rippled surfaces were made using a sine wave microtexture. Projections were made using a 3D sine wave by crossing two sine wave ripples at right angles to each other. Smooth polyimide film was used for controls (Figure 5.1f). The accuracy of the surfaces was confirmed using SEM.

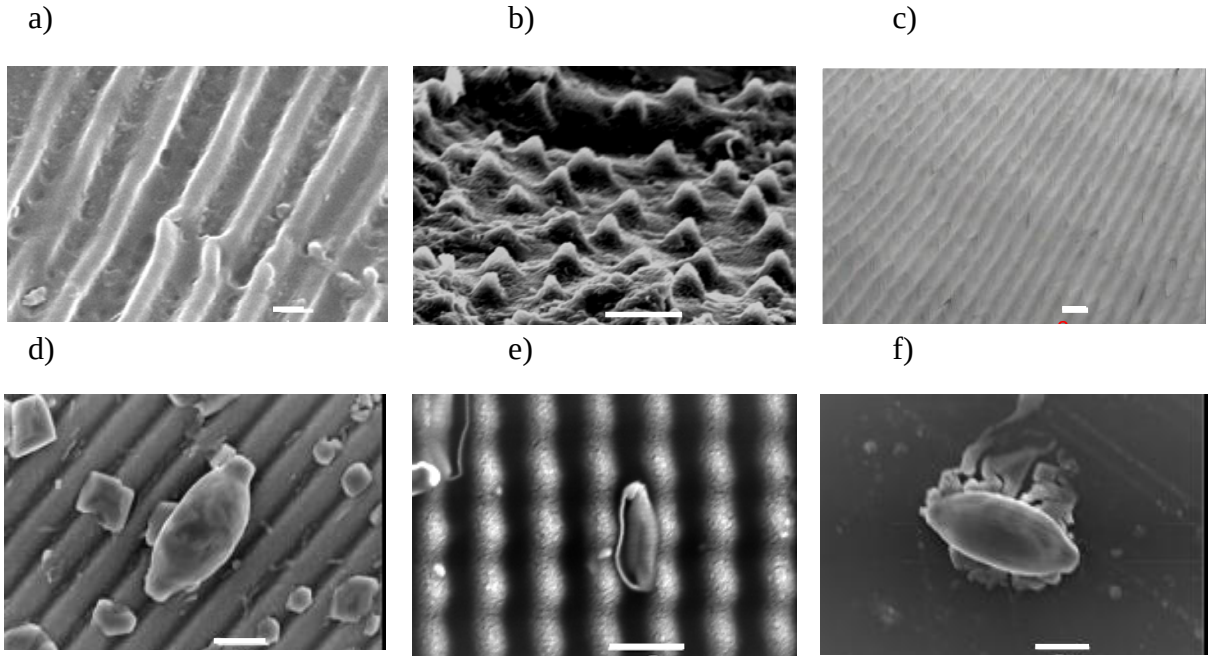

Figure 5.1 Scanning Electron Microscopy (SEM) images of a) modeled *Mytilus galloprovincialis* microripples, scale bar = 1 µm b) modeled *Tellina plicata* microprojections, scale bar = 5 µm c) 2 µm microripples, scale bar = 2 µm d) 4 µm microripples, scale bar = 5 µm e) 4 µm microprojections, scale bar = 5 µm f) smooth polyimide control, scale bar = 5 µm

5.2.3 Bioassay procedures

The test surfaces were rinsed in filtered (0.2 µm) seawater before adding diatom cultures. The surfaces were individually placed in plastic weigh boats and filled with 4 ml of filtered (0.2 µm) seawater and 100 µl of diatom culture suspension with a cell density of approximately 3 x 10^6 cells/ml. Each treatment was repeated in triplicate. The diatoms were left to settle for 4 hours after which they were rinsed by dipping each treatment in a new beaker of filtered (0.2 µm) seawater three times to remove unattached diatoms, the surfaces were briefly exposed to air during this dip-rinse process. Diatoms were then counted in 10 random fields of view (FOV) per dish at magnifications of x 400 (0.16mm^2) and x 1000 (0.025mm^2) for *Fallacia carpentariae*. The mean number of attached diatoms per field of view was analysed using a nested one-way analysis of variance (FOV nested within dish) followed by Tukey's HSD *post hoc* test for each diatom species. Attachment refers specifically to diatoms that have settled on, and adhered to, the surface and have not been removed by the rinsing process. Due to supply of diatom stocks each species assay was conducted independently and the response between species is not compared statistically. All data were normally distributed and variances homogeneous. Analyses were conducted using SPSS v12.0.

5.3 Results

5.3.1 Cell sizes and numbers of attachment points to microtexture

The four diatom species used in this study were all able to settle, glide and attach to polyimide films in static bioassays. The motility of the four species was similar across all surfaces with gliding observed. However, the mean number of cells attached after rinsing varied significantly between the smooth polyimide and micro-textured polyimide treatments. Furthermore, the response to the surfaces was species specific. Cell sizes for the four diatom species and the number of adhesion points on the microtextured polyimide treatments are shown in Table 5.1. Theoretical attachment points are designated as multiple where diatoms fit within surface microtexture, or for smooth controls where the shape of pinnate diatoms allows for multiple attachment sites (Figure 5.2). It is assumed that the highest number of attachment points is possible where the diatom fits within the most 'attractive' microtexture (e.g. Callow et al. 2002). Points of attachment were determined based on the width of the diatom cell and the

wavelength of the surface microtexture when longitudinal to microtexture as cells consistently align with the surface microtexture (Figures 5.3-5.6). For microtextured peaks the length of the cell was also used to determine theoretical attachment points as the longer the cell the more peaks are available for attachment (Table 5.1).

Table 5.1 Cell sizes and the number of attachment points to polyimide microtextures.

Species	**Cell length**	**Cell width**	**# adhesion points on 2 µm ripples**	**# adhesion points on 4 µm ripples**	**# adhesion points on 4 µm peaks**
Fallacia carpentariae	3±0.09 µm	1±0.06 µm	multiple	multiple	multiple
Nitzschia paleacea	7.2±0.4 µm	2±0.07 µm	multiple	multiple	multiple
Navicula jeffreyi	12±0.17 µm	4±0.13 µm	3	2	6
Amphora sp.	14.7±0.24 µm	7.3±0.26 µm	4	2	6

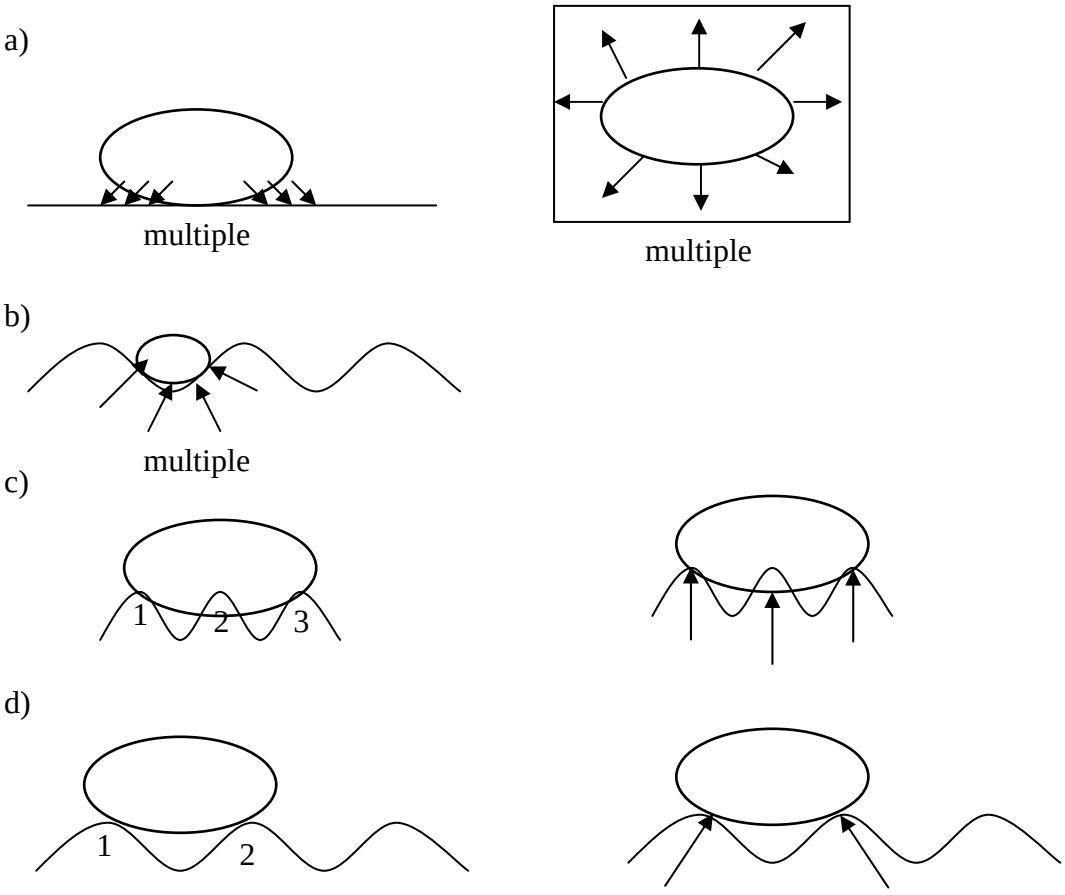

Figure 5.2 A schematic illustrations of theoretical attachment points for settlement by a) all diatoms on a smooth surface – multiple attachment points b) *Fallacia carpentariae* on 2 µm ripples – multiple attachment points c) *Navicula jeffreyi* settling on 2 µm ripples – 3 attachment points d) *Amphora* sp. settling on 4 µm ripples – 2 attachment points

5.3.2 *Fallacia carpentariae* assay

Fallacia carpentariae, the smallest diatom species used, has a cell length of 3 µm and a width of 1 µm. This species can fit inside the microtexture of all treatments, hence has multiple numbers of attachment points to all treatments. The number of attached cells was highest on 4 µm ripples (9.47 cells/fov) however, the mean number of cells was not significantly different between the microtextured polyimide treatments and the smooth control all of which have multiple attachment points (8.63 cells/fov) (ANOVA P = 0.966, Figure 5.3).

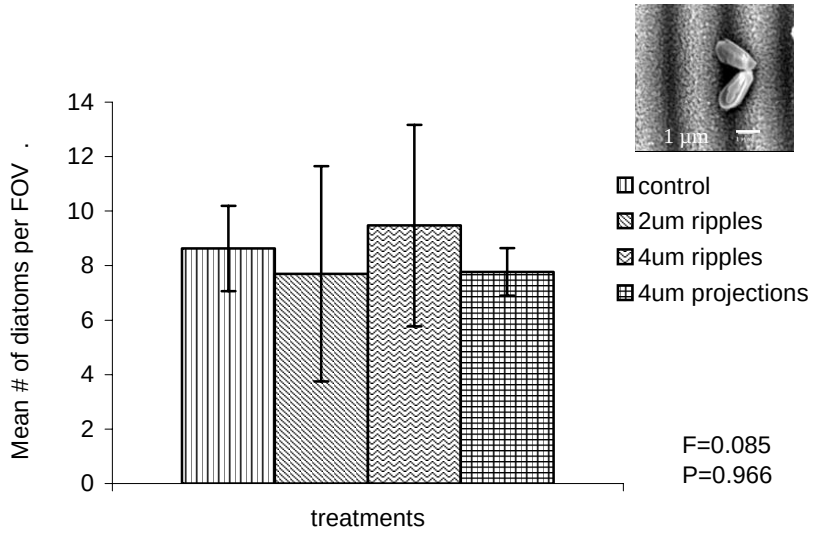

Figure 5.3 Mean cell settlement by *Fallacia carpentariae* to treatments and control. Data shows mean ± one standard error. Analysis was by one-way ANOVA. Thumbnail: *Fallacia carpentariae* on 4 µm ripples

5.3.3 *Nitzschia paleacea* assay

Attachment by the intermediate sized diatom, *Nitzschia paleacea* (cell length 7 µm, width 2 µm), was significantly higher (ANOVA P = 0.003, Tukey's *post-hoc* analysis, Figure 5.4) on the 2 µm ripple treatment than all other treatments with more than twice the cells per FOV (126 cells/fov) than the other surfaces (53-66 cells/fov). This species has the highest number of attachment points on the 2 µm ripple treatment fitting within the width of the microtexture. There was no significant difference in diatom attachment between the other microtextured treatments and the smooth control.

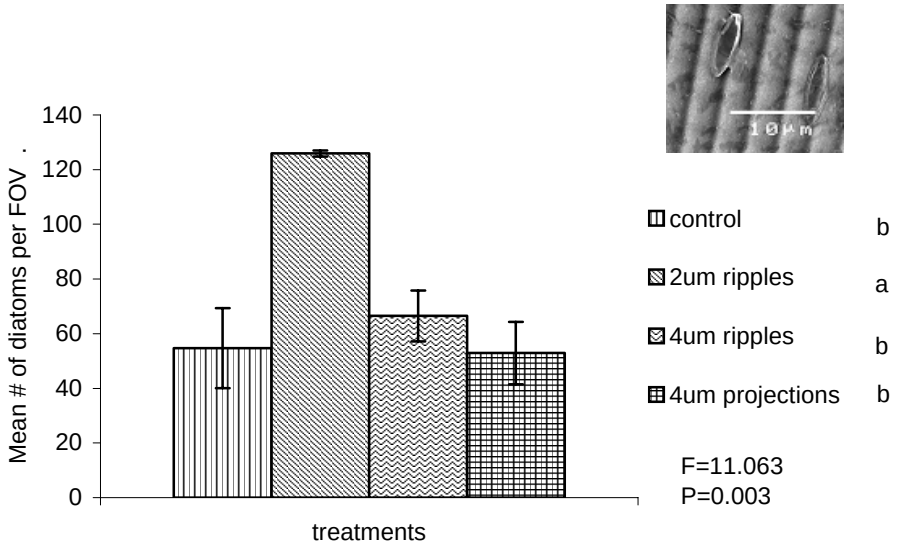

Figure 5.4 Mean cell settlement by *Nitzschia* cf. *paleacea* to treatments and control. Data shows mean ± one standard error. Analysis by one-way ANOVA followed by Tukey's *post hoc* test. Thumbnail: *Nitzschia* cf. *paleacea* on 4 µm ripples

5.3.4 *Navicula jeffreyi* assay

The second largest diatom *Navicula jeffreyi* (cell length 12 µm, width 4 µm) settled in significantly higher numbers on the smooth control (38.5 cells/fov) than the 4 µm ripple surface (24.6 cells/fov) (ANOVA P = 0.035, Tukey's *post-hoc* analysis). This species has the most attachment points on the smooth control and the least number on the 4 µm ripple surface. There was no significant difference in diatom settlement between the microtextured surfaces with 2 µm ripples (30.5 cells/fov) and 4 µm projections (33.9 cells/fov) and any other treatments (see Figure 5.5).

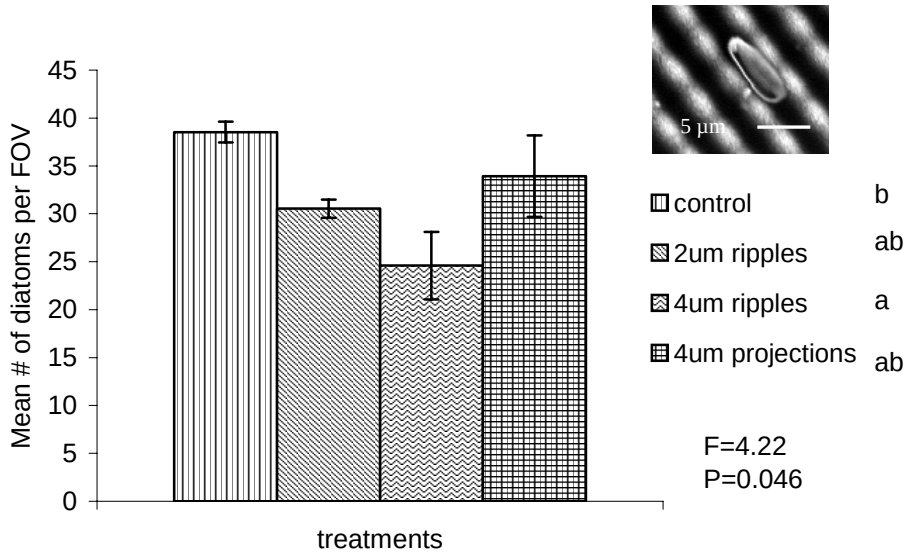

Figure 5.5 Mean cell settlement by *Navicula jeffreyi* to treatments and control. Data shows mean ± one standard error. Analysis by one-way ANOVA followed by Tukey's *post hoc* test. Thumbnail: *Navicula jeffreyi* on 4 µm projections

5.3.6 *Amphora* sp. assay

The largest diatom *Amphora* sp. (cell length 14 µm, width 7 µm) settled in high numbers on all treatments after 4 hours, with the highest number of diatoms settling on the smooth control treatments (279±18.9 cells/fov, Figure 5.6), significantly more than the 4 µm ripple surface (148±15.5 cells, P = 0.039, Tukey's *post-hoc* analysis, Figure 5.6). This species also has the most theoretical attachment points on the smooth control and the least number on the 4 µm ripple surface. Diatom attachment on 2 µm ripples (228±14.4, Figure 5.6) and 4 µm projections (242±15.1, Figure 5.6) were not significantly different to any other treatments.

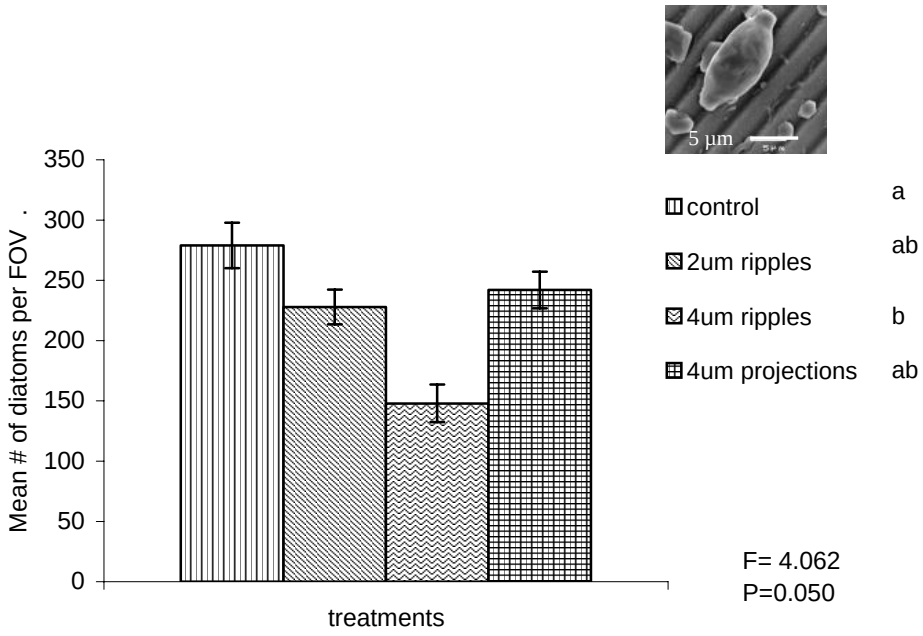

Figure 5.6 Mean cell settlement by *Amphora* sp. to treatments and control. Data shows mean ± one standard error. Analysis by one-way ANOVA followed by Tukey's *post hoc* test. Thumbnail: *Amphora* sp. on 4 µm ripples

5.4 Discussion

The four benthic fouling diatoms used in this study were able to attach and adhere to both smooth and microtextured polyimide. Cells attached in significantly higher numbers on surfaces where the numbers of attachment points are highest. For the smallest diatom, *Fallacia carpentariae*, there was no difference in mean number of cells attached between any treatments. This species has a cell size less than the wavelength of all microtextured treatments and as such the cells of this species have a multiple attachment points on all test surfaces. *Nitzchia paleacea* has a cell width slightly less than 2 µm, the perfect fit for 2 µm microtextured ripples. The cells of this species were observed to line up longitudinally inside the 2 µm microtextured ripples and incidentally had twice the number of cells adhering to this treatment than any other. With increasing cell size the number of attachment points was reduced particularly on the 4 µm ripple surfaces where for both *Amphora* sp. and *Navicula jeffreyi* there were only two theoretical attachment points. Both species had significantly lower attachment to the 4 µm ripple surfaces than the smooth control.

The response of the tested fouling diatoms to microtextured polyimide supports the application of attachment point theory to diatoms, whereby reduced numbers of attachment points results in lower rates of settlement. Changes in surface chemistry resulting from the laser ablation of polyimide is unlikely to be responsible for differences in cell settlement between microtextured surfaces and smooth controls as in all assays at least one microtextured treatment was not significantly different to the smooth control polyimide.

Increased attachment rates with increasing attachment points have been reported for algal spores of *Ulva linza* with spores settling preferentially in 5μm valleys, the same size as their spores (Callow et al. 2002). A majority of spores settled on the angle between the valley floor and sidewall, or the base of pillars regardless of the width of microtexture, and there was a five-fold increase in spore settlement on 5μm deep valleys as opposed to valleys 1.5μm deep (Callow et al. 2002). Therefore, for *Ulva linza* zoospores maximum attachment occurs at the most energetically favourable site where there are optimal numbers of attachment points (Callow et al. 2002, Hoipkemeier et al. 2004).

There is also evidence that barnacle cyprid settlement is reduced when the numbers of attachment points are reduced. For the barnacle *Balanus improvisus* microtextured surfaces with a height of 30-45 μm and width of between 150-200 μm reduced settlement compared to smooth controls by 82% (Berntsson et al. 2000b) whilst PVC riblets with profile height of 350 μm and width of 134μm reduced settlement by 98% (Berntsson et al. 2000a). In a similar study Petronis *et al*. (2000) found that PVC riblets with 69 μm height and 97 μm width reduced *B. improvisus* settlement by 67% compared to smooth controls. In all cases where *B. improvisus* settlement was heavily reduced compared to smooth controls the size of microtexture was slightly less than the width of the cyprid (250-270 μm, Berntsson *et al.*, 2000b) reducing the number of attachment points. Petronis *et al*., (2000) also reported that micropyramids did not deter cyprids as well as microriblets. This is consistent with the present study whereby 4 μm ripples had significantly lower diatom attachment than controls for the two largest species and the 4 μm projections had no settlement differences compared to smooth

controls. This may be due to projections providing a greater number of theoretical attachment points than ripples.

This study reinforces the pattern seen between the size and settlement of larvae and propagules, and the optimal number of attachment points. The ability of microfoulers to settle inside microtexture smaller than the cell width may help explain the loss of fouling resistance over time for biomimics from Chapter 4. To date there have been a limited number of organisms tested against microtextured surfaces, but those that have been tested demonstrate a strong correlation between levels of settlement and the optimal number of attachment points. Conversely, restricted numbers of attachment points correlate with decreased settlement. The biomimetic approach used in this study demonstrates the opportunity to understand and develop new fouling deterrent surfaces using natural models. Further studies examining a range of microtexture scales are needed to apply attachment point theory to the suite of fouling organisms and to develop structured surfaces to control the attachment and development of fouling communities.

CHAPTER SIX

Attachment point theory: the fouling response to a microtextured matrix

6.1 Introduction

The study of surface microtexture has gained some momentum in recent years with the discovery of several naturally fouling resistant organisms that display surface microtexture (Wahl et al. 1998; Ball, 1999; Baum et al. 2002; Scardino et al. 2003; Bers & Wahl, 2004). Artificial surfaces have been produced that are inspired from natural microtextures, and these biomimics have provided promising fouling resistance (Figueiredo et al. 1997; Bers & Wahl, 2004; Scardino & de Nys, 2004). In addition, designed microfabricated surfaces have been tested against diatoms (Scardino et al. 2006), algal spores (Callow et al. 2002; Hoipkemeier-Wilson et al. 2004) and barnacle cyprid larvae (Berntsson et al. 2000; Petronis et al. 2000). These organisms demonstrate mixed attachment (in this case referring to attachment of diatoms, settlement and germination of algae, and settlement and metamorphosis of larvae) preferences depending on the size of the organism tested and the microtexture of the surface. While the variation in attachment on surface structures is well documented, the mechanism of action of how microtexture affects fouling is not well understood. Attachment point theory has been proposed as a possible mechanism for reduced or increased fouling on microtextured surfaces, whereby fouling organism attachment is increased when there are optimal numbers of “potential settling points” (Hills et al. 1999) or “attachment points” (Callow et al. 2002) and reduced with few (sub-optimal) points of attachment (Scardino et al. 2006). The number of attachment points is dependent on the size of the settling larvae/spores and the wavelength of the microtexture. Attachment to microtextures/microrefuges has been explored for barnacle cyprids (Lemire & Bourget, 1996; Hills et al. 1999; Kohler et al. 1999; Lapointe and Bourget, 1999; Berntsson et al. 2000; Petronis et al. 2000) and *Ulva* spores (Callow et al. 2002; Hoipkemeier-Wilson et al. 2004). These studies have found that for various cyprids of various barnacle species attachment is reduced on microgroves and pyramids below the size of the cyprid. Similarly, *Ulva* spore attachment is increased on microtextures slightly larger than the spore size. Attachment also affects adhesion strength. Microrefuges have been shown to be important in protecting *Ulva linza* spores

from hydrodynamic forces, thereby reducing spore removal. These refuges occur when the spore is slightly smaller than the size of the microtexture (Granhag et al. 2004; Hoipkemeier-Wilson et al. 2004).

The concept of attachment point theory was introduced in Chapter 5. For several diatom species attachment was reduced on surfaces with texture below the size of the cell while attachment increased on smooth surfaces and when textures provided multiple numbers of attachments points. In this Chapter I expand on the findings from Chapter 5 and include the major fouling classes comprising a wide range of cell and propagule sizes (7-321 μm), which are tested for attachment preferences across a broad range of microtexture wavelengths (4-512 μm). The aim of this study was to determine if attachment point theory holds for broad classes of fouling larvae and algal propagules in static choice bioassays. The five fouling organisms used are the raphid diatom *Amphora* sp., the green algae *Ulva rigida*, the red algae *Polysiphonia sphaerocarpa* and *Centroceras clavulatum*, and the bryozoan *Bugula neritina*. *Amphora* sp. contacts the surface passively, attaches via the excretion of extracellular polymeric substances (EPS) and can glide across a surface. *U. rigida* spores have flagella and can move freely across a surface to explore. Attachment is initiated by the secretion of a glycoprotein adhesive which rapidly cures on the surface. After this process the spore is non-motile (Finlay et al. 2002b). Red algal spores have no flagella and hence contact the surface passively after which mucilage and adhesive vesicles are released. *B. neritina* larvae are freely motile (for several hours) due to an external covering of cilia. Larvae adhere to the surface through adhesive secretions from the pyriform groove and internal sac, which becomes extruded and forms a permanent disc-like holdfast (Mawatari, 1951).

6.2 Methods

6.2.1 Ablation of polymers

A matrix of microtextured patterns was manufactured by MiniFAB Pty Ltd in 1.5 mm polycarbonate by laser micromachining using an excimer laser system (8000 series, Exitech, UK) equipped with a Lambda Physik LPX210i laser source operating at a wavelength of 248 nm with krypton fluoride (KrF) as the excitation gas. The master template for the polycarbonate pieces was 100 mm x 100 mm and consisted of nine 30

mm x 30 mm squares each with a sinusoidal shaped pattern which varied in both the period (distance from peak to peak) and depth (distance from peak to trough) of the sinusoidal shape.

Full details of the machining process used to produce the microtextured matrix are detailed in Harvey & Rumsby (1997). In brief it involved delivering a laser beam onto a chrome-on-quartz mask. The mask was controlled by an X-Y stage allowing precise lateral and vertical movement. The microtextured polycarbonate master copy was metallised after laser machining. An inverse copy of this master was subsequently electroformed in nickel using a nickel sulphamate bath. This nickel tool was then used as a master for replicating several microtextured parts in polycarbonate by hot embossing. Each polycarbonate piece was arranged as displayed in Figure 6.1. The centre square was un-machined polycarbonate.

256 µm	**16** µm	**64** µm
***512** µm	**smooth**	**32** µm
8 µm	**128** µm	**4** µm

Figure 6.1 The arrangement of microtextured squares on the Polycarbonate matrix. The number in each square represents the depth and period of microtexture with the exception (*) of the 512 µm microtextured square which has a period of 512 µm and a depth of 256 µm due to machining constraints.

6.2.2 Surface characterisation

All microtextures were assessed for accuracy using Scanning Electron Microscopy. For aspect ratios microtextured depths were determined using optical microscope (x 50 objective). Wettabilities of each texture and control (unmodified PC) of polycarbonate were determined using the sessile drop method by measuring advancing water contact angles using a goniometer (Rahme-Hart, NRL-CA, 100-00). The aspect ratio between

the microtextured wavelength and depth was kept constant at 1:1 except for the 512 µm texture, which could not be manufactured at a 1:1 ratio and had a 0.5: 1 ratio. The wettability of microtextured squares was relatively constant for all textures and smooth polycarbonate (69º - 82º) except for the 32 µm texture (100º). The microtextured polycarbonate was characterised for each square and is summarised in Table 6.1.

Table 6.1. Summary of surface characterisation of microtextured polycarbonate

Wavelength (µm)	**Depth (µm)**	**Aspect ratio**	**Wettability (º)**
Smooth (untextured)	0	1:1	70.9 ± 3.4
4	4-6	1:1	69.3 ± 3.3
8	4-6	1:1	71.3 ± 4.2
16	14	1:1	84.3 ± 1.2
32	30	1:1	100.5 ± 7.5
64	59	1:1	84 ± 4.6
128	125	1:1	69.4 ± 4.3
256	245	1:1	82.1 ± 6.9
512	256	1:0.5	78.3 ± 2

6.2.3 Collection of organisms

Five fouling organisms were used in bioassays on microtextured polycarbonate plates. They were the benthic pennate diatom *Amphora* sp. (CS-255), the red algae *Polysiphonia sphaerocarpa* Børgesen and *Centroceras clavulatum* (C. Agardh) Montagne, the green alga *Ulva rigida* (C. Agardh), and the bryozoan *Bugula neritina* Linneaus.

Amphora sp. (CS-255) (Class Bacillariophyceae, Order Bacillariales) stock cultures were obtained from CSIRO microalgal supply service, Tasmania, Australia and assays were conducted at James Cook University (JCU) laboratories.

The algae *P. sphaerocarpa, C. clavulatum* and *U. rigida* were collected from intertidal rock pools at Nth Clovelly, Sydney (33° 55'S; 151° 15'E). Fertile *U. rigida* were checked each day for two weeks before a full moon for the presence of reproductive thalli. A variety of plants from different areas on the rock platforms were collected and

placed in bags with *in situ* seawater and returned immediately to the laboratory at UNSW for assays.

The bryozoan *Bugula neritina* is a cosmopolitan species occurring along the eastern Australian coastline. Bioassays were conducted at UNSW. Colonies of *B. neritina* were collected from boat hulls at Rose Bay, Sydney (33° 53'S; 151° 15'E) and placed in bags with *in situ* seawater and returned immediately to the laboratory.

6.2.3 Bioassay procedures

Amphora sp. (CS-255)

Growth conditions for *Amphora* sp. were 12:12 light: dark cycle with a light intensity - 80µmol photons PAR $m^{-2}S^{-1}$; using Philips daylight or cool white fluorescent tubes. Diatom cultures were supplemented with F/E2 medium (Guillard & Ryland, 1962). *Amphora* sp. was cultured at 25ºC. The cells were re-suspended with an orbital shaker and their concentration determined using a haemocytometer prior to use in assays. The test surfaces were rinsed in filtered (0.2 µm) seawater before adding diatom cultures. The surfaces were individually placed in plastic weigh boats (120 mm x 120 mm) and filled with 40 ml of filtered (0.2 µm) seawater and 150 µl of diatom culture suspension was pipetted into each textured square with a cell density of approximately 1.6 x 10^5 cells/ml. Three replicate microtextured pieces were used. The diatoms were left to attach for 3 hours after which they were dip-rinsed and counted in 10 random fields of view (FOV) per dish at magnifications of x 400 (0.16 mm^2). The dip-rinsing involved immersing each treatment in a new beaker of filtered (0.2 µm) seawater three times to remove unattached cells, the surfaces were briefly exposed to air during this process (technique used in Scardino et al. 2006). This dip-rinsing process is used for all assays in this Chapter.

Ulva rigida

Fertile thalli (with yellow tips) of *U. rigida* were kept in seawater under refrigeration for two hours after collection. They were then dried and placed in new seawater and exposed to light. Gametes (two terminally inserted flagella) were released after 15 minutes and swam towards the light. They were pipetted into a separate beaker under light and stirred to prevent settlement until the solution was light green in colour.

Approximately 150 µl (6.3×10^{-5} cells) were added to each dish (plastic weigh-boat, 120 mm x 120 mm) with a microtextured polycarbonate plate with 40 ml of filtered (0.2 µm) seawater. Gametes were left to settle and germinate for 96hrs after which the dishes were dip-rinsed and the number of plants counted in 5 fields of view (x 200, 0.64 mm^2) on each microtextured square. There were 5 replicate microtextured polycarbonate plates.

Polysiphonia sphaerocarpa

Collected plants were brought back to the laboratory and checked under a dissecting microscope for cystocarps, which were removed and placed in a separate dish. Spores were released from the cystocarps over 30-60 minutes. Approximately 250 spores were randomly dispersed by pipette into each dish (plastic weigh-boat, 120 mm x 120 mm) with a microtextured polycarbonate plate with 40 ml of filtered (0.2 µm) seawater. Red algal spores have no flagella and hence settle passively. They were left to germinate over 48hrs after which the numbers of plants were counted on each microtextured square after dip-rinsing. Five replicate microtextured polycarbonate plates were used.

Centroceras clavulatum

Collected plants were brought back to the laboratory and checked under a dissecting microscope for cystocarps, which were removed and placed in a separate dish. Spores were released from the cystocarps over 30-60 minutes. Approximately 100 spores were randomly pipetted into each dish (plastic weigh-boat, 120 mm x 120 mm) with a microtextured polycarbonate plate with 40 ml of filtered (0.2 µm) seawater. The spores were left to germinate over 48hrs after which the numbers of plants were counted on each microtextured square after dip-rinsing. Six replicate microtextured polycarbonate plates were used.

Bugula neritina

Colonies of *B. neritina* were placed in aerated seawater in the dark for 24 hours after collection. After approximately 15 minutes exposure to light, larvae were released and pipetted into each dish (plastic weigh-boat, 120 mm x 120 mm) with a microtextured polycarbonate plate with 40 ml of filtered (0.2 µm) seawater. Approximately 100 larvae were placed in each dish, covered and allowed to settle in the dark for 24 hours. After

this time the number of settled and metamorphosed larvae in each microtextured square was recorded. There were 5 replicate matrix pieces.

For all bioassays, three unmachined control pieces of polycarbonate were used to ensure cells, propagules and larvae were competent to attach to this material and that there was an even spread of attachment across the polycarbonate piece (no clumping in certain areas).

Measurement of cells, propagules and larvae

All diatoms, gametes, spores and larvae were photographed (Leica, DC300 camera) and sizes were measured with the measurement module of the image analysis program IM50 (Leica Microsystems). 10 replicates were measured for each species.

6.2.4 Statistical analysis

Analysis between microtextures was done using ANOVA with Tukey's *post-hoc* tests where appropriate. The assumptions of ANOVA were met by testing the normality of the data using Q-Q plots of standardized residuals and homogeneity of variance tested using scattergrams of standardized residuals versus predicted means (Underwood, 1981). Where assumptions were not met, data was transformed (arcsine square-root). The statistical package SPSS v 12 was used.

6.3 Results

6.3.1 Cell, propagule and larval sizes

Larvae and spore sizes are shown in Table 6.2. The organisms chosen provide a broad range of sizes for the testing of microtextured polycarbonate. The smallest organisms were the *Amphora* sp. cells, (width 7 µm) and *U. rigida* gametes (7.24 µm diameter) whilst *B. neritina* larvae are much larger (321 µm).

Table 6.2 Cell, propagule and larval sizes of fouling organisms used in bioassays. Data are mean ± one standard error

Larval/cell size	*Amphora* sp.	*Ulva rigida*	*Centroceras clavulatum*	*Polysiphonia sphaerocarpa*	*Bugula neritina*
Width	7 µm	7.24± 0.13 µm	37.49± 1.75 µm	51.66± 0.46 µm	321.4± 5.1 µm
Length	14 µm	N/A spherical	N/A spherical	N/A spherical	N/A spherical

6.3.2 *Amphora* sp. assay

The *Amphora* sp. cells were 7 µm wide and 14 µm long, and could fit inside all textures except the 4 µm. The mean proportion of *Amphora* sp. cells attached to the microtextured squares was not significantly different ($F_{8,36}$ = 1.113, P =0.378, Figure 6.2). The texture with the lowest proportion of *Amphora* sp. cells was 512 µm with 7.9% (46.4 ± 19.2 cells) and 4 µm with 9.18% (49.3 ± 19.4 cells) of cells attached to these textures. In contrast the 8 µm texture which is slightly larger than the width of *Amphora* sp. cells had the highest proportion of attached cells,14.7% (88.3 ± 43 cells) (Figure 6.2).

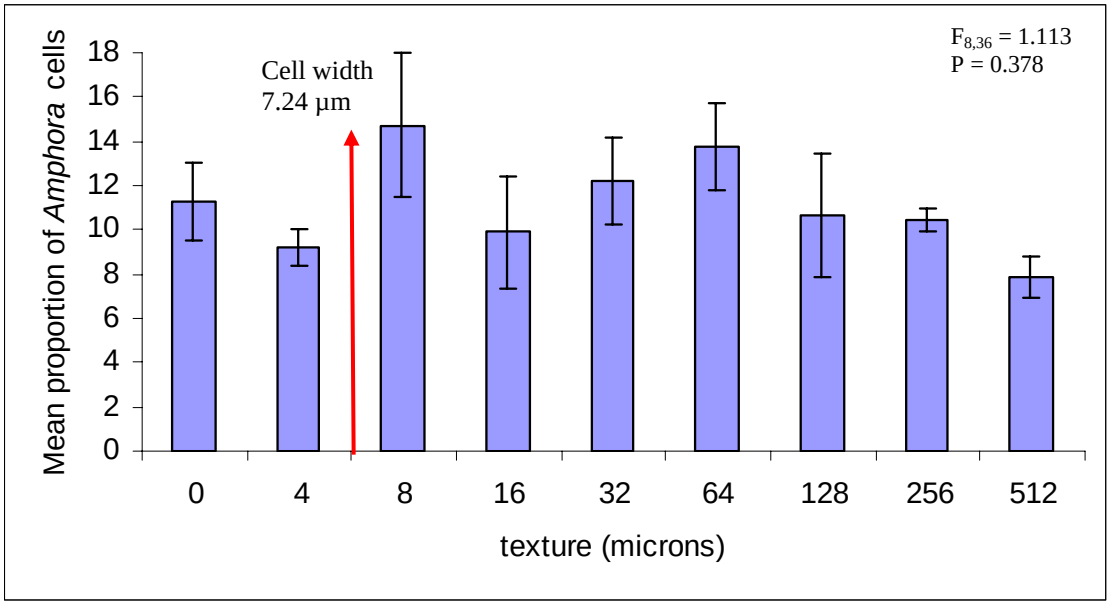

Figure 6.2. The proportion of *Amphora* sp. cells attached to microtextured squares per 200x FOV. Data are means ± 1 SE, n=5. Analysis by ANOVA.

6.3.3 *Ulva rigida* assay

U. rigida gametes were spherical with a diameter of 7.24 µm and could fit inside all textures except the 4 µm. The proportion of *U. rigida* gametes settled and germinated on the untextured and microtextured squares was not significantly different ($F_{8,36}$ = 1.75, P = 0.132, Figure 6.3). The texture with the highest proportion of settled and germinated *U. rigida* gametes was the 64 µm which had 16.7% (76.2 ± 34.5 gametes) of gametes attached to this texture. In contrast the 4 µm texture, the only texture smaller than the *U. rigida* spore size, had the lowest proportion of settled and germinated gametes, 5.4% (16.12 ± 4.34 gametes) (Figure 6.3). The number of gametes settled and germinated increased with increasing texture widths up to 64 µm then decreased for the largest three microtextures. Gametes settled and germinated in moderate numbers on the untextured polycarbonate (20.8 ± 3.4 gametes).

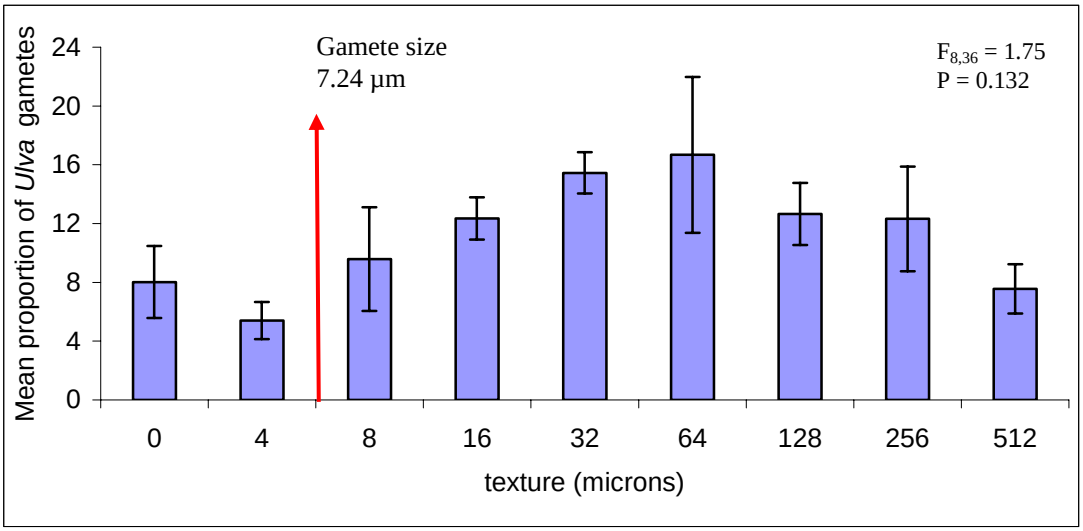

Figure 6.3. The proportion of *Ulva rigida* gametes settled and germinated on microtextured squares per 400x FOV. Data are means ± 1 SE, n=5. Analysis by ANOVA.

6.3.4 *Centroceras clavulatum*

The spore size was 37.5 µm (diameter) and therefore could fit inside all textures above 32 µm however, *C. clavulatum* spores are non-motile. The number of *C. clavulatum* spores settled and germinated on the microtextured squares was not significantly different (F = 0.841, P = 0.572, Figure 6.4). The highest *Centroceras clavulatum* germination occurred on the untextured polycarbonate (21.8 ± 12.3 spores) whilst the

lowest germination occurred on the 256 µm microtexture (6.33 ± 3.2 spores). The proportion of spores settled and germinated was similar across all textures ranging from 9.1% to 10.9% (Figure 6.4).

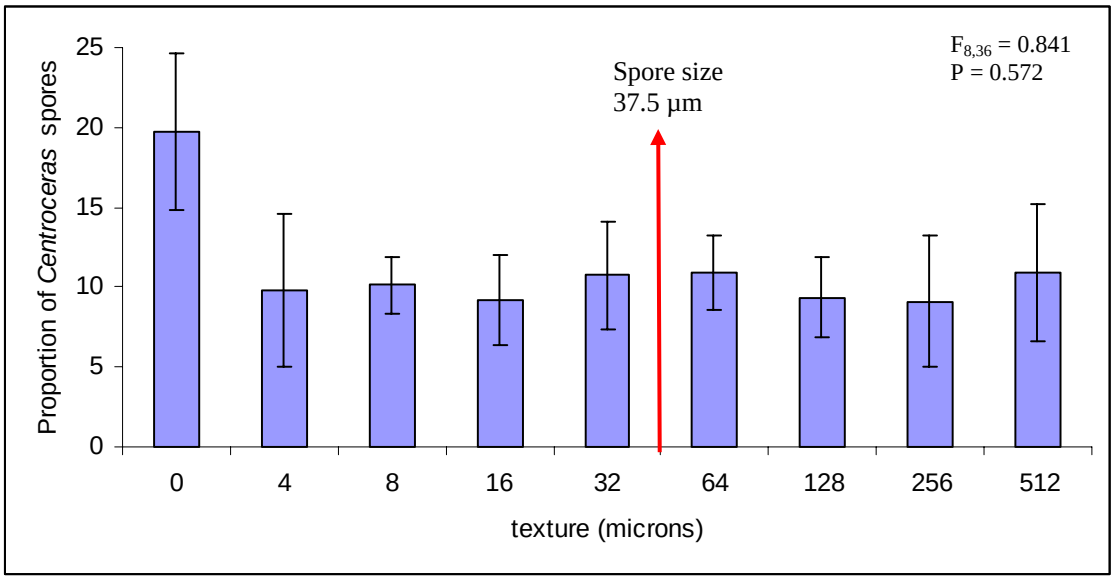

Figure 6.4 The proportion of settled and germinated *C. clavulatum* spores on microtextured squares. Data are means ± SE, n=6. Analysis by ANOVA.

6.3.5 *Polysiphonia sphaerocarpa* assay

The spore size of *P. sphaerocarpa* was 51.66 µm (diameter) and therefore could fit inside all textures above 32 µm. However, *P. sphaerocarpa* spores are non-motile. The numbers of *P. sphaerocarpa* spores that settled and germinated on the microtextured squares was significantly different ($F_{8,36}$ = 3.64, P = 0.003, Figure 6.5) however there was no consistent pattern for increasing scale of texture. The lowest settlement and germination occurred on the 32 µm texture with 5.2% of spores (11.2 ± 1.9 spores) while the highest settlement and germination occurred on the 256 µm texture with 23.4% of spores (50.4 ± 11.7 spores) (Figure 6.5). The 32 µm texture, 4 µm texture (5.3%, 11.4 ± 4.9 spores) and 128 µm texture (5.5%, 11.8 ± 2.7 spores) had significantly less attached *P. sphaerocarpa* spores than the 256 µm texture (Figure 6.5). Spore attachment on the 8, 16, 64, 512 µm textures and the untextured polycarbonate were not significantly different to any other textures.

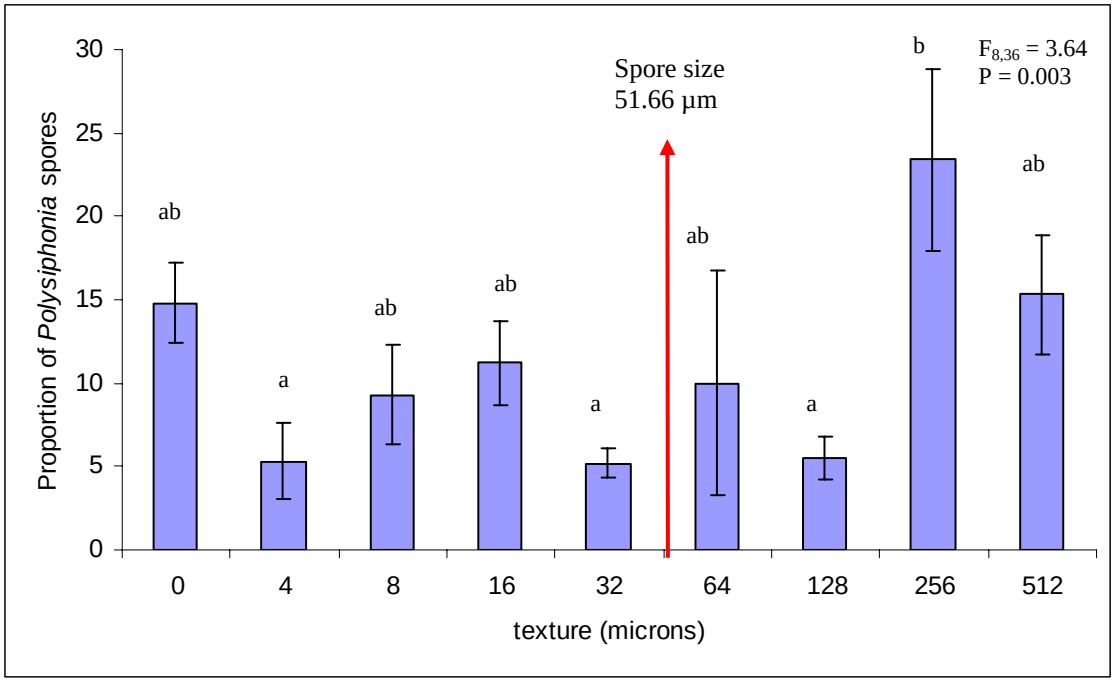

Figure 6.5 Proportion of *P. sphaerocarpa* spores settled and germinated on microtextured squares. Data are means ± SE, n=5. Analysis by ANOVA followed by Tukey's *post hoc* test. Columns with a dissimilar letter are significantly different at α = 0.05.

6.3.6 *Bugula neritina* assay

The size of *B. neritina* larvae was 321.4 µm and therefore could only fit inside the 512 µm texture. The proportion of *B. neritina* larvae settled and metamorphosed on the microtextured squares was significantly different (F = 2.21, P = 0.036, Figure 6.6). The highest proportion of settled and metamorphosed *B. neritina* larvae was on the largest ripples 512 µm (23.4 ± 6.7%, 36 larvae) which is the only texture larger than the larvae. In contrast significantly fewer larvae settled and metamorphosed to the 64 µm and 256 µm textures (5.3% ± 2.7, 16 larvae and 5.8% ± 2.8, 17 larvae respectively). Settlement and metamorphosis to the remaining textures ranged from 8.5% to 15% and was not significantly different to settlement and metamorphosis on any other textures.

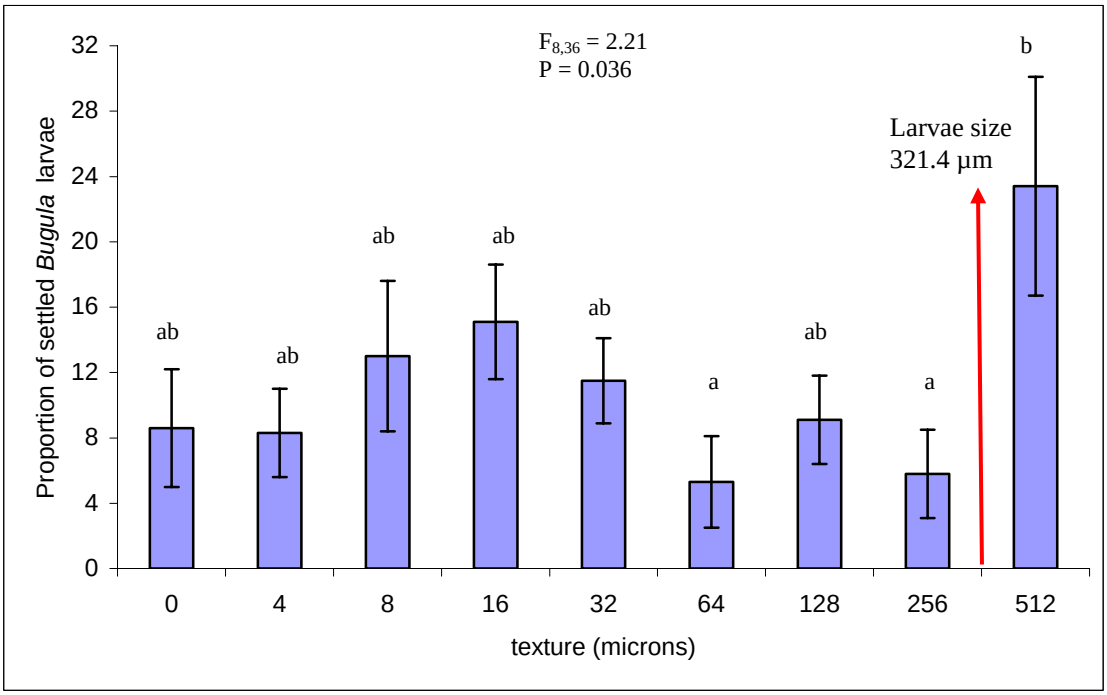

Figure 6.6. Proportions of settled and metamorphosed *B. neritina* larvae to microtextured squares. Data are means ± SE, n=9. Analysis by one-way ANOVA followed by Tukey's *post hoc* test. Columns with a dissimilar letter are significantly different at $\alpha = 0.05$.

Table 6.3. Summary of attachment to microtextured polycarbonate for each species tested. Lower = lower proportion of cells attached compared to other microtextures, Higher = a greater proportion of cells attached compared to other microtextures, Equal = a similar proportion of cells attached compared to other microtextures, n/s = no significant difference in attached cells between microtextures, * = a significant difference in attached cells between microtextures at $\alpha = 0.05$.

Species	**Size (µm)**	**Attachment to first texture smaller than cell size**	**Attachment to first texture larger than cell size**
Amphora sp.	7	(4 µm) Lower	(8 µm) Higher
Ulva rigida	7.2	(4 µm) Lower	(8 µm) Equal
Centroceras clavulatum	37.5	(32 µm) Equal	(64 µm) Equal
Polysiphonia sphaerocarpa	51.7	(32 µm) Lower*	(64 µm) Equal
Bugula neritina	321.4	(256 µm) Lower*	(512 µm) Higher*

6.4 Discussion

The fouling organisms chosen in this study cover the major groups of fouling classes and larval/spore sizes, and demonstrate the influence of attachment points and surface microtexture on attachment. There is a broad range of attachment preferences by the different fouling organisms to varying scales of microtexture (in this case referring to attachment of diatoms, settlement and germination of algae, and settlement and metamorphosis of larva). The most important finding across all the organisms, except *C. clavulatum*, is that attachment is lower on textures slightly smaller than the size of the fouling larvae/cells compared to other microtextures. Furthermore, on the texture immediately greater than the size of the larvae attachment was in general strongly increased. For the diatom *Amphora* sp., (cell size 7 µm), attachment is lower on the 4 µm texture and higher on the 8 µm texture and the green algae, *Ulva rigida*, (gamete size 7 µm) attached in lower numbers on the 4 µm texture. However, these differences were not significant. The red algae *Polysiphonia sphaerocarpa*, (spores size 51 µm) attached in significantly lower numbers on the 32 µm texture while for the bryozoan, *Bugula neritina* (larval size 321 µm), attachment was significantly lower on the 256 µm texture and significantly higher on the 512 µm texture. These findings provide species-specific support for attachment point theory discussed in Chapter 5.

Surface microtexture has previously been tested against *Amphora* sp. (Scardino et al. 2006), and *Ulva linza* (Callow et al. 2002; Hoipkemeier-Wilson et al. 2004), and *Balanus* species (Hills et al. 1999; Berntsson et al. 2000; Petronis et al. 2000). *Amphora* sp. attachment numbers were reduced compared to smooth controls on microtextured surfaces smaller than the width of the cell (Scardino et al. 2006). Whilst this finding is consistent with the present study where the 7 µm *Amphora* sp. cells attached in fewer numbers on the 4 µm texture compared to larger microtextures and a smooth control, the differences in this study were not significant. This is possibly due to the greater range of choices (eight textures and a smooth control) compared to the previous no choice bioassays.

Ulva linza spores have been reported to prefer microtextures slightly larger than the spore size (Callow et al. 2002; Hoipkemeier-Wilson et al. 2004), while in this study *Ulva rigida* showed no preference for microtexture slightly larger (8 µm and 16 µm) than the gamete size (7 µm). However, attachment was lower (non-significant) on microtexture slightly smaller (4 µm) than the spore size. Both *Amphora* cells and *Ulva* gametes attached in relatively high numbers to textures larger than their size. This pattern of settlement could be due to the sinusoidal shape of the microtexture which allows for attachment at the bottom of the texture even though the top of the channel becomes wider. Square channels with an even width throughout the depth of the channel may be better to determine the effect of size of texture on attachment.

Several studies have shown that *Balanus improvisus* cyprids are deterred by microtextures smaller than the cyprid size (250-270 µm) (Berntsson et al. 2000; Petronis et al. 2000) and Hills et al. (1999) found that densities of *Semibalanus balanoides* were positively correlated to Potential Settling Sites (PSS). Although barnacle cyprids were not tested in this study, similar trends were found for bryozoan larvae which are of a similar size. *B. neritina* larvae fitted to attachment point theory as there was significantly lower attachment on the 256 µm texture and compared to the 512 µm texture. *B. neritina* larvae are known to prefer small-scale heterogeneity whereby refuge is often found (Walter, 1992; Walters & Wethey, 1996). Whilst the smallest scale of surface complexity chosen in those studies was in the order of millimeters, it supports the present study's finding that *B. neritina* larvae prefer textures larger than their body size.

The red algae *Polysiphonia sphaerocarpa* and *Centroceras clavulatum* are passive settlers, which mean spores drift onto a surface rather than actively exploring it. It would therefore be expected that all areas of the textured plate would have an even number of attached spores. Any differences in settlement would reflect changes in adhesion strength resulting from the dip-rinsing process. Despite the ubiquitous nature of these species little is known regarding their attachment and adhesion. Considering they do not chose where to settle, it was particularly interesting to see if the attachment point theory would fit for these species. Spores of *C. clavulatum* did not conform to

attachment point theory as expected as spore attachment was similar on all microtextures with the highest attachment occurring on untextured polycarbonate. Spores of *P*. *sphaerocarpa* attached in a random pattern, neither supporting nor refuting attachment point theory. Spores attached in significantly lower numbers on the microtexture slightly smaller than the spore size (32 µm) as well as on the smallest microtexture (4 µm). However, attachment was not significantly higher on the 64 µm texture as would be expected. Instead attachment was significantly higher on the 256 µm texture. Weak adherence to certain mictotextures and subsequent detachment of spores after dip-rinsing may have been the cause of the significant differences in attachment considering these spores do not select where to settle.

Each tested fouling organism was tested on untextured polycarbonate controls to ensure competency to attach to this material. As each polycarbonate piece was designed with the same texture pattern arrangement, cells, larvae and propagules were also checked to ensure there were no conspecifics or clumping on certain areas of the polycarbonate piece, thereby ensuring that any observed differences were due to changes in texture and not edge effects. The etching of the microtextures onto polycarbonate altered the wettability of the surface slightly (70-100º). The range of wettabilities were however quite moderate, considering surfaces can have wettabilities ranging from 0 to 180º. It would therefore be unlikely that any differences in attachment preferences were due to slight increases in surface hydrophobicity.

This study has given limited support to attachment point theory, in that organisms will attach in lower numbers when there are fewer attachment points. The next important research direction will be to determine the attachment strength on microtextures above and below the scale of the fouling organism using the surfaces tested here. Given the potential dampening effect of the curved surface on attachment points it would also be useful to test the sizes tested in this study using alternative shapes such as square edged grooves to remove bias for attachment at the base of larger sinusoidal surfaces. Previous work on adhesion strength under flow has demonstrated the importance of microtopographies/surface roughness on larval and spore removal (Berntsson et al. 2000; Finlay et al. 2002, Shultz et al. 2000; Granhag et al. 2004;). Depending on the

scale of roughness or topography relative to the fouling organism, protection from hydrodynamic forces can occur. For spores of *Ulva linza* (size 5 µm), lower removal after exposure to a water jet was found on microtopographies with profile heights of 25 and 36 µm compared to smooth and large scale topographies (Granhag et al. 2004) while microtextures 5 µm wide and 5 µm deep (perfect fit for spores) had the least spore removal after exposure to a flow channel (Hoipkemeier-Wilson et al. 2004). In contrast microtopographies at a similar scale (30-45 µm) reduced barnacle attachment (Berntsson et al. 2000); in this case topography was smaller than the scale of the fouling organism and did not provide a refuge from hydrodynamics.

The forces required to remove fouling larvae from surface microtexture are an important consideration for the development of fouling-release technologies. Finlay et al. (2002) demonstrated that on a smooth surface (glass) the surface pressure required to remove *U. linza* spores is 250kPa after four hours and increases substantially with time. It is therefore unlikely that spores would be removed under operating speeds of most vessels. With many antifouling surfaces moving towards fouling-release rather than non-stick coatings it is essential that surface roughness/microtexture does not increase adhesion strength and the forces required for fouling removal. A surface with fewer numbers of attachment points and one which does not provide microrefuges may be able to reduce the shear forces required for fouling removal and therefore would be an excellent foul-release candidate.

The applicability of attachment point theory and the influence of surface microtexture in long-term field trials will also be essential in assessing the efficiency of microfabricated biomimics. Of course *in-situ,* fouling larvae come in all sizes as such a successful surface will need a combination of microtextures with fractal dimensions to cover micro and macro fouling organisms.

CHAPTER SEVEN

Micro and nano-scale surfaces with extreme hydrophobicities

7.1. Introduction

Previous Chapters have stressed the increasing need for non-toxic antifouling alternatives. A range of physical surface properties have been investigated in regard to their antifouling potential including microtexture, mean roughness and waviness, skewness, texture aspect ratio and fractal dimension. All of these properties have a demonstrated influence on fouling attachment. To date the properties investigated and manipulated to determine mechanisms affecting the settlement and attachment of fouling organisms have been on the scale of microns. However, with the development of new coatings technologies (Lamb et al. 1998; Sun et al. 2005) there is the possibility to decrease surface properties to the level of nanometers. This provides a new scale of surface that has yet to be investigated for its effects on the settlement and development of fouling communities. Clearly nano-scale surfaces will provide a new scale of roughness and fractal dimension to a surface and these will in turn affect the physical properties of a surface, in particular hydrophobicity (Zhang et al. 2005; Guo et al. 2005). Hydrophobicity is the degree of affinity a solid surface has for a liquid. Hydrophobic surfaces have a low affinity to liquids, in particular water, and hence droplets tend to bead up on the surface. Hydrophobic surface are generally those with a water contact angle of 60-100º. In contrast, liquids spread over hydrophilic surfaces and become highly wettable with water contact angles of < 30º. A water contact angle of 0º indicates complete wetting of a surface and as such any angle greater than 0º has some degree of hydrophobicity. When a rough surface, in particular on the scale of nanometers, is combined with hydrophobic materials a superhydrophobic surface is formed (Zhang et al. 2005; Guo et al. 2005). Superhydrophobic coatings (SHCs) are surfaces with water contact angles of > 150º.

Hydrophobicity and its influence on fouling has been investigated against a range of fouling organisms, often with mixed or contrasting responses. *Ulva linza* (Finlay et al. 2002a), *Balanus improvisus* (Dahlstrom et al. 2004) and *Nitzschia amphibia*. (Sekar et al. 2004) prefer hydrophobic surfaces. In contrast, others fouling organisms such as

Balanus amphitrite cannot attach or adhere well to hydrophobic surfaces (Schultz et al. 1999; Graham et al. 2000; Thomason et al. 2002; Tang et al. 2005; Zhang et al. 2005). In some cases, such as the spores of *Ulva linza*, hydrophobic surfaces increase attachment but decrease adhesion strength (Finlay et al. 2002a), while some species of diatoms including *Amphora coffeaeformis* also have stronger adherence to hydrophobic surfaces (Finlay et al. 2002a; Holland et al. 2004). For species of *Amphora*, hydrophobic surfaces can also reduce motility (Wigglesworth-Cooksey et al. 1999; Finlay et al. 2002a). However, the effects of hydrophobicity often diminish with time (Zhang et al. 2005), or they are overshadowed by other surface properties such as porosity and the extent of cross-linking in the case of sol-gel-derived xerogel materials (Tang et al. 2005). Hydrophobicity is also impacted by initial colonisation processes under natural conditions (Becker et al. 1997).

Recent technological breakthroughs have enabled superhydrophobic surface to be developed by combining nano-scale roughness with hydrophobic materials. Superhydrophobic coatings (SHCs) with water contact angles of up to 175º (Guo et al. 2005; Zhang et al. 2005) can be formed using chemically modified nano-sized particles of hydrophobic silicon based materials. The principles behind the wetting behaviour of SHC have recently been reviewed (Marmur, 2006a; b). The unique physical architecture of SHCs allows exploration of the effects of micro- and nano-scale roughness on fouling to be investigated. A surface can be modified to have either a nano-scale roughness, or nano on micro-scale roughness, and produce a superhydrophobic surface. This allows for the testing of critical roughness parameters (nano versus micro) to determine the scale at which roughness, or the effects of roughness, affect the settlement of fouling organisms. This method also allows for the testing of multiple roughness scales, or fractals (nano, micro, and nano on micro), on one surface in an attempt to develop a coating that affects a broad range of fouling organisms with different surface preferences (see Chapter 6).

Nano-scale roughness and related SHCs (> 150º) have not previously been investigated for their fouling deterrence in quantified laboratory assays. Roughness-related antifouling properties have been limited to micron-scale hydrophobic surfaces (see review Verran & Boyd, 2001; Callow et al. 2002; Hoipkemeier-Wilson et al. 2004;

Carman et al. 2006), primarily due to the technological requirements to produce the smaller nano-scale of roughness.

The aim of this study was therefore to test nano and micro-textured surfaces with extreme hydrophobicities (> 150º) against the major groups of fouling organisms in 'choice' laboratory bioassays to determine their effects on settlement, and in particular to partition any effect of deterrence between the scales of the surfaces (nano - micro) as hydrophobicity is extreme for all surfaces. Four SHCs were used with varying nano- and micro-scale roughness which were coated onto glass Petri dishes. Only half of each dish was coated to allow a 'choice' between hydrophilic glass and the SHC. It should be noted that not all organisms can choose where to settle. Red algal spores and diatoms reach a surface passively, drifting through the water column. Diatoms, however, are motile upon contact with certain surfaces. The fouling organisms chosen covered the major fouling groups and cell/larval sizes and have been used in previous Chapters.

7.2. Methods

7.2.1. Preparation of super-hydrophobic surfaces

The four superhydrophobic coatings (SHCs) were prepared by Dr Hua Zhang at the School of Chemistry, The University of NSW, Sydney, Australia. The SHCs vary in terms of chemical composition, which controls the degree of superhydrophobicity, and surface roughness (nano- and micro- scale). The SHC are termed SCC (Siloxane based, condensation cured), SCAM (siloxane based, condensation + addition cured using methacrylate radical), SCAV (siloxane based, condensation + addition cured using vinyl radical), and TRANS (siloxane based, decomposed organic particles, highly transparent). The production of each is described in detail in patents (SCC (Lamb et al. 1998): WO 9842452 PCT/AU98/00185; SCAV & SCAM (Zhang et al. 2004) WO 2004090065 PCT/AU2004/000462); TRANS (Jones et al. 2004) WO 2004090064 PCT/AU2004/000461). Briefly the chemical mixtures were sonicated, heated and a catalyst added. Films were prepared for each coating by spray coating using a spray cane and subsequent annealing at 150°C for 30 minutes. (Lamb et al. 1998). All SHCs were sprayed onto one half of a glass petri dish (diameter 75 mm).

7.2.2. Surface characterisation of surfaces

The roughness ratio (*r*) and the root mean square roughness (RMS) of SHCs and glass were analysed by Atomic Force Microscopy (tapping mode) using a Digital Dimension-3000 instrument (Table 7.1). To determine if roughness profiles changed at different scales two scans were made over areas of 5× 5 μm and 20 × 20 μm with a resolution of 256 × 256 pixels. The roughness ratio *r* was calculated by dividing scan surface area by projected surface area.

$r = \sum (projected\ area)_i / \sum (scan\ area)_i$

For example, if the scan area is 25 μm^2 and the projected area is 30.16 μm^2 then *r* equals 1.21. *RMS* (the Root Mean Square) roughness is the standard deviation of the Z values (in the vertical direction) within the given area and is height direction roughness.

$$RMS = \sqrt{\frac{\sum_{i=1}^{N} (Z_i - Z_{ave})^2}{N}}$$

where Z_i is the current *Z* value; Z_{ave} is the average *Z* value within the given area. *N* is the number of points within the given area.

The hydrophobic nature of the four coatings and glass was determined by measuring the advancing and receding angles contact angle of water on three points of each coating using a goniometer (Ramé-hart instrument Co. – 100-00) and imaging software (RHI 2001) (Table 7.1).

Glass is a relatively smooth hydrophilic surface with a Root Mean Square roughness of 0.425 nm, a roughness ratio of 1, and a hydrophobicity of 46.5º. Due its smooth nature glass was only scanned by AFM over 25 μm^2.

SCAM:

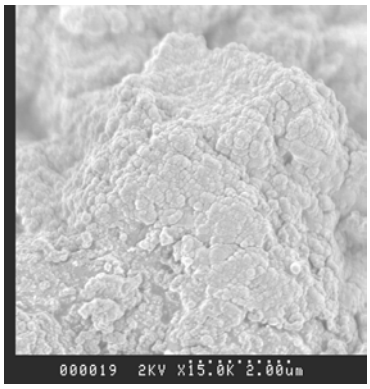

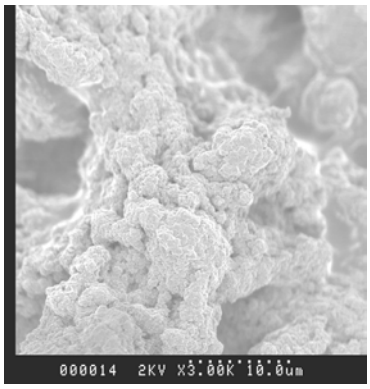

SCAV:

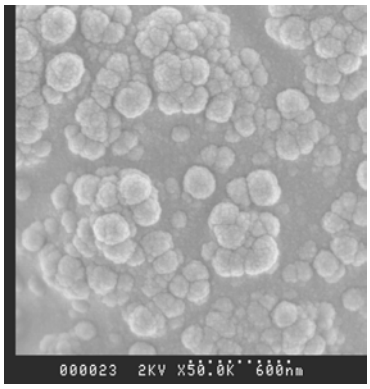

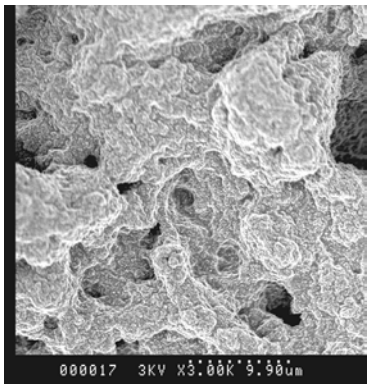

SCC:

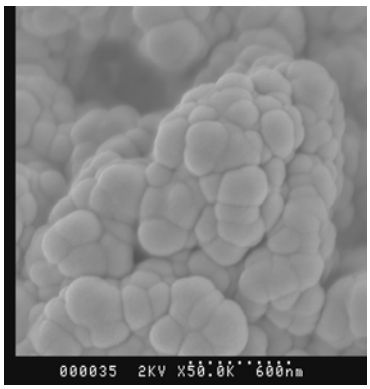

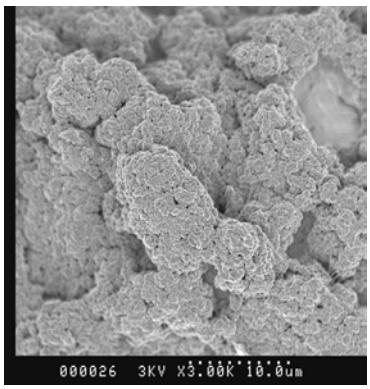

TRANS

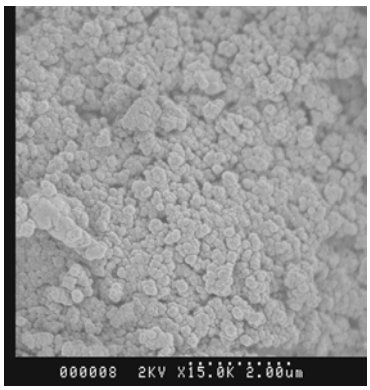

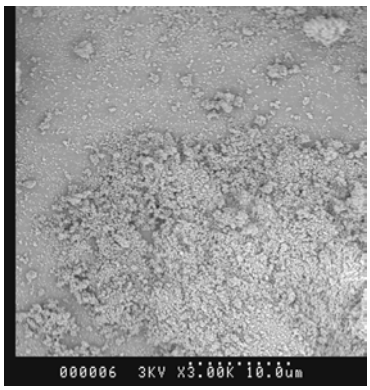

Figure 7.1 Scanning Electron Microscopy images for SHCs (Dr H. Zhang, UNSW) a) SCAM coating at 15000x and 3000x magnification b) SCAV coating at 50000 x and 3000x magnification c) SCC coating at 50000x and 3000x magnification d) TRANS coating at 15000x and 3000x magnification.

Table 7.1 The roughness profiles of the four SHCs and glass: Advancing and receding water contact angles are the means of three points of each SHC and glass, accuracy of ± 1º. The root mean square roughness (RMS) and the roughness ratio (*r*) were recorded with AFM scan sizes of 25 μm^2 and 400 μm^2 (SHCs only).

SHC	*Water contact angle*		*Scan size* (5× 5 μm)		*Scan size* (20× 20 μm)	
	advancing	receding	*RMS* (nm)	*r (roughness ratio)*	*RMS* (nm)	*r (roughness ratio)*
SCAM	161	152	308.72	1.50	1117	2.17
SCAV	155	139	481.71	1.73	1463	1.47
SCC	168	159	252.37	1.21	965.1	1.22
TRANS	169	153	374.11	1.40	607.18	1.44
Glass	66.3	28.9	0.425	1	N/A	N/A

7.2.3. Collection and culture of organisms

Three of the five species used for bioassays, the green alga *Ulva rigida* Areschoug (gametes, 7.24 μm diameter), the red alga *Polysiphonia sphaerocarpa* Børgesen (carpospore, 51.66 μm diameter), and the bryozoan *Bugula neritina* Linnaeus (larva, 321 μm diameter), were all collected and cultured as described in Chapter 6.2.3. However, the diatom *Amphora* sp. (cell, 7 μm diameter) was a different strain to that used in Chapter 6. The cells were collected from the Defence Science & Technology Organisation (DSTO) testing facility at Williamstown, Victoria (37° 52'S; 144° 54'E). Diatoms were isolated (T. Dugdale) and maintained in 200ml Pyrex conical flasks and cultures were supplemented with K-medium plus silicates (K+Si) (Andersen et al. 2005). *Amphora* sp. was cultured at 16ºC under Sylvania 58W Luxline Plus® and Gro-Lux® fluorescent lamps with a 14:10 light/dark cycle. The barnacle *Balanus amphitrite* Darwin (nauplii length: 515 μm, width: 210 μm) was collected from rock platforms in Sydney (33° 55'S; 151° 15'E). Barnacles were maintained with an ambient light cycle (15h light/9h dark) at 23-28ºC in containers with 150 μm filtered seawater and high aeration. Barnacles were feed *Artemia salina* and *Skeletonema costatum* daily. To

induce larval release the water was changed, the aeration stopped, and a 25 watt light source placed on the side of the container. The nauplii larvae are positively phototactic and were collected and cultured at a density of 1/ml (de Nys et al. 1995). Nauplii were cultured with the addition of antibiotics streptomycin (36.5 mg/L) and penicillin (21.9 mg/L) and fed *S. costatum* daily. Barnacle larvae undergo six nauplii moults (Rittschof et al. 1992) and after six days they are ready for use in bioassays.

7.2.4. Bioassay procedures

All bioassays were conducted using glass petri dishes (SCHOTT, Mainz) (7.5 cm diameter) with one-half (22.08 cm^2) of the dish coated and the other half untreated glass.

Amphora sp.

Diatom cells were re-suspended with an orbital shaker and their concentration determined using a haemocytometer prior to use in assays. The dishes were filled with 20 ml of autoclaved seawater with K^+Si medium. l ml of diatom culture suspension was also pippetted in each half of the dish with a cell density of approximately 1.6 x 10^5 cells/ml. Four replicate dishes were used per treatment. The diatoms were left to settle for 3 hours after which they were dip-rinsed three times in new autoclaved seawater with K^+Si medium to remove unattached diatoms (Holland et al. 2004; Scardino et al. 2006) and counted using a digital 3CCD camera set upon a Leica Microsystems inverted DMIL microscope in 10 random fields of view (FOV) per dish at magnifications of x 200 (0.0475 mm^2). SCC and SCAV coatings were too rough to discern individual cells via light microscopy as they were often hidden in micro depressions. To overcome this depth of field issue cells for these treatments were enumerated using autofluorescence of chloroplasts with an Olympus BH-2 confocal laser scanning microscope (CLSM)(FOV – 0.0667 mm^2) with a mercury bulb and a Leica DC300F camera and the image analysis program IM50.

Ulva rigida

Bioassay procedures for this species are described in detail in Chapter 6.2.3. After 96 h dishes were gently dip-rinsed to remove loose unattached material and gametes were enumerated at x 200 magnification in five fov (0.16 mm^2) on both the glass and coated sides of the dish. Five replicate dishes were used for each coating.

Polysiphonia sphaerocarpa

Bioassay procedures for this species are described in detail in Chapter 6.2.3. After 48 h all dishes were gently dip-rinsed to remove loose unattached material and all settled spores counted on both glass and coated sides of each dish. There were five replicate dishes per coating.

Bugula neritina

Bioassay procedures for this species were carried out as described in detail in Chapter 6.2.3. After 48 h all dishes were gently dip-rinsed to remove loose unattached material and the number of adhered metamorphosed larvae were counted on the glass and coating. There were five replicate dishes per coating.

Balanus amphitrite

Barnacle nauplii were monitored for 6 days after release. After they had undergone their sixth nauplii moult the resulting cyprids were pipetted into glass Petri dishes containing filtered seawater. The dishes were covered and left for 68 h after which time dishes were gently dip-rinsed to remove loose unattached material and the number of attached adults were counted on the glass and coating. There were five replicate dishes. Due to limited release of cyprids only two SHC were used in these assays, TRANS and SCAM.

7.2.5 Statistical methods

All bioassays were analysed using a goodness-of-fit test for a single variable (settlement) with two categories (glass and coating) and 1 degree of freedom. Chi-square values were obtained based on the observed and expected numbers of attached cells, spores or larvae on glass and coating. Chi-square distribution tables were used to determine p-values. Significance was taken at $\alpha = 0.05$.

7.3. Results

All graphs represent mean proportions of cells attached on glass and coated portions of dishes. Mean counts per FOV ± one standard error are denoted in brackets for each coating throughout the results.

7.3.1 *Amphora* sp. assay

There were significantly less *Amphora* sp. cells attached to the TRANS (χ^2 = 100.9, P < 0.001), SCC (χ^2 = 7.06, P = 0.0079), SCAM (χ^2 = 12.74, P = 0.0004) and SCAV (χ^2 = 36.9, P = 0.001) coatings than glass. 87.8% (166.5 ± 31.2 cells) of *Amphora* cells attached to glass compared to 12.2% (26.75 ± 10.8 cells) on the TRANS coating (Figure 7.2). This was similar for the SCC coated dishes with 61.8% (58.77 ± 2.4 cells) of cells attached to glass and 38.2% (33.3 ± 7.8 cells) attached to the coating (Figure 7.2). There was also significantly lower attachment to the SCAM coating (33% attachment, 21.2 ± 8.2 cells) than glass (67% attachment, 51.75 ± 17.2 cells) and the SCAV coating (18.5% attachment, 30 ± 11.2 cells) and glass (81.5% attachment, 99 ± 32.9 cells) (Figure 7.2).

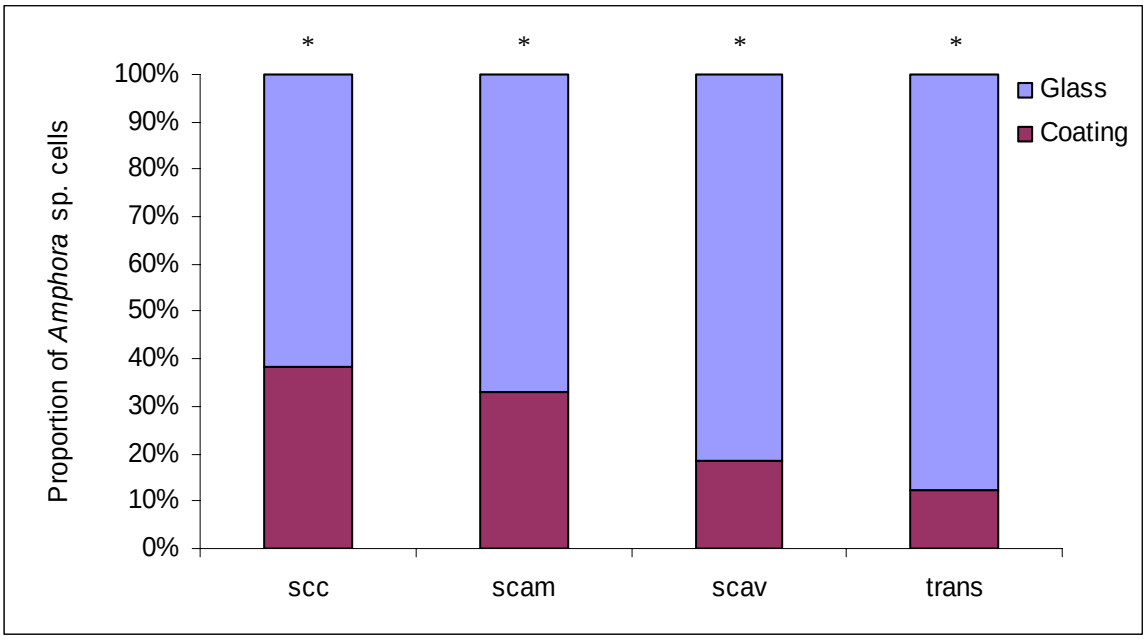

Figure 7.2. Proportion of *Amphora* sp. cells attached post-rinse on glass and SHC (200 x, 0.0475 mm^2 FOV). Data are means, n = 4. Treatments with an asterix have a significantly different proportion of attached spores than expected when compared to glass, Chi-square test.

7.3.2 *Ulva rigida* assay

Gametes attached on all coatings and glass, however, the preference of gametes for glass and coatings varied markedly between the coatings. Significantly more gametes attached on glass compared to the SCC (χ^2 = 44.8, P < 0.001) and TRANS coatings (χ^2 = 18.7, P < 0.001) while the reverse was true for gamete settlement on SCAV coatings

(χ^2 = 6, P = 0.014). There was no significant difference in gamete settlement between the SCAM coating and glass (χ^2 = 2, P = 0.157). Gametes had the strongest preference for glass (strongest deterrence by the coating) on the SCC coated dishes with 87% (71.6 ± 17.2 gametes) of gametes settling on glass compared to 13% (10.2 ± 2.7 gametes) on the coating (Figure 7.3). This was similar for the TRANS coated dishes with 85.4% (32.6 ± 4.4 gametes) of gametes attached on glass and 14.6% (5.6 ± 1.9 gametes) settling on the coating (Figure 7.3). In contrast 66.2% (35.8 ± 10.4 gametes) of gametes attached preferentially on the SCAV coating and 33.8% (18.3 ± 5 gametes) on glass (Figure 7.3). There was no preference between the SCAM coating (58% settlement, 41.6 ± 10.1 gametes) and glass (42% settlement, 29.7 ± 5.5 gametes) (Figure 7.3).

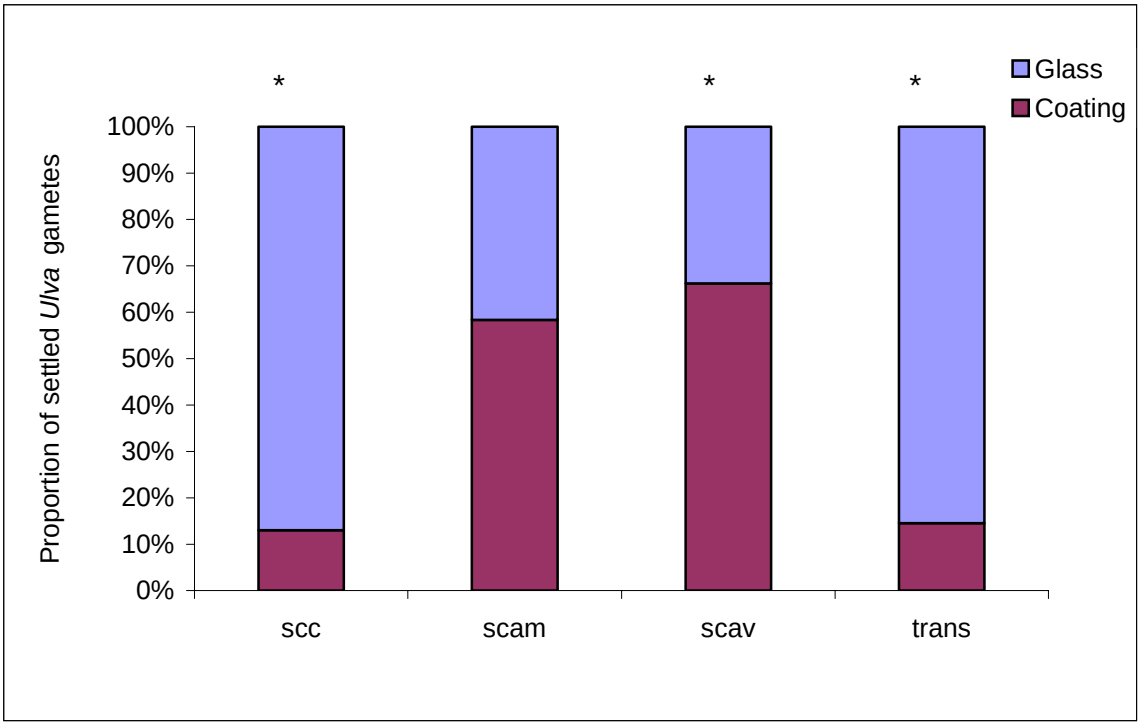

Figure 7.3. Proportion of *Ulva rigida* gametes attached on glass and SHCs (400 x, 0.16 mm^2 FOV). Data are means, n = 5. Treatments with an asterix have a significantly different number of attached gametes than expected compared to glass, Chi-square test.

7.3.3 *Polysiphonia sphaerocarpa* assay

Post rinse, *Polysiphonia sphaerocarpa* spores attached in significantly lower numbers on the SCAM (χ^2 = 6.72, p = 0.01) and TRANS (χ^2 = 57.36, P < 0.001) treatments than expected. There was no difference in spore settlement between the SCAV (χ^2 = 0.157, P = 0.692) and SCC (χ^2 = 0.17, P = 0.68) coatings and glass. After the dip-rinsing 77.2%

(61.6 ± 26.5) of spores were attached to glass compared to 22.8% on the TRANS (18.2 ± 10.2) treatment (Figure 7.4). There was a similar effect on the SCAM coating with 30% (12.8 ± 2.8) of spores adhered to the coating and 70% (29.8 ± 11.1) on the glass (Figure 7.4). There was no difference in the proportion of attached cells between glass (52.9%, 27.8 ± 5.1) and the SCC (47.1%, 24.8 ± 4.5) and glass (51.9%, 52.8 ± 17.3) and SCAV (48.1%, 49 ± 11.2) coatings (Figure 7.4).

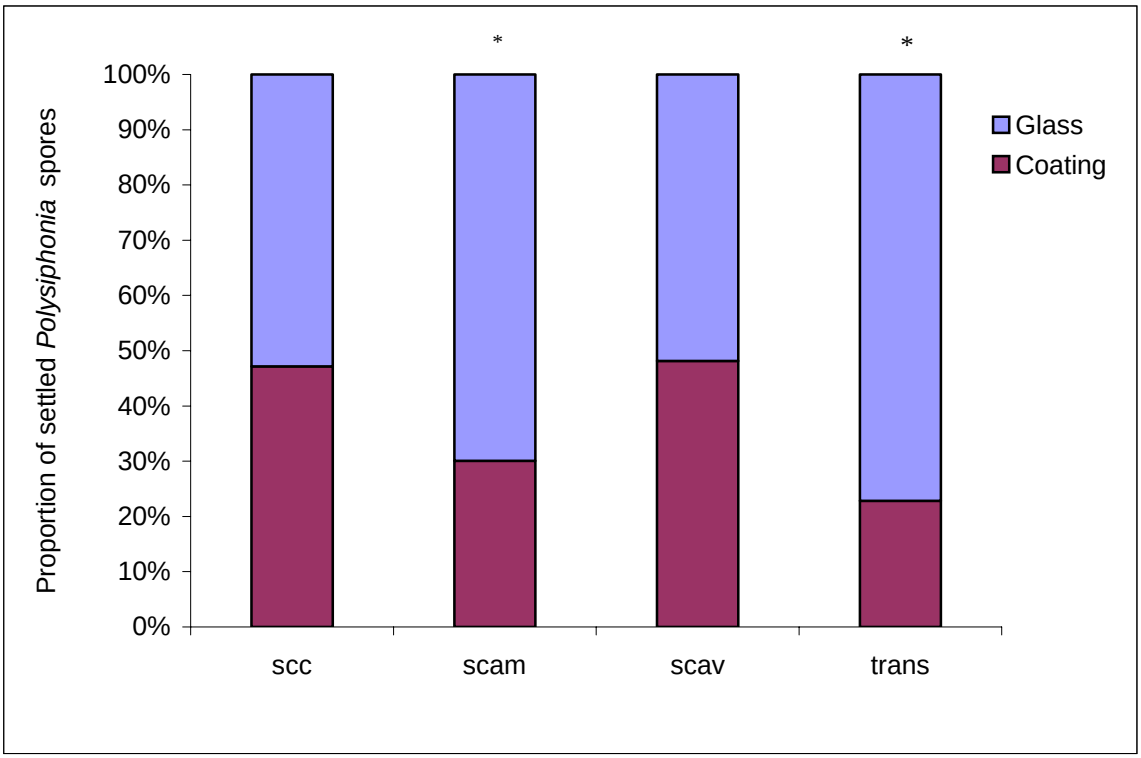

Figure 7.4. Proportion of *Polysiphonia sphaerocarpa* spores attached post-rinse on glass and SHC. Data are means, n = 5. Treatments with an asterix have a significantly different proportion of attached spores than expected compared to glass, Chi-square test.

7.3.4 *Bugula neritina* assay

Bugula neritina larvae settled on all coatings and glass, however the preference of larvae for glass varied very strongly depending on the type of coating. *B. neritina* larvae settled in significantly higher numbers on the SCAM (χ^2 = 4, P = 0.0455) and SCC (χ^2 = 5.4, P = 0.02) coatings than on glass. In contrast significantly fewer larvae settled the TRANS coating than glass (χ^2 = 4.5, P = 0.034). There was no significant preference by *Bugula neritina* larvae for glass or the SCAV coating (χ^2 = 3.27, P =

0.071). *B. neritina* larvae preferred the SCAM (86.6%, 11.6 ± 1.6 larvae), SCC (78.5%, 12.4 ± 1.7 larvae) and SCAV (73.6%, 10.6 ± 2.8 larvae) coatings to glass (13.4%, 1.8 ± 0.5 larvae; 21.5%, 3.4 ± 0.6 larvae and 26.4%, 3.8 ± 3.4 larvae respectively) (Figure 7.5). In contrast *B. neritina* larvae had a very strong preference for glass (91.2%, 7.4 ± 1.9 larvae) and avoided the TRANS coating (9.8%, 0.8 ± 0.5 larvae) (Figure 7.5).

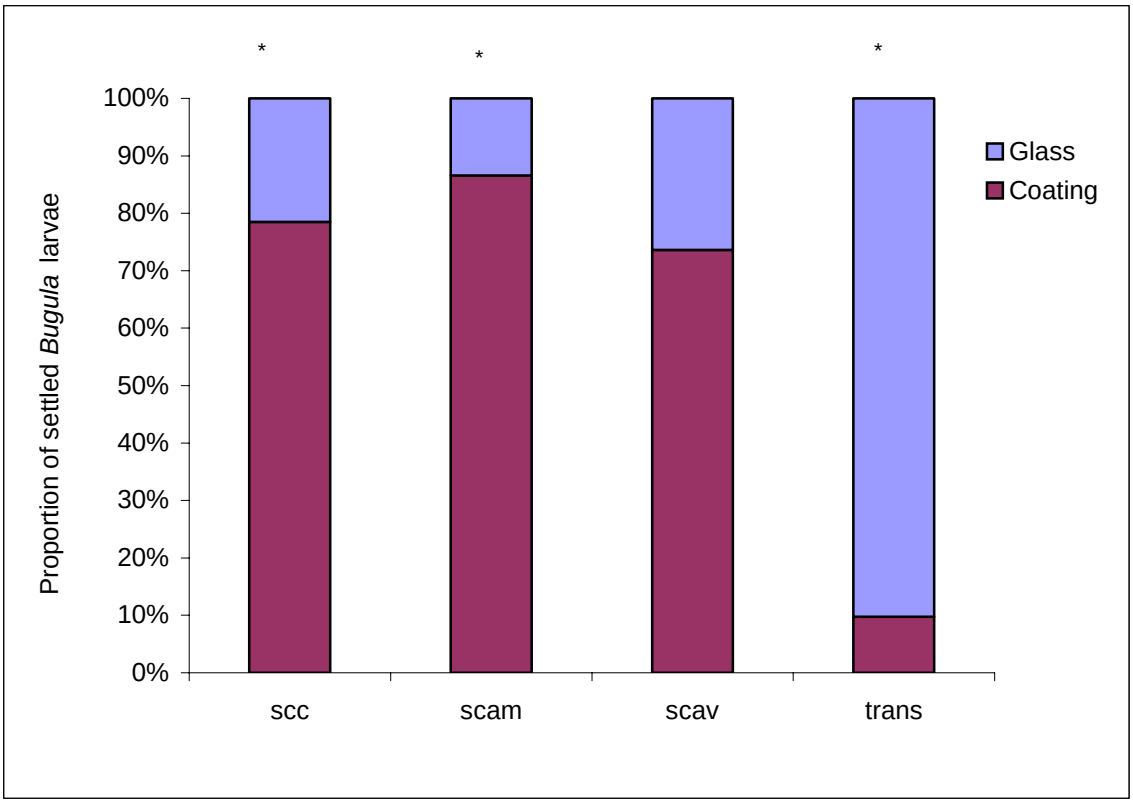

Figure 7.5. Proportion of *Bugula neritina* larvae settled on glass and SHC. Data are means, n = 5. Treatments with an asterix have a significantly different proportion of settled larvae than expected compared to glass, Chi-square test.

7.3.5 *Balanus amphitrite* assay

Balanus amphitrite cyprids settled in significantly higher numbers on glass than the TRANS treatment (χ^2 = 11.65, P = 0.001) while there was no significant difference in cyprid settlement on the SCAM coatings and glass (χ^2 = 0.2, P = 0.665). On the TRANS treatment cyprids preferred glass over coating with 81.9% (25.4 ± 2.7 cyprids) of cyprids settling on glass as opposed to 18.1% (5.6 ± 1.4 cyprids) on the coating (Figure 7.6). There was no preference on the SCAM treatment for glass or coating with 44.9% (7 ± 2.9 cyprids) of cyprids settling on glass and 55.1% (9.6 ± 0.6 cyprids) on

the coating (Figure 7.6). Overall settlement on the SCAM dishes was 31.66% of cyprids placed into the dishes while on TRANS dishes overall settlement was 47.55%.

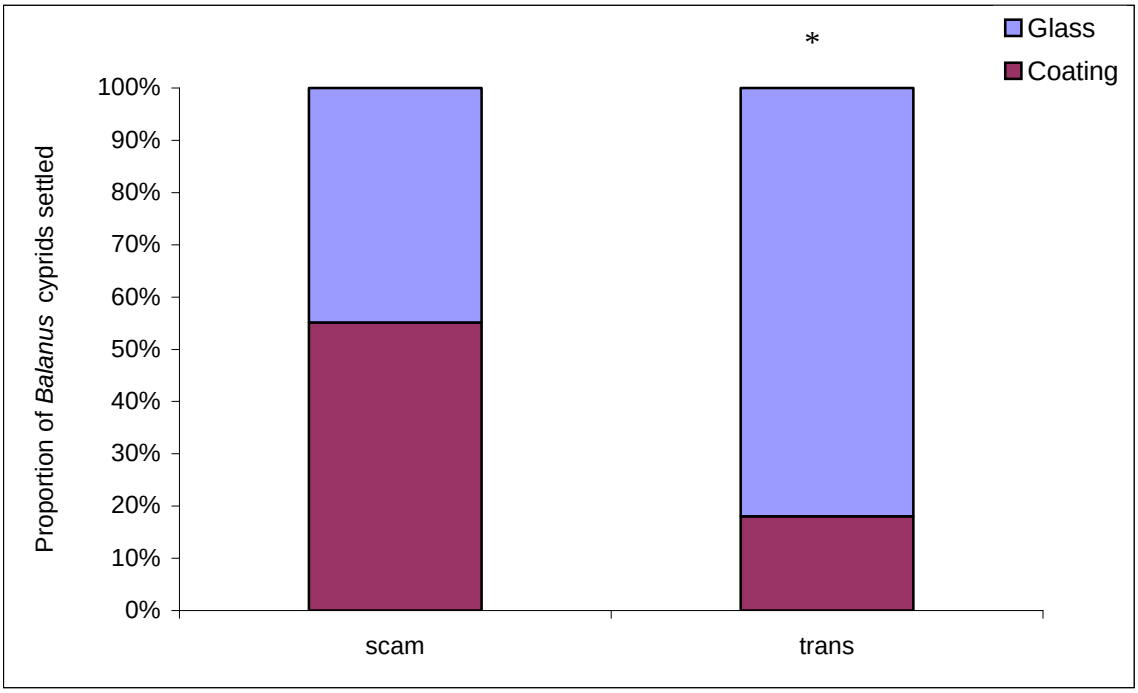

Figure 7.6. Proportion of *Balanus amphitrite* cyprids settled on glass and SHC. Data are means, n = 5. Treatments with an asterix have a significantly different proportion of settled cyprids than expected compared to glass, Chi-square test.

7.4 Discussion

The superhydrophobic coatings (SHCs) used had significant antifouling effects compared to glass across a broad range of fouling organisms in static bioassays. However, the effects were different for each coating and varied between coatings and each organism tested. There was one consistent response across all fouling organisms and this was that TRANS, the only coating to have only nano-scale roughness, significantly reduced settlement (attachment) for all five fouling organisms tested. In contrast, the other three SHCs with nano-scale roughness superimposed on micro-scale roughness were avoided, preferred, or settled in the same numbers as glass.

The overall responses of fouling organisms to SHCs are summarized in Table 7.2. On the TRANS coating, which has only nano-scale roughness, there was a lower proportion of settlement compared to glass across all organisms. In contrast SHCs with

nano and micro-roughness produced mixed preferences. The SCAV coating was attached to in lower numbers only by *Amphora* sp. but was either preferred over glass or there were no attachment differences by all other organisms. The SCC coating was preferred by *Bugula neritina* but attached in lower numbers by *Amphora* sp. and *Ulva rigida*. Similarly the SCAM coating was also preferred by *B. neritina* but there was significantly lower settlement than expected by *Amphora* sp. and *Polysiphonia sphaerocarpa* spores.

Table 7.2. Summary of the fouling response to SHCs and glass. Settlement differences are based on the proportion of cells, spores or larvae settled on either glass or the coating. ↓ = significantly lower settlement; ↑ = significantly higher settlement; N/D = no difference; N/T = not tested as determined by Chi-square Analysis.

	Amphora sp.	*Ulva rigida*	*Polysiphonia sphaerocarpa*	*Bugula neritina*	*Balanus amphitrite*
SCC	↓	↓	N/D	↑	N/T
SCAM	↓	N/D	↓	↑	N/D
SCAV	↓	↑	N/D	↑	N/T
TRANS	↓	↓	↓	↓	↓

From the mixed differences recorded in the bioassays it is clear that factors other than superhydrophobicity play a significant role in the selection of a surface on which to settle. All coatings were superhydrophobic (> 155º) and produced very different settlement responses, however they have different roughness properties. The TRANS coating has nano-scale roughness whilst the SCC, SCAV and SCAM have micro- and nano-scale roughness. The differing settlement response to SHCs also cannot be attributed to mean roughness alone as there are no clear correlations between these variables and settlement preferences. The TRANS coating has intermediate values for both RMS and roughness ratio as compared to the other three SHCs. In contrast glass has low water contact angles (hydrophilic) and a very smooth surface as indicated by the small RMS value and a roughness ratio of 1 (Table 7.1). It should be noted that acid washed glass should have lower water contact angles (< 30 º) than those reported here (46 º). It is possible that some over-spray from the coatings could have contaminated the adjacent glass resulting in slightly higher water contact angles than expected.

Another potential mechanism that could alter the settlement preferences of fouling larvae is the presence of nano-bubbles on the surface. It has been reported that SHCs generate a layer of air bubbles at the water-solid interface due to having extremely rough surfaces (Attard, 2003; Zhang & Jun, 2004; Lafuma & Quere, 2003; Sun et al. 2005) (surface area 2.7 times larger than that of a smooth surface; Zhang et al. 2005). It is proposed that this layer of air bubbles creates a barrier to fouling organisms attempting to establish on the surface, however this is not proven. It is also proposed that the scale and pattern of roughness will influence the size and distribution of air bubbles on a surface. A nano-rough surface will generate nano-scale air bubbles, which will create nano-scale patches on the surface, while a surface with micro-roughness will lead to micro-scale patches. Furthermore, the presence of micro-bubbles will over-ride any nano-effects and this supports a differential effect for the TRANS coating, which has only a nano-scale surface. Quantitative measurements of bubble sizes and geometry have yet to be determined using Small Angle X-ray Scattering.

The only previous study to examine a nano-rough surface and superhydrophobicity in relation to fouling found that the surface, which was largely undefined, was unwetted after 6 months and reduced short-term bacterial attachment (Zhang et al. 2005). However, fouling resistance in the field decreased over a 2 month period (Zhang et al. 2005). The diminishing fouling resistance is attributed to the loss of superhydrophobicity, which can occur due to air dissolving in water over long periods of submersion. This is proposed to be due to the destruction of pores that may remove air physically from the water-solid interface, or the development of conditioning layers of macromolecules which alter the chemical and physical structure of the surface (Zhang et al. 2005).

Research on the response of fouling organisms to superhydrophobic surfaces is limited and it is on surfaces with significantly lower superhydrophobicites than tested here. Fouling reduction by *Ulva linza* zoospores was reported in a recent study examining a range of microtopographical designs on ‘ultrahydrophobic’ PDMSe surfaces (Carman et al. 2006). The most successful surface (86% spore reduction) had the highest water contact angle (135º), however, it was the only surface with topographical widths smaller than the zoospore diameter (Carman et al. 2006). It appears topographical height and spacing are more important than hydrophobicity as surfaces with similar

'ultrahydrophobicities' produced very different settlement responses for *U. linza* zoospores. This is consistent with the present study where superhydrophobic coatings (> 155 º) produced differing settlement responses that cannot be attributed to hydrophobicity or roughness and is more likely to be due to micro and nano-scale effects.

Amphora sp. cells adhere more strongly to hydrophobic surfaces than to glass (Finlay et al. 2002b; Holland et al. 2004). On patterned self-assembled monolayers (SAMs) of increasing hydrophobicity (water contact angles of 20º - 115º) *Amphora coffeaeformis* cells were removed in lower numbers on the most hydrophobic surfaces. Furthermore, Holland et al. (2004) found that adhesion strength by three common fouling diatoms, including *Amphora coffeaeformis*, was stronger on a Polydimethylsiloxane elastomer (115º) (PDMSe) than glass. It had also been observed that diatom slimes often cover hydrophobic low surface energy antifouling coatings (Finlay et al 2002b) and adhere tenaciously to them (Terlizzi et al. 2000). This is in contrast to the present studies findings where all four superhydrophobic coatings had lower *Amphora* sp. attachment than glass.

Bryozoan larvae are known to avoid glass and other highly wettable (hydrophilic) surfaces in preference for non-wettable (hydrophobic) surfaces (Eibern, 1976; Loeb, 1977; Mihm et al. 1981). This is consistent for *Bugula neritina* settlement in this study whereby glass was avoided in preference for the SCC, SCAV and SCAM coatings. However, when compared to the TRANS coating, glass was more attractive to *B. neritina* larvae. Therefore, strong repellent effects must be operating in the presence of the TRANS coating for *B. neritina* larvae to significantly prefer glass to the coating in the present study.

Several studies have examined fouling release coatings as a non-toxic antifouling alternative (see reviews Anderson et al. 2003; Brady 2005; Yebra et al. 2004). These coatings are generally composed of silicone (PDMS), which has excellent fouling release properties based on low surface energy, micro-roughness, low glass transition temperatures and low modulus of elasticity (Swain, 1998; Brady, 2001). These surface characteristics minimize mechanical locking of adhesives and promote slippage (Newby et al. 1995). Fouling-release surfaces are generally only successful on fast-

moving vessels as the decrease in adhesion strength facilitates removal at cruising speeds above 22 Knots (Brady, 2001). However, fouling release is not fool-proof and diatom slimes are reported to have higher attachment strength on hydrophobic surfaces (Finlay et al. 2002b; Holland et al. 2004) and can stick to fouling-release coatings on boats operating in excess of 30 knots (Candries, 2001). This is in contrast to the present studies findings whereby SHCs reduced diatom attachment. This is a particularly encouraging result as diatom films have often been the bane of novel antifouling surfaces and are well known to be a precursor to subsequent macrofouling colonization (Wahl, 1989). Furthermore, given that the chemical nature of the coatings used in this study is primarily siloxane-based we also expect that coatings will have fouling-release properties, however these properties have yet to be quantified. For example spores of the red alga *Polysiphonia sphaerocarpa*, were easily removed from two SHCs after gentle dip-rinsing. As these spores settle passively and therefore do not actively choose where to settle, their reduced attachment could be attributed to their weak adhesion to the SHCs. Quantified cell removal from these SHCs in flow chambers may demonstrate that far lower boat speeds are required to release fouling organisms.

This study has demonstrated the potential of nano-technology and SHCs as non-toxic antifouling alternatives. Future studies will need to test the performance of SHCs with flow as well as examine fouling resistance in long-term field trials and against a broader range of diatoms and bacteria. The loss of superhydrophobicity is possible and needs to be measured and correlated to any changes in fouling resistance. A greater understanding of how nano- and micro- air bubbles interfere with settlement processes and the adhesive mechanisms of fouling organisms is also required. Designing a robust nano-coated surface that can maintain superhydrophobicity or entrap air for long periods of immersion will be crucial to the development of a non-toxic antifouling alternative.

CHAPTER EIGHT

General Discussion

In this thesis I investigated physical fouling defence mechanisms in marine molluscs. I examined natural surface microtopographies on over 100 species of bivalves and gastropods from the Great Barrier Reef (GBR). A wide variety of microtopographical shapes patterns and scales were discovered ranging from pillars through to corrugations and strands. Higher level surface roughness features were quantified for 36 of the most unique species of marine molluscs using confocal scanning laser microscopy. Six selected surface roughness parameters were generated for each natural surface based on the roughness and waviness components of the shell. These same 36 species were then tested for fouling resistance over 3 months and fouling removal after this period. The resistance to fouling and the level of fouling removal (after exposure to a water jet) was correlated to the surface roughness parameters generated. For the first time quantified surface features were correlated to the settlement and removal of specific fouling organisms.

Subsequently, two bivalve species with differing patterns of homogeneous surface microtopography, though of the same scale, and a third species which has no surface topography were mimicked using resin models. The microtextured biomimics resisted fouling longer than the smooth biomimics, and the microtextured shells resisted fouling longer than the smooth shells or the textured biomimics. The loss of fouling resistance over time by microtextured biomimics supports other factors, in particular a chemical defence based on the proteinaceous periostracum, contributing to fouling resistance on bivalve shells (Scardino & de Nys, 2004). Natural surfaces while providing a defence against macrofouling through microtextrue also employ multiple defences to maintain foul-resistant surfaces.

To explain the fouling deterrence observed for textured surfaces the number of attachment points on a microtextured surface was proposed as an important mechanism in fouling attachment. Due to the varying sizes of fouling larvae the numbers of attachment points to a specific microtexture will vary. A fouling larva smaller than the size of the microtexture width will have multiple attachment points as it can fit inside

the texture, in contrast larvae larger than the size of the microtexture will have fewer theoretical points of attachment. This ‘attachment point theory’ was tested against fouling diatoms (Chapter 5) and a range of micro and macro fouling larvae (Chapter 6) on microtextured films of varying texture widths. Fouling was highest on textures larger than the size of the settling diatom, larvae, or propagule. In contrast settlement tended to be reduced on textures slightly smaller than the settling larvae that provide only two attachment points. Finally, surface roughness was reduced by an order of magnitude to incorporate nanometer scale roughness. Nano-rough surfaces are smaller than all fouling organisms and are also superhydrophobic. Nano-roughness and superhydrophobicity have not been tested for antifouling. Nano-rough surfaces overlain on micro-roughness produced mixed results with a range of fouling larvae/propagules. Some surfaces were preferred over glass and others avoided, in contrast the only coating containing only nano-scale roughness deterred all tested fouling organisms. The promising results of nano-rough surfaces under static conditions indicate that this line of research will receive considerable attention in the future.

8.1 Surface roughness and fouling resistance of marine bivalves and gastropods

Some marine bivalves are able to resist fouling despite having no known chemical defences. The blue mussel remains comparatively free of fouling and this resistance to fouling correlates with an intact microtopographical structure (ripple) based on the periostracum (Wahl et al. 1998; Scardino et al. 2003; Scardino & de Nys, 2004). Bivalves and gastropods free of fouling in situ were collected from the GBR and analysed for potential microtopographies. In total over 101 species were characterised and a variety of natural microtopographies were discovered from a broad range of families and genera. Thirty six species (26 bivalves and 10 gastropods) were analysed in greater detail to produce quantifiable surface roughness characteristics. The mean roughness, waviness, Rsk roughness and waviness, anisotropy, fractal dimension and wettability were generated from the shell surfaces. The roughness properties of the molluscs were correlated to each other and one parameter, fractal dimension, can be used to predict the other six surface parameters. The 36 species varied in the surface roughness properties and differences were also observed at higher taxonomic classifications between families and classes of molluscs.

The 36 species were analysed for fouling resistance over 3 months and a range of fouling levels were recorded including changes in species specific fouling levels between families, classes and species. The fouling resistances were correlated to the roughness parameters generated and several key correlations were identified. Total fouling cover was positively correlated to fractal dimension and negatively with Rsk roughness and Wsk waviness, algal cover was negatively correlated with surface hydrophobicity and mean waviness was positively correlated to percent fouling removal.

These findings represent the first time natural surface features have been correlated to fouling resistance. Importantly, the degree of fouling release was also correlated to roughness properties which could have meaningful implications for the design of future foul release surfaces. Particular surfaces features can now be chosen to design a surface for optimal or species specific fouling resistance or fouling promotion as is sometimes required in aquaculture. Future research will focus on biomimetic surfaces which incorporate the surface roughness parameters of the most fouling resistant molluscs. Static and quantified flow will be required to determine attachment strength and the efficacy of biomimics before ship-scale trials can commence.

8.2 Biomimics Vs natural surfaces

As expected from previous research (Wahl et al. 1998; Scardino et al. 2003, Bers & Wahl, 2004) microtextured shells and biomimics outperformed untextured shells and biomimics. However, microtextured biomimics lost fouling resistance earlier than natural shells indicating other properties of the shell contribute to antifouling defence. The surface bound periostracum layer covering bivalve shells has been speculated as a possible antifouling defence mechanism. The removal of the periostracum leads to a rapid increase in fouling (Wahl et al. 1998; Scardino et al. 2003) and boring (Che et al. 1996) on the abraded portions of the shell. Attempts to denature the surface bound proteins on the periostracum have proved inconclusive (Scardino, unpublished data) and potential antifouling periostracal properties remain under investigation. However, the loss of fouling resistance of the microtextured biomimics is attributed to the loss of texture due to the establishment of microfouling (biofilms). This is suggested to be due to the absence of the periostracum which provides a defence against microfouling (Scardino & de Nys, 2004). On the two mimicked species microtextures were between

2-4 µm that is smaller than all macrofouling larvae, however not smaller than bacteria and some diatom species. It was proposed that microtexture smaller than the scale of the settling larvae/propagule will reduce attachment due to fewer attachment points being provided. In contrast, organisms smaller than the size of the microtexture will have multiple attachment points as they can fit inside the texture and therefore will have increased settlement. As such the microtextured biomimics could resist macrofouling though over time microfouling fills the textures creating a smooth surface which results in a loss of macrofouling resistance. This mechanism was termed 'attachment point theory' and was the basis for Chapters 5 and 6.

8.3 Testing attachment point theory

The microtexture from the two bivalves species replicated in Chapter 4 was reproduced onto polyimide films. The microtextured films were tested against four fouling diatoms of varying cell sizes that had either multiple or a reduced number of attachment points to the microtextured film. Diatom attachment supported attachment point theory whereby cells which were smaller than the size of the microtexture had increased attachment and in contrast larger diatoms which had only a few attachment points attached in significantly fewer numbers (Scardino et al. 2006). This study gives further support to the loss of fouling resistance of the biomimicked shells from Chapter 4.

Attachment point theory is not confined to microfouling organisms. A broad range of textures were etched onto a polycarbonate matrix and tested against both micro and macrofouling larvae and propagules. Larvae and cells generally settled in higher numbers on textures larger than the cell size and in fewer numbers on textures slightly smaller than the cell size. All assays were done under static conditions and the introduction of flow may give further support to attachment point theory if adhesion strength is reduced on surfaces providing fewer points of attachment. As fouling propagules come in several shapes and sizes the next challenge will be to design a fractal surface which has multiple levels of microtexture and thereby providing sub-optimal points of attachment for a variety of organisms.

8.4 Nano-rough & superhydrophobic coatings

Advances in materials science have allowed surfaces to be explored and developed at the nano-scale. Previous Chapters have examined roughness and surface features at the

micro-scale, however bacteria and some microalgae are smaller than this scale and hence are not influenced by features at this level. With this in mind surface coatings which incorporated nano-scale roughness were tested for the first time for potential antifouling effects. Creating a nano-rough surface can also result in a superhydrophobic state where the surface has water contact angles in excess of 150º. Considerable attention has recently been given to superhydrophobic surfaces for a variety of applications (Sun et al. 2005), however their influence on biofouling has not yet been examined. The four nano-rough coatings all had superhydrophobicity (158º - 165º) but differed in their roughness characteristics. Interestingly, superhydrophobicity was not important to fouling deterrence as all superhydrophobic surfaces produced vastly different fouling responses. Nano-scale roughness appears to be the driving force behind fouling resistance as the only coating with nano-scale roughness alone significantly deterred all five tested fouling organisms in static choice bioassays compared to varying responses between fouling organisms to the other superhydrophobic surfaces incorporating both micro- and nano- scale structure.

Nano-coatings are a new concept and the promising results from static assays will require further research into the influence of flow and the longevity of resistance in the field. The mechanism of action of fouling deterrence on nano-scale surfaces is yet to be demonstrated and the influence of nano-bubbles on the surface of these coatings will be the focus of future investigations.

8.5 Future directions

This thesis has demonstrated the promising alternatives biomimetic antifouling technologies provide. With the imminent removal of TBT from all vessels and the longer-term phasing out of all toxic coatings the urgency for a non-toxic solution is increasing and biomimetics will contribute to these answers. Whilst this thesis has used marine molluscs as a model for biomimetic technologies, there are many other marine organisms which have evolved antifouling strategies which are waiting to inspire new ideas and designs for fouling control. It is widely recognised that multiple defence strategies are necessary to combat the myriad of fouling organisms, therefore studying several natural models of fouling resistance can only contribute to the knowledge of biomimetic technologies.

Based on the outcomes of this thesis I have identified four key areas for future research into biomimetic antifouling technologies. Firstly, the key roughness parameters identified from mollusc surfaces that influence fouling need to be tested on biomimicked surfaces. Designing a surface with a high degree of isotropy, high skewness values, with a greater distribution of peaks and large waviness profiles, should facilitate fouling resistance and the ease of fouling detachment. The incorporation of these features into a silicone based foul release surface requires testing in the field and in flow chambers. Secondly, attachment points have been demonstrated to be important to fouling attachment for both micro and macrofouling propagules. Designing fractal textures to account for multiple organism sizes will be a requirement for successful fouling resistance in the field. The foul-release ability of reduced attachment points is also unexplored and quantified analysis in flow chambers is necessary. Thirdly, it is clear that other factors combine with surface microtexture to produce extended fouling resistance on natural bivalve shells. For the mussel *Mytilus galloprovincialis* it appears that the periostracum plays a major role in fouling deterrence. Determining the nature of the periostracal properties that contribute to fouling deterrence is a vital link to determine the mechanisms of action. A non-destructive method to denature the Mytilid periostracum will determine the extent to which the periostracum contributes to fouling resistance. This will lead to proteins and other compounds being tethered to foul-release surfaces to combine the chemical and physical surface properties which provide multiple defence strategies. Lastly, the demonstration of nano-scale roughness significantly deterring a range of micro and macro-larvae/propagules/cells under static conditions is a breakthrough concept. Future research into non-toxic antifouling coatings will focus on nano-scale roughness and the determination of the mechanisms of action. Little is known about the formation of nano-bubbles at the surface of nano-rough surfaces. The size, geometry and persistence of these nano-bubbles requires determination along with how they interfere with the settlement and adhesive mechanisms of fouling larvae.

REFERENCES

Abarzua, S., & Jakubowsky, S. (1995) Biotechnological investigation for the prevention of biofouling. 1. Biological and biochemical principles for the prevention of biofouling. *Marine Ecology-Progress Series*, 123, 301-312

Abbott R.T. & Dance P.S. (1986) *Compendium of seashells : a color guide to more than 4,200 of the world's marine shells*. Crawford House, Bathurst.

Alagarswami K. & Chellam A. (1976) On fouling and boring organisms and mortality of pearl oysters in the farm at Veppalodai, Gulf of Mannar. *Indian Journal of Fisheries*, 23, 10-22

Alzieu C. (1986) TBT detrimental effects on oyster culture in France - Evolution since antifouling paint regulation. In: *Proceedings of Oceans 86, Organotin Symposium*, pp. 1130-1134. Marine Technology Society, Washington D.C

Anamalay R.V., Kirk T.B. & Panzera D. (1995) Numerical descriptors for the analysis of wear surfaces using laser scanning confocal microscopy. *Wear*, 181, 771-776

Andersen R.J., Berges J.A., Harrison P.J. & Watanabe M.M. (2005) Recepies for freshwater and seawater media. In: *Algal Culturing Techniques* (ed. Andersen RJ), pp. 429-538. Elseiver Academic Press, Burlington

Anderson C., Atlar M., Callow M.E., Candries M. & Townsin R.L. (2003) The development of foul release coatings for seagoing vessels. *Journal of Marine Design and Operations*, B4, 11-23

Anderson C.D. (1995) Tin vs tin-free antifoulings. In: *Proceedings of protecting the ship whie safeguarding the environment. 5-6 April*, London

Anderson C.D. (1998) TBT and TBT-free antifouling paints: efficiency and track record. In: *IBC UK Conferences Limited*, pp. 1-12, London

Andersson M., Berntsson K., Jonsson P. & Gatenholm P. (1999) Microtextured surfaces: towards macrofouling resistant coatings. *Biofouling*, 14, 167-178

Anon (2002) Anti-fouling coating mimics dolphin skin. *Developments in Waste Technology*, Dec 02/Jan 03, 6

Attard P. (2003) Nanobubbles and the hydrophobic attraction. *Advances in Colloid and Interface Science*, 104, 75-91

Baier R.E. (1968) Adhesion - mechanisms that assist or impede it. *Science*, 162, 1360

Bakker, D.P., Klijnstra, J.W., Busscher, H.B., Van der Mei, H.C. (2003) The effect of dissolved organic carbon on bacterial adhesion to conditioning films adsorbed on glass from natural seawater collected during different seasons. *Biofouling*, 19, 391-397

Bakus G.J., Targett N.M. & Schulte B. (1986) Chemical ecology of marine organisms - an overview. *Journal of Chemical Ecology*, 12, 951-987

Ball P. (1999) Engineering - shark skin and other solutions. *Nature*, 400, 507-509

Barthlott W. & Neinhuis C. (1997) Purity of the sacred lotus, or escape from contamination in biological surfaces. *Planta*, 202, 1-8

Baum C., Meyer C., Roessner D., Siebers D. & Fleischer L.-G. (2001) A zymogel enhances the self-cleaning abilities of the skin of the pilot whale (*Globicephala melas*). *Comparative Biochemistry and Physiology Part A*, 130, 835-847

Baum C., Meyer W., Stelzer R., Fleischer L.-G. & Siebers D. (2002) Average nanorough skin surface of the pilot whale (*Globicephala melas*, Delphinidae): considerations on the self-cleaning abilities based on nanoroughness. *Marine Biology*, 140, 653-657

Baum C., Simon F., Meyer W., Fleischer L.G., Siebers D., Kacza J. & Seeger J. (2003) Surface properties of the skin of the pilot whale *Globicephala melas*. *Biofouling*, 19, 181-186

Bavington C.D., Lever R., Mulloy B., Grundy M.M., Page C.P., Richardson N.V. & McKenzie J.D. (2004) Anti-adhesive glycoproteins in echinoderm mucus secretions. *Comparative Biochemistry and Physiology B-Biochemistry & Molecular Biology*, 139, 607-617

Bechert D.W., Bruse M. & Hage W. (2000) Experiments with three-dimensional riblets as an idealized model of shark skin. *Experiments in Fluids*, 28, 403-412

Becker K. (1996) Exopolysaccharide production and attachment strength of bacteria and diatoms on substrates with different surface tensions. *Microbial Ecology*, 32, 23-33

Becker K., Siriratanachai S. & Hormchong T. (1997) Influence of initial substratum surface tension on marine micro- and macro-fouling in the Gulf of Thailand. *Helgolander Meeresuntersuchungen*, 51, 445-461

Berntsson K.M., Andreasson H., Jonsson P.R., Larsson L., Ring K., Petronis S. & Gatenholm P. (2000a) Reduction of barnacle recruitment on micro-textured surfaces: Analysis of effective topographic characteristics and evaluation of skin friction. *Biofouling*, 16, 245-261

Berntsson K.M., Jonsson P.R., Larsson A.I. & Holdt S. (2004) Rejection of unsuitable substrata as a potential driver of aggregated settlement in the barnacle *Balanus improvisus*. *Marine Ecology-Progress Series*, 275, 199-210

Berntsson K.M., Jonsson P.R., Lejhall M. & Gatenholm P. (2000b) Analysis of behavioural rejection of micro-textured surfaces and implications for recruitment by the barnacle *Balanus improvisus*. *Journal of Experimental Marine Biology & Ecology.*, 251, 59-83

Bers A.V., Prendergast G.S., Zurn C.M., Hansson L., Head R.M. & Thomason J.C. (2006) A comparative study of the anti-settlement properties of Mytilid shells. *Biology Letters*, 2, 88-91

Bers V. & Wahl M. (2004) The influence of natural surface microtopographies on fouling. *Biofouling*, 20, 43-51

Bottjer D.J. (1981) Periostracum of the gastropod *Fusitriton oregonensis*: natural inhibitor of boring and encrusting organisms. *Bulletin of Marine Science*, 31, 916-921

Brady R.F. (2001) A fracture mechanical analysis of fouling release from non-toxic antifouling coatings. *Progress in Organic Coatings*, 43, 188-192

Brady R.F. (2005) Fouling-release coatings for warships. *Defence Science Journal*, 55, 75-81

Branscomb E.S. & Rittschof D. (1984) An Investigation of low-frequency sound-waves as a means of inhibiting barnacle settlement. *Journal of Experimental Marine Biology and Ecology*, 79, 149-154

Brouns J. & Heijs F.M.L. (1986) Production and biomass of the seagrass *Enhalus-Acoroides* (Lf) Royle and its epiphytes. *Aquatic Botany*, 25, 21-45

Brown G.O., Cheng C., Gudipati C.S., Johnson J., Powell K.T. & Wooley K.L. (2004) Nanoscopically-fiesolved amphiphilic coatings: Treacherous terrain to inhibit biofouling. *Abstracts of Papers of the American Chemical Society*, 228, U365-U365

Burke R.D. (1986) Pheromones and the gregarious settlement of marine invertebrate larvae. *Bulletin of Marine Science*, 39, 323-331

Butman C.A. (1987) Larval settlement of soft-sediment invertebrates - the spatial scales of pattern explained by active habitat selection and the emerging role of hydrodynamical processes. *Oceanography and Marine Biology*, 25, 113-165

Callow M. (1990) Ship fouling - problems and solutions. *Chemistry & Industry*, 123-127

Callow J.A. & Callow, M. E. (2006) Biofilms. In: *Antifouling Compounds. Progress in Milecular and sub-cellular Biology: Marine Molecular Biotechnology*. (eds. Fusetani, N., Clare, A.S.) pp. 141-170. Springer-Verlag Press.

Callow M.E., Jennings A.R., Brennan A.B., Seegert C.E., Gibson A., Wilson L., Feinberg A., Baney R. & Callow J.A. (2002) Microtopographic cues for settlement of zoospores of the green fouling alga *Enteromorpha*. *Biofouling*, 18, 237-245

Candries M., Anderson C.D. & Atlar M. (2001) Foul release systems and drag: Observations on how the coatings work. *Journal of Protective Coatings & Linings*, 18, 38-43

Carman M.L., Estes T.G., Feinberg A.W., Schumacher J.F., Wilkerson W., Wilson L.H., Callow M.E., Callow J.A. & Brennan A.B. (2006) Engineered antifouling microtopographies - correlating wettability with cell attachment. *Biofouling*, 22, 11-21

Chabot R. & Bourget E. (1988) Influence of substratum heterogeneity and settled barnacle density on the settlement of cypris larvae. *Marine Biology*, 91, 45-56

Champ M.A. (2000) A review of organotin regulatory strategies, pending actions, related costs and benefits. *Science of the Total Environment*, 258, 21-71

Champ M.A. (2001) New IMO convention to control anti-fouling systems on ships. *Sea Technology*, 42, 48-50

Che L.M., Le Campion-Alsumard T., Boury-Esnault N., Payri C., Golubic S. & Bezac C. (1996a) Biodegradation of shells of the black pearl oyster, *Pinctada margaritifera* var *cumingii*, by microborers and sponges of French Polynesia. *Marine Biology*, 126, 509-519

Che L.M., Le Campion-Alsumard T., Boury-Esnault N., Payri C., Golubic S. & Bezac C. (1996b) Biodegradation of shells of the black pearl oyster, *Pinctada margaritifera* var. *cumingii*, by microborers and sponges of French Polynesia. *Marine Biology*, 126, 509-519

Clarkson N. (1999) The antifouling potential of silicone elastomer polymers. In: *Recent Advances in Marine Biotechnology, Vol 3*. (eds. Fingerman M, Nagabhushanam R & Thompson MF), pp. 87-108. Scientific Publishers, Inc., New Hampshire

Cohn S.A., Farrell J.F., Munro J.D., Ragland R.L., Weitzell R.E. & Wibisono B.L. (2003) The effect of temperature and mixed species composition on diatom motility and adhesion. *Diatom Research*, 18, 225-243

Correa J.A. & Sanchez P.A. (1996) Ecological aspects of algal infectious diseases. *Hydrobiologia*, 327, 89-95

Crisp D.J. & Ryland J.S. (1960) Influence of filming and of surface texture on the settlement of marine organisms. *Nature*, 185, 119

D' Antonio C. (1985) Epiphytes on the rocky intertidal red alga *Rhodomela-Larix* (Turner) C Agardh - Negative effects on the host and food for herbivores. *Journal of Experimental Marine Biology and Ecology*, 86, 197-218

Dahlstrom M., Jonsson H., Jonsson P.R. & Elwing H. (2004) Surface wettability as a determinant in the settlement of the barnacle *Balanus Improvisus* (Darwin). *Journal of Experimental Marine Biology and Ecology*, 305, 223-232

Davenport J. (1999) Antifouling properties of the dogfish egg case and their possible application in developing non-toxic alternatives to antifouling paints. In: *Recent Advances in Marine Biotechnology Vol. III* (eds. Fingerman M, Nagabhushanam R & Thompson MF), pp. 21-36. Scientific Publishers, Inc., New Hampshire

Davenport J., Pugh P.J.A. & McKechnie J. (1996) Mixed fractals and anisotropy in subantarctic marine macroalgae from south Georgia: Implications for epifaunal biomass and abundance. *Marine Ecology-Progress Series*, 136, 245-255

de Nys R., Dworjanyn S.A. & Steinberg P.D. (1998) A new method for determining surface concentrations of marine natural products on seaweeds. *Marine Ecology Progress Series*, 162, 79-87

de Nys R. & Steinberg P.D. (1999) Role of secondary metabolites from algae and seagrasses in biofouling control. In: *Recent Advances in Marine Biotechnology Vol. III* (eds. Fingerman M, Nagabhushanam R & Thompson M-F), pp. 223-244. Science Publishers, New Hampshire

de Nys R., Steinberg P.D., Willemsen P., Dworjanyn S.A., Gabalish C.L. & King R.J. (1995) Broad spectrum effects of secondary metabolites from the red alga *Delisea pulchra* in antifouling assays. *Biofouling*, 8, 259-271

de Nys R., Givskov M., Kumar N., Kjelleberg S. & P.D. S. (2006) Furanones: Antifouling compounds. In: *Progress in Molecular and Subcellular Biology – Subseries Marine Molecular Biotechnology.* (eds. Fusetani N & Clare AS), pp. 55-86. Springer-Verlag Press.

Del Amo B., Giudice C.A. & Rascio V.J.D. (1984) Influence of binder dissolution rate on the bioactivity of antifouling paints. *Journal of Coatings Technology*, 56, 63-69

Duncan A.C., Weisbuch F., Rouais F., Lazare S. & Baquey C. (2002) Laser microfabricated model surfaces for controlled cell growth. *Biosensors & Bioelectronics*, 17, 413-426

Dworjanyn S.A. (2002) Chemically mediated antifouling and the cost of producing secondary metabolites in seaweeds. PhD Thesis. In: *School of Biological Sciences*. University of New South Wales, Sydney

Dworjanyn S.A., de Nys R. & Steinberg P.D. (1999) Localisation and surface quantification of secondary metabolites in the red alga *Delisea pulchra*. *Marine Biology*, 133, 727-736

Dworjanyn S.A., Wright J.T., Paul N.A., de Nys R. & Steinberg P.D. (2006) Cost of chemical defence in the red alga *Delisea pulchra*. *Oikos*, 113, 13-22

Edgar, L. & Pickett-Heaps, J.D. (1984) Diatom locomotion. In: *Progress in Phycological Research*. (eds. Round, F.E. & Chapman, D.J.) Biopress Ltd., Bristol, pp. 47-88

Eiben R. (1976) Influence of wetting tension and ions upon settlement and beginning of metamorphosis in bryozoan larvae (*Bowerbankia-Gracilis*). *Marine Biology*, 37, 249-254

Evans S.M., Birchenough A.C. & Brancato M.S. (2000) The TBT ban: Out of the prying pan into the fire? *Marine Pollution Bulletin*, 40, 204-211

Evans S.M., Leksono T. & McKinnell P.D. (1995) Tributyltin Pollution - a Diminishing problem following legislation limiting the use of TBT-based antifouling paints. *Marine Pollution Bulletin*, 30, 14-21

Figueiredo M., Norton T.A. & Kain J.M. (1997) Settlement and survival of epiphytes on two intertidal crustose coralline alga. *Journal of Experimental Marine Biology and Ecology*, 213, 247-260

Finlay J.A., Callow M.E., Ista L.K., Lopez G.P. & Callow J.A. (2002a) The influence of surface wettability on the adhesion strength of settled spores of the green alga *Enteromorpha* and the diatom *Amphora*. *Integrative and Comparative Biology*, 42, 1116-1122

Finlay J.A., Callow M.E., Schultz M.P., Swain G.W. & Callow J.A. (2002b) Adhesion strength of settled spores of the green alga *Enteromorpha*. *Biofouling*, 18, 251-256

Floerl O. (2002) Intracoastal spread of fouling organisms by recreations vessels. PhD Thesis. In: *School of Tropical Environment Studies and Geography*, p. 278. James Cook University, Townsville

Floerl O. & Inglis G.J. (2003) Boat harbour design can exacerbate hull fouling. *Austral Ecology*, 28, 116-127

Fusetani N. (2004) Biofouling and antifouling. *Natural Product Reports*, 21, 94-104

Gee J.M. & Warwick R.M. (1994) Body-Size Distribution in a marine metazoan community and the fractal dimensions of macroalgae. *Journal of Experimental Marine Biology and Ecology*, 178, 247-259

Gerhart D.J., Rittschof D., Hooper I.R., Eisenman K., Meyer A.E., Baier R.E. & Young C.M. (1992) Rapid and inexpensive quantification of the combined polar components of surface wettability: applications to biofouling. *Biofouling*, 5, 251-259

Gibbs P.E. & Bryan G.W. (1986) Reproductive failure in populations of the Dog-Whelk, *Nucella-Lapillus*, caused by imposex induced by Tributyltin from antifouling paints. *Journal of the Marine Biological Association of the United Kingdom*, 66, 767-777

Gitlitz M.H. (1981) Recent developments in marine antifouling coatings. *Journal of Coatings Technology*, 53, 46-52

Gosling E.M. (2003) *Bivalve molluscs*. Malden, Mass, Oxford.

Graham P.D., Joint I., Nevell T.G., Smith J.R., Stone M. & Tsibouklis J. (2000) Bacterial colonisation and settlement of algal spores and barnacle larvae on low surface energy materials. *Biofouling*, 16, 289-299

Granhag L.M., Finlay J.A., Jonsson P.R., Callow J.A. & Callow M.E. (2004) Roughness-dependent removal of settled spores of the green alga *Ulva* (syn. *Enteromorpha*) exposed to hydrodynamic forces from a water jet. *Biofouling*, 20, 117-122

Greer S.P., Iken K.B., McClintock J.B. & Amsler C.D. (2003) Individual and coupled effects of echinoderm extracts and surface hydrophobicity on spore settlement and germination in the brown alga *Hincksia irregularis*. *Biofouling*, 19, 315-326

Gribben P.E., Marshall D.J. & Steinberg P.D. (2006) Less inhibited with age? Larval age modifies responses to natural settlement inhibitors. *Biofouling*, 22, 101-106

Grigolava I.V. & McKenzie J.D. (1995) Carbodiimide-induced labeling of sea-urchin surfaces (Echinoidea, Echinodermata). *Comparative Biochemistry and Physiology B-Biochemistry & Molecular Biology*, 110, 477-482

Gucinski H. & Baier R.E. (1983) Surface-properties of porpoise and killer whale skin *invivo*. *American Zoologist*, 23, 959-959

Guillard R.R.L. & Ryland J.H. (1962) Studies on marine planktonic diatoms. 1. *Cyclotella nana* Hustedt and *Detonula confervacea* (Cleve). *Canadian journal of Microbiology*, 8, 229-239

Guo Z.G., Zhou F., Hao J.C. & Liu W.M. (2005) Stable biomimetic super-hydrophobic engineering materials. *Journal of the American Chemical Society*, 127, 15670-15671

Harper E.M. (1997) The molluscan periostracum: an important constraint in bivalve evolution. *Palaeontology*, 40, 71-97
Harper E.M. & Skelton P.W. (1993) A defensive value of the thickened periostracum in the Mytiloidea. *The Veliger*, 36, 36-42
Harvey E.C. & Rumsby P.T. (1997) Fabrication techniques and their applications to produce novel micromachined structures using excimer laser projection. In: *Proceedings from SPIE-International Society for Optical Engineering, 3223*, pp. 26-33
Hay M.E. (1986) Associational plant defenses and the maintenance of species-diversity - turning competitors into accomplices. *American Naturalist*, 128, 617-641
Hayden H.S., Blomster J., Maggs C.A., Silva P.C., Stanhope M.J. & Waaland J.R. (2003) Linnaeus was right all along: *Ulva* and *Enteromorpha* are not distinct genera. *European Journal of Phycology*, 38, 277-294
Head R.M., Berntsson K.M., Dahlstrom M., Overbeke K. & Thomason J.C. (2004) Gregarious settlement in cypris larvae: The effects of cyprid age and assay duration. *Biofouling*, 20, 123-128
Head R.M., Overbeke K., Klijnstra J., Biersteker R. & Thomason J.C. (2003) The effect of gregariousness in cyprid settlement assays. *Biofouling*, 19, 269-278
Hedegaard C. & Wenk H.R. (1998) Microstructure and texture patterns of mollusc shells. *Journal of Molluscan Studies*, 64, 133-136
Hills J.M. & Thomason J.C. (1998a) The effect of scales of surface roughness on the settlement of barnacle (*Semibalanus balanoides*) cyprids. *Biofouling*, 12, 57-69
Hills J.M. & Thomason J.C. (1998b) On the effect of tile size and surface texture on recruitment pattern and density of the barnacle, *Semibalanus balanoides*. *Biofouling*, 13, 31-50
Hills J.M., Thomason J.C. & Muhl J. (1999) Settlement of barnacle larvae is governed by Euclidean and not fractal surface characteristics. *Functional Ecology*, 13, 868-875
Hoipkemeier-Wilson L., Schumacher J.F., Carman M.L., Gibson A.L., Feinberg A.W., Callow M.E., Finlay J.A., Callow J.A. & Brennan A.B. (2004) Antifouling potential of lubricious, Micro-engineered, PDMS elastomers against zoospores of the green alga *Ulva* (*Enteromorpha*). *Biofouling*, 20, 53-63
Hoipkemeier-Wilson L., Schumacher J.F., Finlay J.A., Perry R., Callow M.E., Callow J.A. & Brennan A.B. (2005) Towards minimally fouling substrates: surface grafting and topography. *Polymer Preprints*, 46(2), 1312
Holland R., Dugdale T.M., Wetherbee R., Brennan A.B., Finlay J.A., Callow J.A. & Callow M.E. (2004) Adhesion and motility of fouling diatoms on a silicone elastomer. *Biofouling*, 20, 323-329
Holmes S.P., Sturgess C.J. & Davies M.S. (1997) The effect of rock-type on the settlement of *Balanus balanoides* (L) cyprids. *Biofouling*, 11, 137-147
Hunter J.E. & Cain P. (1996) Antifouling coatings in the 1990s - environmental, economic and legislative aspects. In: *Inst of Marine Engineers (IMarE), Pt I, IMAS 96, 10th Intn Maritime & Shipping Conf, Session V, Paper 16, 108(5) 22-24 October*, pp. 61-70, London
Hutchings P. (1984) *An illustrated guide to the estuarine polycheate worms of New South Wales*. Coast and Wetland Society, Sydney.
Iken K., Greer S.P., Amsler C.D. & McClintock J.B. (2003) A new antifouling bioassay monitoring brown algal spore swimming behaviour in the presence of echinoderm extracts. *Biofouling*, 19, 327-334

Jeffries M. (1993) Invertebrate colonization of artificial pondweeds of differing fractal dimension. *Oikos*, 67, 142-148
Jones A.W., Zhang H. & Lamb R.N. (2004) Hydrophobic coating. WO 2004090064 (PCT/AU2004/000461).
Kannan K. & Tanabe S. (1997) Elevated accumulation of tributyltin and its breakdown products in bottlenose dolphins (*Tursiops truncatus*) found stranded along the US Atlantic and Gulf coasts - Response. *Environmental Science & Technology*, 31, 3035-3036
Kelly M.S. & McKenzie J.D. (1995) Survey of the occurrence and morphology of sub-cuticular bacteria in shelf echinoderms from the North-East Atlantic-Ocean. *Marine Biology*, 123, 741-756
Kiil S., Weinell C.E., Pedersen M.S. & Dam-Johansen K. (2001) Analysis of self-polishing antifouling paints using rotary experiments and mathematical modeling. *Industrial & Engineering Chemistry Research*, 40, 3906-3920
Kobayashi N. & Okamura H. (2002) Effects of new antifouling compounds on the development of sea urchin. *Marine Pollution Bulletin*, 44, 748-751
Kohler J., Hansen P.D. & Wahl M. (1999) Colonization patterns at the substratum-water interface: how does surface microtopography influence recruitment patterns of sessile organisms? *Biofouling*, 14, 237-248
Kott P. (1992) The Australian Ascidiacea Part 3, Aplousobranchia (2). *Memoirs of the Queensland Museum*, 32, 375-620
Krug, P.J. Defense of Benthic Invertebrates Against Surface Colonization by Larvae: A Chemical Arms race. In: *Progress in Molecular and Subcellular Biology – Subseries Marine Molecular Biotechnology.* (eds. Fusetani N & Clare AS), pp. 1-54. Springer-Verlag Press.
Lafuma A. & Quere D. (2003) Superhydrophobic states. *Nature Materials*, 2, 457-460
Lamb R.N., Zhang H. & Raston C.L. (1998) Hydrophobic films. WO 9842452 (PCT/AU98/00185).
Lamprell K. & Whitehead K. (1998) *Bivalves of Australia*. Crawford House, Bathurst.
Lamprell K. & Whitehead T. (1992) *Bivalves of Australia*. Backhuys Publishers, Leiden.
Lapointe L. & Bourget E. (1999) Influence of substratum heterogeneity scales and complexity on a temperate epibenthic marine community. *Marine Ecology Progress Series.*, 189, 159-170
Lemire M. & Bourget E. (1996) Substratum heterogeneity and complexity influence micro-habitat selection of *Balanus* sp. and *Tubularia crocea* larvae. *Marine Ecology Progress Series*, 135, 77-87
Letourneux F. & Bourget E. (1988) Importance of physical and biological settlement cues used at different spatial scales by the larvae of *Semibalanus-Balanoides*. *Marine Biology*, 97, 57-66
Liedert R. & Kesel A.B. (2005) Biomimetic fouling control using microstructured surfaces. *University of Applied Sciences, Bremen Germany.*, Bionics - Innovations inspired by nature. Poster presented at the *Society for Experimental Biology Annual Main Meeting* in Barcelona, Spain.
Littler M.M. & Littler D.S. (1995) Impact of clod pathogen on pacific coral reefs. *Science*, 267, 1356-1360
Loeb G.I. (1977) The settlement of fouling organisms on hydrophobic surfaces. *Memoirs and Reports from the U.S Naval Research Laboratory*, 1-9

Lynch J.M., Fletcher M. & Latham M.J. (1979) Biological interactions. In: *Microbial ecology: a conceptual approach* (eds. Lynch JM & Poole NJ), pp. 171-187. Blackwell Scientific Publishing, Oxford

Maki J.S. (1999) The influence of marine microbes on biofouling. In: *Recent Advances in Marine Biotechnology* (eds. Fingerman M, Nagabhushanam R & Thompson M-F), pp. 147-171. Science Publishers, Enfield

Maki J.S., Rittschof D., Schmidt A.R., Snyder A.G. & Mitchell R. (1989) Factors controlling attachment of bryozoan larvae: A comparison of bacterial films and unfilmed surfaces. *Biological Bulletin*, 177, 295

Marmur A. (2006) Underwater superhydrophobicity: Theoretical feasibility. *Langmuir*, 22, 1400-1402

Marmur A. (2006b) Super-hydrophobicity fundamentals: implications to biofouling prevention. *Biofouling*, 22, 107-115

Marrs S.J., Thomason J.C., Cowling M.J. & Hodgkiess T. (1995) A replica method for the study of marine biofilms. *Journal of the Marine Biological Association of the United Kingdom. Plymouth*, 75, 759-762

Marshall D.J. & Keough M.J. (2003a) Effects of settler size and density on early post-settlement survival of *Ciona intestinalis* in the field. *Marine Ecology-Progress Series*, 259, 139-144

Marshall D.J. & Keough M.J. (2003b) Variation in the dispersal potential of non-feeding invertebrate larvae: the desperate larva hypothesis and larval size. *Marine Ecology-Progress Series*, 255, 145-153

Marshall D.J. & Keough M.J. (2004) Variable effects of larval size on post-metamorphic performance in the field. *Marine Ecology-Progress Series*, 279, 73-80

Mawatari, S. (1951) The natural history of the common fouling bryozoan *Bugula neritina* (Linneaus). *Miscellaneous Report from the Research Institute for Natural Resources*. Tokyo Nos. 19-21, pp. 47-54

Maximilien R., de Nys R., Holmstrom C., Gram L., Givskov M., Crass K., Kjelleberg S. & Steinberg P.D. (1998) Chemical mediation of bacterial surface colonisation by secondary metabolites from the red alga *Delisea pulchra*. *Aquatic Microbial Ecology*, 15, 233-246

McKenzie J.D. & Grigolava I.V. (1996) The echinoderm surface and its role in preventing microfouling. *Biofouling*, 10, 261-272

McKenzie J.D. & Kelly M.S. (1994) Comparative study of sub-cuticular bacteria in brittlestars (Echinodermata, Ophiuroidea). *Marine Biology*, 120, 65-80

Mihm J.W., Banta W.C. & Loeb G.I. (1981) Effects of adsorbed organic and primary fouling films on bryozoan settlement. *Journal of Experimental Marine Biology and Ecology*, 54, 167-179

Millar R.H. (1967) Ascidians as fouling organisms. In: *Marine borers, fungi and fouling organisms of wood* (eds. Jones & Eltringham), pp. p185-194. OECD publications, Paris

Milne A. & Hails G. (1974) Patent #1457590 International Paint Plc, Great Britain.

Monniot C., Monniot F. & Laboute P. (1991) *Coral reef ascidians of New Caledonia.* Orstom, Paris.

Newby B.M.Z., Chaudhury M.K. & Brown H.R. (1995) Macroscopic evidence of the effect of interfacial slippage on adhesion. *Science*, 269, 1407-1409

Novak R. (1984) A Study in Ultra-Ecology - Microorganisms on the seagrass *Posidonia-Oceanica* (L) *Delile*. *Marine Ecology-Pubblicazioni Della Stazione Zoologica Di Napoli I*, 5, 143-190

Nylund G.M., Cervin G., Hermansson M. & Pavia H. (2005) Chemical inhibition of bacterial colonization by the red alga *Bonnemaisonia hamifera*. *Marine Ecology-Progress Series*, 302, 27-36
Nylund G.M. & Pavia H. (2003) Inhibitory effects of red algal extracts on larval settlement of the barnacle *Balanus improvisus*. *Marine Biology*, 143, 875-882
Nylund G.M. & Pavia H. (2005) Chemical versus mechanical inhibition of fouling in the red alga *Dilsea carnosa*. *Marine Ecology-Progress Series*, 299, 111-121
Organisation for economic co-operation and development (1967) *Catalogue of main marine fouling organisms*. OECD publications, Paris.
Pal S. & Misra S.K. (1993) Organotin copolymers for self-polishing antifouling paints (SPC's). *Paintindia*, 43, 19-24
Patel P., Callow M.E., Joint I. & Callow J.A. (2003) Specificity in the settlement - modifying response of bacterial biofilms towards zoospores of the marine alga *Enteromorpha*. *Environmental Microbiology*, 5, 338-349
Pawley J.B. (1995) *Handbook of Biological Confocal Microscopy*. 2nd edn. Plenum Press, New York.
Pawlik J.R. (1992) Chemical Ecology of the Settlement of Benthic Marine-Invertebrates. *Oceanography and Marine Biology*, 30, 273-335
Peng Z. (2002) An integrated intelligence system for wear debris analysis. *Wear*, 252, 730-743
Peng Z. & Kirk T.B. (1999) The study of three-dimensional analysis techniques and automatic classification systems for wear particles. *Journal of Tribology-Transactions of the Asme*, 121, 169-176
Peterson C.G. & Stevenson R.J. (1989) Substratum conditioning and diatom colonization in different current regimes. *Journal of Phycology*, 25, 790-793
Petronis S., Berntsson K., Gold J. & Gatenholm P. (2000) Design and microstructuring of PDMS surfaces for improved marine biofouling resistance. *Journal of Biomaterials Science-Polymer Edition*, 11, 1051-1072
Quinn G.P. & Keough M.J. (2002) *Experimental design and data analysis for biologists*. Cambridge University Press, Cambridge.
Rahmoune M. & Latour M. (1995) Application of mechanical waves induced by piezofilms to marine fouling protection of oceanographic sensors. *Smart Materials & Structures*, 4, 195-201
Rascio V.J.D., Giúdice C.A. & del Amo D.B. (1988) Research and development on soluble matrix antifouling paints to be used on ships, offshore platforms and power stations. *Corrosion Reviews*, 8(1-2), 87-153
Rittschof D., Clare A.S., Gerhart D.J., Mary A.S. & Bonaventura J. (1992) Barnacle in vitro assays for biologically active substances: toxicity and settlement inhibition assays using mass cultured *Balanus amphitrite amphitrite* Darwin. *Biofouling*, 6, 115-122
Rittschof D., Hooper I.I. & Costlow J.D. (1988) Settlement and inhibition of marine invertebrate larvae: comparison of sensitivities of bryozoan and barnacle larvae. In: *Marine Biodeterioration* (eds. Thompson M-F, Sarojini R & Nagabhushanam R), pp. 599-608. Oxford and IBH Publishing Co. Inc., New Delhi
Rodriguez S.R., Ojeda F.P. & Inestrosa N.C. (1993) Settlement of benthic marine-invertebrates. *Marine Ecology-Progress Series*, 97, 193-207
Sand-Jensen K. (1977) Effect of epiphytes on eelgrass photosynthesis. *Aquatic Botany*, 3, 55-63

Scardino A., de Nys R., Ison O., O'Connor W. & Steinberg P. (2003) Microtopography and antifouling properties of the shell surface of the bivalve molluscs *Mytilis galloprovincialis* and *Pinctada imbricata*. *Biofouling*, 19, 221-230
Scardino A.J. & de Nys R. (2004) Fouling deterrence on the bivalve shell *Mytilus galloprovincialis*: A physical phenomenon? *Biofouling*, 20, 249-257
Scardino A.J., Harvey E. & De Nys R. (2006) Testing attachment point theory: diatom attachment on microtextured polyimide biomimics. *Biofouling*, 22, 55-60
Schmitt T.M., Hay M.E. & Lindquist N. (1995) Constraints on chemically mediated coevolution - multiple functions for seaweed secondary metabolites. *Ecology*, 76, 107-123
Schultz M.P., Kavanagh C.J. & Swain G.W. (1999) Hydrodynamic forces on barnacles: Implications on detachment from fouling-release surfaces. *Biofouling*, 13, 323-335
Schultz M.P. & Swain G.W. (2000) The influence of biofilms on skin friction drag. *Biofouling*, 15, 129-139
Scott P.J. (1994) *Three dimensional surface topography: Measurement, interpretation and applications*. Penton Press, London.
Sekar R., Venugopalan V.P., Satpathy K.K., Nair K.V.K. & Rao V.N.R. (2004) Laboratory studies on adhesion of microalgae to hard substrates. *Hydrobiologia*, 512, 109-116
Sheppard C.J.R. & Shotton D.M. (1997) *Confocal Laser Scanning Microscopy*. BIOS Scientific Publishers, Oxford.
Steinberg P.D. & de Nys R. (2002) Chemical mediation of colonization of seaweed surfaces. *Journal of Phycology*, 38, 621-629
Steinberg P.D., de Nys R. & Kjelleberg S. (2001) Chemical mediation of surface colonization. In: *Marine Chemical Ecology* (eds. McClintock JB & Baker JB), pp. 355-387. CRC Press, Boca Raton
Sun T.L., Feng L., Gao X.F. & Jiang L. (2005) Bioinspired surfaces with special wettability. *Accounts of Chemical Research*, 38, 644-652
Swain G. (1998) Biofouling control: A critical component of drag reduction. In: *International symposium on seawater drag reduction. 22-24 July*, Newport
Swain G. (1999) Redefining antifouling coatings. *Journal of Protective Coatings & Linings*, 16(9), 26-35
Swain G.W. & Schultz M.P. (1996) The testing and evaluation of non-toxic antifouling coatings. *Biofouling*, 10, 187-197
Tang Y., Finlay J.A., Kowalke G.L., Meyer A.E., Bright F.V., Callow M.E., Callow J.A., Wendt D.E. & Detty M.R. (2005) Hybrid xerogel films as novel coatings for antifouling and fouling release. *Biofouling*, 21, 59-71
Terlizzi A., Conte E., Zupo V. & Mazzella L. (2000) Biological succession on silicone fouling-release surfaces: Long-term exposure tests in the harbour of Ischia, Italy. *Biofouling*, 15, 327-342
Thomas P.A. (1981) Boring sponges destructive to economically important molluscan beds and coral reefs in Indian seas. *Indian Journal of Fisheries*, 26, 163-200
Thomason J.C., Davenport J. & Rogerson A. (1994) Antifouling performance of the embryo and eggcase of the dogfish *Scyliorhinus canicula*. *Journal of the Marine Biological Association of the United Kingdom.*, 74, 823-836
Thomason J.C., Letissier M.D.A., Thomason P.O. & Field S.N. (2002) Optimising settlement tiles: the effects of surface texture and energy, orientation and deployment duration upon the fouling community. *Biofouling*, 18, 293-304

Thomason J.C., Marrs S.J. & Davenport J. (1996) Antibacterial and antisettlement activity of the dogfish (*Scyliorhinus canicula*) eggcase. *Journal of the Marine Biological Association of the United Kingdom*, 76, 777-792

Underwood A.J. (1981) Techniques of analysis of variancee in experimental marine biology and ecology. *Oceanography and Marine Biology: An Annual Review*, 19, 513-605

Uyama Y., Inoue H., Ito K., Kishida A. & Ikada Y. (1991) Comparison of Different Methods for Contact-Angle Measurement. *Journal of Colloid and Interface Science*, 141, 275-279

Verran J. & Boyd R.D. (2001) The relationship between substratum surface roughness and microbiological and organic soiling: a review. *Biofouling*, 17, 59-71

Voulvoulis N., Scrimshaw M.D. & Lester J.N. (1999) Alternative antifouling biocides. *Applied Organometallic Chemistry*, 13, 135-143

Vrolijk N.H., Targett N.M., Baier R.E. & Meyer A.E. (1990) Surface characterisation of two gorgonian coral species: implications for a natural antifouling defence. *Biofouling*, 2, 39-54

Wahl M. (1989) Marine epibiosis. 1. Fouling and antifouling: some basic aspects. *Marine Ecological Progress Series*, 58, 175-189

Wahl M. & Hay M.E. (1995) Associational resistance and shared doom: effects of epibiosis on fouling. *Oecologia*, 102, 329-340

Wahl M., Kroeger K. & Lenz M. (1998) Non-toxic protection against epibiosis. *Biofouling*, 12, 1-3

Walters, L.J. (1992) Postsettlement success of the arborescent bryozoan *Bugula neritina* (L) - the importance of structural complexity. *Journal of Experimental Marine Biology and Ecology*, 164(1), 55-71

Walters, L.J. & Wethey, D.S. (1996) Settlement and early post settlement survival of sessile marine invertebrates on topographically complex surfaces: the importance of refuge dimensions and adult morphology. *Marine Ecology-Progress Series*, 137(1-3), 161-171

Wetherbee, R., Lind, J.L., Burke, J. & Quatrano, R.S. (1998) The first kiss: Establishment and control of initial adhesion by raphid diatoms. J*ournal of Phycology*, 34, 9-15

Wieczorek S.K. & Todd C.D. (1997) Inhibition and facilitation of bryozoan and ascidian settlement by natural multi-species biofilms: Effects of film age and the roles of active and passive larval attachment. *Marine Biology*, 128, 463-473

Wigglesworth-Cooksey B., van der Mei H., Busscher H.J. & Cooksey K.E. (1999) The influence of surface chemistry on the control of cellular behavior: studies with a marine diatom and a wettability gradient. *Colloids and Surfaces B-Biointerfaces*, 15, 71-80

Wikstrom S.A. & Pavia H. (2004) Chemical settlement inhibition versus post-settlement mortality as an explanation for differential fouling of two congeneric seaweeds. *Oecologia*, 138, 223-230

Wilson B.R. (2002) *A handbook to Australian seashells : on seashores east to west and north to south*. Reed New Holland, Sydney.

Wilson B.R., Wilson C. & Baker P. (1993) *Australian marine shells*. Odyssey Publishing, Kallaroo.

Witman J.D. & Suchanek T.H. (1984) Mussels in flow - drag and dislodgement by epizoans. *Marine Ecology-Progress Series*, 16, 259-268

Wooley K.L., Gudipati C., Johnson J. & Gan D.J. (2003) Kinetically-trapped segregated mixtures of hyperbranched fluoropolymers and linear polyethylene glycols: Treacherous terrain to inhibit biofouling. *Abstracts of Papers of the American Chemical Society*, 225, U666-U666

Yebra D.M., Kiil S. & Dam-Johansen K. (2004) Antifouling technology - past, present and future steps towards efficient and environmentally friendly antifouling coatings. *Progress in Organic Coatings*, 50, 75-104

Yuan C.Q., Peng Z., Zhou X.C. & Yan X.P. (2004) Effects of temperature on sliding wear process under contaminated lubricant test conditions. *Wear*, 257, 812-822

Zhang H., Lamb R. & Lewis J. (2005) Engineering nanoscale roughness on hydrophobic surface - preliminary assessment of fouling behaviour. *Science and Technology of Advanced Materials*, 6, 236-239

Zhang H., Lamb R.N. & Jones A.W. (2004) Durable superhydrophobic coating. WO 2004090065 (PCT/AU2004/000462).

Zhang X.H. & Jun H. (2004) Nanobubbles at the solid/water interface. *Progress in Chemistry*, 16, 673-681

Appendix One

Post-hoc multiple pair-wise comparisons for roughness parameters from Chapter 2

Figure 2.4c Ra

Student-Newman-Keuls

Species	N	Subset 1	2	3	4	5	6	7
27.00	3	.0523						
35.00	3	.0524						
26.00	3	.0567						
1.00	3	.0571						
29.00	3	.0672	.0672					
31.00	3	.0694	.0694					
23.00	3	.0724	.0724					
21.00	3	.0753	.0753					
32.00	3	.0840	.0840	.0840				
6.00	3	.0933	.0933	.0933	.0933			
10.00	3	.1140	.1140	.1140	.1140	.1140		
25.00	3	.1153	.1153	.1153	.1153	.1153		
36.00	3	.1187	.1187	.1187	.1187	.1187		
11.00	3	.1224	.1224	.1224	.1224	.1224		
34.00	3	.1230	.1230	.1230	.1230	.1230		
4.00	3	.1245	.1245	.1245	.1245	.1245	.1245	
15.00	3	.1261	.1261	.1261	.1261	.1261	.1261	
24.00	3	.1385	.1385	.1385	.1385	.1385	.1385	
22.00	3	.1507	.1507	.1507	.1507	.1507	.1507	
14.00	3	.1553	.1553	.1553	.1553	.1553	.1553	
28.00	3	.1609	.1609	.1609	.1609	.1609	.1609	
30.00	3	.1637	.1637	.1637	.1637	.1637	.1637	
37.00	3	.1671	.1671	.1671	.1671	.1671	.1671	
20.00	3	.1686	.1686	.1686	.1686	.1686	.1686	
33.00	3	.1717	.1717	.1717	.1717	.1717	.1717	
5.00	3	.1727	.1727	.1727	.1727	.1727	.1727	
18.00	3	.1738	.1738	.1738	.1738	.1738	.1738	
2.00	3	.1792	.1792	.1792	.1792	.1792	.1792	
13.00	3	.1881	.1881	.1881	.1881	.1881	.1881	
12.00	3		.1943	.1943	.1943	.1943	.1943	
3.00	3		.1980	.1980	.1980	.1980	.1980	
16.00	3			.2129	.2129	.2129	.2129	.2129
9.00	3				.2218	.2218	.2218	.2218
8.00	3				.2257	.2257	.2257	.2257
19.00	3					.2389	.2389	.2389
17.00	3						.2561	.2561
7.00	3							.3070
Sig.		.060	.079	.076	.062	.108	.050	.099

*Species sharing the same column are not significantly different at Alpha = .05.

Figure 2.5c Wa

Student-Newman-Keuls

Species	N	Subset 1	2	3	4	5
25.00	3	.0580				
24.00	3	.0612				
34.00	3	.0733				
10.00	3	.0739				
11.00	3	.0762				
22.00	3	.0796				
18.00	3	.0975	.0975			
1.00	3	.0976	.0976			
20.00	3	.1022	.1022			
2.00	3	.1099	.1099			
5.00	3	.1112	.1112			
27.00	3	.1250	.1250			
3.00	3	.1265	.1265			
26.00	3	.1284	.1284			
35.00	3	.1480	.1480	.1480		
6.00	3	.1483	.1483	.1483		
31.00	3	.1488	.1488	.1488		
19.00	3	.1576	.1576	.1576		
29.00	3	.1622	.1622	.1622		
32.00	3	.1663	.1663	.1663	.1663	
23.00	3	.1663	.1663	.1663	.1663	
16.00	3	.1743	.1743	.1743	.1743	
21.00	3	.1825	.1825	.1825	.1825	
8.00	3	.1832	.1832	.1832	.1832	
7.00	3	.1903	.1903	.1903	.1903	
15.00	3	.1952	.1952	.1952	.1952	
36.00	3	.2300	.2300	.2300	.2300	
9.00	3	.2366	.2366	.2366	.2366	
17.00	3	.3087	.3087	.3087	.3087	.3087
33.00	3		.3537	.3537	.3537	.3537
37.00	3		.3545	.3545	.3545	.3545
4.00	3			.3801	.3801	.3801
30.00	3			.3853	.3853	.3853
28.00	3			.3916	.3916	.3916
12.00	3			.3997	.3997	.3997
14.00	3				.4119	.4119
13.00	3					.4818
Sig.		.093	.058	.055	.050	.238

*Species sharing the same column are not significantly different at Alpha = .05.

Figure 2.6c Rsk

Student-Newman-Keuls

Species	N	Subset 1	2	3	4
17.00	3	-.0534			
8.00	3	-.0176			
3.00	3	-.0154			
11.00	3	-.0051			
10.00	3	-.0037			
18.00	3	-.0021			
24.00	3	-.0018			
7.00	3	.0015			
19.00	3	.0024			
25.00	3	.0034			
5.00	3	.0052			
22.00	3	.0080			
9.00	3	.0177			
20.00	3	.0292			
16.00	3	.0922			
2.00	3	.1792			
34.00	3	1.1247	1.1247		
15.00	3	1.8296	1.8296	1.8296	
23.00	3	1.8616	1.8616	1.8616	
36.00	3	2.1267	2.1267	2.1267	
27.00	3	2.2105	2.2105	2.2105	
1.00	3	2.5329	2.5329	2.5329	2.5329
29.00	3	2.5591	2.5591	2.5591	2.5591
13.00	3	2.6297	2.6297	2.6297	2.6297
37.00	3	2.6554	2.6554	2.6554	2.6554
31.00	3	2.7321	2.7321	2.7321	2.7321
26.00	3	2.7960	2.7960	2.7960	2.7960
12.00	3	2.8367	2.8367	2.8367	2.8367
30.00	3	2.9200	2.9200	2.9200	2.9200
33.00	3	2.9936	2.9936	2.9936	2.9936
21.00	3	3.0228	3.0228	3.0228	3.0228
14.00	3	3.3516	3.3516	3.3516	3.3516
32.00	3		3.4967	3.4967	3.4967
6.00	3		3.5733	3.5733	3.5733
28.00	3		3.8597	3.8597	3.8597
4.00	3			4.6171	4.6171
35.00	3				5.4872
Sig.		.065	.203	.178	.088

*Species sharing the same column are not significantly different at Alpha = .05.

Figure 2.7c Wsk

Student-Newman-Keuls

Species	N	Subset 1	2	3	4
9.00	3	-.2974			
19.00	3	-.1160	-.1160		
8.00	3	-.0500	-.0500		
7.00	3	-.0152	-.0152		
25.00	3	.0069	.0069		
11.00	3	.0163	.0163		
3.00	3	.0452	.0452	.0452	
10.00	3	.0567	.0567	.0567	
5.00	3	.0727	.0727	.0727	
18.00	3	.0921	.0921	.0921	
22.00	3	.1194	.1194	.1194	
17.00	3	.1279	.1279	.1279	
24.00	3	.1685	.1685	.1685	
20.00	3	.3277	.3277	.3277	
2.00	3	.4540	.4540	.4540	.4540
16.00	3	.4754	.4754	.4754	.4754
34.00	3	1.2587	1.2587	1.2587	1.2587
31.00	3	1.2916	1.2916	1.2916	1.2916
13.00	3	1.2966	1.2966	1.2966	1.2966
15.00	3	1.3215	1.3215	1.3215	1.3215
37.00	3	1.3590	1.3590	1.3590	1.3590
1.00	3	1.3597	1.3597	1.3597	1.3597
29.00	3	1.3652	1.3652	1.3652	1.3652
26.00	3	1.3840	1.3840	1.3840	1.3840
14.00	3	1.4458	1.4458	1.4458	1.4458
33.00	3	1.4642	1.4642	1.4642	1.4642
36.00	3	1.4767	1.4767	1.4767	1.4767
23.00	3	1.4824	1.4824	1.4824	1.4824
27.00	3	1.4863	1.4863	1.4863	1.4863
12.00	3	1.4933	1.4933	1.4933	1.4933
28.00	3		1.7685	1.7685	1.7685
6.00	3		1.7833	1.7833	1.7833
30.00	3		1.9067	1.9067	1.9067
32.00	3		1.9433	1.9433	1.9433
4.00	3			2.0729	2.0729
21.00	3				2.3049
35.00	3				2.4190
Sig.		.177	.054	.052	.051

*Species sharing the same column are not significantly different at Alpha = .05.

Figure 2.8c Str

Student-Newman-Keuls

Species	N	Subset 1	Subset 2	Subset 3
7.00	3	.7513		
13.00	3	.7566	.7566	
16.00	3	.7699	.7699	.7699
5.00	3	.7776	.7776	.7776
17.00	3	.7781	.7781	.7781
34.00	3	.7852	.7852	.7852
24.00	3	.7878	.7878	.7878
11.00	3	.7908	.7908	.7908
3.00	3	.7909	.7909	.7909
19.00	3	.7921	.7921	.7921
9.00	3	.7958	.7958	.7958
8.00	3		.8005	.8005
22.00	3		.8012	.8012
20.00	3		.8013	.8013
2.00	3		.8021	.8021
25.00	3		.8035	.8035
1.00	3		.8041	.8041
15.00	3		.8057	.8057
18.00	3		.8062	.8062
31.00	3		.8068	.8068
4.00	3			.8084
14.00	3			.8097
10.00	3			.8104
33.00	3			.8104
28.00	3			.8124
30.00	3			.8125
37.00	3			.8142
26.00	3			.8144
32.00	3			.8147
29.00	3			.8154
21.00	3			.8154
27.00	3			.8157
36.00	3			.8170
35.00	3			.8177
23.00	3			.8180
12.00	3			.8225
6.00	3			.8234
Sig.		.075	.062	.082

* Species sharing the same column are not significantly different at Alpha = .05.

Figure 2.9c Fractal dimension

Student-Newman-Keuls

Species	N	Subset 1	2	3	4	5	6
26.00	3	2.3347					
1.00	3	2.3388	2.3388				
35.00	3	2.3513	2.3513	2.3513			
27.00	3	2.3900	2.3900	2.3900	2.3900		
32.00	3	2.3900	2.3900	2.3900	2.3900		
29.00	3	2.3953	2.3953	2.3953	2.3953		
23.00	3	2.4290	2.4290	2.4290	2.4290		
28.00	3	2.4349	2.4349	2.4349	2.4349		
31.00	3	2.4398	2.4398	2.4398	2.4398		
21.00	3	2.4456	2.4456	2.4456	2.4456		
14.00	3	2.4491	2.4491	2.4491	2.4491		
6.00	3	2.4800	2.4800	2.4800	2.4800		
12.00	3	2.4800	2.4800	2.4800	2.4800		
37.00	3		2.5019	2.5019	2.5019		
30.00	3		2.5067	2.5067	2.5067		
33.00	3		2.5076	2.5076	2.5076		
15.00	3			2.5131	2.5131		
4.00	3			2.5198	2.5198		
13.00	3				2.5312		
36.00	3				2.5600		
34.00	3					2.7590	
25.00	3					2.7844	2.7844
24.00	3					2.7869	2.7869
10.00	3					2.8100	2.8100
8.00	3					2.8259	2.8259
11.00	3					2.8393	2.8393
7.00	3					2.8552	2.8552
5.00	3					2.8562	2.8562
22.00	3					2.8642	2.8642
20.00	3					2.8674	2.8674
9.00	3					2.8740	2.8740
2.00	3					2.8944	2.8944
19.00	3					2.9004	2.9004
18.00	3					2.9045	2.9045
3.00	3						2.9343
16.00	3						2.9375
17.00	3						2.9494
Sig.		.141	.051	.057	.058	.155	.070

* Species sharing the same column are not significantly different at Alpha = .05.